United States
Environmental Protection
Agency

Environmental Research
Laboratory
Narragansett RI 02882

EPA-600/3-79-029
March 1979

Research and Development

EPA

Dredge Spoils and Sewage Sludge in the Trace Metal Budget of Estuarine and Coastal Waters

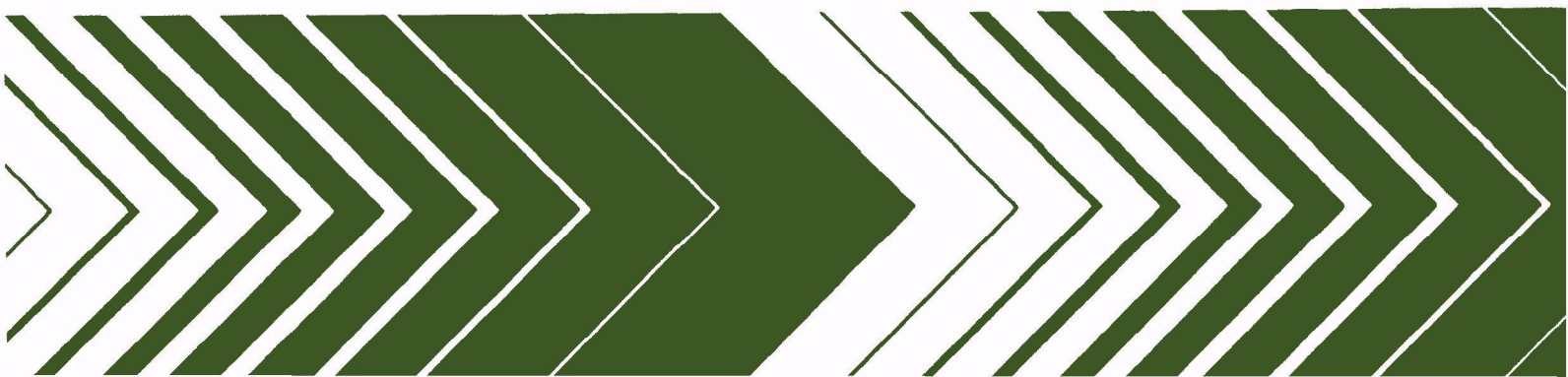

RESEARCH REPORTING SERIES

Research reports of the Office of Research and Development, U.S. Environmental Protection Agency, have been grouped into nine series. These nine broad categories were established to facilitate further development and application of environmental technology. Elimination of traditional grouping was consciously planned to foster technology transfer and a maximum interface in related fields. The nine series are:

1. Environmental Health Effects Research
2. Environmental Protection Technology
3. Ecological Research
4. Environmental Monitoring
5. Socioeconomic Environmental Studies
6. Scientific and Technical Assessment Reports (STAR)
7. Interagency Energy-Environment Research and Development
8. "Special" Reports
9. Miscellaneous Reports

This report has been assigned to the ECOLOGICAL RESEARCH series. This series describes research on the effects of pollution on humans, plant and animal species, and materials. Problems are assessed for their long- and short-term influences. Investigations include formation, transport, and pathway studies to determine the fate of pollutants and their effects. This work provides the technical basis for setting standards to minimize undesirable changes in living organisms in the aquatic, terrestrial, and atmospheric environments.

This document is available to the public through the National Technical Information Service, Springfield, Virginia 22161.

EPA-600/3-79-029
March 1979

DREDGE SPOILS AND SEWAGE SLUDGE IN THE TRACE METAL BUDGET OF ESTUARINE AND COASTAL WATERS

by

H. James Simpson
Lamont-Doherty Geological Observatory
of Columbia University
Palisades, New York 10964

Grant No. R803113

Project Officer

Robert R. Payne
Environmental Research Laboratory
Narragansett, Rhode Island 02882

ENVIRONMENTAL RESEARCH LABORATORY
OFFICE OF RESEARCH AND DEVELOPMENT
U.S. ENVIRONMENTAL PROTECTION AGENCY
NARRAGANSETT, RHODE ISLAND 02882

DISCLAIMER

This report has been reviewed by the Environmental Research Laboratory, Narragansett, U. S. Environmental Protection Agency, and approved for publication. Approval does not signify that the contents necessarily reflect the views and policies of the U. S. Environmental Protection Agency, nor does mention of trade names or commercial products constitute endorsement or recommendation for use.

FOREWORD

In the natural environment, few regions are as complex or as difficult to understand as estuarine and coastal waters. In contrast to the open ocean remote from upwelling areas or a fresh water system where individual chemical cycles may be studied in a relatively constant matrix, coastal waters and especially estuaries show temporal and spatial variability in almost every measurable parameter. The extreme physical, chemical and biological changes encountered in going from fresh water to sea water, and the transport dynamics associated with river flow and tidal cycles almost demand a relatively broad approach to the study of such systems if we are to have any hope of understanding how to manage them.

In recent years, increased need for fresh water and interest in better management of our environmental resources have helped focus attention on the serious degradation of estuarine and coastal regions largely as a result of urbanization. The impact of trace metals, domestic and industrial organic residues, nutrients, and dredge spoils from estuaries on coastal waters has become a major concern in environmental planning. In the case of the estuary of the Hudson River, a major portion of the suspended particles are deposited within the system only to be moved to the continental shelf by dredging. Thus the strong coupling between an estuary and the adjacent coastal waters can be perturbed by man's activities on a scale comparable to natural processes, even in large systems. The following report examines some of these perturbations and their relationships to natural cycles and processes. The impact of dredge spoils and sewage sludge in the natural cycles of trace metals in estuarine and coastal waters are examined for the Hudson River estuary and adjacent region of the continental shelf through the use of a broad range of geochemical approaches, based primarily on data collected on field samples.

Eric D. Schneider
Director, Environmental Research
Laboratory, Narragansett

PREFACE

The research documented here was the result of the combined efforts of a number of people, including several graduate students who were responsible for a major portion of the field and laboratory work, and for the interpretation and reporting of these studies. These current, or former, students include Richard Bopp (Columbia University), Peter Bower (Queens College and Columbia University), Bruce Deck (Columbia University), Douglas Hammond (Columbia University), Gary Klinkhammer (University of Rhode Island), and Curtis Olsen (Columbia University). Dr. Susan Williams (now at Lederle Laboratories, Pearl River, New York) and Dr. Yuan-Hui Li (Columbia University) were Co-Principal Investigators and Professor Michael Bender (University of Rhode Island) was responsible, along with Gary Klinkhammer, for water column measurements of trace metals in the Hudson. Dr. Edward Catanzaro (Lamont-Doherty Geological Observatory) and Professor William Corpe (Barnard College) also participated in this study. The results of portions of our research have been reported in the following abstracts and publications:

ABSTRACTS

Bopp, R.F., H.J. Simpson and C.R. Olsen, PCB's and Cs-137 in Sediments of the Hudson Estuary (Abs.), Trans. Amer. Geophys. Union, 58, 407, 1977.

Hammond, D.E., H.J. Simpson and G. Mathieu, Distribution of Radon-222 in the Delaware and Hudson Estuaries as an Indicator of Migration Rates of Dissolved Species Across the Sediment-Water Interface (Abs.), Trans. Amer. Geophys. Union, 57, 151, 1976.

Klinkhammer, G.P., M. Bender and H.J. Simpson, The Partitioning of Some Trace Metals in the Hudson River Estuary (Abs.), Trans. Amer. Geophys. Union, 57, 255, 1976.

Olsen, C.R., H.J. Simpson and R.M. Trier, Anthropogenic Radionuclides as Tracers for Recent Sediment Deposition in the Hudson Estuary (Abs.), Trans. Amer. Geophys. Union, 58, 406, 1977.

Olsen, C.R., H.J. Simpson and S.C. Williams, Sedimentation Rates in the Hudson River Estuary (Abs.), Amer. Assoc. of Petroleum Geol. Bull., 60, 703, 1976.

Simpson, H.J., T.H. Peng, C.R. Olsen and S.C. Williams, Radiocarbon Dating of Estuarine Carbonates (Abs.), Amer. Assoc. of Petroleum Geol. Bull., 60, 723, 1976.

PUBLICATIONS

Hammond, D.E., H.J. Simpson and G. Mathieu, Methane and Radon-222 as Tracers for Mechanisms of Exchange Across the Sediment-Water Interface in the Hudson River Estuary, In: Marine Chemistry in the Coastal Environment, ACS Symp. Ser., Vol. 18, edited by T. Church, 119-132, American Chemical Society, Washington, D.C., 1975.

Hammond, D.E., Dissolved Gases and Kinetic Processes in the Hudson River Estuary, Ph.D. Thesis, Columbia University, New York, New York, 1975, 161 pp

Hammond, D.E., H.J. Simpson and G. Mathieu, Radon-222 Distribution and Transport Across the Sediment-Water Interface in the Hudson River Estuary, Jour. Geophys. Res., 82, 3913-3920, 1977.

Olsen, C.R., H.J. Simpson, S.C. Williams, T.H. Peng and B.L. Deck, A Geochemical Analysis of the Sediments and Sedimentary Structures in the Hudson Estuary, Jour. Sedimentary Petrology, in press, 1978.

Simpson, H.J., D.E. Hammond, B.L. Deck and S.C. Williams, Nutrient Budgets in the Hudson River Estuary, In: Marine Chemistry in the Coastal Environment, ACS Symp. Ser., Vol. 18, edited by T. Church, 618-635, 1975.

Simpson, H.J., C.R. Olsen, R.F. Bopp, P.M. Bower, R.M. Trier and S.C. Williams, Cesium-137 as a Tracer for Reactive Pollutants in Estuarine Sediments, USA-USSR Symposium-Odessa, U.S. Environmental Protection Agency, in press, 1978.

Simpson, H.J., C.R. Olsen, S.C. Williams and R.M. Trier, Man-Made Radionuclides and Sedimentation in the Hudson River Estuary, Science, 194, 179-183, 1976.

Simpson, H.J., S.C. Williams, C.R. Olsen and D.E. Hammond, Nutrient and Particulate Matter Budgets in Urban Estuaries, In: Estuaries, Geophysics and the Environment, Studies in Geophysics, 94-103, National Academy of Sciences, Washington, D.C., 1977.

Williams, S.C., H.J. Simpson, C.R. Olsen and R.F. Bopp, Heavy Metals in Hudson River Estuary Sediments, Marine Chemistry, in press, 1978.

MANUSCRIPTS SUBMITTED FOR PUBLICATION

Bower, P.M., H.J. Simpson, S.C. Williams and Y.H. Li, Trace Metals in the Sediments of Foundry Cove, Cold Spring, New York.

Friedmann, M., S.C. Williams and H.J. Simpson, A New Enzymatic Method for Analysis of Cellulose in Sediments.

Hammond, D.E. and H.J. Simpson, Methane Distribution and Sediment Flatulence in the Hudson River Estuary.

Simpson, H.J. and D.E. Hammond, Application of One-Dimensional Models to the Hudson River Estuary.

Simpson, H.J., T.H. Peng, C.R. Olsen and S.C. Williams, Radiocarbon Geochemistry in the Estuary of the Hudson River.

ABSTRACT

Many reactive pollutants, such as Zn, Cu, Pb, Cs-137, Pu-239,240 and PCB's appear to be transported and accumulated together in association with fine-grained particles in the Hudson River estuary. Anthropogenic increases of 3-6 times natural levels of Zn, Cu, and Pb were found for Hudson sediments. Mobilization of Cd and Ni in the sediments of a small embayment of the Hudson with very high contamination levels appears to be primarily by resuspension of fine particles, although elevated concentrations of Cd in pore waters were also observed. Radiocarbon measurements indicate the predominant source of organic carbon in New York harbor sediments is recent sewage and not petroleum hydrocarbon contamination. A new enzymatic technique was developed to trace the distribution of cellulose, a significant component of sewage sludge, in coastal sediments. Radon-222, a natural radioactive gas dissolved in the Hudson, is supplied primarily from the sediments at approximately twice the rate predicted by molecular diffusion. Methane measurements provided additional information on the flux of materials from sediments. The behavior of phosphate and trace metals derived from sewage was examined on the basis of field data and the use of simple models to examine management alternatives. The most reasonable course appears to be completion of secondary sewage treatment plants in New York City and major upgrading of primary treatment in New Jersey. Tertiary treatment for nutrient removal does not appear to offer at present the likelihood of significant improvements of receiving water quality in the Hudson estuary. Discharge from the Hudson estuary appears to be the dominant source of soluble metals to the adjacent coastal zone and if soluble trace metal fluxes were the only criterion for placement of discharge sites for dredge spoils and sewage sludge, the present site would appear to be a reasonable one, since estuary discharge will probably dominate soluble metal transport budgets whether or not dumping is continued at that site.

CONTENTS

FIGURES

TABLES

ACKNOWLEDGMENTS

Organization, preparation, and editing of this report were primarily accomplished by the efforts of Karen Antlitz and Bruce Deck, in addition to their normal administrative and research activities at Lamont-Doherty Geological Observatory.

SECTION 1

INTRODUCTION

Sediments dredged from urban and industrial harbor areas and sludges from sewage treatment plants are continuously generated in large quantities by our coastal cities. Disposal of these materials presents a number of difficult management problems. In the New York City metropolitan region, current practice involves discharge of both dredge spoils and sewage sludge to coastal waters within a few tens of kilometers of shore. One concern is that toxic pollutants such as heavy metals will be released from the waste solids to solution in the water column in amounts sufficient to substantially affect the biota of the impacted coastal waters. Another consideration is that many pollutants are associated with fine particles which could be easily transported by currents away from the disposal sites possibly to accumulate in other areas.

Much of the research on mobilization of toxic contaminants has employed laboratory simulations, the results of which are then extrapolated to field situations. We have concentrated on analysis of field samples to help provide a framework into which laboratory experiments of other investigations can be integrated. The field area of our research, the estuary of the Hudson River, is one of the most important components of the estuarine-coastal water system of the New York City metropolitan region. This region has one of the largest dredge spoil and sewage sludge marine disposal operations in the world, and is currently the focus of several major field research programs primarily in the New York Bight. Our research in the Hudson is complementary to that in the Bight, and will help provide critical information for development of the best management approach for disposal of dredge spoils and sewage sludge in the New York areas, and other areas as well.

One of our primary objectives has been to estimate the rate of releases of dissolved heavy metals from polluted sediments and to examine the importance of these releases relative to other heavy metal fluxes and cycles in estuarine and coastal waters. We have examined the distribution of several metals in the sediments, pore waters and water column of the Hudson estuary. To interpret these data in terms of processes and rates of transport, we have also measured a number of additional parameters in both the sediments and water column of the Hudson. New analytical techniques and sampling approaches were developed and used to obtain some of the data, and these innovations should prove useful in studies by other investigators. We have attempted to suggest tentative conclusions directly related to management objectives whenever these seemed warranted, even when more extensive research is obviously needed to reach really firm conclusions.

SECTION 2

CONCLUSIONS

1. Trace metal (Zn, Cu and Pb) concentrations in recent Hudson sediments are 3-6 times background levels for fine-grained sediments, and are comparable to observed metal concentrations of sediments in the New York Bight sewage sludge and dredge spoil dumping area.

2. Foundry Cove, a small embayment in the Hudson 60 km north of New York City, appears to be the site of most intense metal contamination in the Hudson, with Cd and Ni concentrations of up to a few per cent by weight. Mobilization of Cd in this area is apparently primarily via resuspension of fine particles, although the fluxes of soluble Cd from these sediments appears measurable with additional field studies. This site offers an unusual opportunity for further understanding of Cd and Ni mobilization from contaminated sediments in both fresh water and saline environments.

3. Many reactive pollutants in Hudson sediments appear to be transported and accumulated together in association with fine-grained particles. This covariation of Zn, Cu, Pb, Cd, Ni, PCB's, Pu-239,240 and Cs-137 greatly simplifies the task of mapping the distribution of contaminated sediments in the Hudson.

4. Through radiocarbon measurements we have found the organic carbon of New York harbor sediments to be predominantly recent sewage, with fossil fuel carbon making up a considerably smaller proportion of the pollutant carbon than in contaminated sediments from other areas in the Hudson. The hydrocarbon pollutant levels in the harbor sediments are substantial, however.

5. We have developed a new analytical technique for cellulose, utilizing cellulase enzymes to hydrolyze cellulose to glucose. This technique is quite sensitive and specific and has been exploited here for studies of the source of high molecular weight organic matter in shelf sediments.

6. The flux of a soluble, chemically-inert natural tracer, Rn-222, from Hudson sediments to the water column is approximately two times the rate predicted assuming only molecular diffusion rates in the sediment interstitial waters. Thus the transport of some types of materials from sediments to the water column can be estimated reasonably well from simple diffusion models; the integrated effect of a number of processes which might enhance the flux of materials to the water column is roughly comparable to that of molecular diffusion.

7. Dissolved methane in the Hudson appears to be supplied, at least in part, by partial solution of bubbles produced in the sediments and released to the water column. The variation of dissolved methane concentration in Hudson sediments is very large, and may be a valuable indicator of the mobility of some trace metals in sediments.

8. Phosphate is supplied to the Hudson in such large amounts by sewage discharge, and is transported out of the harbor so rapidly by estuarine circulation, that it approximates a conservative tracer of sewage in the lower Hudson. This provides a valuable indicator of discharge rates of soluble trace metals to the New York Bight by estuarine circulation. Tertiary treatment of New York City area sewage for phosphate removal does not appear justified in light of our present information. Completion of secondary treatment plants and major upgrading of primary treatment plants, especially in New Jersey appears to be a more sensible course to pursue.

9. A major fraction of the trace metals discharged to New York harbor in sewage leave the Hudson through the Narrows in solution. To the first approximation the soluble metal levels in the lower Hudson can be described in terms of three end member mixing between fresh Hudson water, New York Bight sea water and sewage.

10. The discharge of soluble metals from the Hudson estuary appears to be the dominant source of soluble metals to the apex of the New York Bight. Release of soluble metals from dumping area sediments does not seem to be a significant source compared to estuarine discharge. If the only criteria for the placement of a site for discharge of dredge spoils and sewage sludges was consideration of soluble trace metal fluxes, the present site would appear to be a reasonable one, since soluble metal transport budgets will probably be dominated by estuarine discharge whether or not dumping is continued at that site.

SECTION 3

RECOMMENDATIONS

1. We suggest that studies of the impact of specific activities such as dredge spoil or sewage sludge disposal in coastal waters require integrated field research efforts which exploit a wider range of geochemical tracers and other approaches than are commonly employed. Research of wide scope is necessary to develop the understanding necessary to place the impact of specific activities in perspective.

2. Although more efforts should be devoted to the understanding of trace metal transport pathways in polluted estuarine and coastal waters, it is at least equally important to intensify studies of the environmental pathways and significance of pollutants such a PCB's and other toxic compounds, especially for the New York City area.

SECTION 4

SOURCES OF HEAVY METALS IN SEDIMENTS OF THE HUDSON RIVER ESTUARY

INTRODUCTION

Heavy metals discharged into estuaries and coastal waters with domestic and industrial wastes are often present as particulates, or have strong affinities for solid phases in the receiving waters (Morel et al., 1975). Present distributions of metals in sediments can serve as an indication of the time history and extent of pollutant discharge in specific areas (Chow et al., 1973; Bruland et al., 1974; Erlenkeuser et al., 1974; de Groot et al., 1976). To interpret the present metal content of sediments, several factors must be considered including the "natural" preindustrial metal content of sediments in the area in question. Components such as clay minerals, organics and iron and manganese oxides are important phases in both the natural and pollutant heavy metal content of sediments. Other phases such as quartz and calcium carbonate, which tend to occur in relatively large particles, are usually less important in binding heavy metals, and thus serve primarily to "dilute" the heavy metal bearing phases which dominate the fine particle size fraction. In environments where particle size distributions and mineralogy are heterogeneous, substantial variability in heavy metal concentrations would thus be expected, even in the absence of significant local sources of metal contamination (de Groot et al., 1976). The pattern of sediment accumulation in environments such as estuaries or coastal waters is generally sufficiently complicated to make it difficult to establish the time history of accumulation at any particular sampling site.

We have analyzed sediments from the Hudson estuary and adjacent coastal area for zinc (Zn), copper (Cu), lead (Pb), manganese (Mn) and iron (Fe), as well as man-made radionuclides such as cesium-137, to establish the present distribution of heavy metals in a system subject to substantial pollutant loading. We have related the present sediment metal concentrations to those typical of the Hudson prior to industrial pollutant discharge, and to the patterns of recent sediment accumulation.

SAMPLING AND ANALYTICAL METHODS

Cores were taken from near the upstream limit of saline water intrusion in the Hudson to the middle of New York harbor (Figure 1) where salinities are usually about two thirds of deep ocean water salinities. Large grab samples of the upper 10 centimeters of sediment in the coastal waters adjacent to the Hudson were collected out to beyond the edge of the continental shelf (Figure 2). Most of the cores were collected in plastic liners with a six centimeter diameter gravity corer, and were usually about

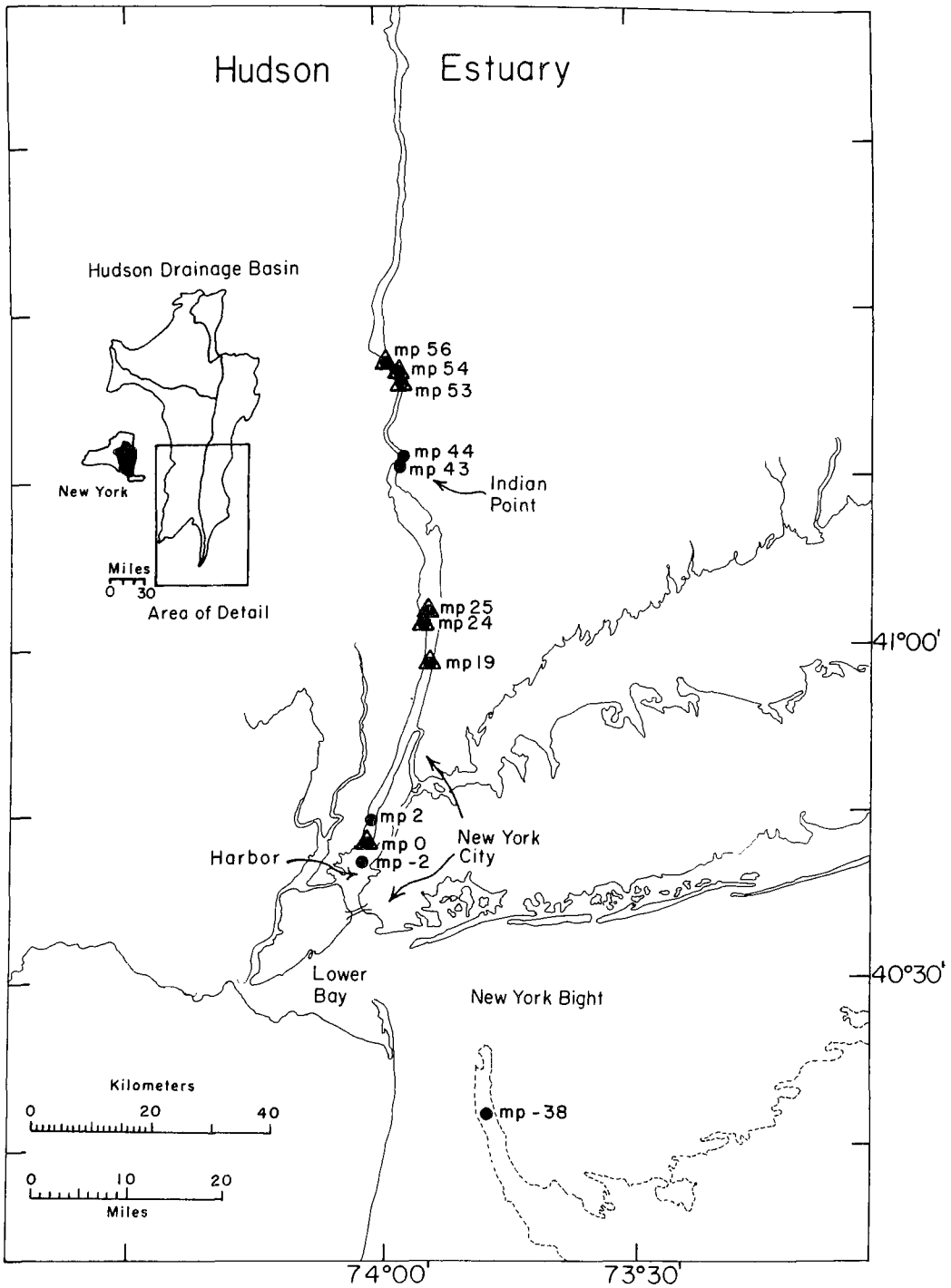

Figure 1. Location map for cores collected in the Hudson River Estuary. Sites where background levels of heavy metals were observed at some depth in the core are indicated with triangles. Locations in the Hudson are generally described in terms of the number of miles (mile point = mp) upstream of the southern tip of Manhattan Island.

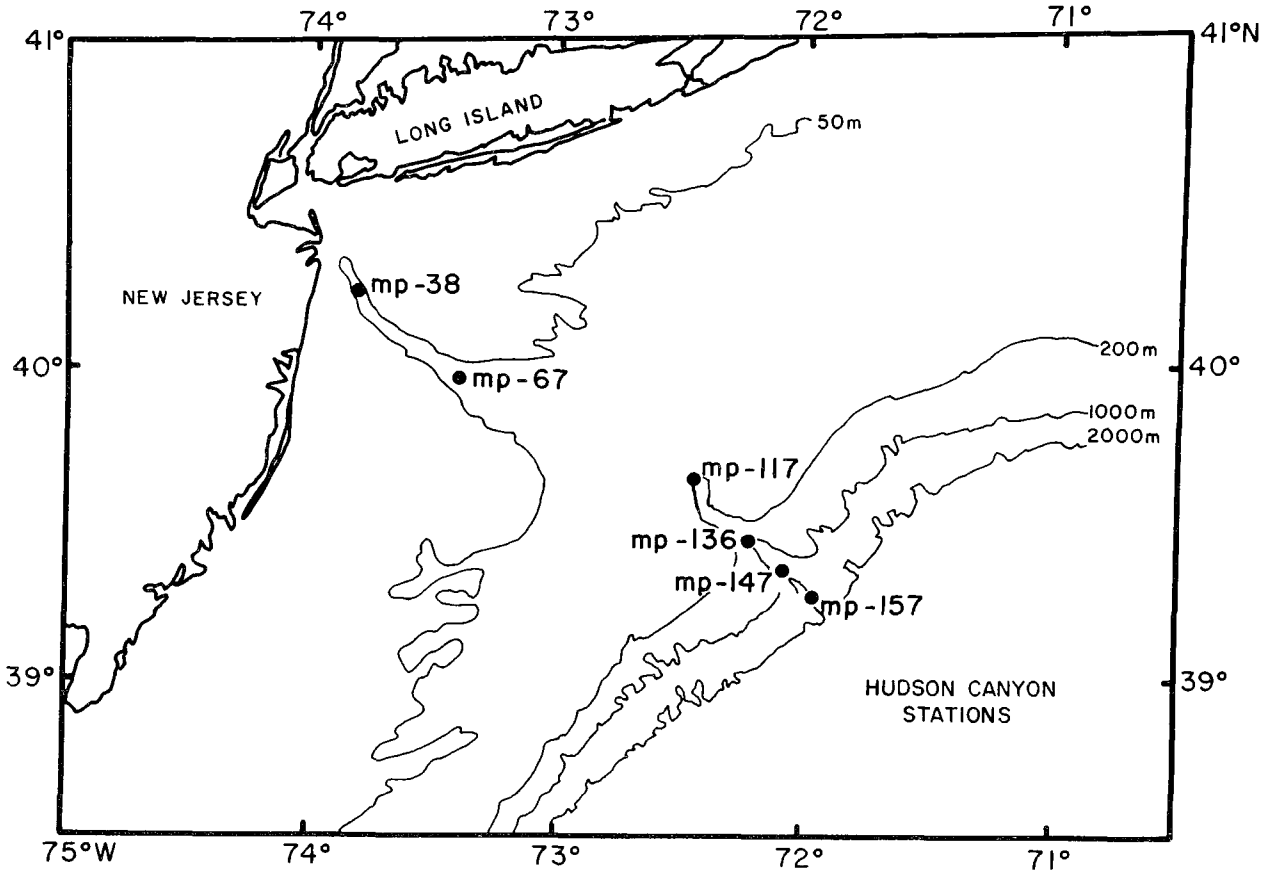

Figure 2. Location map for cores collected on the continental shelf. Sites are indicated with negative numbers, indicating the number of miles downstream from the origin of the mile point reference system. The sampling sites generally follow the narrow band of fine-grained sediments in the Hudson Shelf Valley and Hudson Submarine Canyon.

0.5 meters in length. One of the cores from nineteen miles upstream of the southern tip of Manhattan Island (mile point 19) was a 6 meter piston core taken from one of Columbia University's oceanographic vessels (R/V VEMA). Another of the cores (mp 24) which had a total length of about 12 meters was taken in sections by hand drilling in a marsh which currently is under water during only very high tides.

Sediment samples were air dried, ground in a mortar and pestle and passed through a 250 μ nylon sieve. Samples for heavy metal determinations were dried at 105°C to constant weight and stored in a dessicator, while those for measurement by gamma spectrometry were sealed in teflon-lined aluminum cans and counted with a large volume lithium-drifted germanium detector and multichannel analyzer.

Metals were leached from sediments by fuming samples with concentrated HCl/HNO_3 (1:3) for several hours, followed by treatment with 70% $HClO_4$ until the solid phase was essentially pure white. Final solutions of acid were made up to approximately 5% in HCl after driving off most of the $HClO_4$. Sediment suspensions were filtered and washed through a Gooch crucible with preweighed glass fiber filters. Filtrates were diluted and analyzed by flame atomic absorption spectrometry and the white sediment residue was reweighed after drying. The difference in sediment weight resulting from treatment with strong acids is reported as "loss on leaching" (LOL). The difference in weight for fresh sediment samples dried at 105°C to constant weight and then heated to 500°C for a number of hours is reported as "loss on ignition" (LIG). Quartz was determined by monitoring the α-β transition in a differential scanning calorimeter, potassium from the gamma ray emission peak for ^{40}K at 1.46 Mev and ^{137}Cs from the gamma ray emission peak at 0.662 Mev.

RESULTS AND DISCUSSION

Heavy metal data and related measurements are reported in Tables 1, 2 and 3 for 56 samples of sediment and one of sewage sludge from a large New York City sewage treatment plant. The data are listed beginning at the upstream end of the sampling locations in the Hudson, with the data in Table 2 from New York harbor and in Table 3 from the sediments of the continental shelf. Samples from the Hudson estuary were generally fine-grained silts relatively uniform in physical properties, while several of those from the shelf were predominantly sand despite our attempts to sample the narrow zone of fine-grained sediment between the mouth of the Hudson Estuary and the Hudson Submarine Canyon.

We chose the analytical scheme outlined above for Hudson sediments after trying a number of procedures. The reported data for Zn, Cu, Pb and Mn are probably good estimates of the total metal concentration in our samples, but the reported values for Fe may be systematically low (15-20%). We have analyzed a number of samples after total dissolution with HF and found the procedure to be somewhat less convenient and reproducible than the strong acid leaching method employed here. Data reported in Table 4 provide some comparison of metal concentrations in a Hudson sample which has been analyzed by three separate procedures. The sample (mp 43) used for the intercomparison of analytical techniques is typical of recent Hudson Estuary sediments upstream of New York harbor. We have also analysed seven replicates of a sample typical

Table 1

Hudson Estuary Sediment Composition

Location (Mile Point)	Depth (cm)	Cs-137[a] (pCi/g)	Zn (µg/g)	Cu (µg/g)	Pb (µg/g)	Mn (mg/g)	Fe (%)	LIG[b] (%)	LOL[c] (%)	K[d] (%)	Quartz[e] (%)	Fine Fraction (% < 63µ)
56	0-5	0.9	190	58	66	1.70	3.3	6.6	19	2.2		
	5-10	0.0	100	26	22	2.40	3.6	7.0	20	2.4		
54	0-5	2.5	315	88	150	0.75	3.7	9.6	25	2.2	25	
	5-10	1.8	320	86	130	0.75	3.8	9.4	25	2.5	24	
	10-15	0.2	305	80	120	0.73	3.7	9.6	24	2.4	25	
	15-20	0.0	225	65	110	0.66	3.5	8.8	23	2.2	24	97
	20-25	0.0	125	31	49	0.57	3.4	7.1	24	2.4	29	98
	25-30		97	24	33	0.57	3.5	7.2	21		30	98
	30-35		90	18	25	0.55	3.5	6.8	21		31	96
	35-40		80	17	20	0.51	2.8	6.9	20		31	96
	40-45		84	18	20	0.51	3.4	6.9	21		29	96
	45-50		80	17	23	0.52	3.3	7.3	20		30	96
	50-55	0.0	82	17	23	0.52	3.5	7.5	21	2.2	32	97
53	0-5	2.7	290	110	175	1.15	2.4	8.4	20	2.2		
	5-10	2.1	295	97	130	1.05	2.9	7.7	18	2.2		
	10-15	0.7	245	83	105	.92	3.0	7.4	18	2.3		
	15-20	0.0	170	55	74	.77	2.7	6.3	16	2.3		
	20-25	0.0	87	18	13	.61	2.2	6.0	14	2.0		
44	0-7	0.6	125	29	45	0.53	2.3	3.5	14	1.9		
	7-14	0.0	96	27	45	0.65	2.3	4.6	15	2.1		
	14-21		65	26	37	0.44	1.8	3.2	10			
43	0-10	2.7	315	107	140	1.39	3.3			2.1		95
25	0-6	1.2	190	99	92	0.45	2.6	4.6	14	2.2		
	6-12	0.8	205	115	92	0.51	2.5	4.9	16	2.3		
	12-16	0.3	220	105	98	0.52	2.8	5.6	16	2.0		
	16-21	0.1	170	89	72	0.48	2.6	4.5	14	2.2		
24	0-3	( )	230	115	175	2.45	3.1	38.5	50			
	633-635		82	23	22	0.52	3.2	6.8	20			
	1175-1177		105	26	24	0.48	4.0	7.5	24			
19	0-10	( )	48	35	55	0.32	0.7	2.6	9	1.7	57	
	22-29		81	16	39	1.15	3.2	7.1	23	2.4	26	
	83-85		83	20	24	0.84	3.6	6.6	24	2.0	24	
	150-153		82	20	28	1.00	3.8	6.0	24	2.4	27	
	240-241		68	14	28	0.96	2.9	4.7	18	2.2	35	
	325-328		77	20	24	0.84	3.5	4.7	23	2.4	27	
	430-438		77	21	27	0.90	3.4	4.9	23	2.3	29	
	545-548		81	15	21	0.83	3.1	4.6	19	2.2	37	90

a) Cs-137 was measured by gamma spectrometry (photo peak at 0.662 MEV). Samples reported as 0.0 were analyzed and found to be free of Cs-137; those indicated with dashed lines ( ) were assumed to be free of Cs-137.

(b) Loss on Ignition (LIG) indicates weight loss upon heating from 105°C to 500°C.

(c) Loss on Leaching (LOL) indicates weight loss of a sample dried at 105°C after treatment with strong acids (HCl, HNO_3, $HClO_4$).

(d) Potassium (K) was measured by gamma counting of the K^{40} peak at 1.46 MEV.

(e) Quartz was measured by monitoring the α-β transition with a differential scanning colorimeter.

TABLE 2

New York Harbor Sediment Composition

Location (Mile Point)	Depth (cm)	Cs-137[a] (pCi/g)	Zn (µg/g)	Cu (µg/g)	Pb (µg/g)	Mn (mg/g)	Fe (%)	LIG[b] (%)	LOL[c] (%)	K[d] (%)	Quartz[e] (%)	Fine Fraction (% <63µ)
2	0-5	1.2	345	225	830	0.31	3.7	9.2	26	2.1		
	20-25	0.0	235	145	165	0.29	3.3	6.5	22	2.1		
	50-55	0.0	245	180	245	0.26	3.2	7.8	23	1.9		
0	0-5	0.7	260	180	140	0.26	3.3	8.5	24	2.1		~ 95
	18-25	1.5	215	200	200	0.30	4.0	9.8	28	2.3		~ 95
	45-53	0.7	225	285	175	0.33	3.3	8.8	24	2.0		~ 95
	60-65	0.0	53	12	<28	0.56	3.6	4.9	23	2.0		~ 95
-2	0-5	0.4	337	248	202	0.55	3.3	7.5	22	1.8		
	12-20	0.6	434	344	271	0.50	3.3	9.4	25	2.1		
	25-30	0.4	459	348	253	0.60	4.2		27	2.2		
	35-40	0.6	399	294	247	0.47	3.6	9.4	23	1.9		
	45-50	0.6	472	338	286	0.53	3.5	10.0		1.9		
	55-60	0.9	557	416	345	0.46	3.7	11.0		1.9		

a) Cs-137 was measured by gamma spectrometry (photo peak at 0.662 MEV). Samples reported as 0.0 were analyzed and found to be free of Cs-137; those indicated with dashed lines (-) were assumed to be free of Cs-137.

b) Loss on Ignition (LIG) indicates weight loss upon heating from 105°C to 500°C.

c) Loss on Leaching (LOL) indicates weight loss of a sample dried at 105°C after treatment with strong acids (HCl, HNO_3, $HClO_4$).

d) Potassium (K) was measured by gamma counting of the K^{40} peak at 1.46 MEV.

e) Quartz was measured by monitoring the α-β transition with a differential scanning calorimeter.

TABLE 3

New York Bight Sediment Composition

Location (Mile Point)	Depth (cm)	Cs-137[a] (pCi/g)	Zn (µg/g)	Cu (µg/g)	Pb (µg/g)	Mn (mg/g)	Fe (%)	LIG[b] (%)	LOL[c] (%)	K[d] (%)	Quartz[e] (%)	Fine Fraction (% < 63µ)
Sewage Sludge		0.1	692	1440	375	0.20	1.1	72.4	84	0.7	1	
-38	0-10	0.2	110	27	67	0.18	2.1	5.0	14	1.5		33
-67	0-10	0.1	38	3	< 20	0.10	1.0	2.5	7	1.5		17
-117	0-10	0.0	17	2	< 20	0.28	0.7	1.3	6	1.3		5
-136	0-10	0.0	79	19	< 20	0.28	2.6	9.3	28	2.3		87
-147	0-10	0.0	90	25	< 20	0.30	2.6	10.2	30	2.3		98
-157	0-10	0.1	69	20	30	0.32	2.6	10.8	33	2.1		93

a) Cs-137 was measured by gamma spectrometry (photo peak at 0.662 MEV). Samples reported as 0.0 were analyzed and found to be free of Cs-137; those indicated with dashed lines (-) were assumed to be free of Cs-137.

b) Loss on Ignition (LIG) indicates weight loss upon heating from 105°C to 500°C.

c) Loss on Leaching (LOL) indicates weight loss of a sample dried at 105°C after treatment with strong acids (HCl, HNO_3, $HClO_4$).

d) Potassium (K) was measured by gamma counting of the K^{40} peak at 1.46 MEV.

e) Quartz was measured by monitoring the α-β transition with a differential scanning calorimeter.

TABLE 4

Comparison of Metal Concentration by Several Analytical Techniques

	Zn (µg/g)	Cu (µg/g)	Pb (µg/g)	Mg (mg/g)	Fe (%)
mp 43[a]	336	111	141	1.42	3.5
mp 43[a]	327	103	145	1.30	3.3
mp 43[a]	302	105	144	1.25	2.8
mp 43[a]	294	107	131	1.57	3.5
Average mp 43	315	107	140	1.39	3.3
2σ	(12%)	(9%)	(14%)	(18%)	(25%)
mp 43[b]	(570)	79	144	1.27	4.0
mp 43[b]	255	108	114	1.09	3.5
mp 43[c]	305	102	-	1.39	4.3

a) Each of these samples was analyzed by the technique used for all of the data reported in Tables 1, 2 and 3. They were analyzed on different days with groups of other samples.

b) These samples were analyzed by a total dissolution technique using HF. Erratic Zn values were common in a number of other samples we analyzed by total dissolution.

c) Reported analytical data for a blind determination of sample composition of a commercial instrument company using emission spectroscopy.

of preindustrial Hudson sediments (mp 19, 525 cm) which has substantially lower concentrations of Zn, Cu and Pb than the mp 43 sample. Statistical variation (2σ) in that data set was: Zn 8%, Cu 13%, Pb 39%, Mn 3% and Fe 6%. The uncertainties of Pb and Cu were higher than for the sample at mp 43 because we were approaching the detection limits by our procedures for those two metals (Pb: average 23 ppm, detection limit $\sim$ 10 ppm; Cu: average 19 ppm, detection limit $\sim$ 4 ppm).

During the past several years we have developed some understanding of the general accumulation patterns of recent sediments in the Hudson through the use of ^{137}Cs (Simpson *et al.*, 1976; Olsen *et al.*, 1977). This tracer has been added to the Hudson estuary from two sources: (1) global fallout from atmospheric nuclear weapons testing over the last two decades with peak deliveries from rainfall during the years 1963-1965; (2) low level releases from a nuclear power reactor at Indian Point (mp 43) over the last decade, with peak discharges in the years 1971-1972. Enough ^{137}Cs is associated with particles in the Hudson to provide a readily measureable tracer of sediment accumulation rates in areas of high deposition, and of transport along the axis of the Hudson downstream of the reactor site, when used in conjunction with two other radionuclides, ^{134}Cs and ^{60}Co which have been supplied to the Hudson almost exclusively by reactor releases. Cesium-137, which has a half life of about 30 years, is an unequivocal indicator of sediment which has been in contact with the water column within the last two decades, and primarily serves here as a "label" for recent (last two decades) sediments. Using this tracer we have found that accumulation rates of fine-grained sediments in the Hudson range over approximately two orders of magnitude, with the dominant deposition zone being New York harbor. We have found cores with ^{137}Cs to nearly 3 meters below the sediment surface, and accumulation rates of 10-20 cm per year typical of large areas of the harbor. Marginal coves in the lower salinity reaches of the estuary (mp 45 - mp 56) have sediment accumulation rates of a few cm per year (Wrenn *et al.*, 1971; Simpson *et al.*, 1976) while most of the total area of the estuary has little net accumulation of recent fine-grained sediments labeled with ^{137}Cs (less than a cm per year).

From Tables 1 and 2 it is clear that sediments containing ^{137}Cs are significantly higher in the metals Zn, Cu and Pb. Two of the reported cores (mp 54 and mp 19) penetrate well into sediments with relatively low and constant concentrations of Zn, Cu and Pb which appear to be typical of pre-industrial sediments in the Hudson. One of the cores (mp 19) contains many subsurface layers of estuarine carbonate shells, four of which we have analyzed for ^{14}C and found apparent ages of 1000-2000 radiocarbon years. Interpretation of radiocarbon data from estuarine carbonates is not unambiguous, but we are confident that the lower half of this core (3-6 meters), which lies below the four radiocarbon dated carbonate layers in the upper 3 meters, is representative of preindustrial fine-grained sediments in the Hudson.

When data from Tables 1 and 2 are plotted in terms of the concentrations of Zn and Cu, (Figure 3) the samples fall into three relatively distinct groups. Approximately one third of the Hudson samples, from seven of the eleven coring sites, contain similar Zn and Cu concentrations below some level in each of the cores. This can be seen most clearly in three cores (mp 56, mp 24 and mp 19) two of which were the longest collected. Similar "baseline" values were found throughout the salinity range in the estuary, and none of the

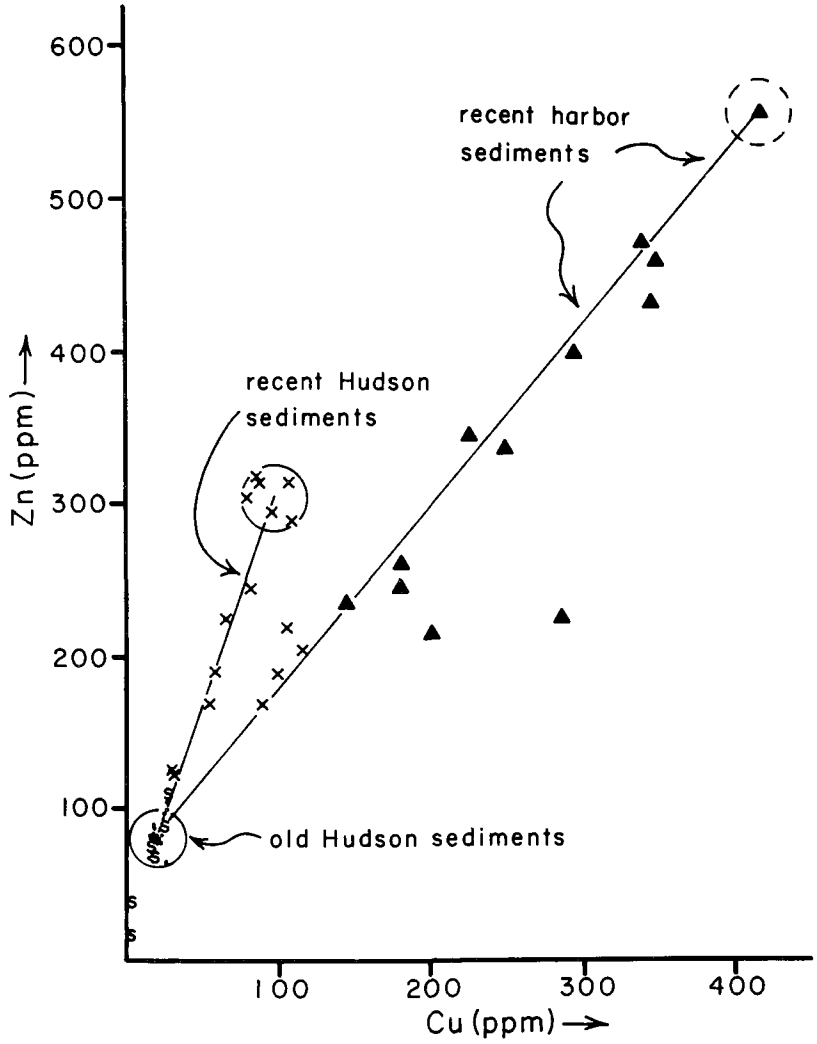

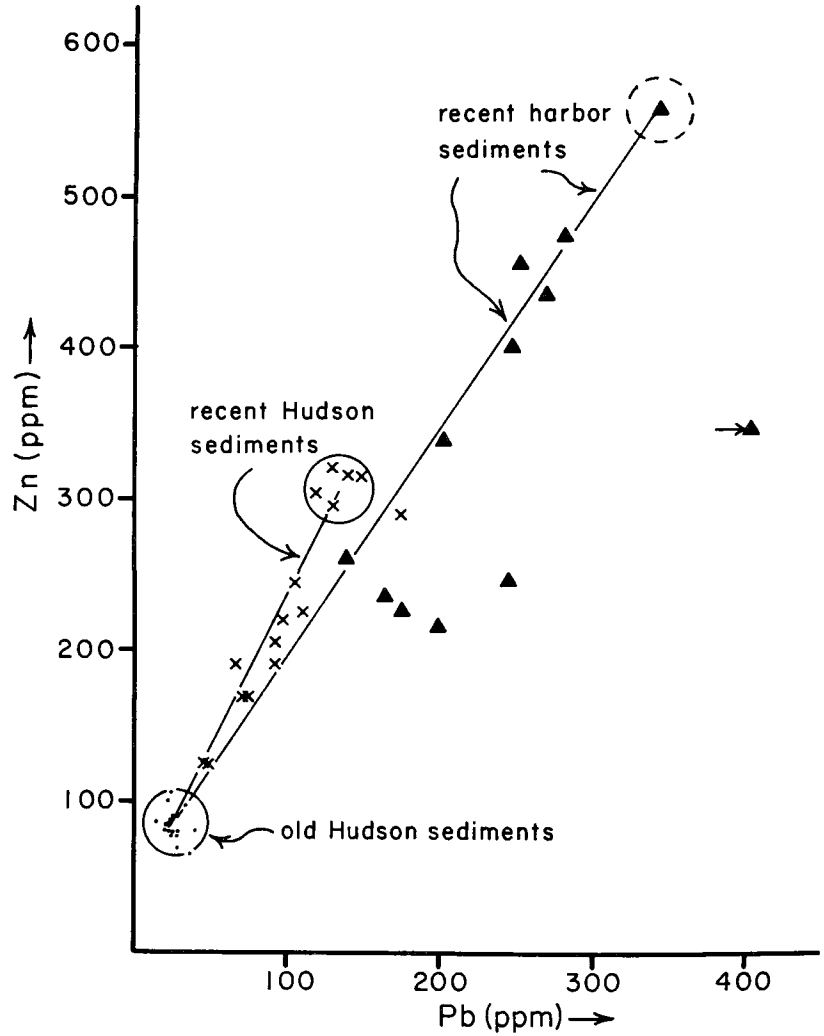

Figure 3. Plot of zinc and copper concentrations in Hudson sediments, with individual samples indicated by one of four symbols. Dots indicate old sediments, free of any cesium-137 or elevated metal levels. Triangles indicate recent harbor sediments (mp 2 to mp -2) containing 137-Cs, and x's indicate recent estuary sediments upstream of the harbor containing 137-Cs. Shelf samples are indicated with S's.

Figure 4. Plot of zinc and lead concentrations in Hudson sediments. The format and conventions are the same as for Figure 3.

estuary samples in the group with Zn concentrations of ∿ 80 ppm and Cu concentrations of ∿ 20 ppm contain ^{137}Cs. We consider these samples to be typical of preindustrial fine-grained sediments throughout the Hudson.

The remainder of the samples (all of which contain ^{137}Cs and thus are recent sediments) can be represented as members of two groups. One group has a number of samples with Zn concentrations of ∿ 300 ppm and Cu concentrations of ∿ 100 ppm, as well as others which fall along a mixing line between these values and preindustrial sediment Zn and Cu values. All of these samples were collected upstream of New York harbor (Table 1) and appear to be representative of the level of heavy metals in recent Hudson sediments upstream of New York City resulting from many diffuse sources of Zn and Cu. One of the upstream sites for which we are reporting data (mp 54) is a small cove which is grossly contaminated with Cd and Ni effluent from a battery factory (Kneip et al., 1974). Bower (1976) has found Zn, Cu and Pb concentrations in this cove to be unrelated to the local metal contamination of Cd and Ni (up to ∿ 0.1% by weight of both metals) and to be typical of other recent estuarine sediments in the Hudson in terms of these three metals. The third group of samples all from New York harbor (Table 2), fall off of the trend line for recent sediments upstream of the harbor (Figure 3) and extend up to considerably higher concentrations of both zinc (∿ 550 ppm) and copper (∿ 400 ppm). Metal contamination added directly to New York harbor sediments appears to be richer in Cu relative to Zn than the diffuse recent contamination of sediments transported down the Hudson toward the harbor. The sewage sludge sample we analyzed had very high Cu (∿ 1400 ppm) relative to Zn (∿ 700 ppm), supporting the suggestion of relatively high Cu proportions in the metal discharge to the harbor (Table 3).

A similar distribution of data from Tables 1 and 2 is produced if Zn is plotted against Pb (Figure 4) rather than Cu, although the relative proportions of contaminant Pb and Zn appear more similar in both recent harbor sediments and those upstream of the harbor than was suggested for Cu and Zn. Approximate concentrations for Zn, Cu and Pb in the three "end member" types of fine grained Hudson sediments indicated on Figures 3 and 4 are listed in Table 5. The recent harbor sediments do not have metal contents which tend to cluster around a small concentration range and thus an end member composition for recent harbor sediments is more artificial than for preindustrial or for recent sediments upstream of the harbor, but a representative high concentration sample is included for comparison purposes.

Heavy metal data have been used to delineate the extent of spreading of wastes such as sewage sludge and dredge spoils dumped in the coastal area about 15 km outside of the mouth of the Hudson Estuary (Gross et al., 1971; Gross, 1972; Carmody et al., 1973). The sensitivity of such tracers is relatively high because the dumped wastes are rich in heavy metals, and because most of the coastal sediments off New York City are sandy and thus have low natural levels of heavy metals. Three of the coastal sediment samples reported here (Table 3) from the vicinity of the shelf break (mp -136, mp -147 and mp -157) have Zn and Cu concentrations similar to preindustrial Hudson sediments (Figure 3). These samples are very fine-grained and are from an area far enough off shore to be reasonably free of much recent metal contamination. The metal data for the other three shelf samples in Table 3 (mp -38, mp -67 and mp -117) are more difficult to interpret. All three samples are relatively

TABLE 5

Trace Metal End Members in Hudson Sediments

		Zinc (ppm)	Copper (ppm)	Lead (ppm)
1.	Old Hudson sediments	80	20	25
2.	Recent Hudson sediments	300	100	135
3.	Recent Harbor sediments	550	400	350
4.	(Recent - Old) Hudson sediments [#2 - #1]	220	80	110
5.	Recent (Harbor - Hudson) sediments [#3 - #2]	250	300	215

low in Zn, Cu and Pb but all three have relatively high proportions of sand (> 63 μ) which would tend to dilute the metal concentrations. Conceptually, it is logical to "correct" metal concentration data in samples with a high percentage of sand to provide a more representative comparison with fine-grained sediments and thus to perhaps obtain an indication of the source of the metals in a particular sample of sandy sediment. The most satisfactory procedure for developing such a correction is not clear, however. A number of possibilities are reasonable to suggest: (1) assume the metals in sediments are primarily bound in organic phases, and multiply the observed concentration of metals in sandy sediments by the ratio of organic content in fine-grained sediments to that of organic matter in the sandy sediments; (2) assume that particles below a certain size (such as 63 μ) are the only ones important in binding heavy metals (de Groot et al., 1976), and multiply metal data from sandy sediments by the ratio of the proportion of sample weight less than 63 μ particles in typical fine-grained sediments to that in the sandy sediments; (3) assume quartz or other metal poor phase is not significant in binding metals and calculate metal concentrations on a "quartz free" basis (Thomas, 1972; Thomas, 1973). There are many other possible approaches, such as normalizing to a constant surface area, but no single procedure appears conceptually superior.

We have tried several normalization procedures for metal data on the three sandy shelf samples mentioned above (Table 6). All of the procedures increase the observed metal concentrations but the amount of increase varied from one approach to another. The "corrected" values based on weight loss on ignition (LIG), weight loss on acid leaching (LOL) and the Fe content of sediments were all reasonably similar, and the "corrected" values are plotted in Figure 5, which is an expanded version of the preindustrial sediment portion of Figure 3. Two of the sandy shelf samples (mp -67 and mp -117) appear to be relatively free of recent metal contamination, whereas the shelf sample (mp -38) closest to the estuary mouth and to the area of dredge spoil and sewage sludge discharge (∿ mp -25) appears to have a significant proportion of recent contamination. The "corrections" suggested are obviously crude and simple minded, but are relatively convenient to apply from observational data on sediment properties, and suggest reasonable conclusions on the basis of the few shelf samples discussed here.

A previous study of the distribution of cation exchange capacity, and organic material in Hudson sediments (McCrone, 1967) indicated that the estuarine silts of the Hudson had relatively uniform properties (when compared with variations found on the adjacent continental shelf) over an extended reach upstream of ∿ mp 22. We have not tried to apply any normalization scheme to metal data from the estuary sediments reported in Tables 1 and 2. Some variations in grain size proportions and organic content do occur within the estuary samples, as indicated by the reported values for LIG and LOL. These variations probably contribute to some of the spread in Zn, Cu and Pb concentrations observed in Figures 3 and 4.

Concentrations of Fe are relatively constant in Hudson sediments, but Mn has considerable variation. Except for the surface sample at mp 24, which is really more of a marsh soil than an estuarine sediment sample, the range of Mn to Fe ratios is 0.008 to 0.067. At locations with significant variation down the core, the highest values of Mn/Fe are usually near the surface. This observation is consistent with upward diffusion of reduced Mn

TABLE 6

Normalization Procedures for Comparing Heavy Metals in Sandy Sediments with Fine-Grained Sediment

Sediment Parameter	Fine-Grained Hudson and/or Shelf Sediment	Shelf Sediments mp -38	mp -67	mp -117
Weight fraction $< 63\ \mu$	$\sim$100%	33%	17%	5%
Normalization Factor	1	3.0	5.5	20
Weight loss on ignition (LIG)	8%	5%	2.5%	1.3%
Normalization Factor	1	1.6	3.2	6.2
Weight loss on acid leaching (LOL)	25%	14%	7%	6%
Normalization Factor	1	1.8	3.6	4.2
Weight fraction iron	3.5%	2.1%	1.0%	0.7%
Normalization Factor	1	1.7	3.5	5.0

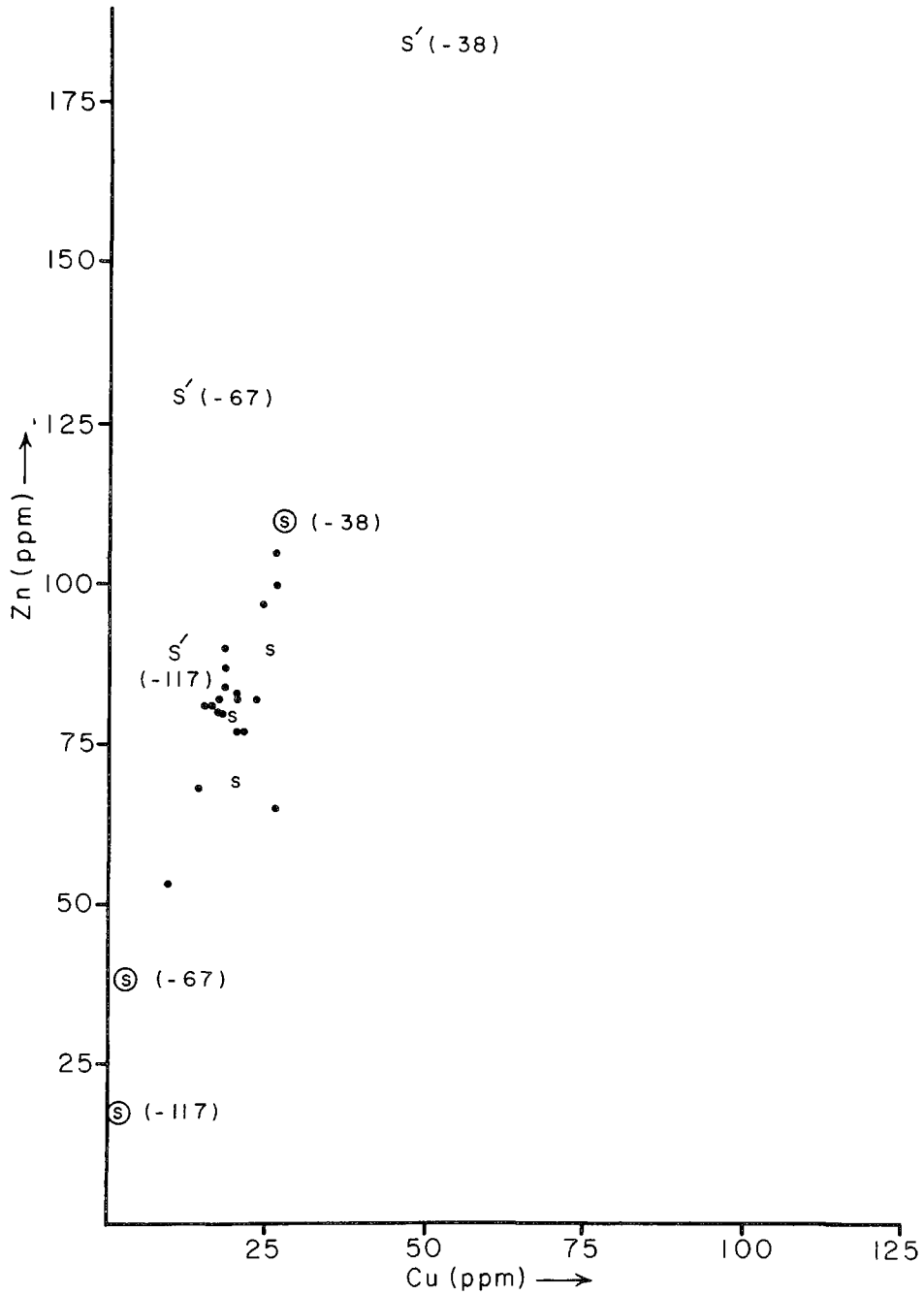

Figure 5. Expanded plot of a portion of Figure 3 to illustrate the effect of transforming observed metal concentrations in sandy shelf (mp -38, mp -67 and mp -117) sediments by the use of normalizing factors for comparison with fine-grained sediments. Normalized shelf sediment metal concentrations are indicated as S's in the figure.

followed by precipitation of oxidized Mn near the sediment-water interface. Although we have no direct evidence that this process actually takes place in Hudson River sediments, the mobility of Mn(II) in reducing sediments is well-known (Lynn and Bonatti, 1965; Li et al., 1969; Bender, 1971; Elderfield, 1976). Manganese is quite reactive in the transition zone between river water and sea water, and a number of studies of Mn in estuaries have been made (Lowman et al., 1966; Windom et al., 1971; Evans and Cutshall, 1973; Graham et al., 1976; Evans et al., 1977). A recent study in Narragansett Bay (Graham et al., 1976) which summarized the behavior of Mn in estuarine environments, suggested that Mn is desorbed from particles as salinity increases, but slowly oxidized to Mn(IV). The time constant suggested for Mn oxidation in Narragansett Bay at salinities of ∿ two-thirds of sea water was on the order of two days, whereas the desorption time constant was much shorter. In the Hudson, lower values of Mn/Fe especially in the upper sediment layers are more common in the harbor and shelf sediments, compared with sites in the Hudson where fresh or low salinity waters are found (mp 40-60). This suggests that desorption of Mn from suspended particles and accumulation of these particles in New York harbor is one of the major processes affecting the behavior of Mn in this estuary. Precipitation of Mn within the Hudson Estuary does not appear to be nearly as important as in Narragansett Bay. If Mn precipitation is primarily the result of slow oxidation of Mn(II), the short residence time of dissolved components in the Hudson during high river discharge (∿ 5 days), and heavy sewage loading from the New York City area (∿ 100 m^3/sec) may explain the lack of evidence for this process within the Hudson Estuary. A similar conclusion has been reached by Klinkhammer (1977) on the basis of an extensive survey including both dissolved and suspended Mn phases in the Hudson.

SUMMARY AND CONCLUSIONS

Concentrations of Zn, Cu and Pb in Hudson sediments indicate those metals can be considered in terms of three general sources of comparable magnitude: (1) preindustrial natural sources of weathering; (2) diffuse recent contamination throughout the estuary; and (3) sewage, industrial effluent and urban runoff, reaching the harbor from the New York City area.

The preindustrial levels of Zn, Cu and Pb in Hudson sediments are comparable to those reported for average shale (Turekian and Wedepohl, 1961) and average continental crust (Taylor, 1964) except for relatively low Cu in the Hudson (Table 7). Our data for Hudson sediments is very similar to background values suggested for Ottawa River sediments (Table 7, Oliver, 1973). A previous study of sediments from an engineering boring at about mp 60, an area which is now usually fresh water (Owens et al., 1974), reported heavy metal data on seven "estuarine" silt samples which averaged as follows: Zn ∿ 80 µg/g, Mn ∿ 1.6 mg/g, Fe ∿ 4.2%. Except for Fe, where our values are ∿ 20% lower, these data are quite consistent with our values from a large number of cores throughout the range of salinity.

The distribution of ^{137}Cs in Hudson sediments corresponds well with that of sediments with recent metal contamination, and provides a good indication of the pattern of pollutant metal accumulation. The depth to which pollutant metals are found in Hudson sediments is usually very similar to the depth distribution of ^{137}Cs.

TABLE 7

Natural Abundances of Heavy Metals

	Zn	Cu	Pb
Hudson Sediments (this study) (preindustrial)	80	20	25
Average Shale (Turekian and Wedepohl, 1961)	95	45	20
Average Continental Crust (Taylor, 1964)	70	55	12
Ottawa River Sediments - Background (Oliver, 1973)	84	28	26

The metal concentration of shelf sediments consisting of appreciable fractions of sand-sized particles can be compared with fine-grained estuarine sediments by normalizing the sandy sediment metal data on the basis of empirical measurements of sediment properties. Similar conclusions about the amount of recent metal contamination in sandy shelf sediments were reached using several normalization parameters including the fraction of weight loss upon heating from 105°C to 500°C, the fraction of weight loss due to leaching with strong oxidizing acids, and the Fe concentration in the sediment.

The amount of Fe in fine-grained Hudson estuary sediments is reasonably constant, but the concentration of Mn varies over approximately an order of magnitude, with greater values near the sediment surface in low salinity and fresh water areas and lesser values deep in cores and in the higher salinity zones such as New York harbor.

The harbor sediments are relatively enriched in Cu, and a first order budget for Cu released to the harbor can be estimated. Assuming a mean concentration of 250 ppm Cu in harbor sediments, and 100 ppm Cu for recent fine-grained sediments delivered to the harbor from upstream, the net increase is 150 ppm Cu. Approximately 4×10^6 tons per year (dry weight) of dredge spoils are discharged in the coastal water off New York City (Gross, 1972). We do not have any direct information on the average metal composition of the dredge spoils which would be significantly influenced by the proportion of the total which was sandy sediment removed from areas such as lower New York Bay. Most of the dredge spoils do appear to be derived from New York harbor in areas of fine particle deposition (Panuzio, 1965). If we assume half (this estimate is probably a reasonable minimum value) of the total mass of dredge spoils consists of recent fine-grained harbor sediment, then $\sim$ 300 tons of Cu per year added to the harbor sediments are being removed from the harbor by dredging. From the data of Klein *et al.* (1974) a total delivery of $\sim$ 2 tons/day of Cu to New York harbor can be estimated. Thus based on an assumption that at least half of the dredge spoils consist of recent harbor sediments, the current removal rate of Cu by dredging appears to be at least half of the loading rate of Cu. For Zn, since $\sim$ 5 tons/day are added (Klein *et al.*, 1975) the fraction ($\sim$ 15-20%) going into the harbor sediments appears considerably smaller than for Cu. A similar suggestion about the relative behavior of Zn and Cu added to New York harbor has been made by Klinkhammer (1977) on the basis of dissolved phase distributions of Zn and Cu in the Hudson.

SECTION 5

HEAVY METALS IN THE SEDIMENTS AND PORE WATERS OF FOUNDRY COVE

INTRODUCTION

Sediments of rivers and estuaries in urban areas frequently have increased heavy metal concentrations due to the discharge of industrial wastes and domestic sewage. Usually metal contamination from many sources is superimposed, producing an increase of a number of "trace" elements over "background" levels which varies in magnitude with the strength of the pollution source and total area of dispersion. In most cases metals such as zinc, copper and lead - derived from a number of distributed sources - are found in sediments of urban waterways at levels of a few times pre-industrial concentrations, up to perhaps an order of magnitude higher. In some situations, metals derived from single sources form a "halo" of very high concentrations, decreasing away from discrete discharge sites. Foundry Cove, a small embayment of the Hudson River (about 60 km north of New York City) is a site where very high concentrations (up to 5% by weight) of cadmium (Cd) and nickel (Ni) in sediments are found as the result of waste discharge from a battery factory (Figure 6).

Foundry Cove has received alkaline discharges of approximately equal amounts of Cd and Ni (Cd/Ni $\sim$ 1.8 by weight) since the construction in the early 1950's of a battery fabrication facility operated for the U.S. Department of Defense in the town of Cold Spring, New York. The cove is located in a relatively pristine reach of the Hudson, with substantial areas of park land nearby, and is remote from other industrial metal discharges of any significance. Foundry Cove has a total surface area of approximately 0.5 km^2 extending eastward from the main channel of the Hudson River. The cove is shallow (1-3 meters at low tide) and divided into two segments by a railroad causeway with a channel of about 25 meters width connecting the two areas. The Hudson River is tidal for more than 200 km upstream of New York City, with semi-diurnal stage changes of 1-2 meters, producing relatively vigorous tidal current flushing of the outer part of Foundry Cove, and also the inner cove through the connecting channel. Foundry Cove and the adjacent main channel of the Hudson contain fresh water during much of the year. Saline water - up to 3-6°/$_{oo}$ - is present most years during low fresh-water flow months, especially during years of lower than average river discharge.

PREVIOUS WORK

Beginning about 1971, several studies were made of the distribution of Cd and Ni in Foundry Cove (Kneip et al., 1974; Buehler and Hirshfield, 1974). Much of this research was related to a court-ordered dredging operation which

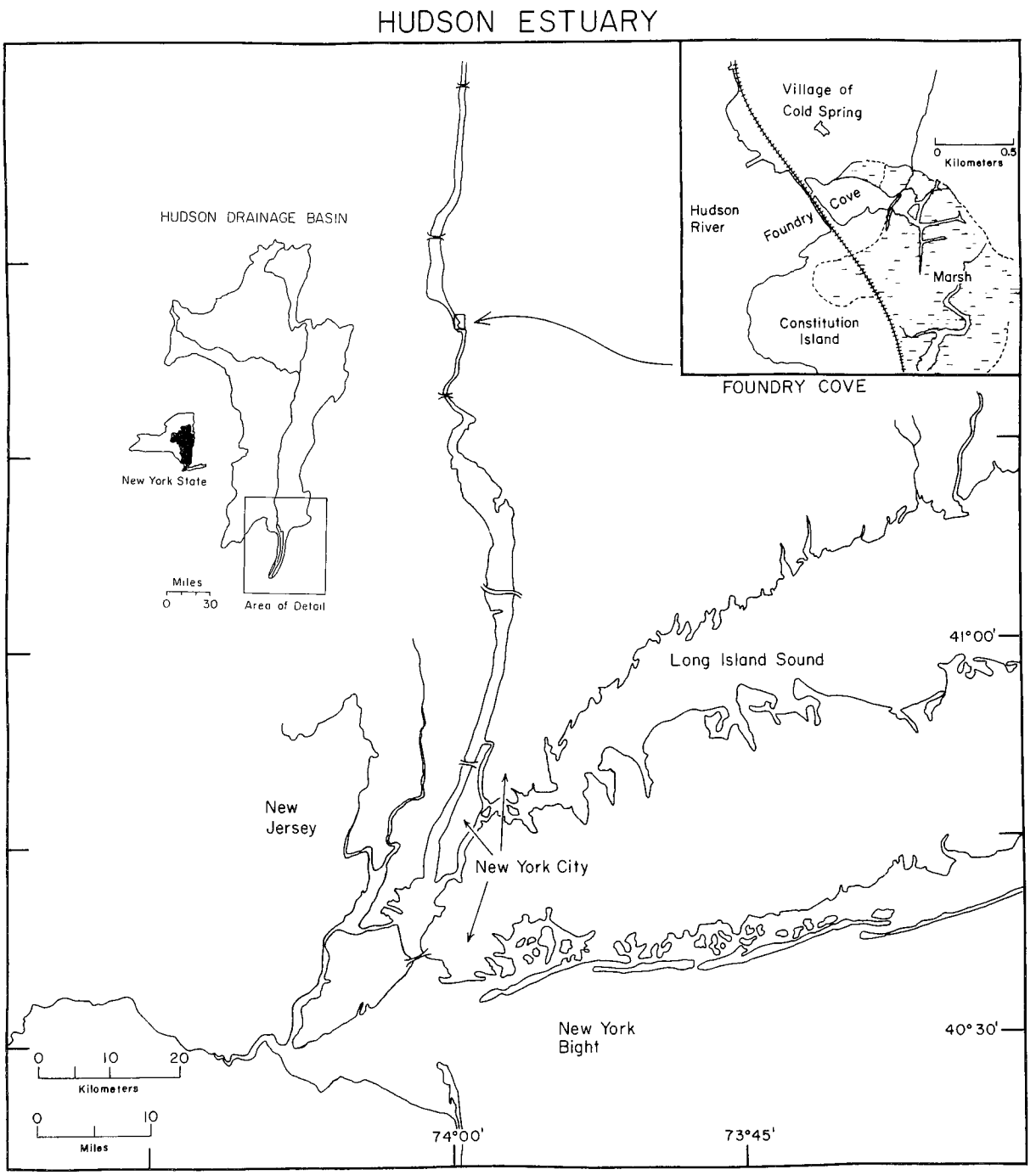

Figure 6. Location map of Foundry Cove in the Hudson River Drainage Basin.

involved the most heavily contaminated zone of sediments (up to 5.0×10^4 ppm for both Cd and Ni) in the eastern end of the inner cove. Most of the published data is from the highly contaminated portion of Foundry Cove on the landward side of the railway. Surveys of sediment Cd and Ni in the inner cove indicate significant differences in the distribution pattern before and after dredging, with the primary change being a shift in location and a broadening of the zone of highest concentration (Kneip, 1975). From reported data we estimate that the total area of the zone of Cd concentrations greater than 10,000 ppm increased from about 5% of the inner cove to about 10%. The quantity of Cd in the inner cove prior to dredging has been estimated to be about 25 tons (Kneip, 1974). The discharge rate of Cd from the inner cove has been estimated to be 0.2-2 tons/year based on water column data over a tidal cycle in the channel connecting the inner cove with the outer cove (Kneip, 1975).

SAMPLE COLLECTION AND ANALYTICAL PROCEDURES FOR SEDIMENT METALS

We collected gravity cores at 15 sites in Foundry Cove, 13 of which were in the outer cove (Figure 7). The cores, which were about 6 cm in diameter and up to 50 cm in length, were sectioned into 5 cm intervals at the field site, transported to the lab and frozen. Following thawing, the samples were dried overnight at 100°C and pulverized with a mortar and pestle. Aliquots of about 2 grams of the total sample weight of 80 grams were leached with 20 ml of conc. HNO_3 and 5 ml of conc. HCl at room temperature for 30 minutes. The samples were heated slowly until most of the organic matter was destroyed, and then reduced in volume on a hot plate to $\sim$ 10 ml. After cooling, 20 ml of 70% $HClO_4$ was added and the sample slowly evaporated to near-dryness. After cooling, 10 ml of conc. HCl and $\sim$ 40 ml of distilled water were added to the white residue of sediment. Then the sediment was filtered, the residue rinsed, and the final filtrate volume brought to 100 ml in a volumetric flask.

Analysis of the resultant acid solutions was performed by flame atomic absorption spectrometry (Perkin-Elmer 303), using mixed-metal standards for Cd, Ni, Zn, Cu, Pb, Co, Mn and Fe. The residual sediment, which consisted of a fine white powder, was dried and weighed and the fraction of weight loss of the original sediment sample is reported as "loss on leaching" (LOL) by strong acids. Separate dry sediment samples were heated overnight to 500°C and the weight loss, which is related to the organic content of the sediments, is reported as "loss on ignition" (LIG).

Small aliquots ($\sim$ 40 mg) of dry sediment were analyzed for quartz content by monitoring the α-β transition in a differential scanning calorimeter a 1 atmosphere and 573°C. After the frozen sediment samples were thawed, dried, and ground to a fine powder, and before subsampling and treatment with strong acids for metal analysis, they were placed in 100 cc aluminum cans and counted on a lithium-drifted germanium (Ge[Li]) gamma ray detector. The spectrum of gamma ray emission from each sample allows the measurement of several naturally occurring radionuclides, including ^{40}K and a number of radioactive daughters of ^{238}U and ^{232}Th. Anthropogenic radionuclides from global fallout (^{137}Cs) and from a nuclear power reactor (^{137}Cs, ^{134}Cs and ^{60}Co) located about 15 km downstream of Foundry Cove were also measured.

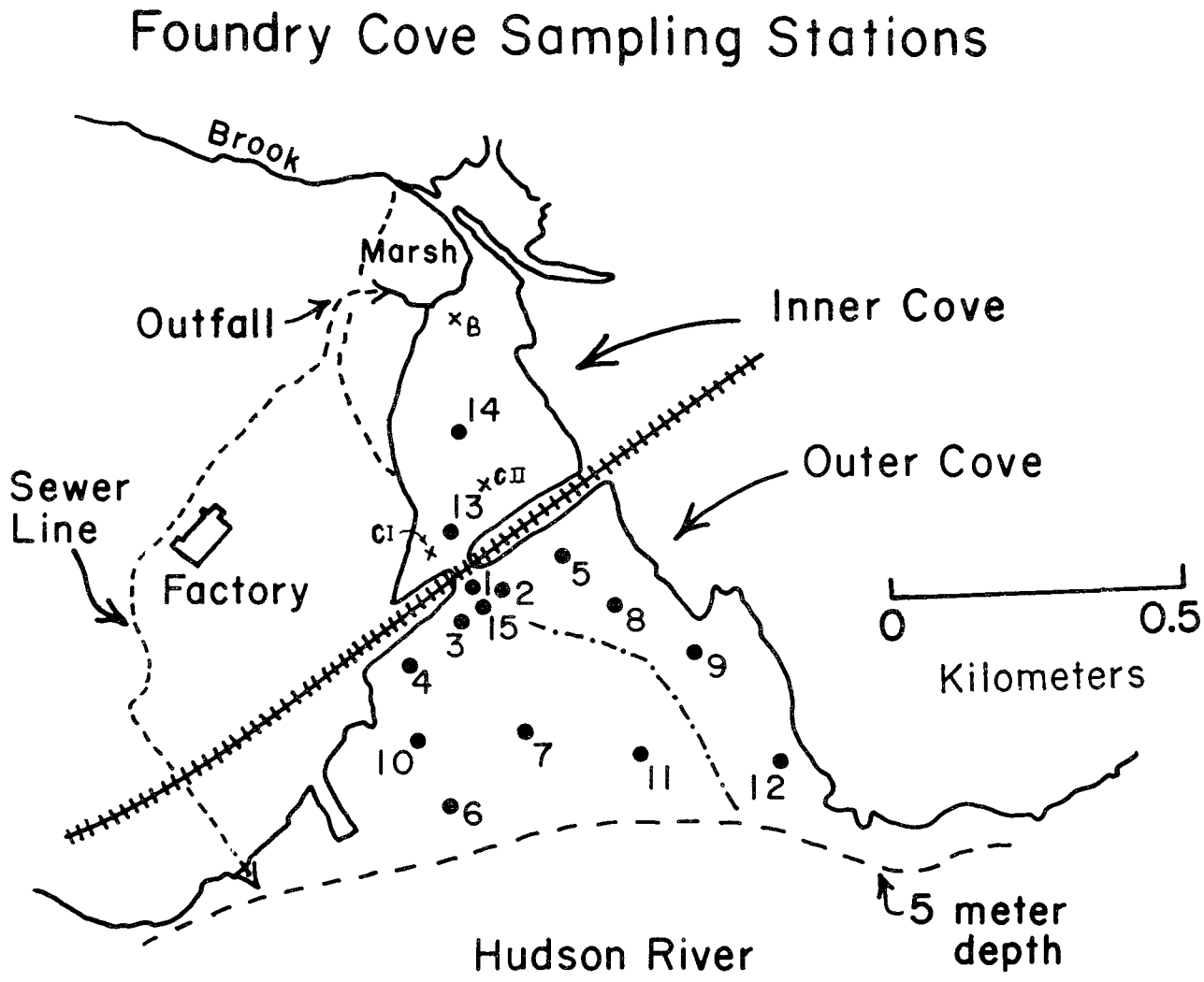

Figure 7. Sampling locations for cores from Foundry Cove with "peeper" sites marked.

Several of the samples have also been analyzed for plutonium isotopes by alpha spectrometry ($^{239,240}Pu$).

ANALYTICAL DATA FOR SEDIMENT METALS

Concentrations of metals in Foundry Cove sediments are reported in Tables 8, 9 and 10, while the radionuclide data are reported in Table 11. Cd contents in samples analyzed here ranged between ∿ 1 ppm, which is the same order of magnitude as average shale (0.3 ppm, Turekian and Wedepohl, 1961) and ∿ 900 ppm. Ni contents ranged between ∿ 30 ppm, which is somewhat less than average shale (68 ppm), and ∿ 300 ppm. In general, Cd and Ni had comparable concentrations with the concentrations of Cd (Figure 8a) and Ni (Figure 8b) in surface sediments (0-5 cm) of the outer cove decreasing away from the connecting channel to the inner cove. Approximate contours of the more highly contaminated inner cove surface sediments are included in Figures 8 and 9 based on data reported elsewhere (Kneip, 1975).

In the outer cove, the sediments contaminated with significant quantities of anthropogenic Cd and Ni are confined to the upper 15 cm in the three cores analyzed up to now (Tables 8, 9; Figure 9). In all three cores concentrations of Cd and Ni as a function of depth in the sediment are similar. In the case of Cd, the surface sediments of the outer cove are more than two orders of magnitude above "background" levels while Ni is about one order of magnitude greater. In the inner cove surface sediments Cd and Ni concentrations up to two orders of magnitude higher than our data in the outer cove have been reported (Kneip, 1975).

The concentrations of Zn, Cu and Pb in Foundry Cove surface sediments (Tables 8, 9, 10) are approximately 3-6 times higher than background levels reached at the bottom of the cores. The depth profiles of these three metals are similar and show elevated levels to depths approximately twice that for Cd and Ni (Tables 8, 9; Figure 10). There is no horizontal gradient in surface sediment concentrations of Zn, Cu and Pb, indicating that the discharges from the battery factory have not significantly increased the levels of these metals in Foundry Cove sediments.

Concentrations of Fe and Mn are also reported in Tables 8, 9 and 10. These metals do not appear to have been significantly increased by localized pollutant discharges. Manganese in the upper 20 cm of the core samples is slightly higher than deeper in the cores. The cause of this increase may be diffusion of Mn from lower in the core, as has been observed in deep sea sediments, or it could be due to other processes such as a generalized recent increase in particulate Mn concentrations, as for Zn, Cu and Pb.

The surface sediments in Foundry Cove contain activities of ^{137}Cs comparable to continental soils (Hardy, 1974). There are measurable amounts of ^{134}Cs and ^{60}Co derived from the reactor located about 15 km downstream, but the dominant source of ^{137}Cs in Foundry Cove sediments is fallout. $^{239,240}Pu$ concentrations in the sediments are also comparable to fallout levels typical of soils.

In general, the distribution of ^{137}Cs in the outer cove sediments is similar to that of Cd and Ni. Several cores have Cd and ^{137}Cs almost down

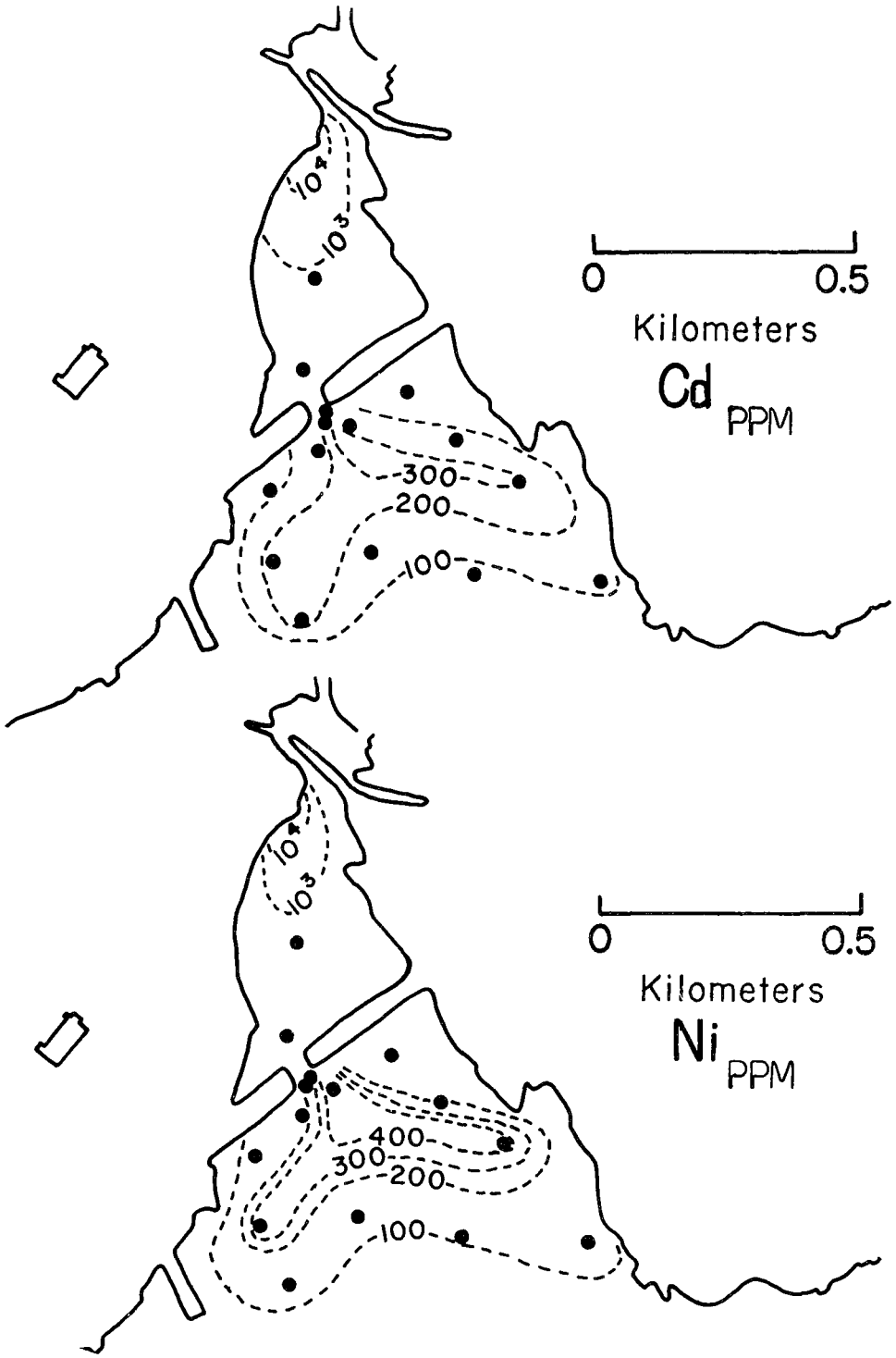

Figure 8a. Contours of cadmium in surface sediments of Foundry Cove. Data for 10^3 and 10^4 contours from Kneip, 1974; Kneip, 1975; and Kneip *et al.*, 1974.

Figure 8b. Contours of nickel in surface sediments of Foundry Cove. Data for 10^3 and 10^4 contours from Kneip, 1974; Kneip, 1975; and Kneip *et al.*, 1974.

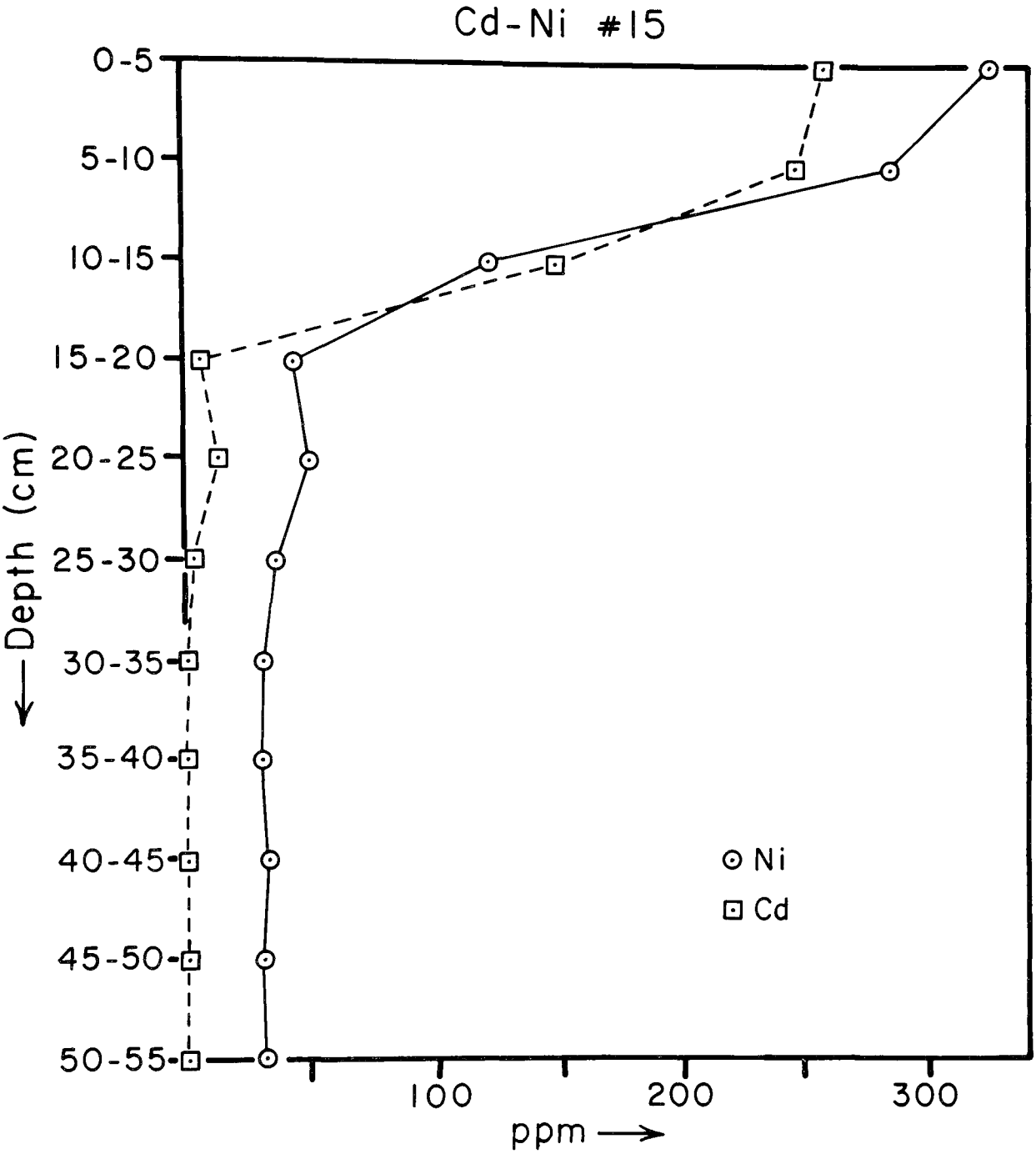

Figure 9. Depth distribution of cadmium and nickel in core #15.

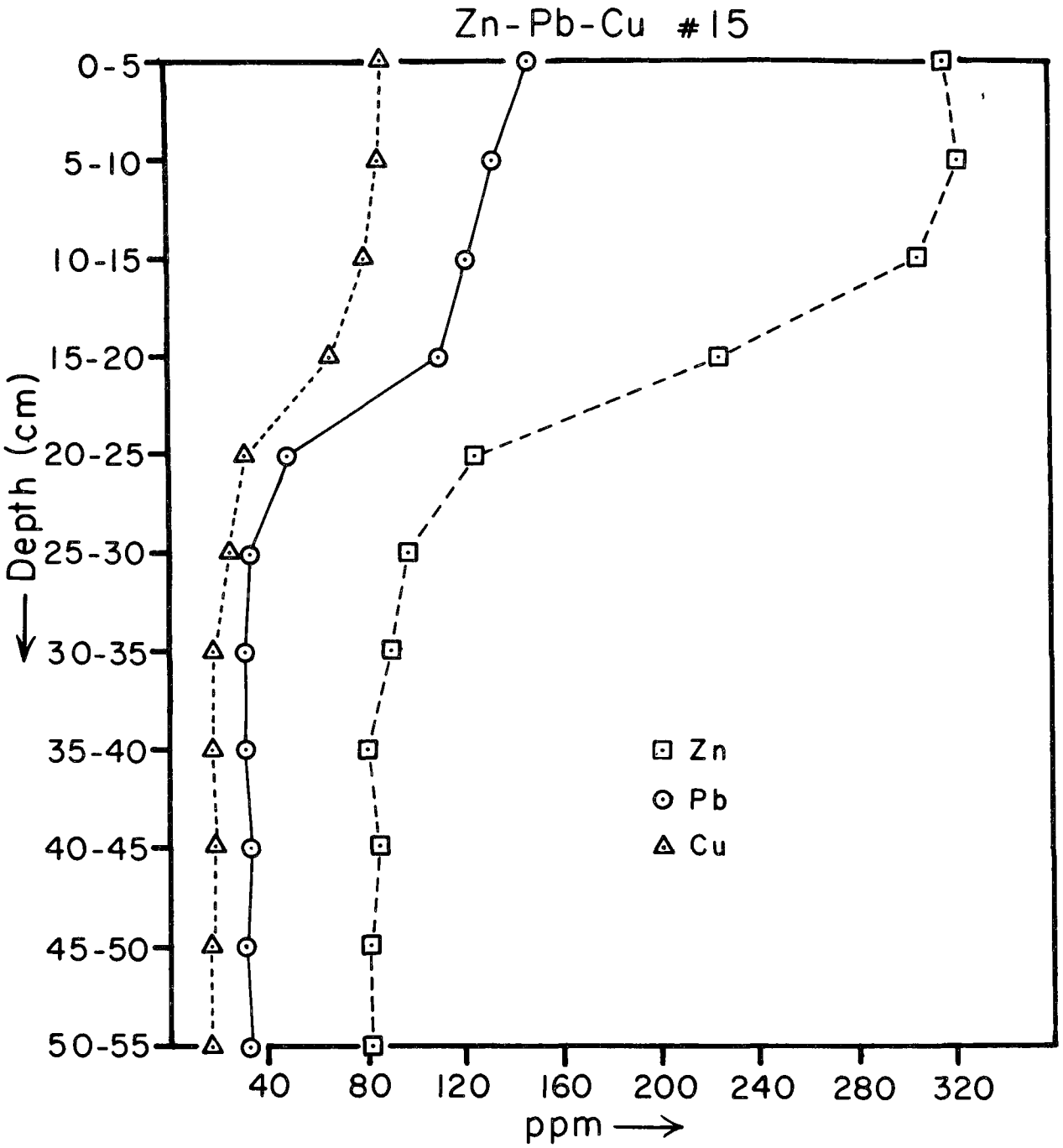

Figure 10. Depth distribution of zinc, lead and copper in core #15.

TABLE 8

Foundry Cove Trace Metals - Core #15

Depth (cm)	Cd (ppm)	Ni (ppm)	Zn (ppm)	Cu (ppm)	Pb (ppm)	Co (ppm)	Mn (ppm)	Fe (%)	Quartz (%)	LIG[a] (%)	LOL[b] (%)
0-5	258	325	316	88	147	23	752	3.7	25	9.6	25
5-10	246	284	321	86	132	24	751	3.8	24	9.4	25
10-15	147	120	305	80	121	20	729	3.7	25	9.6	24
15-20	7	44	224	65	109	21	656	3.5	24	8.8	23
20-25	14	49	124	31	49	20	571	3.4	29	7.1	24
25-30	4	36	97	24	33	20	567	3.5	30	7.2	21
30-35	2	31	90	18	25	16	546	3.5	31	6.8	21
35-40	2	30	80	17	20	16	513	2.8	31	6.9	20
40-45	2	33	84	18	20	16	510	3.4	29	6.9	21
45-50	1	31	80	17	23	15	518	3.3	30	7.3	20
50-55	2	32	82	17	23	15	524	3.5	32	7.5	21

a) LIG - Weight loss on ignition from 105°C to 500°C.

b) LOL - Weight loss on leaching with strong oxidizing acids.

TABLE 9

Foundry Cove Trace Metals - Core #'s 6 and 10

Depth (cm)	Cd (ppm)	Ni (ppm)	Zn (ppm)	Cu (ppm)	Pb (ppm)	Co (ppm)	Mn (ppm)	Fe (%)	LIG[a] (%)	LOL[b] (%)
Core No. 6										
0-5	214	152	358	104	179	25	920	3.9	9.0	28
5-10	261	184	342	100	174	28	1090	4.2	9.1	28
10-15	79	115	314	87	124	22	790	4.1	8.8	27
15-20	4	44	235	67	109	19	590	3.6	8.7	25
20-25	4	42	219	59	97	19	630	3.5	7.9	25
25-30	2	31	119	28	60	15	440	2.9	5.4	19
30-35	2	30	79	15	26	14	420	3.2	4.5	18
Core No. 10										
0-5	249	356	309	85	129	23	740	4.0	8.3	24
5-10	69	119	307	85	133	20	710	3.8	8.3	25
10-15	7	59	274	82	125	20	720	3.7	8.2	24
15-20	4	56	238	70	111	19	610	3.5	8.1	24
20-25	2	42	168	45	87	18	530	3.5	6.8	23
25-30	-	-	-	-	-	-	-	-	-	-
30-35	2	40	106	26	43	17	550	3.5	5.6	26
35-40	2	40	107	26	31	17	560	3.4	-	23

a) LIG - Weight loss on ignition from 105°C to 500°C.

b) LOL - Weight loss on leaching with strong oxidizing acids.

TABLE 10

Foundry Cove Trace Metals - Surface Sediments

Sample	Cd (ppm)	Ni (ppm)	Zn (ppm)	Cu (ppm)	Pb (ppm)	Co (ppm)	Mn (ppm)	Fe (%)	LIG[a] (%)	LOL[b] (%)
1	417	211	320	97	169	29	710	-	9.3	30
2	4	31	76	16	24	14	440	-	5.0	19
3	170	179	323	86	134	22	750	-	11.5	29
4	89	122	369	99	165	21	770	-	8.6	25
5	118	139	388	84	119	22	710	-	8.5	28
6	214	152	358	104	179	25	920	3.8	-	28
7	115	108	247	95	132	22	780	-	8.5	28
8	214	200	323	88	125	20	940	-	7.9	26
9	301	429	324	83	130	23	830	-	7.1	25
10	249	356	309	85	129	23	740	4.0	-	24
11	51	105	328	83	118	22	920	-	14.9	26
12	153	137	379	100	173	25	1040	-	8.9	27
13	5	28	82	14	25	13	320	-	5.0	16
14	908	325	362	94	158	33	690	-	7.8	33
15	258	325	316	88	147	23	750	3.7	9.6	25

a) LIG - Weight loss on ignition from 105°C to 500°C.

b) LOL - Weight loss on leaching with strong oxidizing acids.

TABLE 11

Foundry Cove Radionuclide Data

Core No.	Depth (cm)	^{137}Cs (pCi/kg)	^{134}Cs (pCi/kg)	^{60}Co (pCi/kg)
1	0-5	2135 ± 96	8 ± 24	103 ± 43
2	0-5	71 ± 44	1 ± 30	8 ± 49
3	0-5	1840 ± 115	17 ± 32	69 ± 64
5	0-5	2220 ± 135	2 ± 32	32 ± 60
6	0-5	2785 ± 135	118 ± 43	257 ± 84
7	0-5	670 ± 83	83 ± 39	66 ± 70
8	0-5	1610 ± 105	37 ± 32	11 ± 55
9	0-5	1725 ± 66	10 ± 17	34 ± 37
10	0-5	2250 ± 81	14 ± 10	42 ± 17
10	0-5	2320 ± 55	-	-
11	0-5	1485 ± 54	34 ± 14	66 ± 29
12	0-5	2135 ± 135	43 ± 36	148 ± 72
13	0-5	42 ± 35	15 ± 23	72 ± 41
14	0-5	1835 ± 69	21 ± 21	96 ± 47
15	0-5	2475 ± 63	98 ± 26	69 ± 27
15	5-10	1825 ± 68	17 ± 32	19 ± 29
15	10-15	210 ± 17	- 8 ± 10	15 ± 17
15	15-20	26 ± 17	-15 ± 11	30 ± 25
15	20-25	35 ± 23	0 ± 12	7 ± 27
15	50-55	9 ± 14	7 ± 9	13 ± 20

		$^{239,240}Pu$ (pCi/kg)
15	0-5	76 ± 7
15	5-10	57 ± 5
15	10-15	6 ± 1

to background levels at the surface, apparently due either to dredging or tidal current scouring of the recent sediments. Cd and ^{137}Cs also have similar distributions with depth in the sediments (Figures 9 and 11).

DISCUSSION OF SEDIMENT METAL DATA

The data reported here indicate that significant quantities of Cd and Ni from the battery factory discharge are present in the outer portion of Foundry Cove. Estimates of the sediment burden in the outer cove (Bower, 1976) based on the analytical data reported here are about 2-3 tons of Cd and about the same amount for Ni. These quantities are 5-10% of the total burden of Cd and Ni in Foundry Cove sediments (25-50 tons) estimated (Bower, 1976) from data on the inner cove sediments reported elsewhere (Kneip, 1975).

The distribution of Cd and Ni in Foundry Cove sediments are quite similar, indicating comparable transport pathways for these two metals. The most reasonable explanation is that particulate phase transport has been dominant in establishing the present distribution of both metals in the sediments of the outer cove.

The depth distribution of Cd and ^{137}Cs in the outer cove sediments are very similar. There are no major differences in grain size, mineralogy, or organic content in the Foundry Cove sediments sampled here as indicated by the data for quartz, weight loss on ignition, and weight loss by leaching with strong acids. Particulates less than 62 microns accounted for between 85% and 99% of the total mass of each sample, with the median value about 96%. The similarity in depth distribution of ^{137}Cs and Cd is somewhat surprising since the sources of these metals are obviously quite different. However, both are recent (last few decades), and could be expected to bind strongly to fine-grained, organic-rich sediments.

There is some indication of slight differential movement of Cd and Ni in Foundry Cove, if data from the outer cove from this study are considered together with those for the inner cove from other sources (Kneip *et al.*, 1974; Kneip, 1975). Cd appears to be slightly less mobile than Ni, as indicated by a possible decrease in Cd/Ni ratios away from the discharge site. This trend is only barely suggested by the data, and is clearly of minor importance in the overall transport of Cd and Ni in Foundry Cove.

The levels of Cd and Ni in Foundry Cove sediments appear to be definitely a potential local health hazard, especially if indigenous organisms such as crabs are consumed in any significant quantities by sport fisherman. As has been pointed out elsewhere (Kneip *et al.*, 1974, Kneip, 1975) the court-required dredging in 1972-1973 did not eliminate Cd and Ni contaminated sediments from the cove, and could possibly have enhanced the spread of these metals within the system by mobilizing heavily-contaminated fine-grained particles during dredging. We do not suggest, however, that renewed dredging would be the best policy for Foundry Cove. Until a better solution is found, the most prudent course to follow would appear to be to discourage human consumption of organisms such as crabs from the cove.

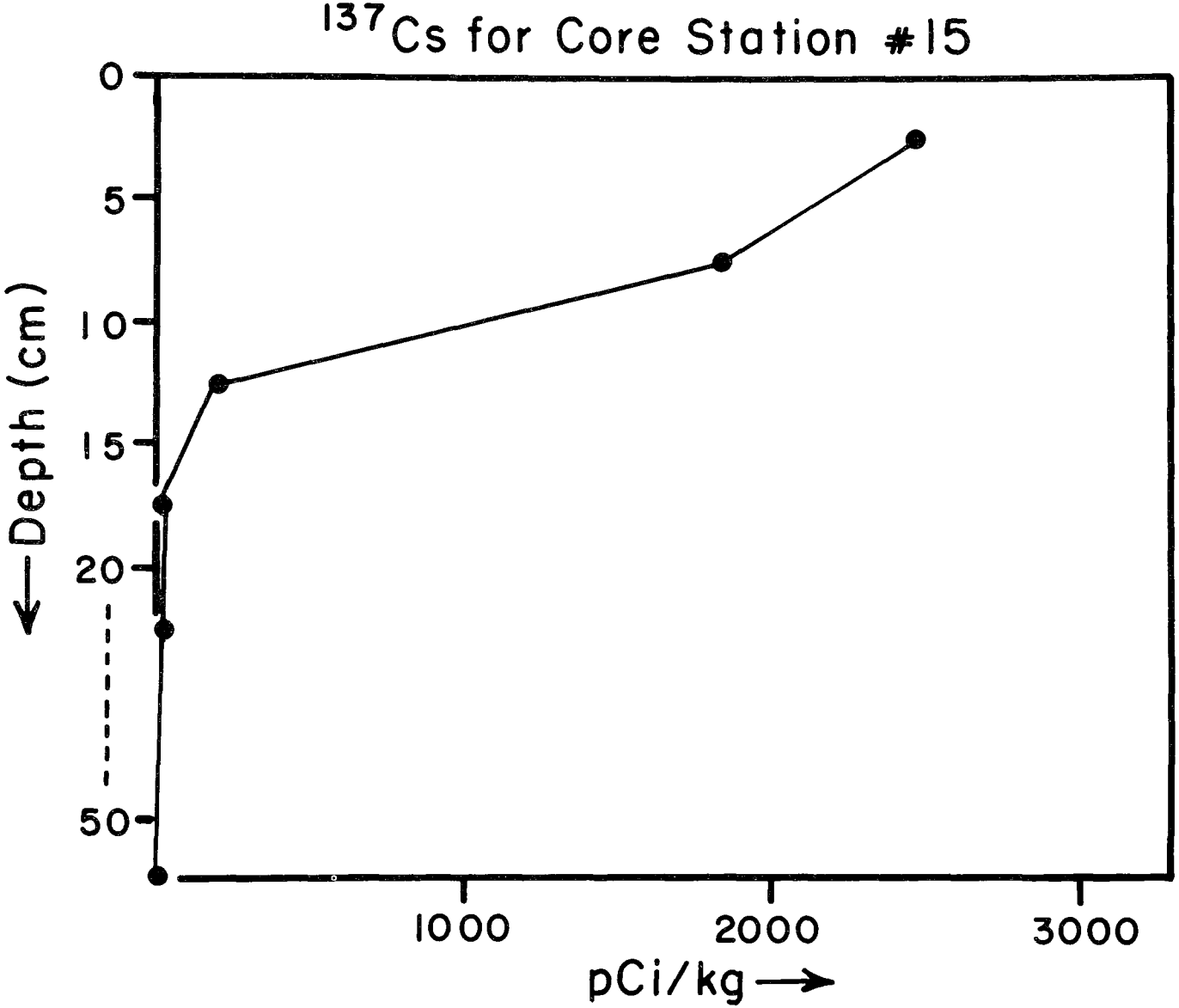

Figure 11. Depth distribution of ^{137}Cs in Foundry Cove, core #15.

PORE WATER SAMPLING - IN SITU METHODS

We have devoted considerable effort in the last year to the development of a relatively new tool for sampling sediment interstitial water (pore waters). This tool, called a pore water "peeper" is based on equilibrating water-filled chambers with pore waters through a permeable membrane which prevents the passage of sediment particles. The peeper was conceived by Ray Hesslein, a former graduate student at Lamont-Doherty, and tested at LDGO and at the Experimental Lakes Area, in Ontario, Canada. The peepers used in our studies were designed with 4.5 cm^3 chambers (5.5 cm x .9 cm x 1 cm) milled at 1 cm intervals. For all but one of the peeper profiles run in 1976, Spectropore™ 2 dialysis membrane (cellulose base) was used. This material has an effective molecular weight cutoff of 12000 to 14000 MWU and a wall thickness of 25 microns. This is similar to the type prescribed by Hesslein (1976) for which he determined a half time for equilibration of a peeper cell with a well-mixed outer reservoir of about 120 minutes. On the basis of measurements made in lake sediments (porosity of > 90%) and through numerical modeling he predicted 92 to 96% equilibration after 7 days. In the sediments of the lower Hudson River (mile point 18), the dialysis membrane was partly destroyed in one week, apparently by bacterial activity, while farther upstream (mp 54), minimal damage occurred to the membrane over a two week period. An attempt was made with one of the peeper samplers to use Nuclepore™ polycarbonate membrane of 0.2 micron pore size as a substitute for the dialysis membrane. The half time for 0.2 micron Nuclepore with a well-mixed outer reservoir is similar (80 min.) to that of the dialysis material. In other experiments in which the inner cell as well as the outer reservoir were continuously mixed, equilibration half times were only 20 to 30 minutes for either material, indicating that diffusion through the membrane is a minor factor in the overall rate of equilibration. Lab experiments measuring the flux of chloride and metal radioisotopes were made by Dennis Adler, a graduate student at Lamont-Doherty, who attempted to fit the results to a numerical model describing the diffusion and transport within both the sediments and pore water sampler. These experiments indicated that after one week 70-80% equilibration should be attained if the diffusion occurs only perpendicular to the sampler (one dimensional diffusion from a planar source). If these results are extrapolated to the actual diffusion geometry of the sampler in the sediment, which is closer to radial symmetry, the degree of equilibration is predicted to be 85-90%.

In preparing the peeper for implacement, the plexiglass shell and cover plate were soaked in dilute nitric acid overnight. Open cell polyurethane foam which was used as a gasket to seal the membrane tightly was washed in hot water and dried. The peeper cells were filled with distilled water and the dialysis membrane placed on top so as to exclude air bubbles (for one of the peepers [C III] the reloading was done in the field and only a distilled water rinse was possible, also no attempt was made to exclude oxygen dissolved in the cells; as later shown, the data does not differ significantly from the other profiles and it is reasonable to assume that oxygen introduced into the pore water from the peeper cells is rapidly consumed by organic oxidation and that the effect on the chemistry of the surrounding pore water is small and short lived). The foam gasket and cover plate were placed on top and the entire assembly held together and compressed with nylon screws. The peeper

was next transferred to an enclosure and purged with nitrogen. This was repeated at later times to remove air that had diffused out of the cells and any that might leak into the container. The length of time the peeper remained in the container varied but was greater than 2 hours and should have allowed for more than 50% oxygen removal from the cells. The peepers were transported to Foundry Cove in their containers and were removed just before emplacement in the sediments. When inserting the peepers into the sediments, care was taken to insure that at least two cells remained above the sediment-water interface. The length of time the peepers remained in the sediment was originally chosen as two weeks to allow the cells to approach reasonably close to equilibrium with the pore waters, but deterioration of the membrane, presumably due to microbiological activity, required a decrease to one week equilibration time.

The peeper was removed from the sediments at the end of the equilibration period by pulling on a rope attached to a surface float. Most of the adhered mud was washed off in the surface water and the peeper transferred in a horizontal position to the boat. The upper cover plate was covered with plastic kitchen wrap to decrease evaporation and gas exchange and the peeper was brought to shore. (The last peeper [C VI] was wrapped in the plastic and then replaced in the air tight enclosure and purged with nitrogen followed by a 1.5 hour trip back to the lab where it was sampled.) After removing the cover plate and foam material, the membrane was washed clean of particles with a light stream of distilled water and a fine brush. Samples for each of the tests were then transferred to test tubes or serum bottles by syringe (gas samples) or plastic tiped micropipettes. The dissolved gases CH_4 and CO_2 were sampled first followed by sulfide, iron, phosphate, ammonia, metals, silicate, specific conductance, chloride, and pH. The volume of water in each cell was limited to 4.5 ml so that each test could only be performed approximately every 3 cells. With the help of several persons, the entire 80 cell peeper could be sampled in under an hour. The analytical techniques used followed closely standard wet chemical seawater or freshwater procedures with reduction in size of all samples and reagents so the final test volume was between 4 and 7 ml. The references and procedure modifications are given below:

Specific Conductance

Two types of determinations were made using this parameter. A special micro cell consisting of two platinum electrodes in a .5 ml volume teflon sample holder was made. This cell was standardized with .01 N KCl solution and against a 1.0 constant cell in the field and determinations made on samples of the peeper pore water. Temperature correction was based on the measured air temperature. Relative conductivity measurements were made in the sediments directly by a long PVC rod which had two platimum electrodes mounted on the side near the end. The open water cell constant was determined before and after each run by comparison to overlying water conductance measured with a standard cell. Temperature correction was obtained by measuring the temperature profile in the sediment at the same time with a thermistor mounted between the electrodes. In both the determinations, a Leed and Northrup #4959 conductance bridge at 1000 cps was used.

Temperature

In situ measurements of the sediment temperature were made using a Fenwald

glass bead thermistor mounted between the conductivity electrodes on the sediment probe. The resistance was measured with an AC Wheatstone conductivity bridge and the temperature determined by substitution into a cubic equation relating temperature and resistance over the range 5°-30°C using a high accuracy 0.1°C thermometer.

pH

pH measurements were made in the field with a Beckman model G pH meter using microreference and glass electrodes. Standard pH 7 buffer was used as a reference. One ml of sample plus wash was required.

Chloride

Chloride was determined by electrochemical titration with silver using an American Instrument Co. Chloride Titrator; .5 ml of sample and 1.5 ml dilution water were titrated with 2 ml conditioning reagent. Standards were prepared from sodium chloride.

Silicate

The silicate test approximates that of Strickland and Parsons (1968) for seawater scaled down by a factor of 10. Distilled water blanks were carried into the field and standards of sodium silicofluoride in distilled water were used. The ammonium molybdate reagent could not be added before the sample so it was added rapidly to the plastic test tube containing the .2 ml sample and 2.3 mls of dilution water at the start of the sample preparation procedure.

Phosphate

The phosphate test is identical to that of Strickland and Parsons (1968) for seawater with a 1:10 reduction in sample and reagent volume. Acid rinsed test tubes were used.

Iron

Iron was determined using a wet chemical method for "reactive" iron following Stookey (1970). Total iron was determined after reduction for 15 min. in aqueous hydroxylamine at boiling water temperatures. Boyle and Edmond (1977) have found that the procedure approximates total dissolved iron as determined by direct injection graphite tube atomic absorption spectrophotometry.

Manganese and Cadmium

For both Mn and Cd determinations direct injection graphite tube atomic absorption spectrophotometry was employed. One ml samples were taken in the field from the peeper cells using plastic tipped Finn pipettes and placed in acid washed (8N HCl) glass test tubes. Samples for Mn had .02 ml 5N HCl added while those to be analyzed for Cd had .02 ml 5N HNO_3 added. Reagents used were chosen for low blanks. Standards were diluted from Fisher 1000 ppm solutions.

Methane and Carbon Dioxide

A 2 ml sample was injected into a helium-purged 10 ml serum bottle which previously had 0.05 ml concentrated H_2SO_4 added. Gas samples of 1 ml were withdrawn and analyzed by gas chromatography using Porapack Q and 5A columns with thermal conductivity (for CO_2) and flame ionization (for CH_4) detectors.

Sulfide

The sulfide test was a modification of the Methylene Blue comparison test for total dissolved sulfide given in Standard Methods (13th Ed., 1971) section 228B. The sample size was reduced to 2 ml which was added to tubes containing 1.5 ml distilled water and 0.05 ml zinc acetate solution in the field: 0.25 ml of the ammine solution 1 was used with 0.05 ml of ferric chloride and 0.8 ml of ammonium phosphate. The color produced was measured with one cm cells at 660 nm against distilled water blanks and standards made from sodium sulfide in nitrogen purged water.

Ammonia

The ammonia procedure follows that of Solozono (1969) run at a scale reduction of 1:10. The samples were either processed immediately after returning from the field or "fixed" by the addition of the phenol reagent. Special cleaning and care was used to reduce the blank and avoid contamination. All ammonia determinations were run by Dennis Adler.

DISCUSSION OF INTERSTITIAL PORE WATER RESULTS

The development of the pore water peeper as a tool provides a new approach to obtaining samples of sediment pore waters over closely spaced intervals. As with any new technique, however, great care must be taken to insure that the resultant data is valid. We have tried lab tracer experiments and model calculations to determine the rate of equilibration of the sampling chambers with interstitial waters. We have also attempted to compare the results of a peeper profile in Narragansett Bay to those of a core taken and centrifuged by Mike Bender's group at the University of Rhode Island. Apparently, lateral homogeneities over a small horizontal distance ($\sim$ 1.3 meters) of the Narragansett Bay sediments contributed substantially to disagreement between two peepers 1 meter apart and a box core taken between them. The best information that we currently have on the operating characteristics of our sampler comes from careful examination of field data from Foundry Cove and by comparison to data from other areas collected by different methods.

In the summer of 1976 nine separate peepers were placed in Foundry Cove at three separate sites (B, C I and C II) as shown in Figure 7. Table 12 gives the times of emplacement and removal for each peeper and information on procedures used for each run. Site B was located about 20 m from the mouth of the channel through which the battery wastes had entered the cove. This site was next to the dredged area and is thought to represent originally deposited material containing about 2000-5000 ppm Cd. Two peeper profiles were made here about 20' apart (B I and B II). Special procedures were used with B II to determine soluble pore water metal concentrations in the highly

TABLE 12

Foundry Cove (mp 54) Site	Peeper Designation	Dates	Duration (days)
B	B I	052076	14
	B II	062476	14
C I	C I	052076	14
C II	C II	061076	14
	C III	062476	14
	C IV(a,b)	071576	7
	C V	072276	6 (Nuclepore)
	C VI	080576	6.5
Hudson River (mp 18)	ALP A	08 74	7
	ALP I	062775	14
	ALP II	072876	7 (Nuclepore)

contaminated sediments. C I is the only peeper profile made at site C I. Later profiles were made at site C II due to currents near the mouth of the causeway and sediment type (river-derived mud). The majority of peeper profiles were made at site C II, which represents a 200 square meter area on the western side of the large shallow area which makes up the central portion of the cove. Peepers C II - C VI were positioned at this site. Cd and Ni concentrations in the surface sediments are between 100 and 400 ppm.

One important piece of information that must be determined before the pore water data is closely examined is the degree of horizontal homogeneity in the Foundry Cove sediments. At site C II, in situ conductivity measurements were made for each peeper profile using a plastic probe with platinum electrodes. Results of the sediment conductivity probe are shown in Figure 12a. The solid line represents an approximate fit of the data, while the dotted line marks the upper 15 cm of peeper C V's curve showing salt intrusion from the overlying water. The similarity of the curves from different locations is clear. The data points below 25 cm show only at $\pm$ 10% spread while those above show a somewhat greater range, which is not unexpected since the sediment above 25 cm contains local vertical irregularities related to biological and physical processes at the surface. A closer examination of individual peeper curves shows that the $\pm$ 10% zone is not the result of random noise in each profile. The major ions supporting the specific conductance are HCO_3^-, Cl^- (from measurements) and Na, K and Ca (ratio unknown) to maintain charge balance. Since the concentration of these major ions swamps the minor ion effects the latteral distribution of the major ions can be assumed to be fairly uniform within sediments of the same type in the cove if the conductivities at each site are the same.

Figure 12b shows the peeper pore water conductivity data as collected. The construction of the micro-conductivity cell and operator error caused large calibration shifts during several of the peeper runs. Only two of the profiles may be accurate as plotted although several others can be made to approach these if assumptions on the nature of the error are made. The erroneous profiles are included to show the relatively small scatter of points within a single profile indicating that dilution of individual peeper samples did not occur during removal or the washing of the membrane.

The temperature profiles determined by the sediment probe are shown in Figure 13. Differences in the profiles reflect unequal heat inputs possibly caused by differences in the amount of sediment exposure during tidal cycles. The slopes of the profiles are nearly constant at approximately 7.5^{o}C per meter.

Figure 14 shows the pH values determined on the peeper pore waters. All of the profiles show the same general shape as approximated by the solid line; initial values at the overlying water value of 7.3 decreasing to 6.6 at 10 cm, and remaining constant at 6.6 to 6.5 cm where a slight increase occurs. The only profile not following this trend is C VI which was not sampled until 1.5 hours after removal. The pH shift of about 0.25 units could be explained by about 20% loss of the $\Sigma\ CO_2$.

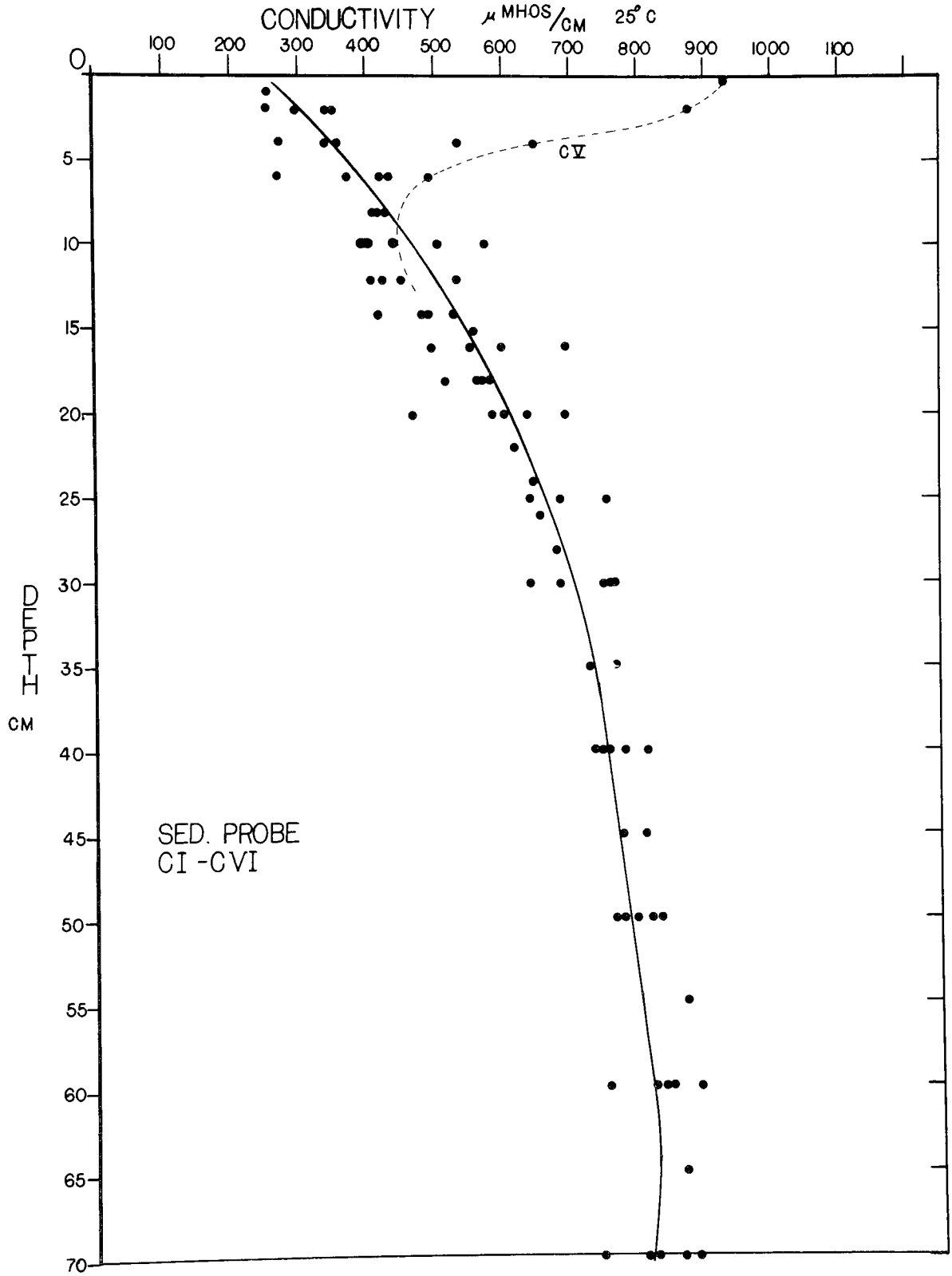

Figure 12a. In situ specific conductance in $\mu MHO^{s}/cm^{3}$ of Foundry Cove sediments with depth. Measured with platinum electrodes and standardized against aqueous solutions. The solid line is an approximate fit of the data.

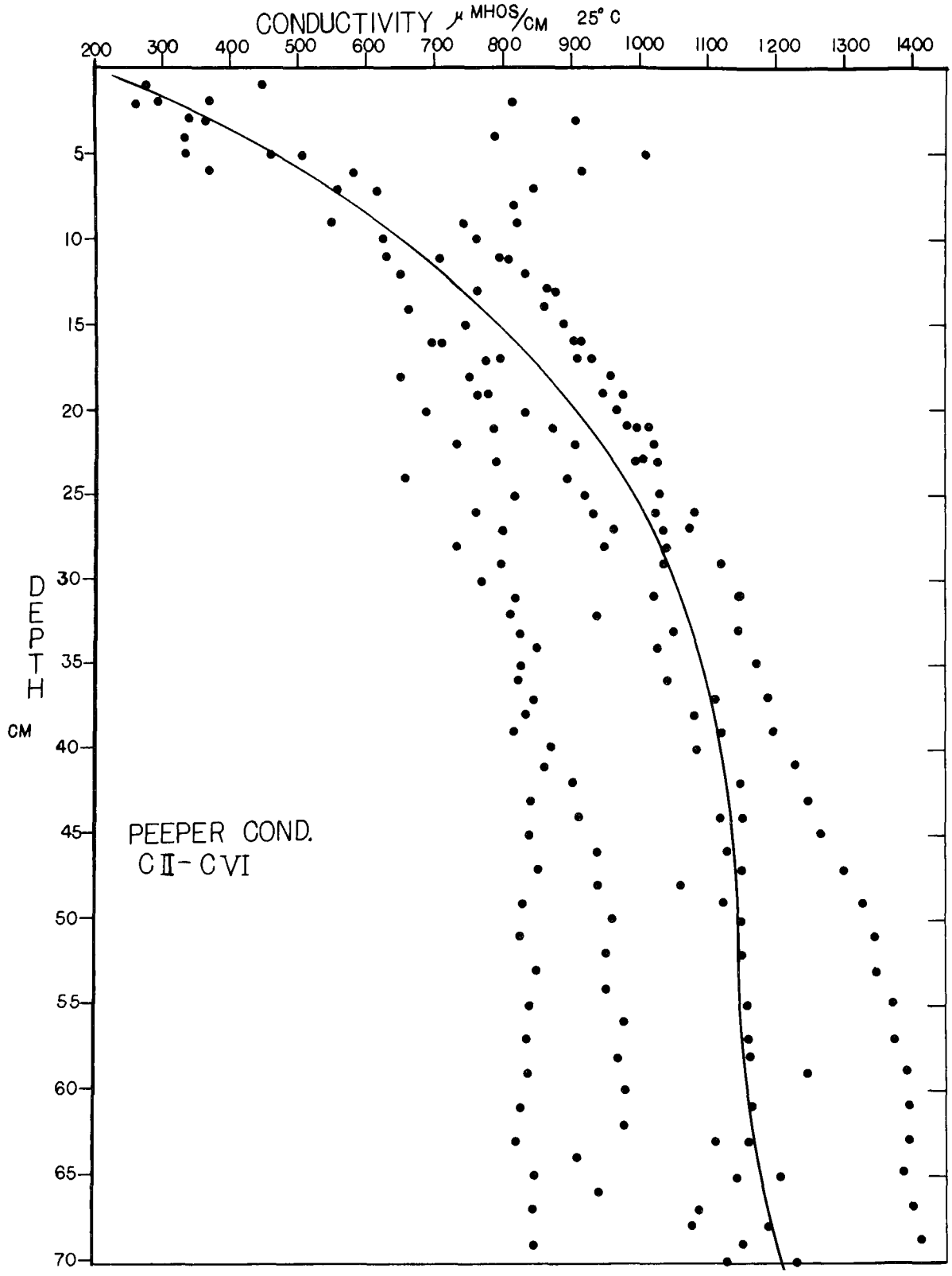

Figure 12b. Specific conductance in $\mu MHO^{S}/cm^{3}$ of "peeper" pore water samples vs. depth in sediment. Measured with platinum electrodes in micro-conductivity cell and standardized against .01 N KCl.

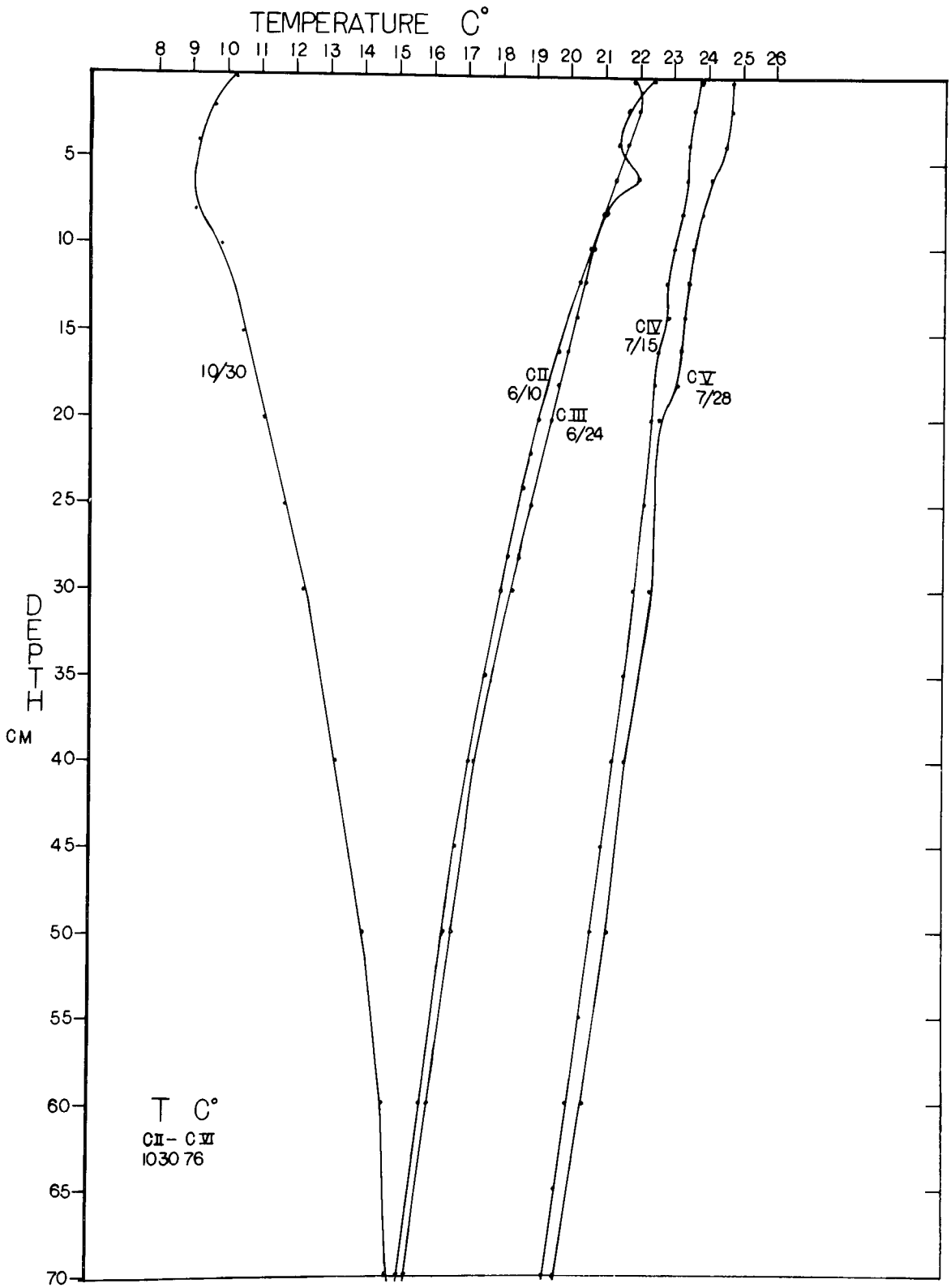

Figure 13. In situ sediment temperatures vs. sediment depth measured with glass bead thermistor and wheatstone bridge.

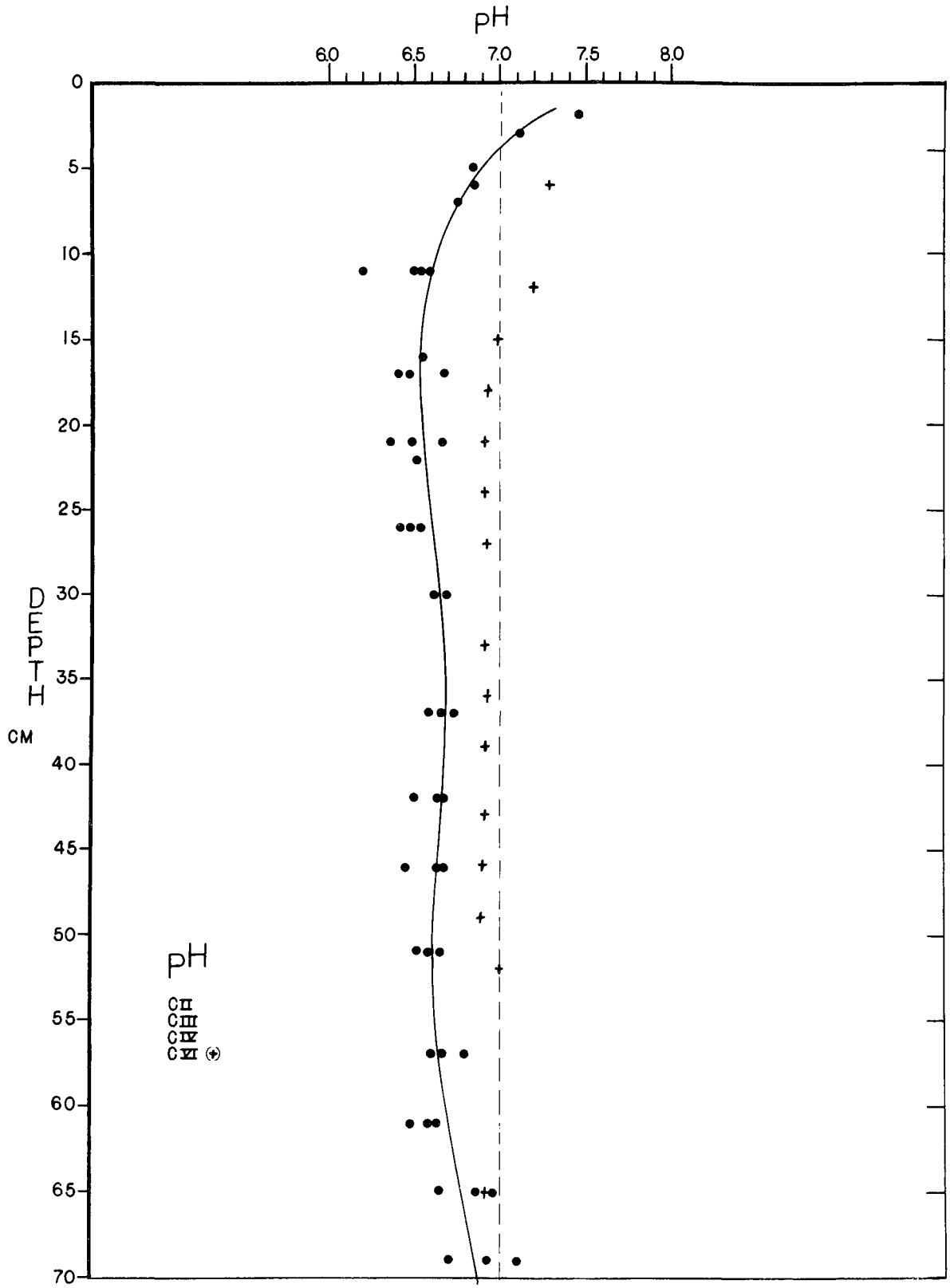

Figure 14. pH of "peeper" pore water samples vs. depth in sediments. Measurements made in the field with Beckman model G pH meter and microelectroded pair, except CVI (+).

The pH values in Foundry Cove sediments are generally lower than those of surface marine sediments (see Narragansett Bay data) but are in good agreement with reducing lake sediment values.

Figure 15 shows peeper pore water chloride values in ppm. The spread of data from the approximated fit represented by the solid line is about ± 10%. Some of the variation can be explained by considering the nature of the individual profiles comprising the figure. The profile from peeper C I shows the lowest chloride values at any depth which might be expected since C I was at a different site than C II - C VI. The high chloride values between 5 and 40 cm are from profile C VI and result from continued diffusion downward of saline water in contact with the surface at the time of C V (dotted line). These observations on the minor variability of sediment chloride concentrations must be taken into consideration in any discussion on the degree of equilibration attained. From the comparison of chloride profiles C I, C II and C III which represent two week equilibration times and those of C IV, C V and C VI which were only equlibrated 6-7 days, it can be clearly shown that no significant differences exist in chloride concentrations between the two sets. This implies that equilibration of a peeper cell with its surrounding is probably greater than 90% complete for conservative materials after 7 days.

Molybdate reactive silicate values are shown in Figure 16. Again, there is a ± 15% spread around the fitted approximate curve with considerable overlap in individual curves. (The 7 high points between 8 cm and 26 cm are from peeper C IVa and probably represent poor data.) The striking difference between this property and that of chloride is in the shape of the curve. The chloride profiles show an almost uniform linearly increasing concentration with depth while those for silicate indicate the importance of exchange reactions, the presence of and/or dissolution in maintaining a uniform concentration of 750 μ M/l. The equilibration reactions are complex and involve clays, organic silica and quartz (Garrel and Christi, 1965) but they appear to be the same in marine sediments also. An examination of data on cores from Narragansett Bay shows that the 750 μ M/l concentration is often reached but only rarely are higher values found. The general bow shape of the Foundry Cove curve is also found in many of the ocean cores (Fanning and Pilson, 1974; Schink et al., 1975).

The molybdate reactive phosphate values from the peeper pore water samples are shown on Figure 17. The values observed at site C II are enclosed by the heavy lines while the light line represents the profile for peeper C IV. The large spread in values is probably partly due to particulate contamination. A study of the individual profiles shows similarity of shape but slightly different concentrations for the different locations. The concentration differences may reflect horizontal inhomogeneities in the phosphate distribution while the similarity in shape between profiles suggests vertical similarity in diagenetic and chemical changes with depth from location to location.

Phosphate values observed in the Foundry Cove sediments are only 1/4 the values found in Hudson River sediments at mp 18 and probably reflect the absence of sewage inputs into the cove. In comparison to cores in Narragansett Bay reported by the URI group, the unpolluted Jamestown N cores

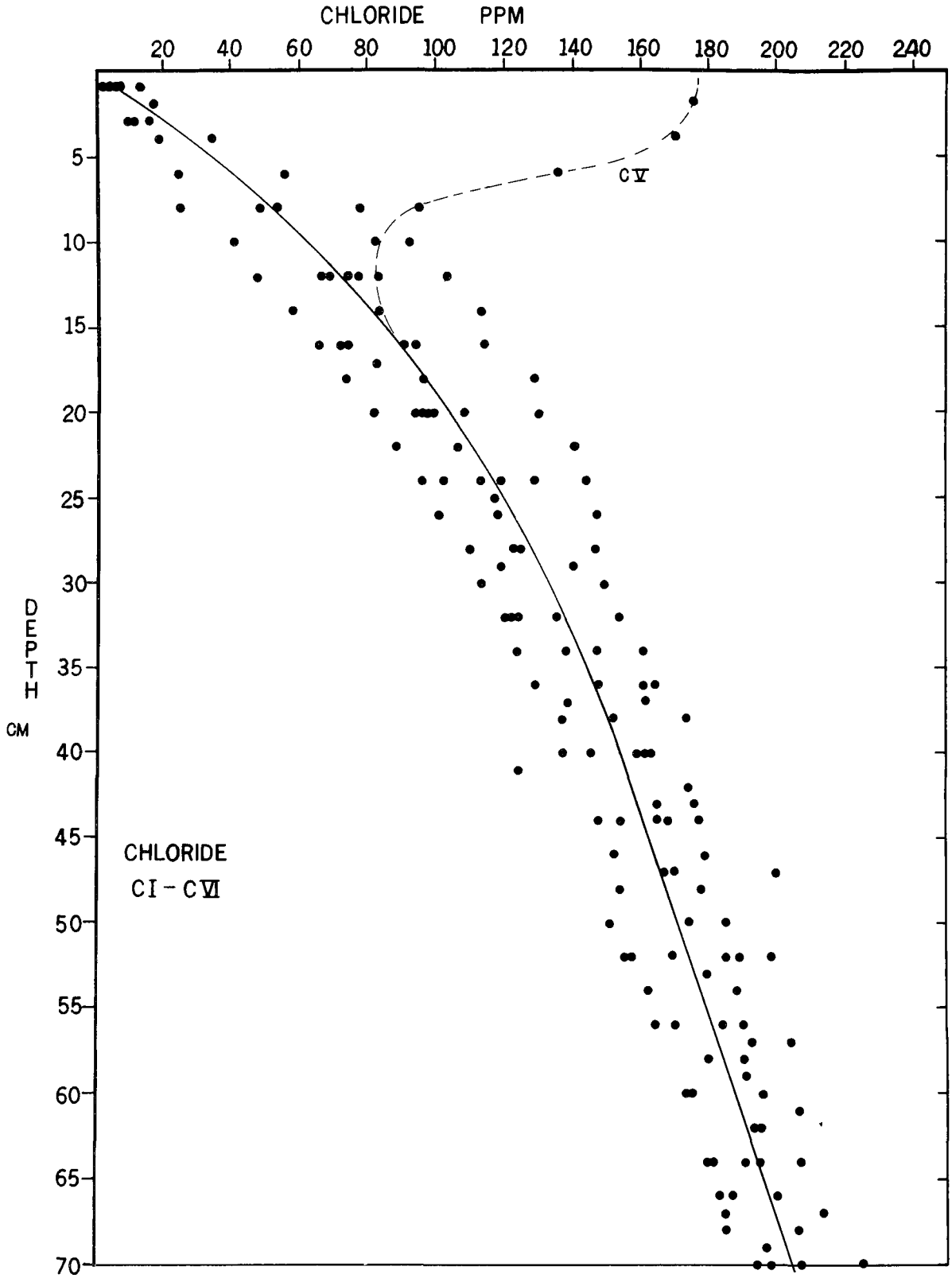

Figure 15. Chloride concentration vs. depth in sediment of "peeper" pore water samples in ppm. Measured by silver ion electrochemical titration. The solid line is an approximate fit of the data.

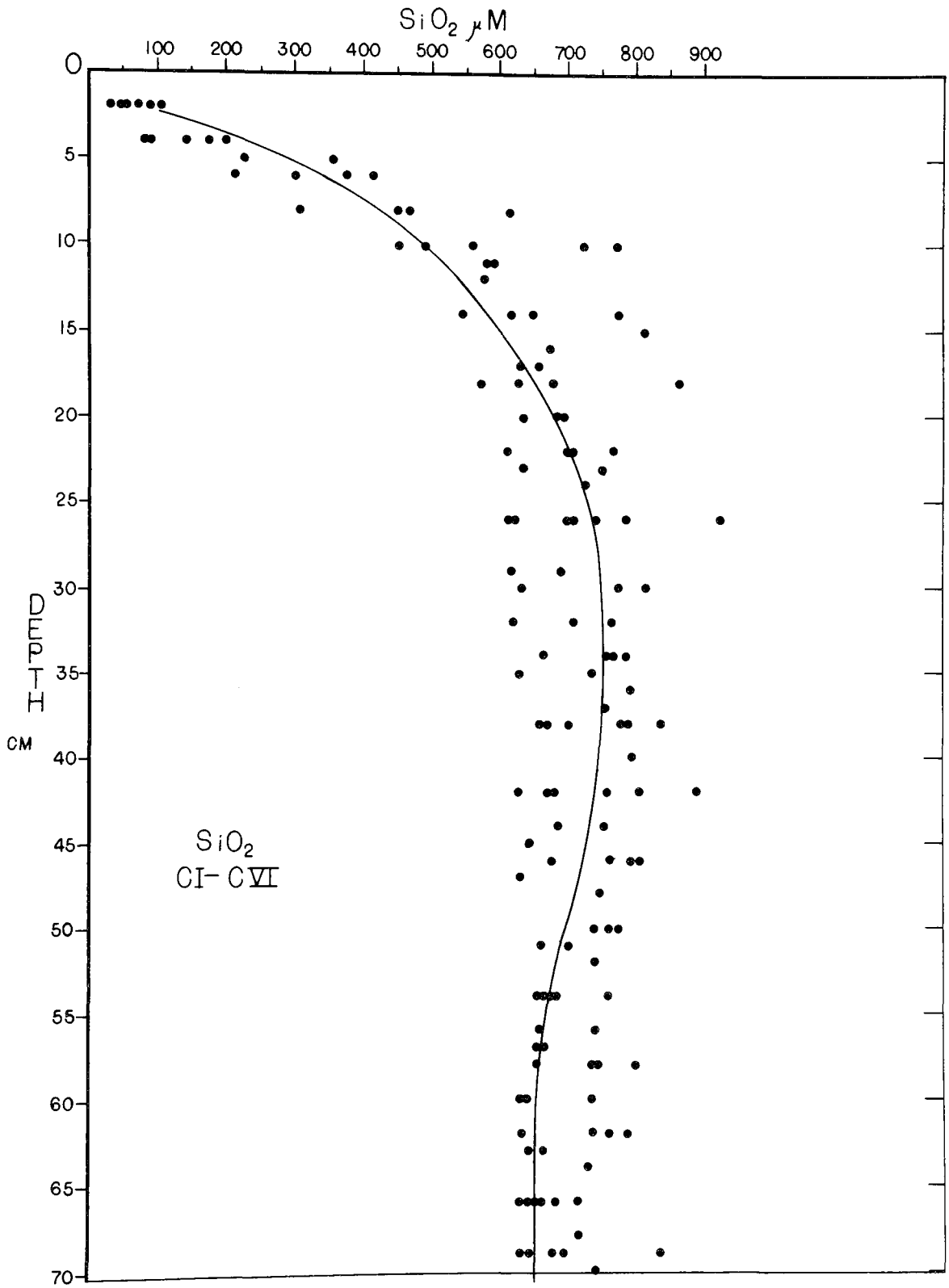

Figure 16. Reactive silicate concentration in μM/l vs. sediment depth. The solid line is an approximate fit of the data.

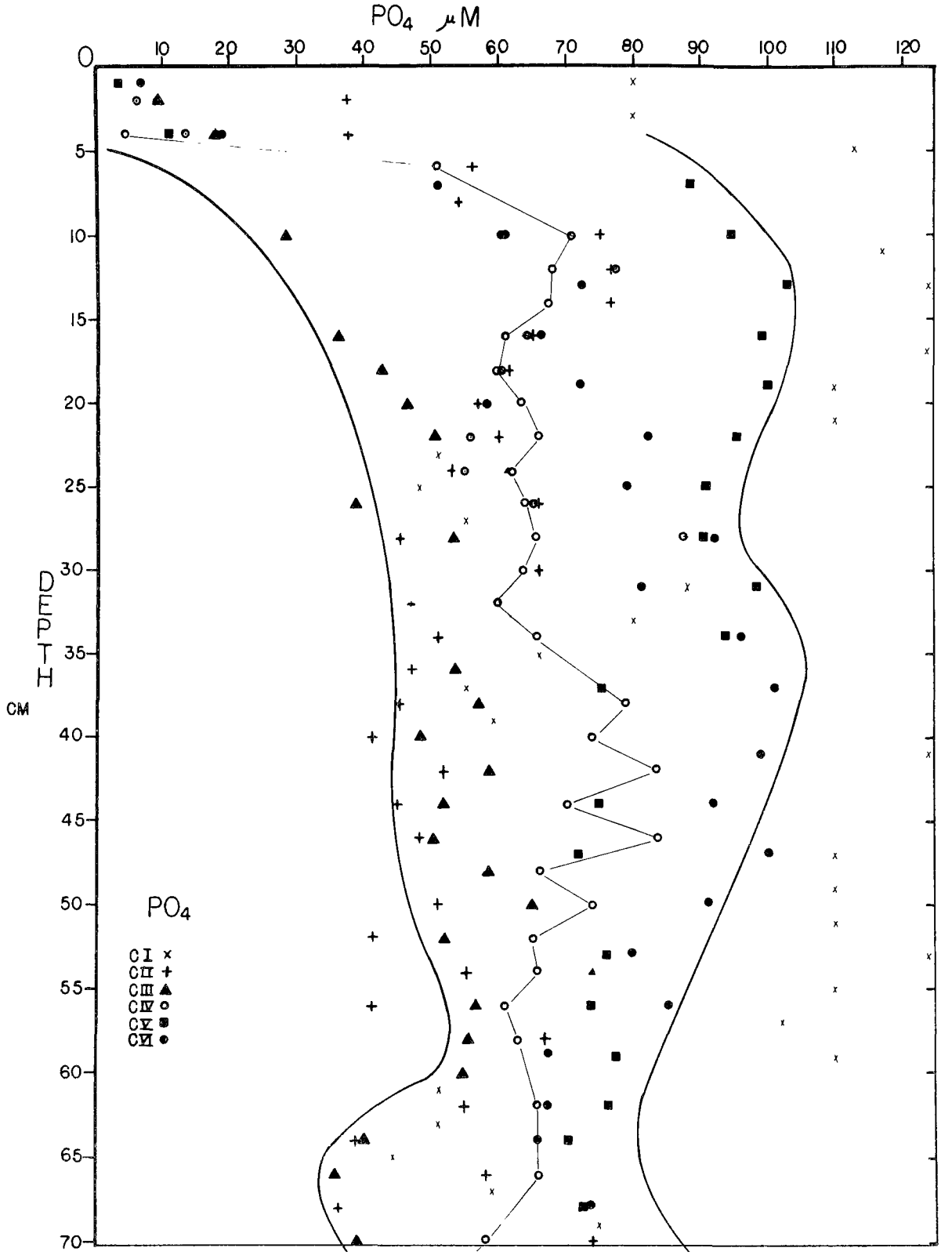

Figure 17. Molybdate reactive phosphate concentration in µM/1 vs. sediment depth. The heavy solid lines represent the limits of concentrations found at site CII. The light line is the profile from "peeper" CIV.

have concentrations similar to those of Foundry Cove (50-100 μ M) while values in the more polluted Rumstick Neck and Sabin Point cores are approximately 4 and 10 times higher respectively.

The manganese and iron data are presented as Figure 18 and 19. With these metals as with phosphate, horizontal inhomogeneities in the sediment could possibly control the variation of the values: Considerably lower values were found for the peeper C I Mn profile than those of peepers C II - C IV taken at site C II. The general uniformity of the Mn values at 2.5 to 3.5 ppm and those of iron around 16 to 22 ppm over nearly the total length of the peeper suggest that the reducing conditions necessary for the mobilization of these metals are attained at or above the 10 cm depth and remain constant to at least 70 cm. Comparison of Fe and Mn in Foundry Cove sediments which have sulfide levels < 30 μM, to the sulfide-rich marine sediments of Narragansett Bay (> 1000 μM sulfide) would not be valid. However, a comparison to low sulfide lake iron (18 to 20 ppm) and manganese (1 to 3 ppm), suggesting that similar chemical equilibria are controlling the values.

The profile for peeper C V on Figure 19 does not agree with the other iron data and presents a major problem in interpretation of all the iron data. This peeper was the only Foundry Cove peeper to use Nuclepore (polycarbonate) filter membrane rather than cellulose-based dialysis membrane. The other parameters do not display any variation resulting from type of material used, but the probability exists that one or the other or both of the sets of values for iron are incorrect. Unfortunately, Mn data was not run for peeper C V which would have told us whether or not any other metals were similarly affected. Clearly, more work must be done to understand this problem.

The primary reason for choosing Foundry Cove as the site of our major effort in peeper studies was the high concentrations of cadmium and nickel found in the sediments. The concentration of dissolved Cd in the pore waters must be known accurately if the flux of the metal into the overlying water is to be determined. Cadmium profiles are shown for three locations in Foundry Cove (Site C I, C II and B I). Approximate metal concentrations in the sediment at the three locations are 200 ppm, 400 ppm and 5000 ppm Cd (dry weight) respectively. The Cd profiles obtained for peeper C I (site C I) peepers C II, C III and C IV (site C II) and those for peepers B I and B II (site B I) are shown as Figure 20. A major problem in sampling procedures was discovered during the B I run. With the extremely low pore water concentrations of soluble Cd relative to the sediment, inclusion of even a very small particle of sediment in the sample causes massive contamination of the sample. This is the most likely explanation for profile B I and probably accounts for the large number of data points with values over 100 ppb. Since peeper C I was sampled at the same time as B I, the same type of contamination could be expected. Due to the lower sediment concentration at the C I site and a better washing of the membrane surface before sampling, the number of contaminated samples was less. To overcome this problem a special peeper was used for B II. This peeper had a convex curved front and did not have a plastic cover plate. This peeper was transported back to the lab where the foam and membrane were removed together thus decreasing the possibility of any particles entering the cells.

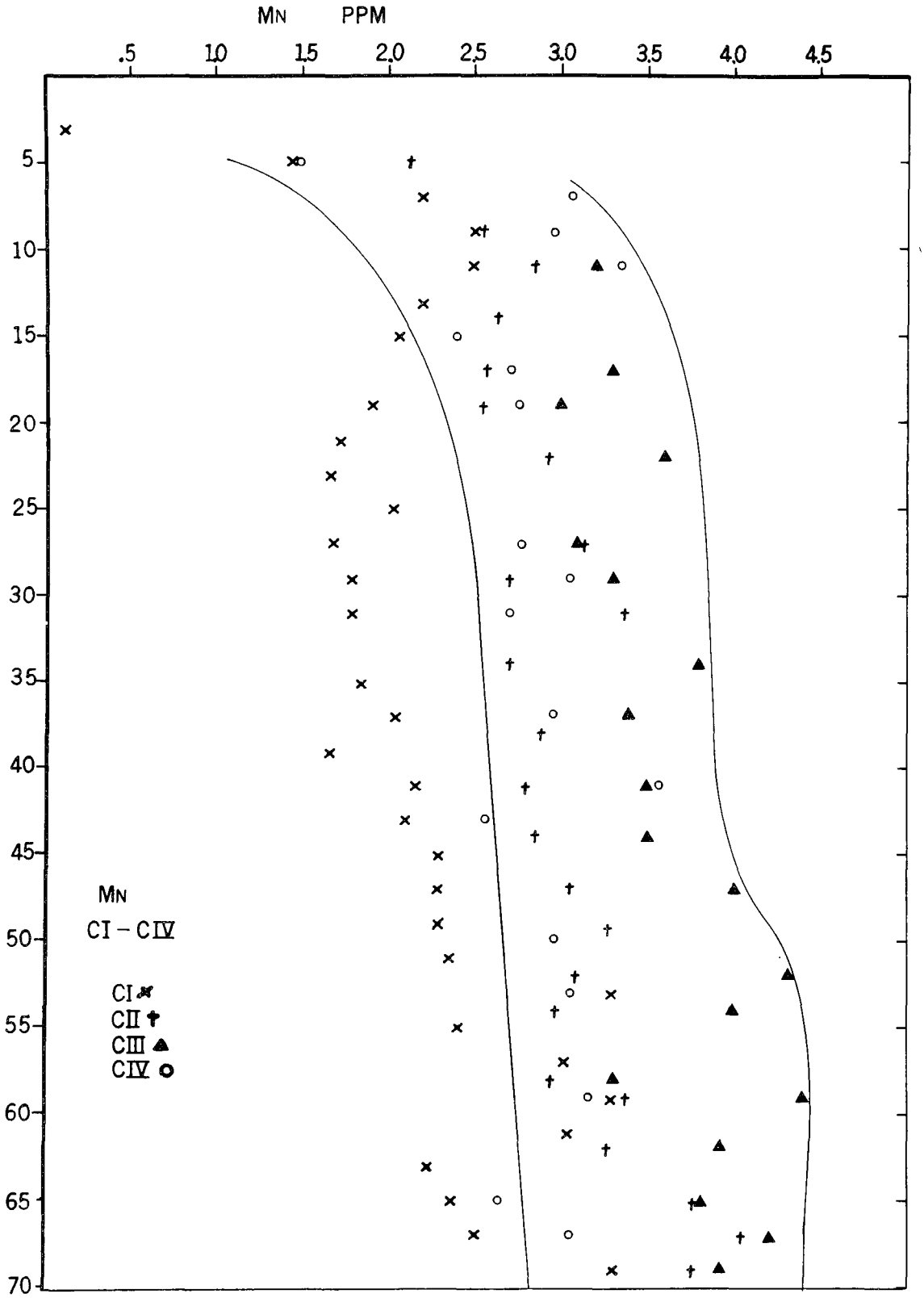

Figure 18. Total manganese concentration of "peeper" pore water samples in ppm vs. depth in sediment by graphite furnace A.A. The solid line represents limits to the data observed at site CII

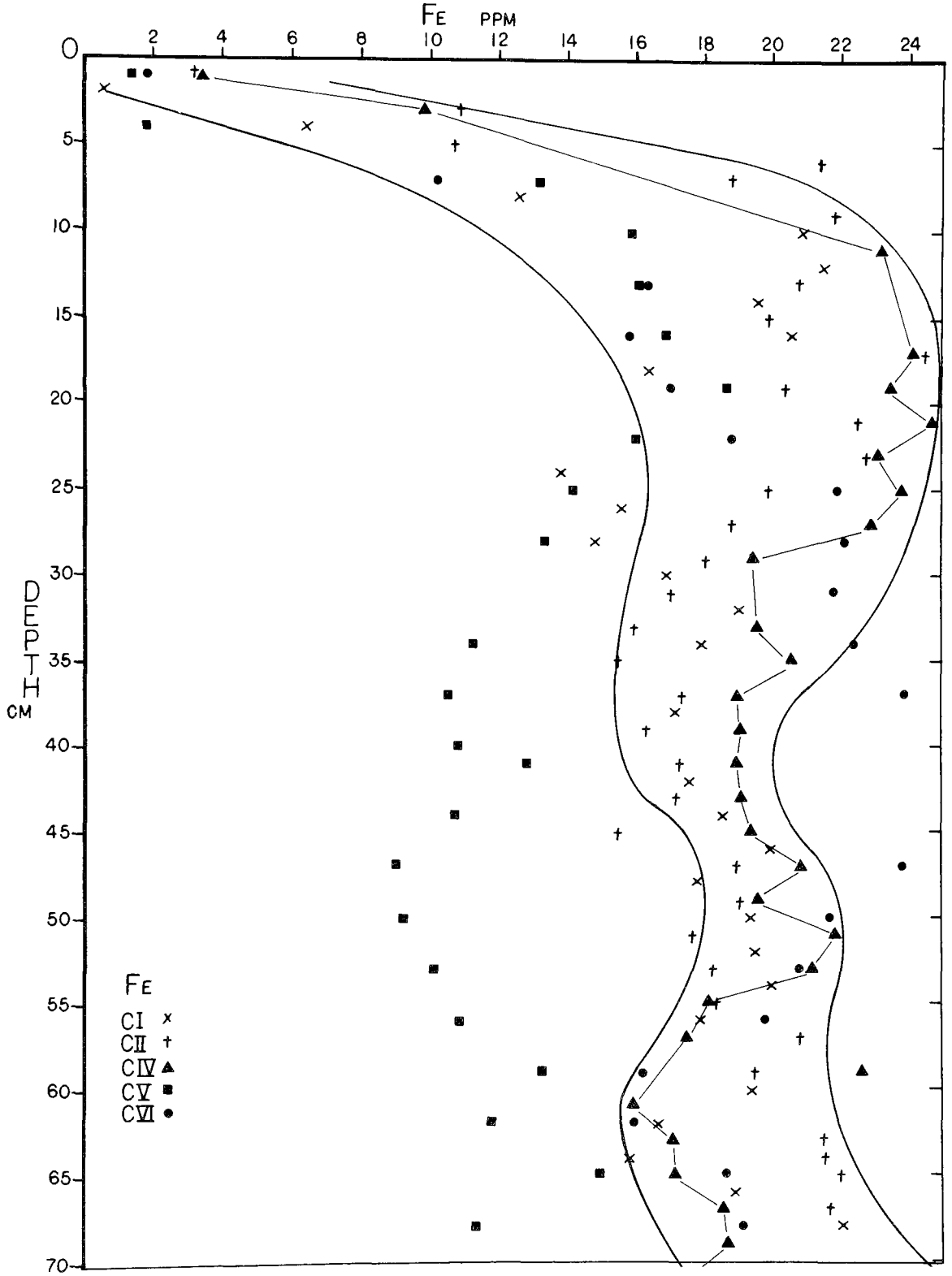

Figure 19. "Colorimetric" iron concentration in ppm of "peeper" pore water samples. The method approximates total iron concentration. The heavy solid lines indicate the range of concentrations found at site CI and CII. The light line is the profile for "peeper" CIV.

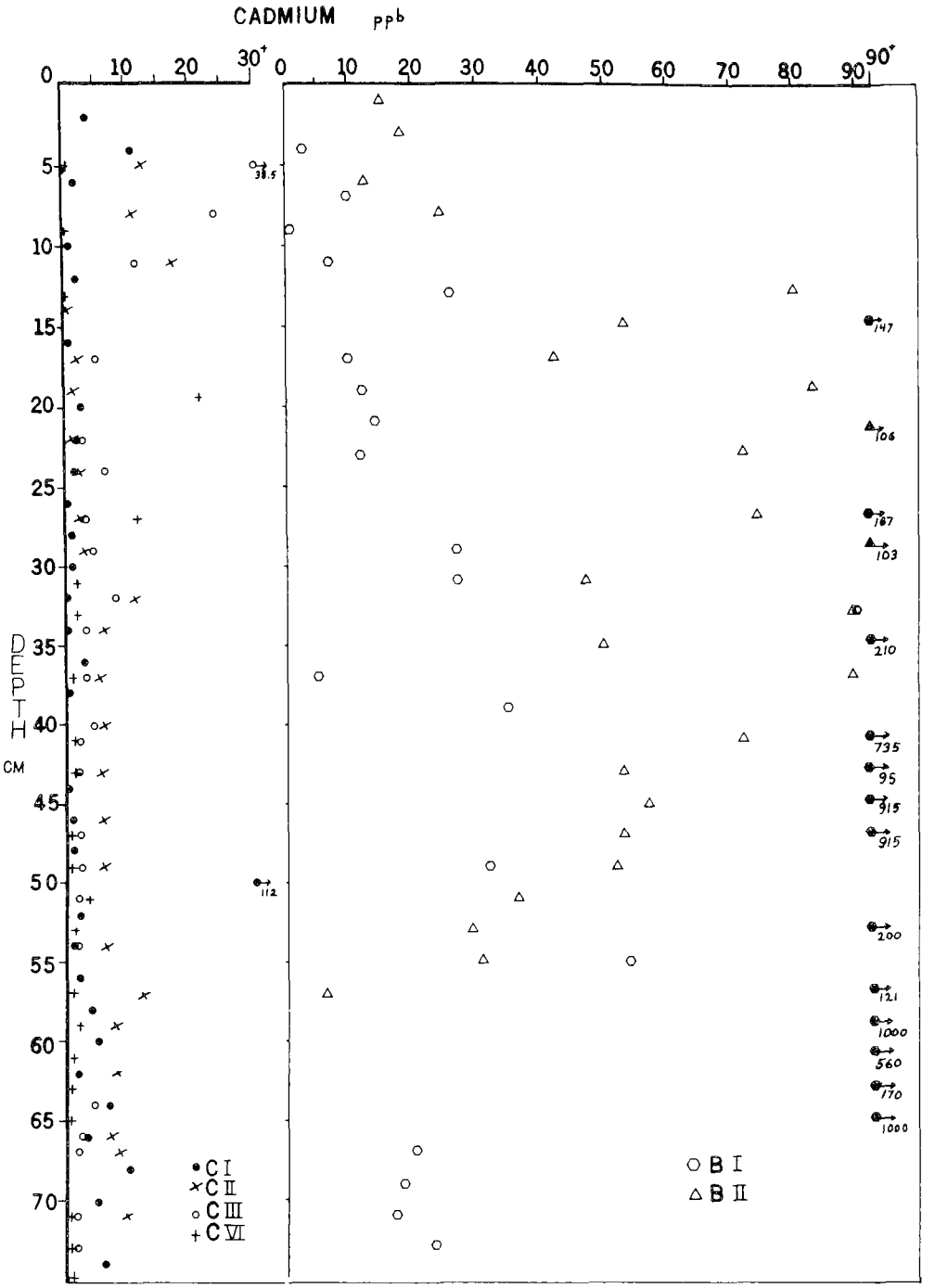

Figure 20. Cadmium concentration of "peeper" pore water samples with depth. The samples from peepers CI, CII, CIV and CVI are on the left. Samples from peepers BI and BII (near plant outfall) are presented center to right. All concentrations are in ppb. (The large number of points on the right margin represent off scale values from "peeper" BI where particulate contamination of the "peeper" water sample resulted in contamination.)

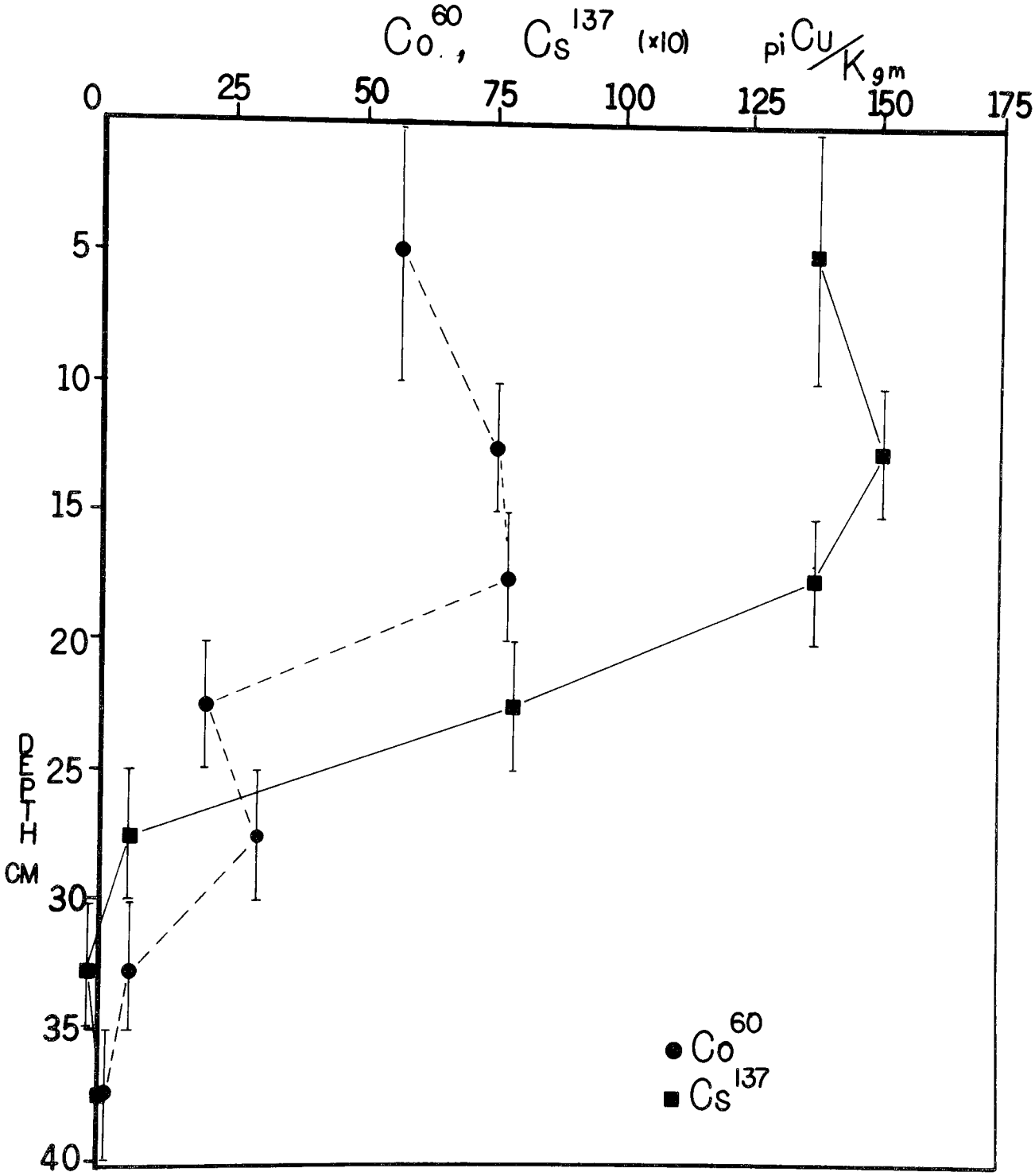

Figure 21. Profiles of cobalt-60 and cesium-137 radioactivities with depth in the sediment at Foundry Cove site CII (middle of inner cove). Concentrations in pico(10^{-12}) curies per kg dry sediment.

(Acid was added to the chambers before the samples were removed to redissolve any material that might have left solution during the 3 hour time period before sampling.) As can be seen from the graph, none of the points for peeper B II have values greater than 110 ppb, and the scatter of the data in the profile has been reduced. While the error with the sampling and chemical analysis may be as great as $\pm$ 30%, the approximate shape of the profile is clear. Low values of 10-20 ppb are found in the top 10 cm rapidly increasing to 70-90 ppb in the 10 to 30 cm region, after which values again drop. This profile is in sharp contrast to the values from peepers C I through C VI where the majority of values are below 10 ppb and close to 3.0 $\pm$ 2 ppb. This factor of 10 difference is approximately equal to the difference in total sediment Cd concentrations. This difference is not in agreement with the findings of Bondietti *et al.* (1973) who found approximately equal pore water solution levels ($\sim$ 10 ppb) in high (35,000 ppm) and low (2100 ppm) Cd sediments in the cove.

Figure 21 shows the distribution of ^{60}Co and ^{137}Cs in pico curies per kilogram of dry sediment at peeper site C II. The main injection of these isotopes to the Hudson from weapons testing (^{137}Cs) and reactor releases (^{137}Cs and ^{60}Co) occurred over the last 20 years and their present distribution gives some indication of the depth to which mixing (turbation) may have occurred and/or the rate of sediment accumulation at the site. We have not used the term bioturbation since, while this may be important, we have observed that considerable thicknesses (10-20 cm) of sediment can become frozen to the bottom of the overlying ice during low tides in the winter with resulting movement and mixing when the ice melts. The profiles indicate that mixing to a depth of 20 cm may have occurred at site CII since the late 1950's (cores taken in other parts of the cove show similar profiles including the one taken at site B). If the input of Cd-Ni wastes began in the mid-1950's, contamination of the sediment might be expected to 25 or 30 cm. Cadmium data from peeper profile B II shows high values to a sediment depth of 35 to 40 cm. At present we don't have any definite explanation of why the pore water data indicate deeper contamination with Cd than the sediment ^{137}Cs data, but one possibility is compression of the sediment column during coring and extrusion of the sediment cores.

Several other tests were run on pore water samples that are included as figures. Ammonium concentrations in Foundry Cove sediments are between 10 and 500 μ M with approximately linear profiles from the surface to 70 cm. Positive sulfide concentrations have been randomly found but never have the values exceeded 15 μ M. Methane profiles are variable and reflect bubble formation and gas loss during sampling. The methane concentrations are high (200+ μ M) which are comparable to those found for Narragansett Bay by the URI group. $\Sigma\ CO_2$ measurements of Foundry Cove peepers have been made and are in the range of 1 to 10 m M/l. Other trace metals (Cu, Zn and Ni) were run on a few sets of samples but technical and blank problems cast some suspicion on their accuracy.

In conjunction with the development of the peeper, several profiles were measured in the lower Hudson estuary off Alpine, New Jersey (mp 18) during 1974-1976. The profiles of PO_4, SiO_2 and Cl^- with depth are presented in Figures 22, 23a and 23 b respectively. In comparison to Foundry Cove, the Alpine site is distinctly brackish for the majority of the year with salinities of 5°/$_{oo}$ to 10°/$_{oo}$. The overlying water contains 6 to 10 times the soluble

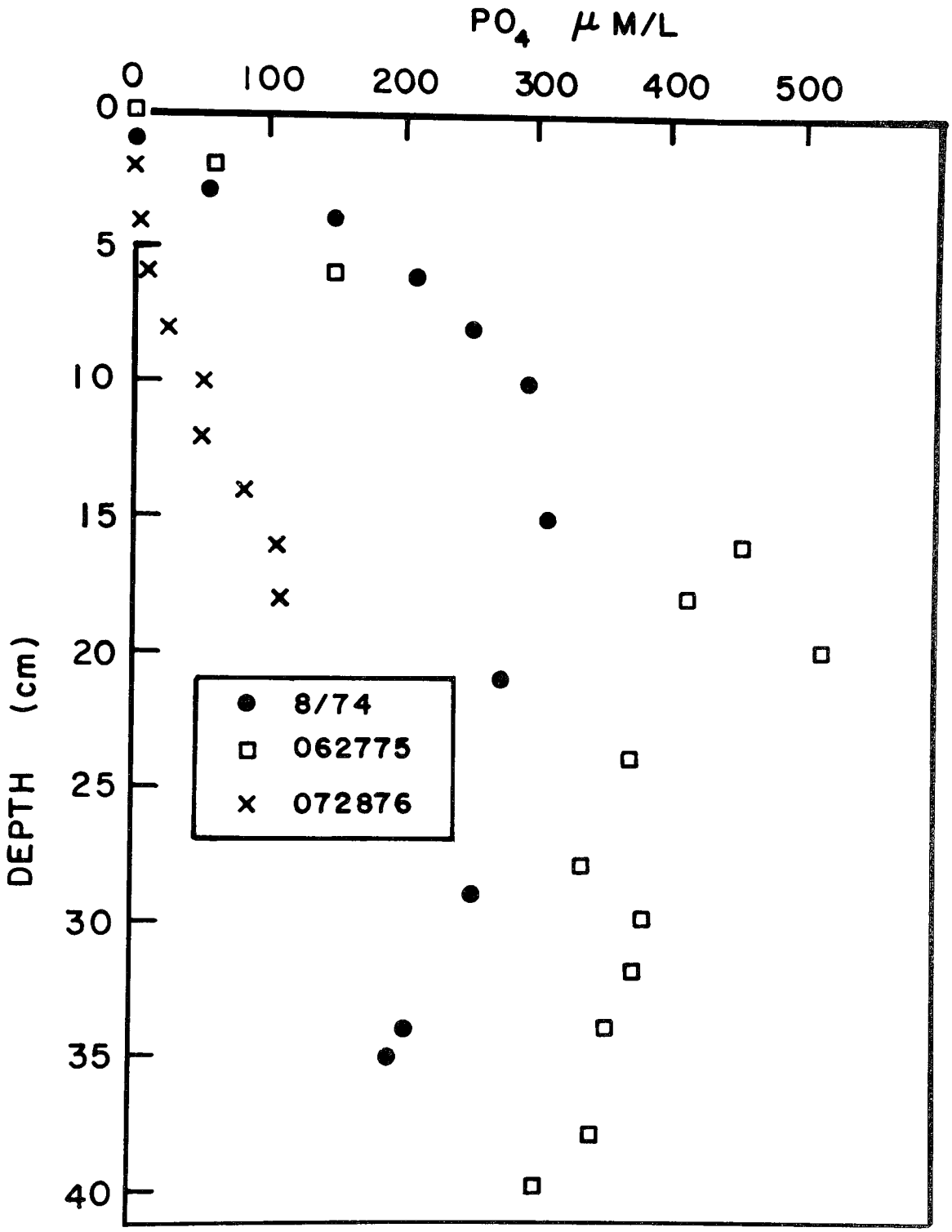

Figure 22. "Peeper" pore water molybdate reactive phosphate values in μM/1 vs. depth in Hudson sediments off Alpine, New Jersey.

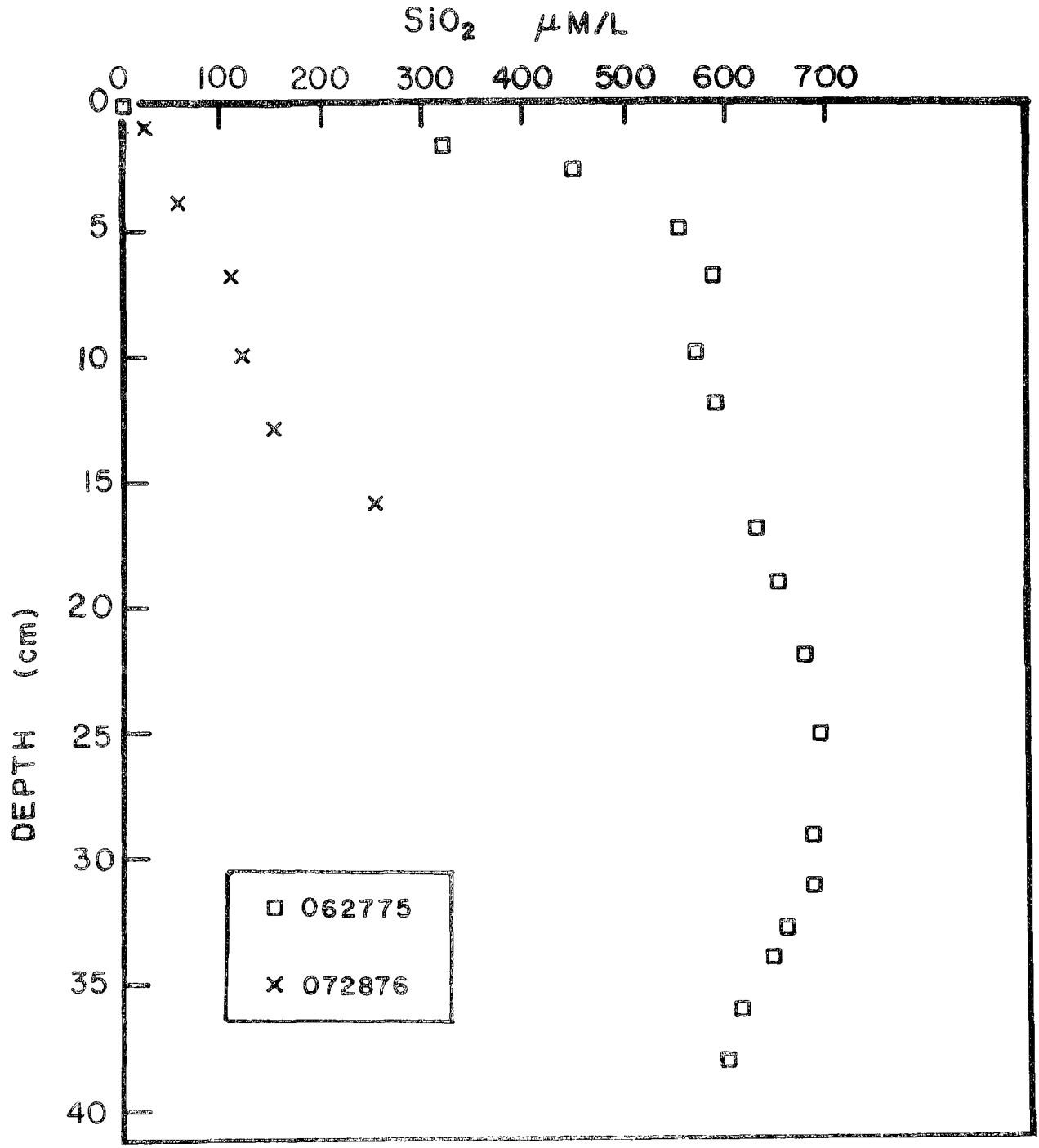

Figure 23a. "Peeper" pore water reactive silicate in μM/l vs. depth in Hudson sediments off Alpine, New Jersey.

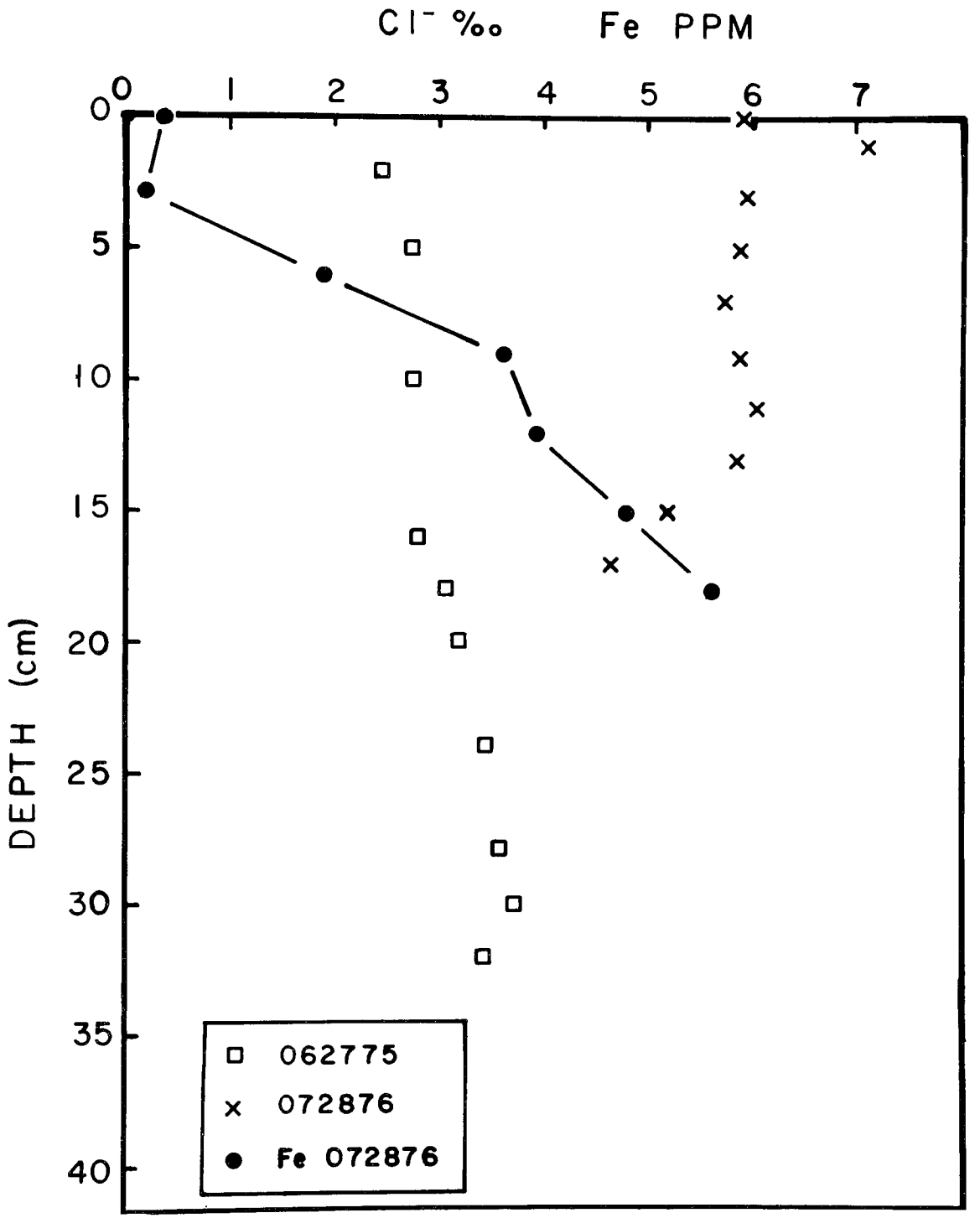

Figure 23b. Chloride concentration in ppt and "colorimetric" iron values in ppm vs. sediment depth for Hudson/Alpine peepers.

phosphate and substantially greater quantities of sewage derived particulates than at Foundry Cove. This difference may be the reason the peeper phosphate profiles at Alpine (Figure 22) are 3 to 4 times higher than those at Foundry Cove, reflecting the large sewage input rate to the lower Hudson The SiO_2 peeper profile from Alpine on 22 June 1975 (062775) (Figure 23a) is very similar to those from Foundry Cove except that the maximum values are slightly less. The SiO_2 profile for 072876 presents a major problem in interpretation. This profile and the corresponding PO_4 profile (Figure 22, 072876) are both approximately 3 times lower than they were in previous years and do not show the sharp gradients at the surface that the other profiles do. Several explanations are possible for these discrepancies. The two which seem the most likely are that the peeper was not inserted correctly and substantial exchange with the overlying water occurred along the back, sides, and face or that the peeper was inserted into a pocket of recently resuspended or deposited sediment. The chlorinities for two of the profiles are shown in Figure 23b and represent the average of many tidal cycles. A single iron profile for the peeper (072876) is also shown on Figure 23b.

SUMMARY OF PORE WATER RESULTS

The data from Foundry Cove indicates that for conservative species such as chloride, the equilibration of the peeper cells with the pore waters is nearly complete after a week and approximately linear curves were observed. Non-conservative materials were controlled by dissolution and/or absorption reactions in the sediment and either reflect a quasi equilibrium state as in the case of silica or display considerably more variability as in the case of PO_4 and the metals Fe and Mn. The species which display variability in the sediment with depth also appear to have greater horizontal variability than Cl^-, silica, or the major ions. The difference in PO_4 concentration between Foundry Cove and the Hudson estuary at Alpine is consistent with the direct correlation found by the URI group between PO_4 levels in the pore water and level of sewage contamination in the overlying water. The measurements of Cd in Foundry Cove have shown that with suitable care to avoid contamination trace metals with low solubilities can be measured in pore waters. Finally, with the proper choice of models, reaction rates, and diffusion constants some estimate of the exchange between the sediments and the water column could be made from the pore water data for each species.

SECTION 6

CESIUM-137 AS A TRACER FOR REACTIVE POLLUTANTS IN ESTUARINE SEDIMENTS

INTRODUCTION

A substantial number of the pollutants discharged to natural waters can be classified as "reactive" in terms of their propensity to be associated with particles, either in the original effluent or after becoming dispersed in the receiving water. For example, metals from the electroplating industry and some types of artificial radionuclides released from nuclear power plants are transported and accumulated on particles in natural waters, as well as in solution. The particles which are most important in reactive pollutant transport are usually relatively small and often contain both organic and inorganic components. We will not discuss the composition or sorption characteristics of these fine particles, but instead will describe some of their characteristics as vectors of pollutant dispersal and accumulation.

In estuaries, fine particles (< 63 microns) are quite mobile and often undergo many episodes of deposition and resuspension by the variable currents of tidal waters. In theory, it should be possible to describe and predict the pathways of fine particle transport in estuaries, based on the physics of the particle motions and numerical models of sufficient complexity or from properly-scaled physical models. Actually, it is more practical to make direct field measurements of particle transport or to use tracers to infer the net motion of particles over extended periods of time. The approach described here uses a "natural" tracer (cesium-137), which has become associated with fine particles in estuaries, as a guide to the distribution and transport of fine-grained sediments and several types of pollutants. The pattern of accumulation of fine particles in estuarine sediments is complex and essentially unique to each estuary. As a first approximation, estuarine sediments can be grouped into three end members: (1) large mineral particles, such as quartz sands, which are relatively unimportant in the transport of reactive pollutants; (2) fine particles (generally < 63 microns) which have not acquired significant quantities of pollutants, primarily because they have had relatively little contact with soluble phase pollutants; and (3) fine particles with readily-measurable quantities of pollutants, which will be referred to here as "recent" fines. Obviously the degree of contamination of recent fines can be extremely variable, but as will be shown in the case of the Hudson River estuary (U.S.A.), there is often a relatively uniform dispersal of reactive pollutants in recent fine particles over large areas and a surprisingly coherent distribution of several types of pollutants.

CESIUM-137 AS AN INDICATOR OF RECENT SEDIMENTS

Atmospheric testing of large nuclear weapons during the 1950's and early 1960's, predominantly by the U.S.A. and U.S.S.R., dispersed a great variety of radionuclides over the entire earth. A number of these nuclides have sufficiently long radioactive half-lives to be valuable as tracers of global scale processes. The pattern and time scale of deposition of strontium-90 (t 1/2 $\sim$ 29 years), especially in the northern hemisphere, have been followed closely (Volchok, 1966; Volchok and Kleinman, 1971) because of its long half-life, potentially serious biological impact, and the existence of relatively direct pathways by which this nuclide can reach man. The depositional history of Cs-137 (t 1/2 $\sim$ 30 years) has not been documented as well as Sr-90 because it does not appear to be of nearly as much biological concern to man as Sr-90. Available data indicate that the pattern of delivery of atmospheric fallout Cs-137 to the earth's surface can be assumed to be identical to Sr-90, with an activity ratio of Cs-137 to Sr-90 of $\sim$ 1.5 (Harley et al., 1965; Hardy, 1974). The peak delivery of fallout Cs-137 to the earth's surface by rain and snow occurred during the years 1962-1964, and the quantities deposited since then have been relatively small. Most of the Sr-90 (and Cs-137) fallout on land has been retained in the upper 10-20 cm of the soil profile and the total activity present per unit area is proportional to the annual rainfall (Hardy and Alexander, 1962) as well as being a function of the latitude (Volchok, 1966).

In the open ocean, both Sr-90 and Cs-137 appear to have remained predominantly in solution (Broecker et al., 1966; Folsom et al., 1970; Bowen and Roether, 1973), although there is some indication of preferential removal of Cs-137 into the sediments (Noshkin and Bowen, 1973). The fraction of total fallout Cs-137 delivered to the ocean which is now in the sediments is quite small. In most fresh water lakes, Sr-90 stays in solution to the first approximation, but Cs-137 is nearly completely removed onto particles (Wahlgren and Marshall, 1975; Farmer et al., 1977). In rivers and estuaries, the fraction of fallout Cs-137 associated with sediment particles (compared with that which passed through these systems in solution) is not well-defined (Riel, 1972), but readily measurable amounts are found in the sediments of estuaries which we have studied.

We usually measure Cs-137 in estuarine sediments by gamma counting 50-100 gram samples of dried sediment which have not undergone chemical steps to enrich the specific activity of the samples. Our counting equipment consists of a high resolution lithium-drifted germanium detector and a multichannel analyzer, which allows us to simultaneously measure the activity of many other radionuclides (both natural and artificial) as well as the Cs-137 gamma emission peak at 662 Kev. Because of our ability to measure Cs-137 at "normal" environmental levels in sediments with non-destructive gamma counting we are able to process a large number of samples with relatively little effort in laboratory preparation, compared with the analytical techniques required for most pollutant measurements. The detection limit for most of our samples was 10-20 pCi/kg, which is a few percent of the activity typical of surface soils in the northern hemisphere.

CESIUM-137 AND OTHER ANTHROPOGENIC COMPONENTS IN HUDSON ESTUARY SEDIMENTS

The total delivery of fallout Cs-137 to the Hudson estuary, decay corrected to 1975, has been about 120 mCi/km^2 (USERDA, 1975). There is an additional supply of Cs-137 from a nuclear electrical-generating facility located near the upstream end of the salinity intrusion in the Hudson. The total release of Cs-137 from this facility over more than a decade of operation has been comparable to the amount supplied by rain to the surface of the Hudson estuary from global fallout. Thus the direct supply of Cs-137 to the Hudson estuary is roughly a factor of two greater than might be expected if fallout were the only source.

The specific activity of Cs-137 in surface sediments in the Hudson ranges over more than two orders of magnitude, with the lowest values in sandy sediments (typical of areas scoured of fine particles by strong currents). Fine-grained surface sediments (< 63 μ) usually range between 0.2 and 2 pCi/g of Cs-137, which is comparable to fallout Cs-137 activity in surface soils throughout the northern hemisphere (Hardy, 1974; Ritchie et al., 1975). There is large variation in the depth to which Cs-137 is found in sediment cores. In most areas Cs-137 activity is confined to the upper 5 cm of the sediment column whereas in some it extends to nearly 3 meters below the sediment surface. Thus the integrated amount of Cs-137 per unit sediment area is not uniform, and ranges over more than two orders of magnitude. As a result, relatively limited geographical areas account for large portions of the total sediment burden of Cs-137. In the Hudson estuary (Figure 24) the dominant areas of Cs-137 accumulation are the harbor and shallow coves upstream of the harbor. These areas are not in close proximity to the site of localized discharge of Cs-137 to the Hudson, and primarily reflect the zones in which fine particles are rapidly accumulating (Simpson et al., 1976).

We have found the distribution of other man-made reactive contaminants in Hudson sediments to be very similar to that of Cs-137, despite significant differences in chemistry, and mode of input to the system. The locations of sediment sampling sites for data reported here are shown in Figure 24. These sites extend from approximately the upstream limit of salinity intrusion during summer months, to the harbor area which typically has salinities of approximately two-thirds that of sea water.

In Figure 25, activities of Pu-239,240, determined by alpha spectrometry following chemical separation procedures as described by Wong (1971), are plotted against Cs-137 in the same samples. The covariance over two orders of magnitude of these two parameters in Hudson sediments is clear. Thus, if the present distribution of Pu-239,240 in Hudson sediments (mostly derived from fallout) were to be measured, the most efficient procedure would be to use the distribution of Cs-137, which is relatively easy to measure by gamma spectrometry, to guide the selection of samples for Pu-239,240 analysis. (The alpha particle energies of Pu-239 and Pu-240 are nearly identical and the sum of their activities is usually reported.)

In Figure 26, the concentration of polychlorinated biphenyls (PCB's) in Hudson sediments is plotted against Cs-137. Although our data is limited at this time, the covariance of these constituents is also obvious. The levels of PCB's are high in sediments over large areas of the Hudson because of

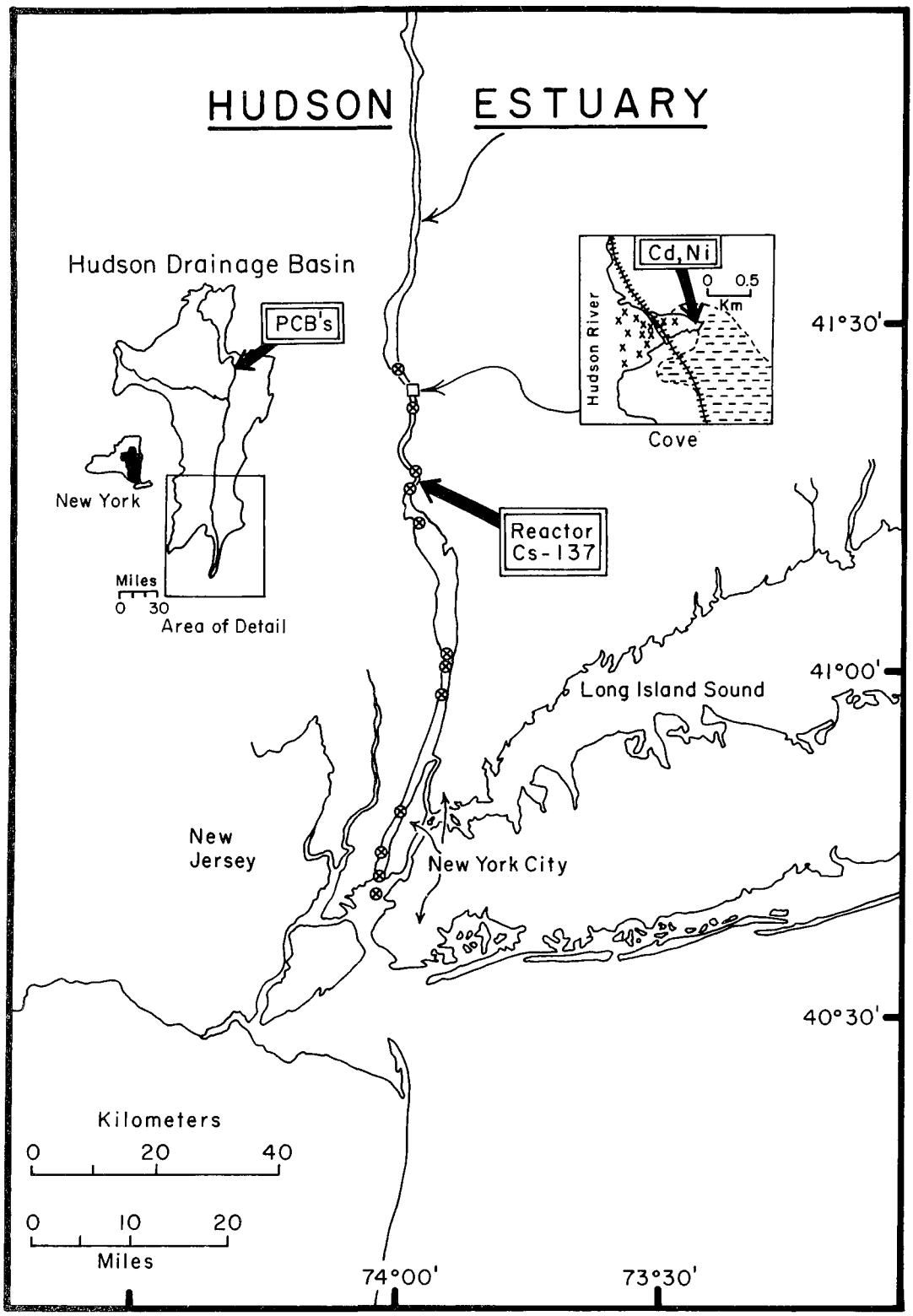

Figure 24. Locations (⊗) for which data in Figures 25, 26, 27 and 28 are reported. Locations of discharge of polychlorinated biphenyls (PCB's), cadmium and nickel (Cd, Ni) and radioactive cesium (Cs-137) are also indicated.

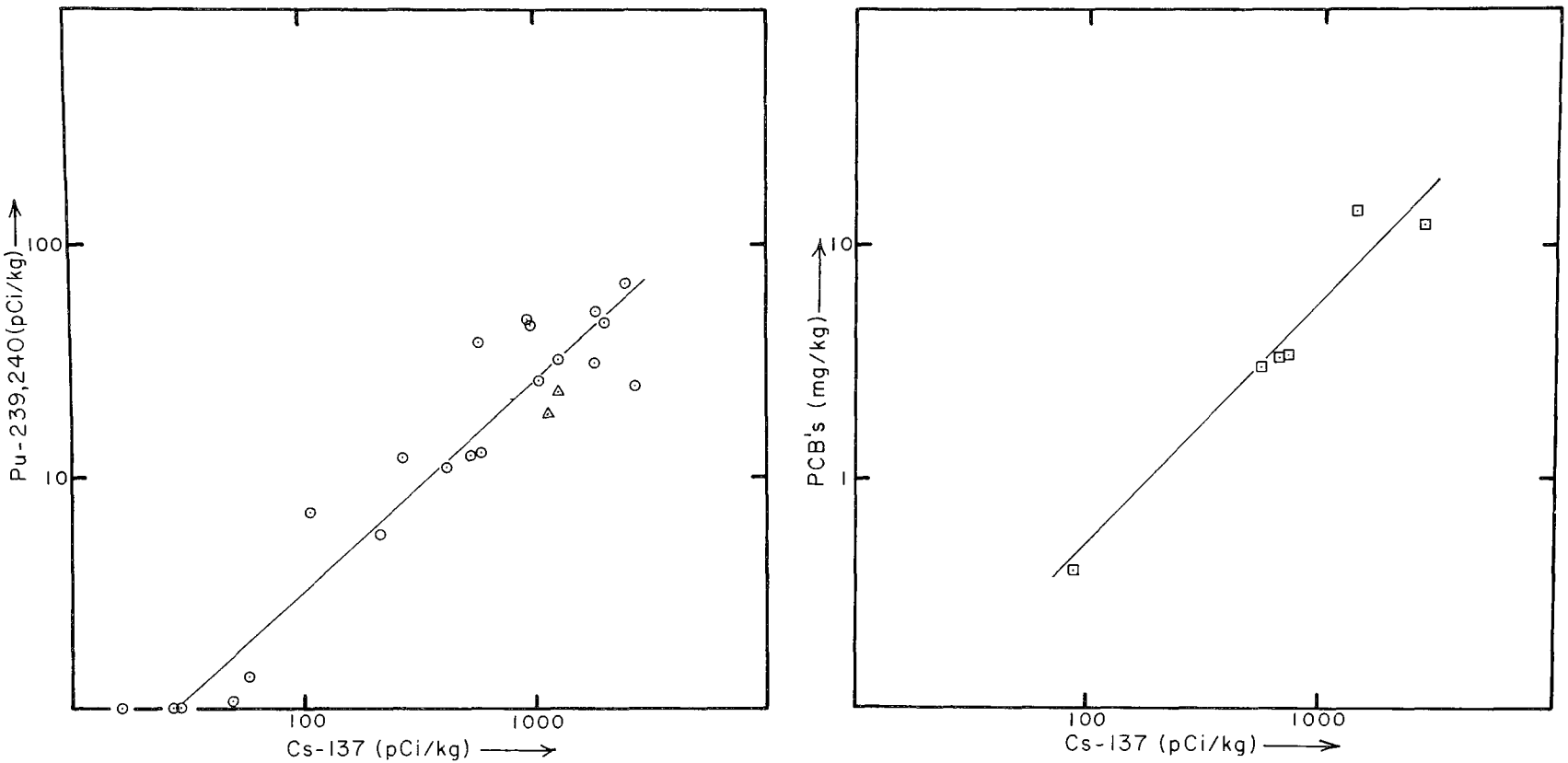

Figure 25. Activities of ^{137}Cs and $^{239,240}Pu$ in Hudson Estuary sediment (dry weight) core samples (Figure 24) including both surface samples and a number from well below the sediment-water interface. Two suspended particulate samples (⧋) collected near the middle of the sampling range are included.

Figure 26. Activities of ^{137}Cs and concentrations of polychlorinated biphenyl's (PCB's) in samples of surface sediment (Figure 24). All data is expressed in terms of dry weight.

industrial releases during the 1950's and 1960's at two sites more than 200 km upstream of the locations of our sampling area. Considering the great differences in chemistry between Cs-137 and PCB's, it is perhaps surprising to find their sediment distributions to be as similar as they are, but their covariance is a good indicator of the ability of fine particles to transport and accumulate quite a variety of reactive pollutants.

In Figure 27 is shown the concentration of several trace metals relative to Cs-137. Zinc, copper and lead concentrations in recent Hudson sediments are several times the concentration levels in pre-industrial sediments. All of the samples shown in Figure 27 are upstream of the harbor area, and thus reflect diffuse sources of these metals to the Hudson over a number of decades. Sediment samples from New York harbor have somewhat higher concentrations for all three metals because of electroplating and other industrial discharges. Vertical distributions of all three metals in harbor sediments also are similar to that of Cs-137.

In Figure 28 the concentrations of cadmium and nickel in Foundry Cove at mp 53 are plotted against Cs-137 activity. High level contamination of the sediments of this small ($\sim$ 0.5 km^2) shallow (mean depth $\sim$ 1-2 meters) area by effluent from a battery factory has resulted in Cd concentrations ranging from a few percent to $\sim$ 100 ppm (Bower, 1976). Some surface sediments in the cove which are apparently in areas of active current scouring contain relatively low concentrations of Cd, Ni and Cs-137. Thus Cs-137 is useful in mapping the pattern of trace metal accumulation in sediments in relatively small, highly contaminated areas, as well as for diffuse sources over large areas.

All of the "reactive" pollutants we measured in Hudson estuary sediments are found preferentially on fine particles and in sediments rich in organic matter, as would be expected. However, many sediment samples with very similar particle size distributions and organic carbon contents did not have appreciable reactive pollutant concentrations (and they did not have measurable Cs-137). Thus the activity of Cs-137 was a much more accurate indicator of probable pollutant concentration than were classical sedimentological techniques, especially in estimating the depth to which appreciable pollutant concentrations would be found in estuary sediment cores.

CESIUM-137 AS A POLLUTANT TRACER IN OTHER AQUEOUS SYSTEMS

Fallout Cs-137 has been used as an indicator of recent sediments in the Delaware Estuary. Sites with appreciable activity of Cs-137 in surface sediments also have hydrocarbon constituents typical of recent pollution, whereas surface sediments free of Cs-137 have hydrocarbons typical of unpolluted marsh sources (Wehmiller, personal communication). In lake sediments, the distribution of Cs-137 has been shown to be nonuniform in large lakes and to be closely related to that of fallout Pu-239,240 (Edgington *et al.* 1976).

The concentration of a number of reactive pollutants in Hudson estuary sediments, although extremely variable in both surface and depth distributions, has been shown to have considerable coherence from one pollutant to another and to have a strong correlation with Cs-137. Thus the task of mapping contaminated sediment distributions in complicated sedimentary regimes can be simplified through the use of a "natural" tracer, Cs-137.

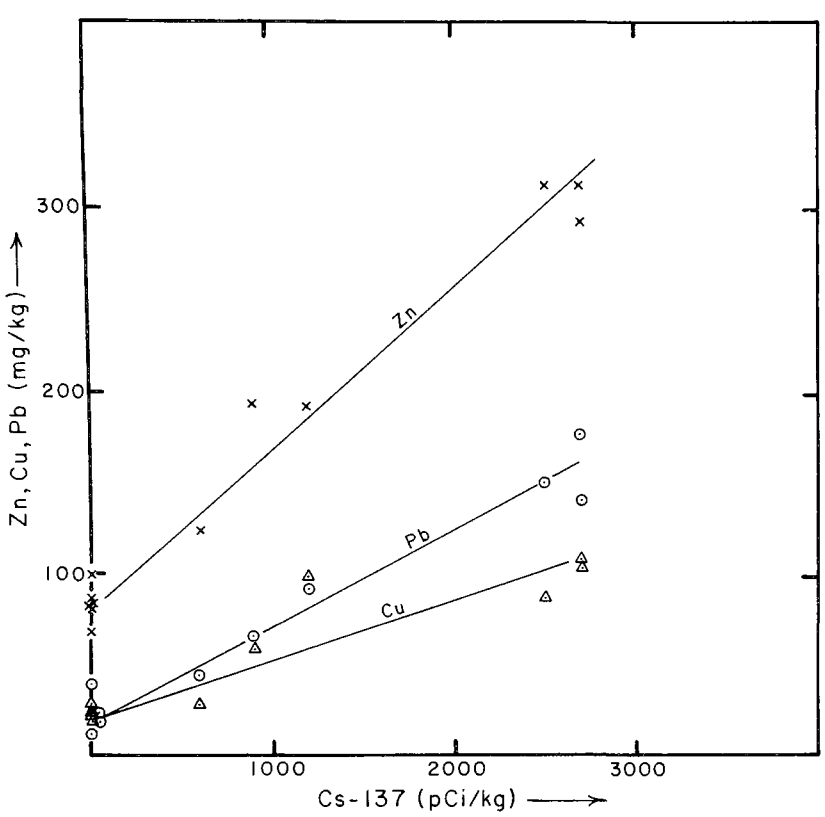

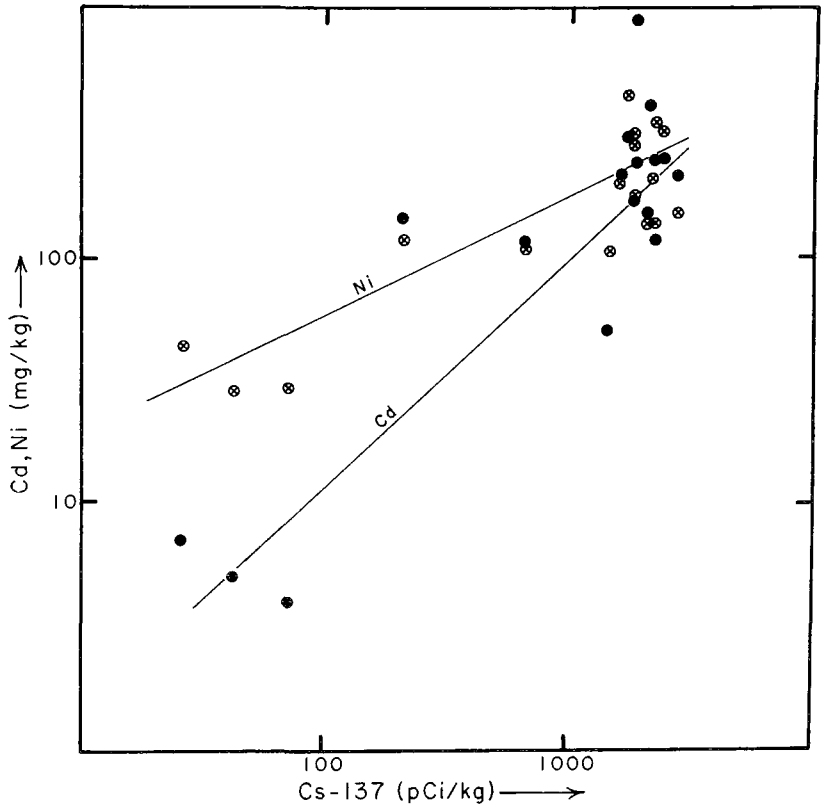

Figure 27. Activities of ^{137}Cs and concentrations of zinc (X), copper (▲) and lead (○) in sediments (Figure 24) from both surface samples and samples well below the sediment-water interface.

Figure 28. Activities of ^{137}Cs and concentrations of cadmium (●) and nickel (⊗) in sediments from the least contaminated area of Foundry Cove (Figure 24).

SECTION 7

RADIOCARBON GEOCHEMISTRY IN THE ESTUARY OF THE HUDSON RIVER

INTRODUCTION

Estuaries can be characterized as complex, three-dimensional zones of mixing of river water and sea water in semi-enclosed areas bounded by land surfaces. Many processes in estuaries are variable on several scales in both time and space. Since a number of estuaries have become the sites of major population centers, the spectrum of natural estuarine processes is now often intricately interwoven with the effects of urban industrial activities. Thus, estuarine processes are important not only to understanding natural chemical cycles but also for management of activities as diverse as disposal of sewage and industrial wastes and maintenance of adequate navigation depths in rapidly shoaling harbors.

Although radiocarbon (C-14) has been extensively used in reconstructing sedimentation history in estuaries, especially over the period since the end of the last glacial maximum, it has been exploited in relatively few studies of processes in urban estuaries. One type of tracer application which has been made is in studies of organic material in aqueous systems significantly perturbed by man (Rosen and Rubin, 1964; Kolle et al., 1972; Zafiriou, 1973; Erlenkeuser et al., 1974; Spiker, 1976; Spiker and Rubin, 1975; Wakeham and Carpenter, 1976). Another potentially valuable application is in establishing the rate of gas exchange between the atmosphere and estuarine waters, one of the critical processes in maintaining the balance of oxygen in estuaries receiving large amounts of sewage.

There are a number of factors which make the distribution of C-14 in estuarine sediments difficult to interpret. Sediment accumulation patterns tend to be complex, with large variations in net deposition rates from area to area within an estuary and considerable reworking and movement of materials likely to occur after they reach the sediment surface. In addition, dredging activities can greatly perturb natural sediment deposition patterns (Simmons and Hermann, 1972). Thus the apparent C-14 age of carbon in sediments is likely to be a complicated function of the deposition and reworking history of the sediment. In many estuaries, most of the carbon in fine-grained sediment is in organic matter, as opposed to calcium carbonate shells or detrital carbonate from the drainage basin. This presents additional difficulty due to the number of important sources of organic carbon in estuarine sediments. Even carbonate shells, which are probably more desirable as dating materials for estimating accumulation rates of estuarine sediments, also present difficulty in interpretation. Fresh water dissolved inorganic carbon in many lakes (Deevey et al., 1954) and rivers (Broecker and

Walton, 1965) has long been known to be deficient in C-14 relative to the atmosphere. Estuaries can also be expected to have C-14 deficient inorganic carbon. The magnitude of the effect is a function of the proportion of weathering of carbonate rocks relative to silicate rocks which occurs in the drainage basin, and the degree of equilibrium with atmospheric C-14 by gas exchange which is accomplished in the riverine (Broecker and Walton, 1959) and estuarine portions of the system. The extent to which carbonate shells reflect the carbon isotopic ratio of dissolved inorganic carbon is somewhat in question (Keith and Anderson, 1963; Rubin and Taylor, 1963; Broecker, 1964; Keith, Anderson and Eichler, 1964; Mook and Vogel, 1968; Fritz and Poplawski, 1974) but appears less of a source of uncertainty than other factors in estuarine systems. Equilibration of the C-14/C-12 ratio of fossil estuarine carbonate shells with dissolved inorganic carbon cannot be directly verified by studies of currently-forming carbonate shells because of the presence in the atmosphere and aqueous carbon systems of C-14 produced from atmospheric testing of nuclear weapons. This perturbation does, however, provide additional opportunities for using bomb C-14 as an estuarine tracer.

HUDSON ESTUARY MORPHOLOGY AND SEDIMENTATION HISTORY

Estuaries are transitory coastline features produced primarily by the rapid rise in sea level as ice melted following the most recent maximum of continental glaciation ($\sim$ 18,000 B.P.). Along the eastern coast of the United States, much of the detrital load of rivers settles out before reaching the continental shelf (Emery, 1967), the estuaries of the isostatically-more stable southeastern U.S. coastline becoming filled with sediments to a greater extent than those farther north (Mead, 1969).

The Hudson River (Figure 29) is tidal for approximately 250 kilometers between New York City and a dam located north of Albany, New York. Upstream of the tidal waters, fresh water is derived from two main sources, the upper Hudson River draining crystalline rocks of the Adirondack mountains and the Mohawk River flowing through sedimentary terrain with large areas of carbonate rocks as well as evaporites. About two thirds of the total fresh water runoff of the Hudson is derived upstream of tidal waters, and much of the dissolved inorganic carbon comes from the Mohawk. Mean annual discharge of the Hudson to New York harbor is about 550 m^3/sec, with monthly means usually ranging between 150 m^3/sec and 1500 m^3/sec. Saline water intrudes one-third to one-half of the total reach of tidal water during low fresh water flow but occupies only the area downstream of the northern end of Manhattan Island during seasonal high flow. Upstream of the southern tip of Manhattan (mile point 0), the Hudson has a remarkably constant total cross-sectional area for approximately half of the reach to the head of tidal influence, despite the fact that the channel transects at least four quite distinct geomorphic provinces (see Sanders, 1974). Downstream of mile point (mp) 0, to the mouth of the estuary at approximately mp -15, the geometry is extremely complex, and includes a number of tidal straits connecting several segments of New York harbor with the New York Bight and Long Island Sound.

The entire Hudson channel is believed to have been excavated by fluvial processes during the Tertiary, and over-deepened by ice scouring during the glacial maxima (Lovegreen, 1974). Downstream from about mp 100, where basement lies about 60 meters below current sea level, the bedrock channel

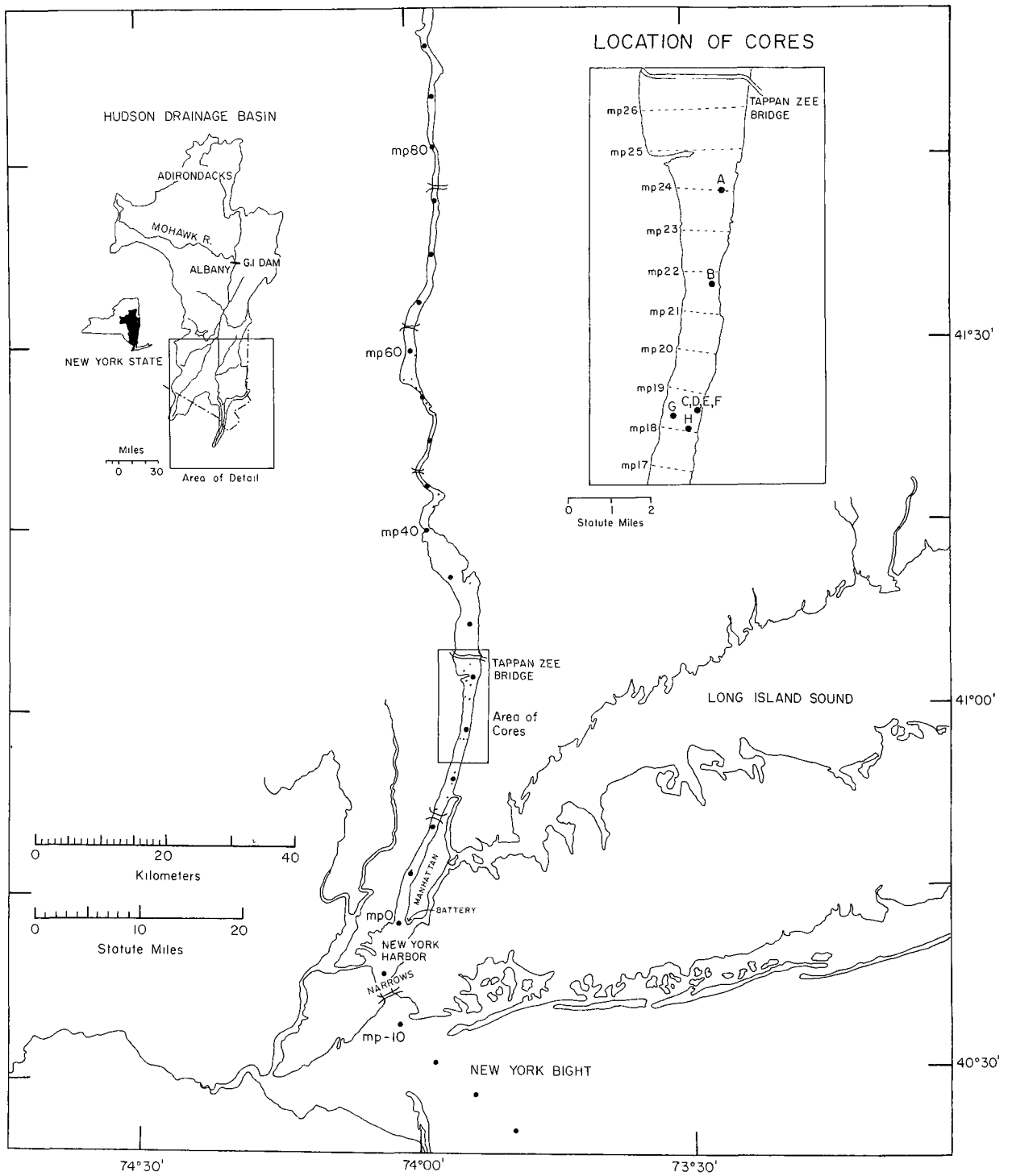

Figure 29. Location of cores for which ^{14}C data are reported in shell layers.

deepens to about 200 meters between mp 50 and 20 (Worzel and Drake, 1959) and then shallows again to about 60 meters at the Narrows (mp -6), indicating that the Hudson estuary probably should be described as a fjord (Newman et al., 1969) which is now largely filled with sediment. Seismic profiles (Worzel and Drake, 1959) and boring information (Wiess, 1974; Newman et al., 1969) have established the general nature of the material accumulated in the Hudson since ice scouring ceased. The lower fill is glacial drift, consisting of gravels and till, which is overlain in most borings by one or more sequences of lacustrine varved sediments representing 2000-3000 years of accumulation. The lake sediments were apparently formed when a terminal moraine crossing the Narrows near the mouth of the present estuary served to dam up the glacial melt waters. The uppermost layer of sediments is estuarine organic silt, representing in most sections a third or less of the total sediment thickness. The oldest reported C-14 dates of fill materials are 12-13,000 radiocarbon years (Newman et al., 1969) for peats formed at the base of the estuarine silt accumulation. Newman et al. (1969) believe that there was a substantial errosional event between the end of lacustrine sediment deposition and the onset of estuarine silt accumulation, possibly related to a catastrophic decanting of the large proglacial lake(s) occupying the Hudson Valley. The deposits of estuarine silt are generally continuous between the top of the lacustrine sediments and the present sediment surface. The total thickness of estuarine organic silt is generally between 10 and 60 meters, with the greatest accumulation in areas with deepest bedrock. Pollen zonation and a limited number of C-14 dates from samples of engineering borings have been used to establish the history of silt accumulation and foraminifera assemblages have been used to delineate the variations in mean salinity intrusion since estuarine conditions were established (Newman et al., 1969; Weiss, 1974). The published data are not sufficient to establish a detailed history of sedimentation of estuarine silts, but accumulation rates appear to have been reasonably uniform with time. Assuming a mean total accumulation of 30 meters of estuarine sediment in 10-12,000 years, the sedimentation rate in the Hudson estuary averaged over the Holocene has been about 3 mm/yr.

There have been major perturbations of the sedimentary regime of the Hudson over the past century. During the past 70 years, extensive dredging has occurred in New York harbor mostly between the mouth of the estuary (mp -15) and mp 12. Initially, dredging was primarily for deepening of docking facilities and some navigation channels, but during the past twenty years or so, sediment removal has been largely directed at maintaining the present harbor depth in the face of rapid shoaling in a few zones, especially between mp 0 and mp 12 (Panuzio, 1965). Dredging activities since World War II have annually removed on the average about 4 million metric tons (dry weight) (Panuzio, 1965; Gross, 1972). Dredging in the main channel of the Hudson outside of New York harbor has been confined to a few areas. The most extensive was in the tidal river reach of the Hudson north of mp 100 to allow Albany to be developed as a port for deep water vessels.

During the past few years we have obtained a considerable amount of information about recent (last two decades) sediment accumulation in the Hudson by measuring the distribution of cesium-137 in sediments (Olsen et al., 1978). This nuclide has been supplied to the Hudson since the middle 1950's by global fallout from nuclear weapons testing, with peak delivery from rainfall during the years 1963-1965, and since the middle 1960's by low-level

releases from a commercial nuclear power plant located at mp 43, with peak discharges in 1971-1972 (Simpson et al., 1976). The relative contributions of fallout and reactor Cs-137 can be estimated from the activities in the sediments of Cs-134 and Co-60, both of which were derived almost exclusively from the reactor. Using Cs-137, which is found in the fine-grained estuarine sediments of the Hudson in readily-measurable activities, as an indicator of sediments which have been in contact with the water column during the past two decades, we have mapped the accumulation pattern of recent sediments. Deposition rates range over approximately two orders of magnitude, with New York harbor between mp 10 and mp -2 being the dominant zone of sedimentation, having accumulations of 10-20 cm/yr of fine-grained particles over large areas of the harbor. Outside of the harbor, recent net deposition rates are considerably less than a cm/yr over most of the total area, with marginal coves between mp 56 and mp 43 and areas of the western side of the broad reach of the estuary between mp 40 and mp 20 having accumulations of up to a few cm/yr. Downstream migration of remobilized fine sediment particles from mp 40 to mp 20 in the harbor occurs on the time scale of a few years, as indicated by the history of arrival in the harbor of Cs-137 released at the reactor site at mp 43. Thus, present sediment accumulation patterns in the Hudson estuary are extremely variable, ranging from areas of active scour and little net deposition to those in which dredging is employed to maintain channel depths in zones accumulating sediment at a rate two orders of magnitude greater than the average accumulation rate over the past 10,000 years.

SAMPLE DESCRIPTION AND PREPARATION PROCEDURES FOR HUDSON RADIOCARBON MEASUREMENTS

We have determined C-14/C-12 ratios in several types of samples from the Hudson: (1) dissolved inorganic carbon from above the upstream end of tidal water (mp 154) to the coastal waters adjacent to the mouth of the Hudson estuary; (2) organic matter from sediments between mp 41 and mp 0, and in recent sewage sludge; (3) shells from sediment cores in a restricted reach of the estuary between mp 24 and mp 18, plus shells collected from the fresh water reach of the tidal Hudson in 1887.

Data are reported in Table 13 for the C-14/C-12 ratio in dissolved inorganic carbon in a number of large water samples (100-200 liters) from the Hudson collected during the last several years. Suspended particles were usually removed from the samples with a high flow continuous centrifuge and carbon dioxide was chemically precipitated in concentrated NaOH with a closed circulating gas system after acidifying the centrifuged water samples. Counting data are given in terms of δC-14 in which:

$$\delta\text{C-14 } (^\circ/_{oo}) = \frac{(\text{C-14/C-12})_{\text{sample}} - (\text{C-14/C-12})_{\text{standard}}}{(\text{C-14/C-12})_{\text{standard}}} \times 1000$$

The standard for which our data are reported is modern wood (0.95 x NBS Oxalic Acid Standard). In this notation, modern wood, free of bomb C-14, would have δC-14 = $0^\circ/_{oo}$, a sample with no C-14 would have δC-14 = $-1000^\circ/_{oo}$ and the atmosphere in 1975 had a δC-14 of approximately $+400^\circ/_{oo}$ due to the presence of bomb C-14. The standard error (1σ) we have quoted is based on counting statistics and variations in the background characteristics of our

TABLE 13

C^{14} Measurements of Inorganic Carbon in Water Samples from the Hudson River Drainage Basin

Lamont-Doherty Sample No.	Sample Description	Collection Date	δC^{14} (‰)	δC^{13} (‰)
1439 G	Mohawk River	10/3/76	+ 120 ± 17	
1439 H	Upper Hudson River	10/3/76	+ 151 ± 18	
1439 C	Hudson River (mp 61; S=0‰)	7/30/76	+ 140 ± 17	
1439 A	Hudson Estuary (mp 18; S∿5‰)	7/28/76	+ 200 ± 17	
1439 B	Hudson Estuary (mp 18; S∿5‰)	7/29/76	+ 191 ± 17	
1439 D	Hudson Estuary (mp -7; S∿24‰)	8/2/76	+ 171 ± 17	
1439 E[a]	Coastal Seawater (Barnegat Lighthouse) (S∿31‰)	8/5/76	+ 155 ± 17	
1371 B	Hudson River (mp 75; S=0‰)	9/9/74	+ 195 ± 23	- 9.8
1371 A	Hudson Estuary (mp 18; S∿12‰)	5/30/74	+ 367 ± 14	- 8.2

a) This sample was from nearshore coastal waters ∿ 100 km south of the mouth of the Hudson Estuary

counters. Stable carbon isotope ratios for all of our samples were measured on splits of the purified CO_2 used for C-14 countings and not from a separate preparation. The δC-13 data are quoted relative to the PDB-scale (Craig, 1957) with standard errors of replicates approximately $\pm$ 0.2°/₀₀, not including fractionation and effects during the CO_2 separation and purification. All of the water samples had δC-14 values greater than modern (0°/₀₀) and thus contained appreciable bomb C-14. Most of the reported data were from a relatively short period of time and are indicative of the water column inorganic carbon C-14 for 1976 during flow conditions somewhat less than mean annual flow.

Samples of organic matter in surface sediments from three sites in the Hudson estuary were analyzed for C-14 (Table 14). All of the organic matter samples were leached with dilute acid (2% HCl) to remove carbonates and dilute base (2% NaOH) to remove humic acids before burning to collect carbon dioxide from the residual organics. The humic acid fraction of two of the samples were also analyzed for C-14. These fractions from mp 41 and mp 18 yielded apparent C-14 ages of 1500-1900 radiocarbon years, while the residual organics had apparent C-14 ages of 4100-4600 radiocarbon years. Sediment organic matter from a rapidly shoaling area of New York harbor (mp 0) and sewage sludge (preparation of this sample did not include treatment with acid and base) from a New York City secondary treatment plant both had appreciable bomb C-14, yielding future ages when expressed in terms of C-14 dates.

Carbonate shell materials are not common in Hudson sediments. We have collected gravity cores ($\sim$ 0.5 meter length) at approximately a hundred sites in the Hudson between mp 60 and mp -2 and have found only one zone with significant shell material. This area, between mp 24 and mp 18, currently appears to have little net accumulation of fine-grained recent sediment except on the shallow subtidal bank along the western shore, based on the distribution of Cs-137 in the sediment (Simpson *et al.*, 1976). Considerable net downstream transport of fine particles bearing Cs-137 occurs through this reach, but the main channel is predominantly covered by a coarse sand lag deposit. The main channel is not an area of active dredging, and is deeper ($>$ 15 meters) than the project depths maintained by the Corps of Engineers in New York harbor. Near the navigation channel of the Hudson between mp 24 and mp 18 we have observed a number of distinct subsurface shell layers, up to 10 cm in thickness. These layers consist almost exclusively of many single valves of *Mulinia lateralis*, a small marine mollusk, and coarse sand fragments, predominantly quartz. At several sites containing shell layers, we collected a number of duplicate $\sim$ 0.5 meter gravity cores, a few small diameter 3 meter piston cores and two 6 meter piston cores, the latter from Lamont-Doherty's oceanographic vessel VEMA. In general, the shell layers are lenticular and appear to be continuous only on a horizontal scale of less than 50 meters, and cannot be visually correlated between cores except when duplicate cores are collected or precisely located sites are reoccupied.

The locations of the sediment samples from which shell materials have been analyzed for C-14 are shown in Figure 29. All but four of the reported samples with C-14 dates between 1000 and 3000 radiocarbon years (Table 15) were from subsurface layers of *Mulinia lateralis*. Four samples consisted of detatched valves of *Macoma balthica* and large oyster fragments (*Crassostrea virginica*) two of which were collected from the top of cores and a third from

TABLE 14

C^{14} Measurements of Organic Carbon in Surface Sediments from the Hudson Estuary

Lamont-Doherty Sample No.	Sample Description	δC^{14} (‰)	δC^{13} (‰)	Apparent Age (Radiocarbon Years)
1378 BH	Humic acid fraction of organic matter (mp 41)	-167 ± 35	-36.1	1470 ± 340
1378 B	Residual organic fraction after removal of humic acids (mp 41)	-403 ± 12	-27.3	4140 ± 160
1378 AH	Humic acid fraction of organic matter (mp 18)	-209 ± 51	-	1890 ± 520
1378 A	Residual organic fraction after removal of humic acids (mp 18)	-436 ± 35	-	4600 ± 500
1378 C	Organic matter - whole sample with no fractions removed (mp 0)	+381 ± 46	-27.4	Future Age
1439 F[a]	Sewage sludge - N.Y. City treatment plant (1975)	+226 ± 17	-	Future Age

a) This sample was from the Ward's Island Sewage Treatment Plant in New York City and was not a sediment sample from the Hudson.

Table 15

C^{14} Dates of Carbonate Shells from Hudson Sediments[a]

Lamont Sample No.	Core No.	Core Location (mp)	Depth (cm)	δC^{14} (‰)	Age (Radiocarbon years)	δC^{13} (‰)	δC^{14} Initial (‰)	Corrected $\delta^* C^{14}$ (‰)	Estimated Minimum Age (yrs)
1363I	A	24	260-270	-315±13	3040±160	-	(-20)±10[d]	-295±16	2810±180
1363D	B	22	35-45	-244±21	2240±230	-11.4	-68±5	-176±22	1550±210
1363C	B	22	130-140	-289±17	2740±190	- 7.2	-43±5	-246±18	2270±190
1363B	B	22	200-210	-310±11	2980±130	- 1.6	-10±5	-300±12	2860±140
1363G	C	18.6	0-5	+455±14	-3010±80	- 3.2	(bomb C^{14})		0-20
1363E	C	18.6	21-23	-148±10	1290±100	- 2.2	-13±5	-135±11	1160±100
1363J	C	18.6	27-31	-149±14	1290±130	-	(-20)±10	-129±17	1110±160
1363F	C	18.6	45-47	-152±14	1320±130	- 4.1	-25±5	-127±15	1090±140
1363K	D	18.6	75-80	-208±14	1880±140	-	(-20)±10	-188±17	1670±170
1363L	E	18.6	110-116	-288±19	2720±220	-	(-20)±10	-268±21	2510±230
1363M	E	18.6	200-212	-138±12	1190±110	-	(-20)±10	-118±16	1010±150
1363N	E	18.6	222-228	-261±30	2430±330	-	(-20)±10	-241±33	2210±350
1387A[b]	F	18.5	0-10	+58±19	-450±150	-	(bomb C^{14})		0-20
1387D	F	18.5	109-111	-130±33	1120±300	-3.1	-19±5	-111±33	950±300
1387C	F	18.5	127-130	-170±13	1490±130	-2.6	-16±5	-154±14	1340±130
1387E	F	18.5	199-201	-241±35	2210±370	-	(-20)±10	-221±36	2010±370
1387B	F	18.5	266-271	-228±26	2080±270	-	(-20)±10	-208±28	1870±280
1363H[c]	G	18.3	0-5	+356±16	-2450±100	-4.2	(bomb C^{14})		0-20
1363A	H	18	137-142	-232±11	2120±110	-2.9	-18±5	-214±12	1930±120
1377A[e]		98	Surface	-76±11	630±100	-11.2	-67±11	-	-

[a] All samples were from discrete subsurface layers of Mulinia lateralis unless otherwise noted.

[b] Core top layer of oyster fragments (Crassostrea virginica) and clam shells (primarily Macoma balthica).

[c] Oyster fragments (C. virginica) and clam valves (M. balthica) from a composite of about a dozen grab samples.

[d] Initial δC^{14} for samples without δC^{13} data were estimated from the observed range of δC^{13} values for similar samples.

[e] Lampsilus radiatus Gmel. (fresh water mollusk) collected by W.S. Treator at Barrytown, New York (mp 98) in 1887.

a surface grab sample. The three surface shell samples all contained bomb C-14, and hence give future ages when expressed as C-14 dates (Table 15). One of the subsurface samples (1387 C) consisted of a single oyster valve and yielded a date of 1490 ± 130 radiocarbon years, in agreement with adjacent layers of Mulinia lateralis. The subsurface shell layers for which dates are reported in Table 15 were obtained during seven separate coring operations. Four of the cores (B, C, E, F) have C-14 dates reported for more than one depth interval in the sediments. Two of the four cores (B, F) which have more than one depth interval dated show increasing ages with depth. Dates from one core (C) were obtained by preparing composite samples for several shell layers from about half a dozen 0.5 meter gravity cores which were collected sequentially while anchored at one site in the estuary. In this core, the surface layer of oyster fragments contains bomb C-14, while the three subsurface layers between 20 and 50 cm have the same age (∿ 1100 years) within the uncertainty of the measurements. One core (E) has an apparent age reversal with depth. We believe the reversal in core E is real, but there is a possibility that it resulted from an error in labeling following extrusion of the core from its plastic liner or during later sampling. Sample G represents a composite of oyster fragments and clam shells from a large number of surface grabs collected while anchored at one site.

We have been able to obtain some fresh water mollusk shells which were collected in 1887 from the Hudson River at mp 98 (tidal fresh water reach of the Hudson). Measurement of C-14 in one sample consisting of about half a dozen large single valves gave an apparent age of 630 ± 100 years (Table 15). The shells were quite fresh in appearance, having their organic coatings intact, and were apparently collected alive.

DISCUSSION

Water column δC-14 values in the Hudson (Table 13) indicate the presence of appreciable bomb C-14 in the inorganic carbon pool, but that complete equilibration with atmospheric C-14 does not occur. Our water samples from 1976 indicate a downstream increase in δC-14, with the highest value (+200°/₀₀) about mp 18, followed by decrease toward the coastal ocean as salinity increased. This decrease is probably largely due to mixing of fresher water with coastal sea water having a lower value of δC-14 (+155°/₀₀). One explanation of the increase of δC-14 downstream to the maximum at +200°/₀₀ is exchange of atmospheric CO_2 with the dissolved CO_2 in the Hudson as water moves downstream. We can estimate the change which might be expected to occur as fresh water with δC-14 of +140°/₀₀ at mp 61 flowed downstream to mp 18, exchanging carbon dioxide with the atmosphere, using an expression derived from Broecker and Walton (1959):

$$(C_A - C_{R_2}) = (C_A - C_{R_1})_e - Rt/kh$$

where C_A = δC-14 of atmospheric carbon dioxide (estimated to be ∿ +400°/₀₀ in 1976)

C_{R_1} = δC-14 of river inorganic carbon at the upstream end of the flow segment of interest (+140°/₀₀)

C_{R_2} = δC-14 of river inorganic carbon at the downstream end of the flow segment of interest (to be calculated)

R = gas exchange rate (estimated to be ≤ 10 moles/m^2/year)

t = time to transect segment of river ($\sim$ 0.1 year at flow conditions of $\sim$ 400 m^3/sec and volume of channel $\sim$ 1.1 x 10^9 m^3)
k = concentration of total inorganic carbon in Hudson ($\sim$ 1 mole/m^3)
h = mean depth ($\sim$ 10 meters)

If atmospheric δC-14 was +400°/$_{oo}$, the dissolved inorganic carbon would increase from +140°/$_{oo}$ to +164°/$_{oo}$ as the Hudson flowed between mp 61 and mp 18, assuming only downstream advective flow. Our measured data indicates higher than predicted δC-14 for mp 18 (average of two samples = +195°/$_{oo}$). There are several possibilities which could explain the data. We do not have a well established value for the δC-14 of the atmosphere in 1976 which was used in our calculation (+400°/$_{oo}$), but it is not likely that the actual value is significantly higher than the one we used, and thus cannot explain the higher value at mp 18 than predicted from our gas exchange calculation. We obtained our value of +400°/$_{oo}$ by extrapolating the trend of Rafter and O'Brien (1972) beyond 1972. Published tree-ring data (Cain and Suess, 1976) from adjacent to Hudson (Bear Mountain, $\sim$ mp 45) in 1970 and a value of +413 $\pm$ 12°/$_{oo}$ reported for atmospheric C-14 in Monaco in 1975 (Rapaire and Hugues, 1977) are in good agreement with the trend of Rafter and O'Brien (1972). Another potential explanation is that the actual gas exchange could be greater than the first order estimate we made of 10 moles/m^2/yr, but this does not seem very likely in light of observed gas exchange rates in marine and fresh water systems (Broecker and Peng, 1974; Emerson, 1975). The gas exchange rate which we used is that derived by Broecker and Peng (1974) as an average for the world ocean (equivalent to a stagnant boundary layer thickness of 50 microns in a one parameter gas exchange model). Most other published estimates of carbon dioxide exchange rates in the ocean based on the distribution of natural C-14 and bomb C-14 (see Broecker and Peng, 1974 for references), have ranged between a factor of 2-3 faster down to a value approximating that used here. Thus the value we have used is a reasonable upper limit for the Hudson, and the most probable value for summertime gas exchange rates is approximately half of that used for the calculations reported here (Hammond et al., 1977).

We can also calculate the expected effect of gas exchange on δC-14 in the Hudson as water moves downstream from the head of tidal water (mp 154) to mp 61. From the δC-14 data in the Mohawk and Upper Hudson for early October, the δC-14 of water in the Hudson was probably about +125°/$_{oo}$, since the Mohawk supplies more than two thirds of the dissolved inorganic carbon to the water entering the tidal Hudson at the upstream end. Using C_A = +40°/$_{oo}$, C_R = +125°/$_{oo}$, R = 10 moles/m^2/year, t = 0.09 year (flow conditions in October were also $\sim$ 400 m^3/sec and volume of $\sim$ 1.0 x 10^9 m^3 between mp 154 and mp 61), k = 1 mole/m^3, h = 7.5 meters, the calculated δC-14 value at C_R (mp 61) is +157°/$_{oo}$, which is greater than the measured value of +140°/$_{oo}$. If we were to use a model gas exchange rate of 5 moles/m^2/yr measured and calculated δC-14 would agree. If the total change in δC-14 between mp 154 (+125) and mp 18 due to gas echange were estimated from the same parameters as used for the two segments of the total length (R = 10 moles/m^2/yr), the calculated δC-14 value at mp 18 would be +176°/$_{oo}$, compared with a measured value of +195. Thus the change in δC-14 measured between two points near the extreme ends of the tidal Hudson is the right order of magnitude to be produced primarily by gas exchange with the atmosphere, but the rate of change indicated near the downstream end appears substantially higher, suggesting the possibility of a second important mechanism for increasing δC-14

in the dissolved inorganic carbon in the water column near New York City. Oxidation of sewage particles, which have a higher C-14/C-12 ratio than inorganic carbon in the Hudson, seems likely to be important in the C-14 budget of the dissolved inorganic carbon the estuarine reach of the Hudson near New York harbor. Two other measurements of dissolved inorganic carbon δC-14 are reported for 1974 (Table 13). These two samples were collected at different times and with differing flow conditions (May $\sim$ 950 m^3/sec, September $\sim$ 400 m^3/sec) and thus are not nearly as useful for gas exchange calculations as 1976 data. Both of the 1974 samples had higher δC-14 than samples collected at similar locations in 1976.

Spiker and Rubin (1975) have found the proportion of C-14 in dissolved organic carbon in a number of streams to be dependent upon the amount of domestic sewage wastes and industrial fossil fuel wastes dicharged. They calculated the proportion of fossil carbon in the dissolved organic carbon assuming the contribution of dissolved organic carbon from other sources, including municipal wastes, had a C-14/C-12 ratio equivalent to the present atmosphere. Our data indicate that the discharge of municipal wastes also affects inorganic carbon δC-14 and tends to bring the water column values toward equilibrium with the atmosphere. Kolle et al. (1972) attributed downstream increases in C-14/C-12 in the inorganic carbon of the Rhine River to the oxidation of municipal wastes dominated by sewage. The downstream trends of C-14/C-12 in the Rhine are complicated and difficult to interpret in detail because of the contribution of large quantities of industrial contamination of C-14 free carbon. In the Hudson, the primary locus of both sewage and industrial discharge is adjacent to New York City and the level of pollutant carbon loading to the tidal river section of the Hudson north of this is relatively low. A sediment sample from New York harbor (mp 0, Table 14) had a δC-14 value of $+381°/_{oo}$, indicating a significantly higher component of bomb C-14 than we observed in our water column inorganic carbon measurements. Sewage sludge from one of the dozen or so large treatment plants in the New York City area also had appreciable bomb C-14 (Table 14, $+226°/_{oo}$). Very large discharges of sewage are made to the harbor complex ($\sim$ 100 m^3/sec) from a number of point sources (Simpson et al., 1975). Fine-grained sediments from the harbor lose about 8% of their weight upon heating from 100°C to 500°C overnight, while sediments farther upstream lose only about 4% of their original weight. The sediments near New York City have approximately twice as much organic carbon as average Hudson sediments, and a much higher fraction of recent sewage organic particles, based on the C-14 data reported in Table 14. The levels of algal growth in the Hudson estuary are surprisingly low (Malone, 1976; Simpson et al., 1976B) and cannot contribute a significant proportion of the organic particles in harbor sediments compared with sewage.

The old apparent C-14 ages of organic matter in surface sediments of the Hudson upstream of the harbor (mp 41, mp 18, Table 14) are not simple to explain. The ages we observed are comparable to those reported for surface sediments in the Baltic Sea (Erlenkeuser et al., 1974) and Lake Washington (Wakehom and Carpenter, 1976), and somewhat younger than reported for Narragansett Bay (Zafiriou, 1973). In the Baltic, the apparent age of organic matter in surface sediments extrapolated from deeper sediments free of recent trace metal contamination was $\sim$ 800 years, but the measured apparent age of one site was $\sim$ 2000 years. The apparent increase in age of surface sediments was attributed to recent fossil fuel contamination, primarily coal. In Lake

Washington and Narragansett Bay, the contamination was assumed to be primarily petroleum hydrocarbons. In the Hudson, based on our knowledge of general sediment accumulation and pollutant discharge patterns we would expect the extent of fossil fuel contamination to be greater at mp 0 than at mp 41. Recent unpublished gas chromatography data on solvent extracts of Hudson sediments suggest that a higher proportion of the normal hydrocarbons upstream of the harbor area are natural, whereas the harbor sediments are dominated by a complex mixture of unresolved peaks (J. Wehmiller and E. Keenan, personal communication). The weight fraction of a total pentane extract (TPE) and normal hydrocarbons (NH) in the harbor sediment sample analyzed for C-14 (mp 0) are greater (TPE = 0.8%, NH $\leq$ 0.15%) than the weight fractions in the upstream sample (mp 41) analyzed for C-14 (TPE = 0.32%, NH $\leq$ 0.057%). Thus our chemical data suggest a greater extent of recent petroleum pollution at mp 0 than in the sample at mp 41, yet the apparent C-14 age is much older in the upstream sample, the opposite of that which would be predicted if recent petroleum pollution were dominant in the C-14 data. Both of the samples we analyzed have higher weight fractions of hydrocarbons than the surface sediments of Lake Washington, and thus are definitely contaminated with fossil fuel carbon. However, in the harbor sediments, despite the highest level of hydrocarbon contamination in our samples, the effect on bulk organic carbon C-14 dates is overwhelmed by recent sewage organic particles.

The C-14 data on fossil carbonate shells reported in Table 15 present a substantial geochemical problem in interpretation. The apparent ages, except for the three surface samples of oyster fragments containing bomb C-14, are all between $\sim$ 1000 and $\sim$ 3000 radiocarbon years. Apparent ages of this magnitude have been found for modern carbonate shells in fresh waters (Broecker and Walton, 1959; Keith and Anderson, 1963; Rubin and Taylor, 1963). We believe the shell layers in Hudson sediments that we analyzed for C-14 to have been deposited prior to the last 50-100 years, and were probably formed up to several thousand years ago. We will present several qualitative arguments in support of the above statement, and one semi-quantitative approach to estimating the true time of growth of the estuarine carbonate shells we analyzed.

During a recent study of trace metal concentrations (Zn, Cu and Pb) in Hudson sediments, we have been able to establish good estimates of pre-industrial heavy metals in this estuary. Samples from the longest core reported here (F) have "base-line" heavy metal concentrations below the upper 20 cm. All of the subsurface C-14 data on this core are found between laminated layers of fine-grained sediment with no recent metal contamination. These data are the strongest evidence we have that if reworking of the carbonate layers has occurred, it predated the period of heavy metal contamination which presumably has occurred over at least the last 50 years.

Modern fresh water carbonate shells with apparent C-14 ages of several thousand years (Broecker and Walton, 1959) generally come from carbonate rock drainage basins, the water of which usually have bicarbonate concentrations on the order of 2 mM or more. The Hudson drainage basin is not, however, predominately carbonates or other sedimentary rocks. The Upper Hudson (bicarbonate $\leq$ 0.3 mM) drains crystalline metamorphic rocks of the Adirondack mountains, and the mean bicarbonate of the Hudson below the confluence with the Mohawk is about 1 mM. Thus, qualitatively one would expect considerably less depletion

of C-14 in Hudson inorganic carbon than that equivalent to an apparent age of a few thousand years. We can make a somewhat more quantitative attempt to estimate the original C-14/C-12 ratio of shells formed in the Hudson Estuary based on our one measurement of carbonate shells formed in the Hudson River at a well-known date prior to the arrival of bomb C-14. If we assume the shells collected in 1887 from mp 98 (Table 15) have a C-14/C-12 ratio (δC-14 = -76°/$_{oo}$, apparent age 630 years) which is representative of the fresh water carbonates formed in the pre-nuclear era Hudson, then after correcting for the known age, an upper limit of 540 years (δC-14 = -67°/$_{oo}$) can be placed on the extent of age correction which should be applied to carbonate shell material formed in the saline reach of the Hudson.

We can also attempt to use stable carbon isotope data for the estuarine carbonates to estimate the original δC-14 of these samples. Fresh water carbonate shells from the Hudson prior to significant sewage pollution probably had a δC-13 value of -11°/$_{oo}$ (Table 15 - assuming the one sample we analyzed from 1887 is typical), whereas carbonate shells formed from surface sea water have δC-14 values of $\sim$ 0°/$_{oo}$. Pre-nuclear era δC-14 in marine carbonates was $\sim$ 0°/$_{oo}$ (Broecker and Olson, 1959; Broecker and Olson, 1961). If δC-14 of shells formed in the saline reach of the pre-nuclear Hudson are assumed to lie on a mixing line between a marine carbonate value of 0°/$_{oo}$ and a fresh water carbonate endmember of -67°/$_{oo}$ (age corrected value of 1887 Hudson shells), and δC-13 of carbonate shells also lie on a mixing line between marine carbonates (0°/$_{oo}$) and fresh water shells from the Hudson (-11°/$_{oo}$), then δC-13 of a carbonate shell layer can be used to estimate the initial δC-14 of that shell layer (see Figure 30). We have applied age corrections by this procedure to all of the dates reported in Table 15. The maximum correction was -690 years, with most of the changes being on the order of -190 years. In the absence of a measured δC-13 value, we estimate the original δC-14 of a sample to be equivalent to about -190 years based on the average δC-13 of similar samples. The uncertainty of the correction for these samples is obviously greater than for the samples for which measured δC-13 values were obtained. Dates corrected for initial δC-14 are plotted in Figures 31 and 32, with the uncorrected dates in radiocarbon years also included to indicate the magnitude of the correction terms. No major changes in estimates of sedimentation rate result from using corrected dates rather than the original dates, except for core B (Figure 31) where the effect is to reduce the estimated sedimentation rate from about 2 mm/yr to about 1 mm/yr.

The procedure we have suggested for estimating original δC-14 of estuarine carbonates is obviously oversimplified in that it ignores a number of processes which could be significant, but it does provide a relatively simple conceptual framework. One weakness to our approach is the assumption that the one sample of pre-bomb fresh water carbonates in the Hudson we analyzed is representative. We cannot support that assumption much beyond the statement that one sample is a whole lot better than none. The magnitude of suggested corrections in original δC-14 would not be greatly altered by choosing another tie point on the δC-13 - δC-14 graph, provided δC-13 and δC-14 were varied roughly parallel to the line drawn. Gas exchange would be the most likely process to cause variation in δC-14 of the fresh water endmember, and as can be seen from the dotted line on Figure 30, the computed effect of gas exchange on δC-13 and δC-14 is similar but not identical to mixing of fresh water with marine bicarbonate. The magnitude of suggested corrections in original δC-14

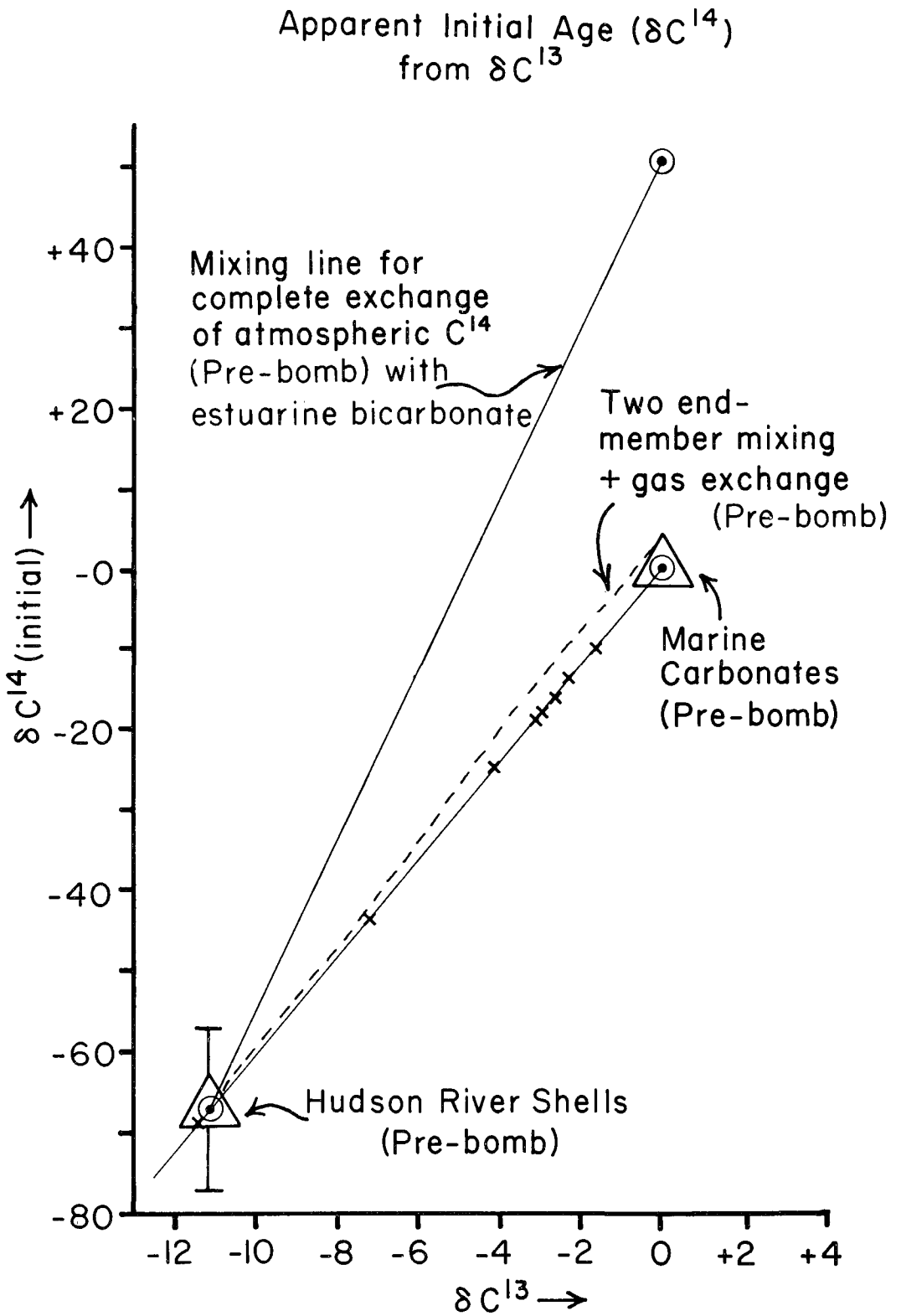

Figure 30. Measured δC^{13} in Hudson Estuary shells can be used to estimate the original δC^{14} value of the estuarine shells, assuming mixing of only two end members. Gas exchange does not cause a major deviation (dashed line) from this mixing line for the Hudson prior to bomb testing.

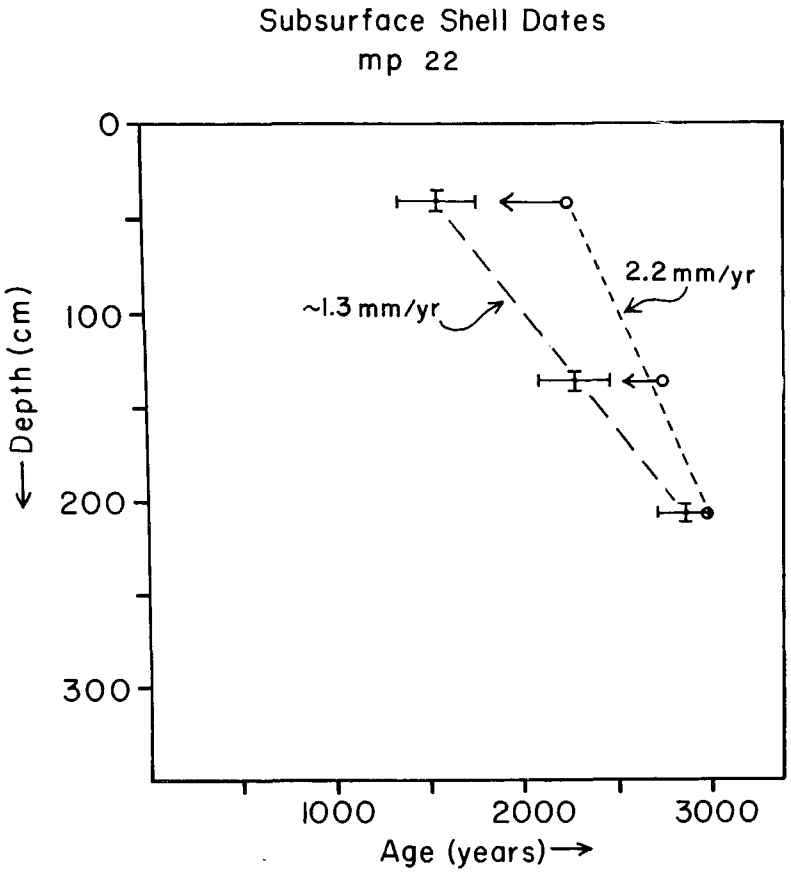

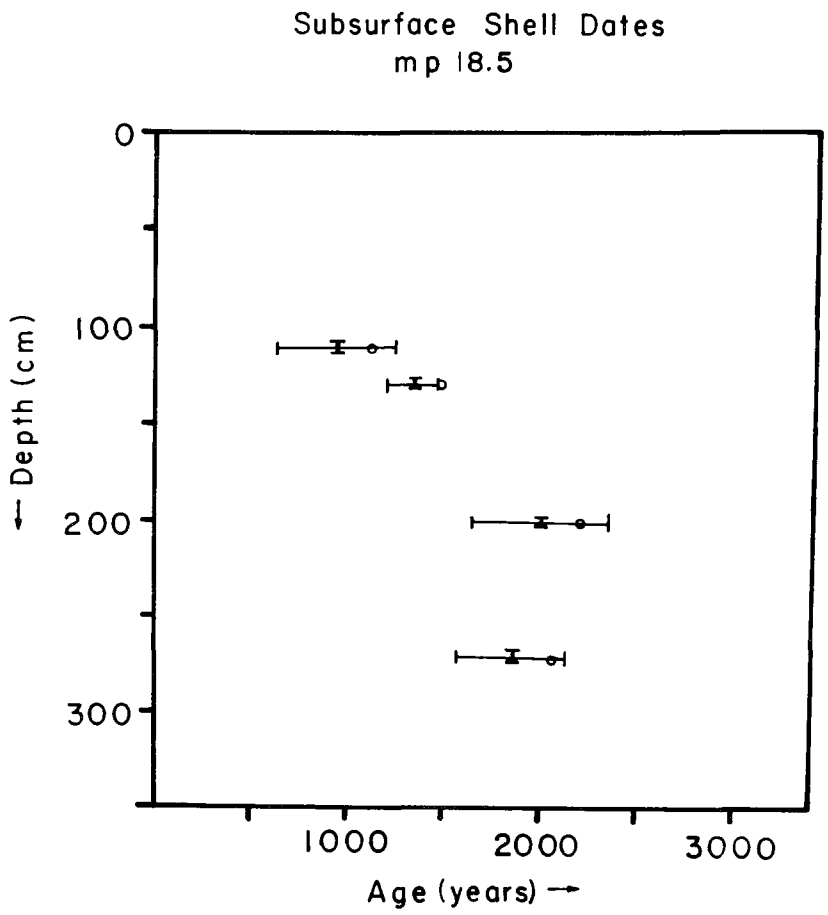

Figure 31. Data points indicated by circles are ages derived from measured radiocarbon values. Data points with error bars were corrected for estimated initial δC^{14} values using δC^{13} (Figure 30). The most probable ages for the shell layers lie between the two plotted ages at each depth.

Figure 32. Symbols have the same meaning as in Figure 31. The core extends another 3 meters below the deepest shell layer.

of the samples in Table 15 is not large compared to the measured δC-14. Thus, changes in the details of Figure 30 would not greatly alter the magnitude of the "corrected" ages.

Another weakness in the approach we have taken in estimating initial δC-14 on the basis of δC-13, is the lack of detailed knowledge of the variation of δC-13 in the Hudson. We have no way to obtain such data for the "pre-pollution" era of interest. Three transects of δC-13 and salinity have been reported for the Hudson in 1963-1964 (Sackett and Moore, 1966). All three of these sets of data have different δC-13 - salinity slopes, but appear to indicate conservative mixing between two endmembers within each data set (Mook and Vogel, 1968). Only one of the salinity transects approached fresh water, and that data set, collected in April 1964, extrapolates to δC-13 = $-9°/_{oo}$ in fresh water, which is certainly compatible with the value of δC-13 = $-11°/_{oo}$ which we used for a location considerably farther up the estuary in the construction of Figure 30.

Another possible perturbation of δC-13 in the Hudson is production of methane and carbon dioxide of greatly different δC-13 than the values we have used for Figure 30. A recent study of methane geochemistry in the Hudson (Hammond and Simpson, 1977) indicates that methane supplied to the water column is derived primarily from methane bubbles produced in the sediments which partially dissolve ($\sim$ 5-10%) on the way up through the water column. Methane oxidation does not occur in the water column to any appreciable extent, and dissolved methane is lost primarily by gas exchange. The total production rate of methane which forms bubbles and passes through the water column is $\sim$ 1.5 mole/m^2/yr. This is an order of magnitude less than our estimate of the gas exchange rate of carbon dioxide in the Hudson. CH_4 is not very likely to significantly perturb inorganic carbon δC-13 since about 90% of the bubble flux passes through the water column without dissolving. Assuming a δC-13 = $-60°/_{oo}$ for CH_4 in the water column and that 1% of the total bubble flux is oxidized (we believe this is a fairly strong upper limit) the effect on the inorganic δC-13 value would be $\sim -0.5°/_{oo}$.

CONCLUSIONS

The dissolved inorganic carbon in the present day (1976) Hudson River and estuary contains appreciable bomb C-14, but is not in equilibrium with atmospheric C-14/C-12 ratios. The downstream increase in δC-14 in the water is compatible with reasonable values of gas exchange rate and physical transport of the water, and thus could conceivably be used to compute gas exchange rates for the Hudson. There appears to be at least one additional mechanism, oxidation of sewage organics, which can significantly increase the δC-14 of the inorganic carbon in the Hudson estuary near New York City.

Surface sediments in New York harbor, despite measurable contamination with petroleum hydrocarbons, have a large component of organic carbon with appreciable bomb C-14, presumably mostly recent sewage particles since primary production of organic carbon in the lower Hudson is an insignificant fraction of the discharge rate of sewage organics. This recent sewage contamination dominates the C-14/C-12 ratio in bulk organic matter in New York harbor sediments, resulting in apparent future C-14 ages of that material as opposed to apparent C-14 ages of a few thousand years in surface sediments in the

Hudson upstream of New York harbor. The mean accumulation rate of sediments in the Hudson since the onset of estuarine condition ∿ 12,000 B.P. has been about 3 ± 2 mm/yr, based on a total accumulation of 10-60 meters. Such a rate of sediment accumulation is approximately the rate of subsidence of the New York area during the last century (Fairbridge and Newman, 1968) and is also compatible with the early Holocene eustatic submergence (0.5 mm/yr). Cores collected in or adjacent to the present main navigation channel of the Hudson between mp 18 and mp 24 penetrate up to several thousand years of sedimeint within a few meters, and sedimentation rates calculated from C-14 dating of subsurface marine shell layers are in the range of 2 ± 1 mm/yr. The age of the tops of these cores, extrapolated from uncorrected C-14 dates of subsurface shell layers, are in the range of 1000 to 2000 radiocarbon years, although oyster and clam shell fragments at the tops of cores contain bomb C-14.

Our best estimate of the pre-bomb C-14 for inorganic carbon in the Hudson estuary indicates a correction of ∿ -200 years should be applied to C-14 dates of estuarine shell materials from the sediments with ages of 1000-3000 years, if no additional information on the initial δC-14 of the sample is available. A simple correction using δC-13 based on two component mixing between surface sea water and fresh Hudson River water can be made. The magnitude of this correction in our sample was as high as ∿ -700 years, but most commonly was on the order of -200 years as suggested above, and thus represents a relatively small change for shell materials with ages of 1000-3000 radiocarbon years. Conceptually, a correction for the effect of gas exchange on δC-14 downstream of the fresh water endmember composition should be included, but equilibration with the pre-bomb atmosphere would have increased the values for both δC-13 and δC-14 of inorganic carbon in the Hudson Estuary in a similar manner as an increased contribution from the sea water endmember.

None of the corrected shell dates we obtained extrapolate to the present at the sediment surface. We collected our cores from an area (mp 18 to mp 24) for which there was no evidence available to us indicating that dredging had occurred, but it is possible that some of the most recent sediment from the core sites had been removed, either by dredging or current scouring, before the recent oyster fragments containing bomb C-14 were accumulated. Another possibility is that sediment accumulation at the core sites had not been appreciable over the past 1000 years or so until quite recently. Sediment in the harbor region (mp 0) is presently accumulating quite rapidly in a number of places. Assuming the dredge spoils of 4×10^6 tons/yr (dry weight) were spread uniformly over the bottom between mp 12 and mp 0, the rate of accumulation would be ∿ 25 cm/yr. We know from dredging records that one large shoaling area has a sediment accumulation rate of at least this value (Panuzio, 1965). We also know from the distribution of other anthropogenic radionuclides (e.g., cesium-137) in harbor sediments that shoaling rates of comparable magnitude (10-20 cm/yr) are found over considerable areas (Simpson *et al.*, 1976). Thus sediment currently accumulating over substantial areas of New York harbor is being deposited at a rate of 10-100 times faster than the mean for the past 12,000 years, and could be expected to bury significant amounts of sewage organic carbon before oxidation could occur (Figure 33).

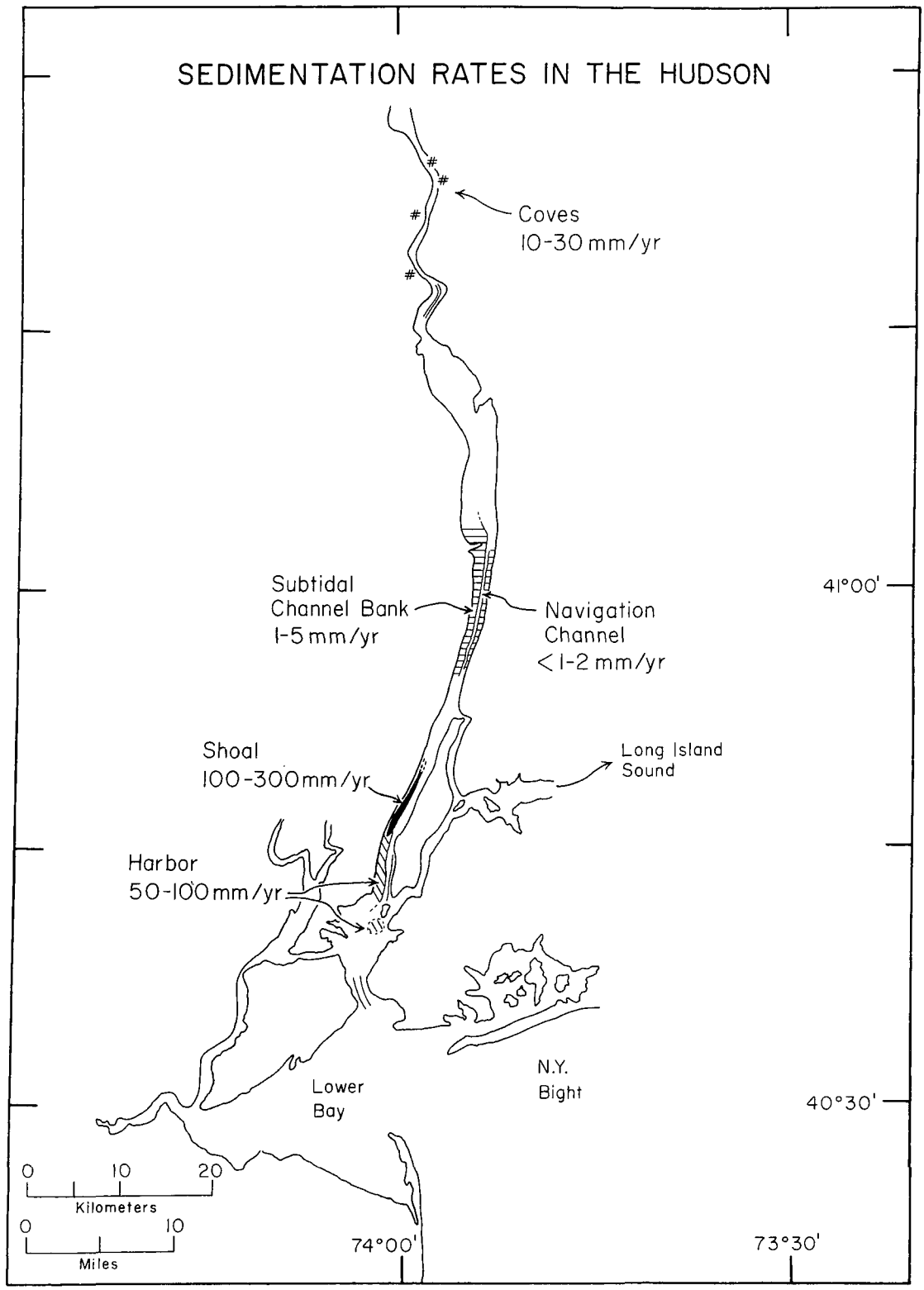

Figure 33. Sedimentation rates in the Hudson from the measured distribution of ^{137}Cs in the sediments.

SECTION 8

A NEW ENZYMATIC METHOD FOR ANALYSIS OF CELLULOSE IN SEDIMENTS

Sediments in natural systems such as estuaries, lakes and the ocean consist of a complicated mixture of materials derived from biological processes, as well as from chemical and physical processes which could be classified as "geological" in origin. The organic fraction (non-calcium carbonate) of sediments ranges from less than a tenth of a percent in slowly accumulating sediments of large areas of the deep ocean up to more than 30% in some lakes. The history of production, preservation and destruction of sedimentary organic matter is strongly dependent on the type of organic compounds involved, as well as on environmental factors. For example, within one group of compounds (the carbohydrates) glucose, a simple sugar, and starch, a polymer consisting of a α-linked glucose monomers, are rapidly cycled by bacterial communities, while cellulose, a polymer consisting of repeating β-linked glucose units, is much less reactive in sediments.

Carbohydrates have been measured in environmental samples at many localities (Lewis and Rakestraw, 1955; Rogers, 1965; Biggs and Wetzel, 1968; Artem'yev, 1970), using relatively simple chemical procedures which have evolved over the past several decades (Dreywood, 1946; Morris, 1948; Dubois et al., 1956; Zein-Eldin and May, 1958; Handa, 1966; Strickland and Parsons, 1968; and Gerchakov and Hatcher, 1972). These are based on forming colored solutions by the reaction of simple sugars or polysaccharides with anthrone or phenol or similar reagents in sulfuric acid. The anthrone and phenol and other similar procedures provide some measure of the total carbohydrate content of a sample, including a substantial variety of both monomeric and polymerized carbohydrates. Pre-treatment with acid and base leaches can be used to remove water-soluble monomeric carbohydrates (Strickland and Parsons, 1968). Thus the same analytical procedure can be used to measure two operationally-defined quantities, "total carbohydrates" and "crude fiber", the latter including what is left after strong acid and base leaches.

The amount and type of compounds present in sedimentary organic matter can be expected to vary substantially, depending upon the original source of the organic matter and upon processes occurring after deposition in the sediment. Our present knowledge of the details of source composition and post-depositional changes of sedimentary organic matter is very primitive. This is perhaps to be expected, considering the structural complexity and range of compounds encompassed by environmental organic materials included under terms such as "humic acids". One additional factor which tends to perpetuate the present level of understanding is the collection of laboratory data with analytical techniques which aggregate a large range of compounds into one measurement. Thus a measurement of "total carbohydrates" provides a convenient

indicator of the amount of one large class of organic molecules which could make up anywhere from a few percent to more than one half the carbon content of a sample of sediment, but it incorporates a tremendous range of compounds, some of which are monomers with molecular weights on the order of a few hundred, while others are highly polymerized, having molecular weight in the millions.

We have developed a new analytical technique, based on the use of a sequence of enzymes, to measure cellulose in sediments. This technique introduces a new type of analytical approach to the study of sedimentary organic matter, and provides a procedure for the measurement of one specific type of highly polymerized carbohydrates which is an important, relatively stable component of most recent sediments. Use of enzymes in analytical procedures is common in biochemical research and in routine biomedical laboratory tests, but has not, to our knowledge, been previously exploited in organic geochemistry.

One possible application of the enzymatic analytical method for cellulose we have developed is for establishing the amount of sewage sludge in sediments. Sewage sludge contains large amounts of cellulose (Hunter and Heukelekian, 1965), which potentially could be used as a very sensitive indicator of the presence of such pollutants. Total carbohydrate measurements have already been made in the area of the coastal ocean near New York City (Hatcher and Keister, 1976) in an attempt to map the present distribution of sewage sludge which has been discharged for a number of decades into a dumping zone about 15 kilometers from the mouth of the Hudson River estuary.

METHODS

Chemical methods for carbohydrate measurements in environmental samples use strong acid solutions to break up polymers and produce colored complexes of basically unknown structure, using reagents such as anthrone or phenol. These methods are nonspecific and have varying sensitivities, depending upon the type of sugar monomer. Interference from non-carbohydrate materials occurs, and empirical corrections for these effects must be made.

Cellulose may be hydrolyzed enzymatically under mild conditions of temperature and pH. Cellulytic enzymes cleave only the β-D-(1→4) glucosidic bonds linking the glucose units, and act only on cellulose and certain of its derivatives. Enzymatic hydrolysis, therefore, lends itself to the selective analysis of one type of compound, leaving other components of the system unaltered.

Materials

- Extracting acid: 20 ml of concentrated H_2SO_4 added to distilled water and brought to a total volume of 1 liter.

- Extracting base: 25 g of NaOH added to distilled water and brought to a total volume of 1 liter.

- Acetate buffer: 0.05 M, pH 5.0.

- Glucose stock solution: 1 g β-D-glucose (Fisher Chemical Company) was dissolved in acetate buffer and diluted to make 1 liter of stock solution (1 mg/ml).

- Glucostat Reagent Set (Worthington Biochemical Company).

- High activity cellulase, lyophilized preparation from Trichoderma viride (obtained from Dr. E.T. Reese, U.S. Army Labs, Natick, Massachusetts, Lot No. 9414). Prepared by dissolving 400 mg of enzyme in acetate buffer and diluting with buffer to 200 ml.

- Redistilled chloroform.

- Avicel microcrystalline cellulose, TG 101 (FMC Corporation).

Pretreatment of Samples

Sediments were dried and ground with mortar and pestle. Approximately 800 mg of sediment was weighed out for each sample and transferred to 100 x 18 mm polypropylene centrifuge tubes. Extracting acid (10 ml) was added and the tubes were thoroughly mixed by shaking and stirring, and placed in a boiling water bath for 30 minutes, after which the tubes were centrifuged for 15 minutes at 15,000 RPM. Supernatant was removed by vacuum pipet, care being taken not to dislodge any solids from the pellet. Extracting base (10 ml) was then added, followed by mixing, heating, centrifuging and removal of supernatant. Then distilled water (10 ml) was added, mixed, centrifuged, and the supernatant removed. The rinsing procedure was repeated to remove soluble residues from the sediment.

The residual sediment from the acid-base treatment was transferred to an Erlenmeyer flask as follows: 5.0 ml of acetate buffer was drawn into a Finnpipet; about half was delivered to the centrifuge tube, and the tube was mixed on a tube buzzer or stirred, until all of the pellet had broken loose; the contents were then rapidly poured into an Erlenmeyer flask. The remainder of the 5.0 ml buffer was then used to wash out the residual sediment in the same manner. This two-step procedure was found to effectively transfer all of the sediment in a precise volume of buffer.

To each flask 80 µl of chloroform was added as a bacteriostat, and the suspensions were ultra-sonically homogenized, sealed with parafilm and stored overnight in a refrigerator.

Enzyme Procedures

For each sample of sediment to be analyzed, three 800 mg aliquots of sediment were treated with acid and base. Sample A was used as a zero reaction-time blank and samples B and C were incubated with cellulase for 24 hours. All reactions were carried out in 50 ml Erlenmeyer flasks, with a total liquid reaction volume of 10 ml, consisting of 5 ml of sediment suspension in acetate buffer and 5 ml of cellulase solution.

The enzyme reactions were begun on the day following initial acid-base leaching by repipeting 5.0 ml of cellulase solution into flasks B and C of each

sample. The flasks were then sealed with parafilm, a pinhole punched in each, and placed in a gyrotory shaker bath set at 50°C.

When 24 hours had elapsed the contents of the three flasks were poured into centrifuge tubes. To flask A of each sample, 5 ml of the cellulase preparation used for flasks B and C was added, and the contents immediately transferred to polypropylene tubes; all three samples were centrifuged 15 minutes at 15,000 RPM. It was essential to keep flask A cold until addition of the enzyme, and to centrifuge immediately, before any enzymatic hydrolysis could take place. From the supernatant of each tube, a 2 ml aliquot was withdrawn, with a Finnpipet, and placed in 20 x 150 mm glass test tubes, for glucose determination.

Glucose, the product of the hydrolosis of cellulose was then analyzed enzymatically, using the glucostat macro method. One vial each of chromogen and glucostat reagent were injected with distilled water, the contents transferred to a graduated cylinder and diluted to 80 ml. Multiples of these quantities were prepared depending on the number of samples to be analyzed. The dissolved reagent was dispensed with a repipet: to each 2.0 ml sample aliquot, 8.0 ml of glucostat reagent was added, and the tubes were agitated with a tube buzzer. After exactly 10 minutes, 2 drops of 4N HCl were added to terminate the reaction and the tubes were mixed again on the tube buzzer. It was found to be convenient to deliver the glucostat and later the HCl to one tube every 15 seconds.

After an interval of at least 5 minutes to allow full color development, the absorbance of the solutions was measured in 1 cm cuvettes against distilled water at a wavelength of 420 nm and a slit width of 1 mm. The absorbance of sample A was subtracted from the mean of samples B and C to give the corrected absorbance due only to glucose produced by the enzymatic hydrolosis of cellulose.

Glucose Standards

The most suitable standardization procedure was found to be addition of glucose to a reaction mixture exactly like the actual samples, containing sediment, buffer, cellulase and chloroform. For each batch of samples to be analyzed, an extra aliquot of a representative sample was weighed out and acid-base treated exactly like the other samples. The residue was transferred to an Erlenmeyer flask with 5 ml of glucose standard instead of acetate buffer. This standard was prepared by diluting 20 ml of stock solution (1 mg/ml) to 100 ml with acetate buffer (0.2 mg/ml). After addition of 5 ml of cellulase, the total reaction volume of 10 ml yielded a standard addition of 0.1 mg/ml of glucose. The flask was incubated for 24 hours with the other samples and then analyzed for glucose content. The absorbance of the same sample without the glucose spike was subtracted from that of the standard; this difference was set as the absorbance due to 0.1 mg/ml of glucose.

To determine the percent of cellulose in a sample the following formula was used:

$$100 \times \frac{\text{abs. B} + \text{abs. C}}{2} - \text{abs. A} \times \frac{0.1 \text{ mg/ml}}{\left(\text{abs. std.} - \text{abs.} \frac{(B+C)}{2}\right)} \times 10 \text{ ml}$$

$$\text{weight of sample (mg)}$$

This number represents the weight percent of enzyme-hydrolyzed cellulose in the sediment expressed in terms of glucose (see Discussion of Method).

In addition, a fresh glucose standard of 0.1 mg/ml was made up and measured at the time of the glucostat analysis, and an acetate buffer blank was run as well. The difference of these two absorbances was calculated, and the two values were compared as a check for bacterial activity, contamination or inhibition of glucostat enzymes.

Discussion of Method

A cellulase preparation of high specific activity was necessary to achieve good results. Several commercial cellulase preparations were found to have too low an activity or were found to cause significant background absorbance at 420 nm. Worthington's cellulase II typically yielded only 30 µg/hr per mg of enzyme when assayed as recommended with Avicel microcrystalline cellulose as substrate. The only enzyme preparation which proved suitable for quantitative analysis of sediment samples was a lyophilized *T. viride* cellulase provided by Dr. E.T. Reese (U.S. Army Labs, Natick, Massachusetts). When assayed under the same conditions as for commercial cellulases the enzyme supplied by Dr. Reese (50°C, 1 hour), produced 1200 µg glucose/hr per mg of enzyme, 40 times the rate we found for commercial cellulases. This preparation caused negligible interference at 420 nm, thereby increasing the sensitivity at low levels and eliminating another source of error. With the procedure described here, 30 mg of lyophilized enzyme was required for each sample analysis including a blank and two duplicates.

The acid-base treatment derived from Strickland and Parsons (1968), was found to be necessary for several reasons. Untreated Hudson River sediment was found to inhibit the Natick enzyme. Inhibition of the cellulase was tested by saturating with Avicel cellulose: to one group of tubes no sediment was added; to a second and third group 400 mg of acid-base treated sediment and 400 mg of untreated sediment were added, respectively. The first and second groups of tubes showed similar activity while the third was about 40% lower, indicating inhibition of untreated sediment.

Treatment of the sediment by boiling acid and base, ultra-sonic dispersion and overnight soaking prior to addition of enzyme undoubtedly increased the rate of enzymatic hydrolysis by swelling the cellulose fibers. Reese and Mandel (1963) report that the reactivity of cellulose fibers is enhanced by increasing the surface available to the enzyme. The acid-base treatment also served to remove soluble substances which might interfere with or inhibit the glucostat measurement.

The glucostat reagent set (Worthington Biochemical Company) provided a highly specific and accurate colorimetric method for measuring glucose produced by cellulolytic activity. The set utilizes a coupled enzyme system

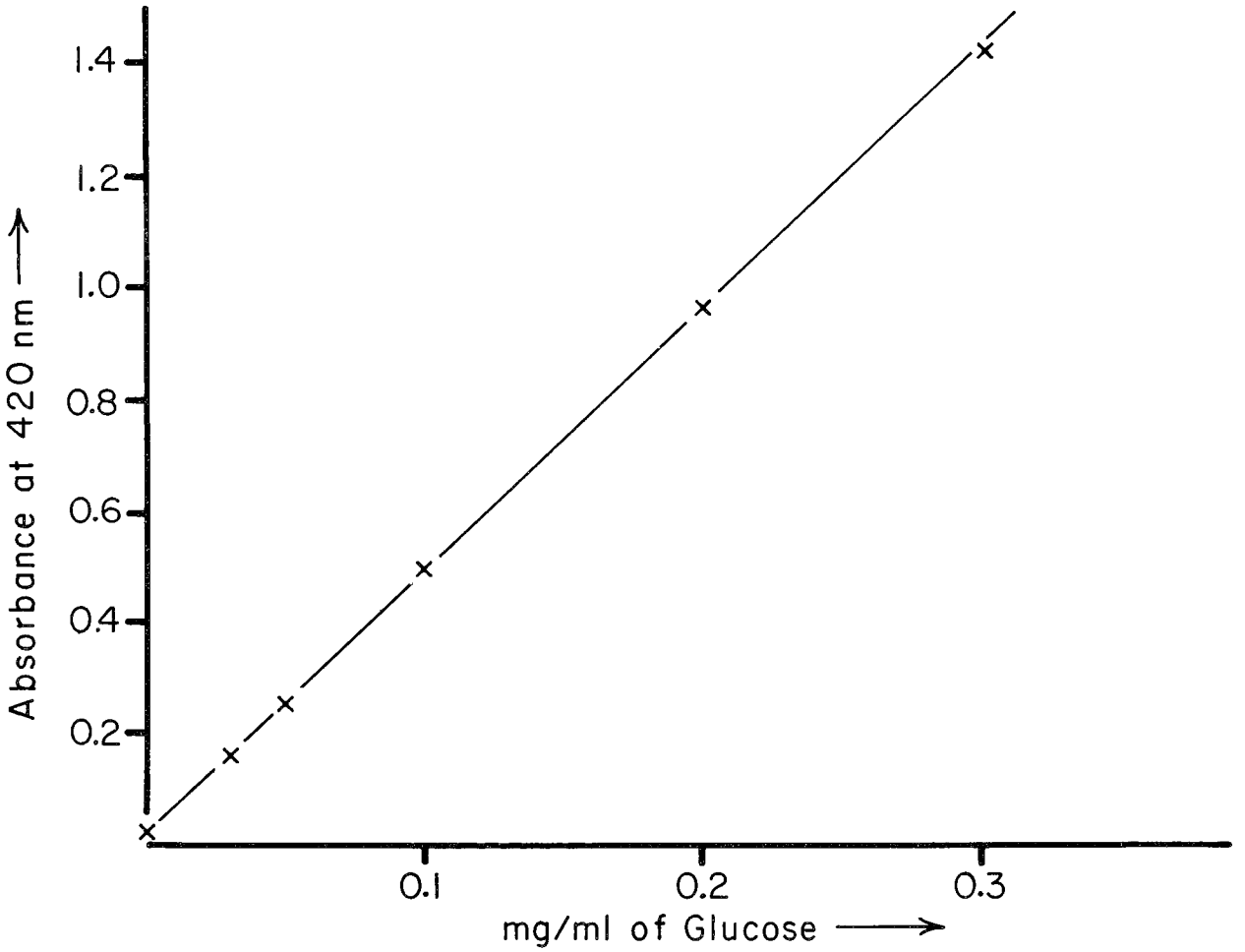

Figure 34. Standard curve of absorbance at 420 nm as a function of the amount of glucose added to a sample.

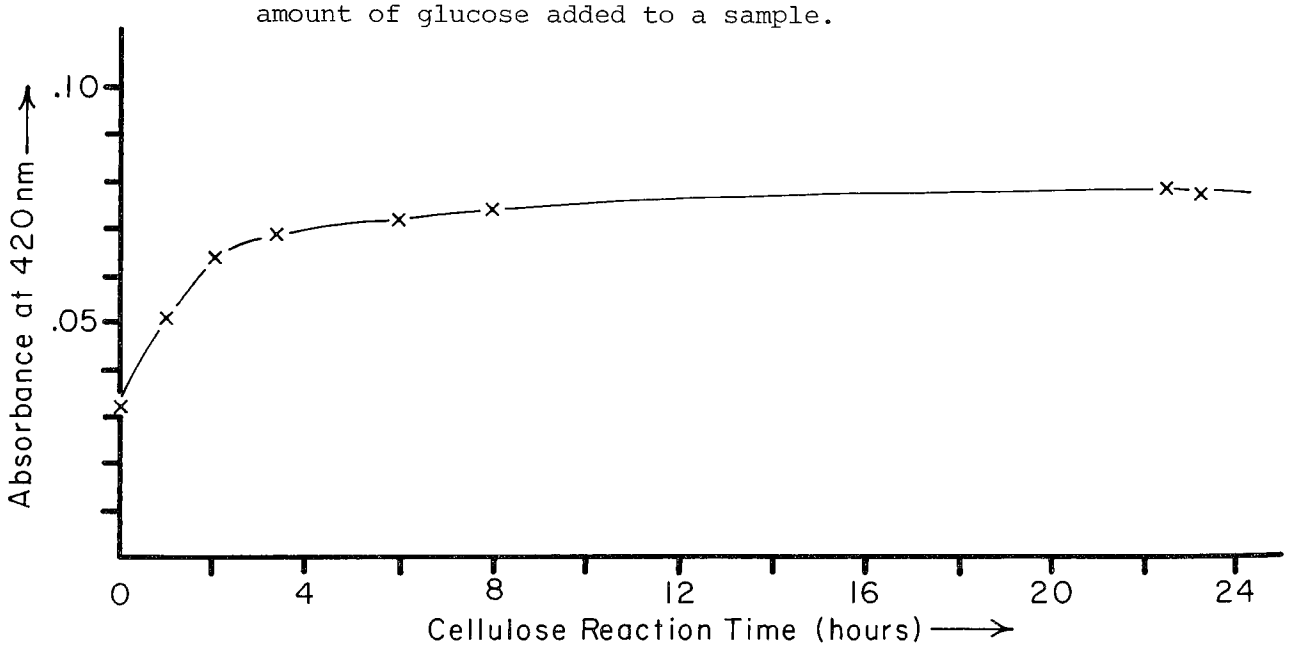

Figure 35. Time response of glucose production by the enzymatic hydrolysis of cellulose in a sample of Hudson Estuary sediment (mile point 43).

consisting of glucose-oxidase and peroxidase enzymes. Figure 34 shows a standard curve obtained by diluting glucose stock with acetate buffer. Chloroform was found not to inhibit the response of the glucostat system. It was found, however, that turbidity or discoloration of the solution to be analyzed caused a depression of values. Thus high speed centrifugation of the reaction mixture resulting in a clear supernatant proved to be essential. Sediment samples that were not acid-base treated often produced yellowish supernatants which caused interference at 420 nm.

With each batch of samples separate glucose standards and standard additions to sediment samples were run; the glucostat response of the standard additions to samples were consistently only several percent lower, indicating that no significant inhibition of the glucostat system was occurring in the cellulase-sediment suspensions, and that no bacterial degradation of glucose was taking place during the course of the reaction.

Figure 35 shows a time curve for the cellulytic hydrolysis of Hudson River sediment relatively high in cellulose. Most of the hydrolysis occurs within the first few hours, and then the rate of hydrolysis falls off rapidly. Assay of reaction mixtures after 24 hours by saturation with 200 mg of Avicel substrate showed that considerable cellulase activity remained, so that cessation of cellulose hydrolysis in the samples was not due to enzyme denaturation. Twenty-four hours was chosen as a standard reaction time for analysis of sediments because it is far enough into the flat part of the curve to minimize the effect of differences in the initial rate of hydrolysis. Susceptibility of cellulose to enzymatic attack varies with great many factors and the relatively long reaction time allows less susceptible forms of cellulose to be fully hydrolyzed.

Cellulose Standards

Addition of known amounts of pure cellulose (Avicel) to sediment samples prior to any treatment other than drying yielded only about 70% of the glucose theoretically available. However, the amount of glucose produced was directly proportional to the amount of cellulose added. A standard curve was prepared in the following manner: 5, 10, 20, 30, 40, 1000 and 2000 mg of Avicel were weighed out and transferred to 150 ml beakers. After 100 ml of distilled water was added to each beaker, and while the suspensions were ultrasonically homogenized, 1 ml aliquots were withdrawn using a Finnpipet, and added to identical 400 mg weights of Hudson River sediment in centrifuge tubes. These samples were then acid-base treated and incubated with cellulase enzyme exactly as described above. Figures 36 and 37 show a standard curve prepared by plotting absorbance produced against weight of cellulose added. On the basis of molecular weights 162 grams of cellulose should produce approximately 180 grams of glucose when hydrolyzed completely due to the addition of a molecule of water at each glycosidic linkage. We found the quantity of glucose produced to be consistently about 70% of the theoretical value, whatever weight of Avicel was added. The pretreatment of Avicel with acid and base, as was also done for samples, results in some loss of weight by the Avicel. We subjected 4 different aliquots of Avicel, ranging in weight from $\sim$ 10 mg to $\sim$ 80 mg, to pretreatment with acid and base and then reweighed the Avicel after drying. The average weight loss for the 4 samples was 36%. Correcting for this weight loss from acid and base pretreatment, the yield of glucose from Avicel was very

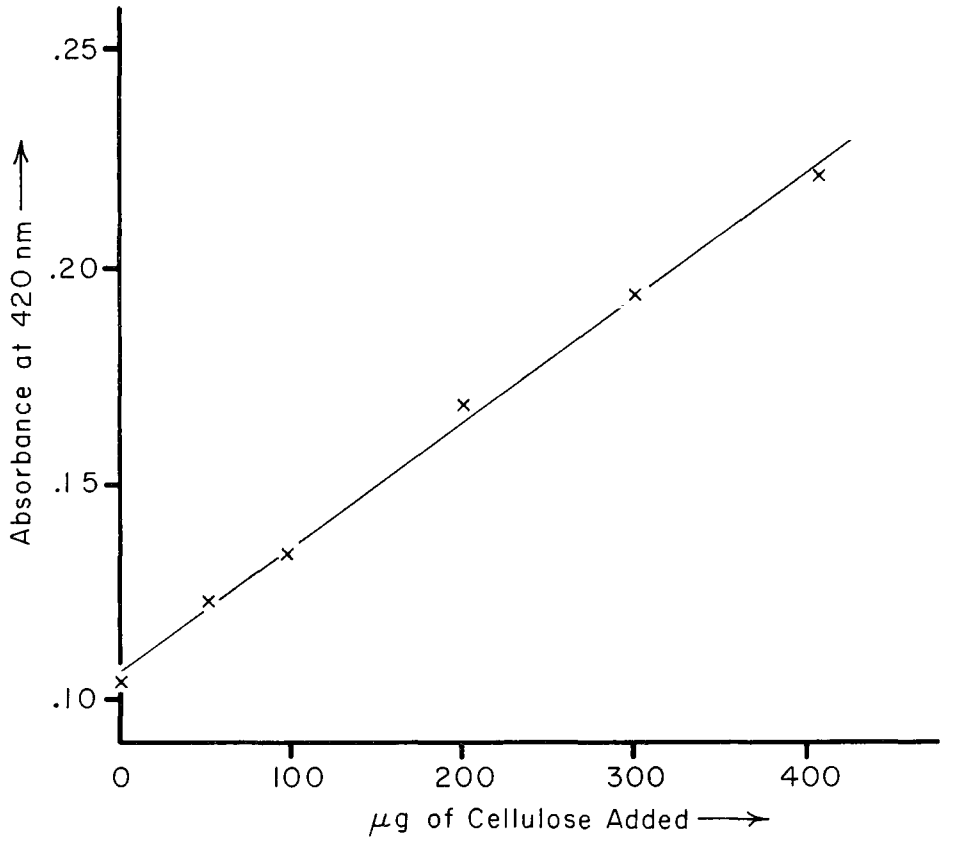

Figure 36. Standard curve of absorbance at 420 nm as a function of the amount of cellulose added to a sample of Hudson Estuary sediment (mile point 43 - 400 mg).

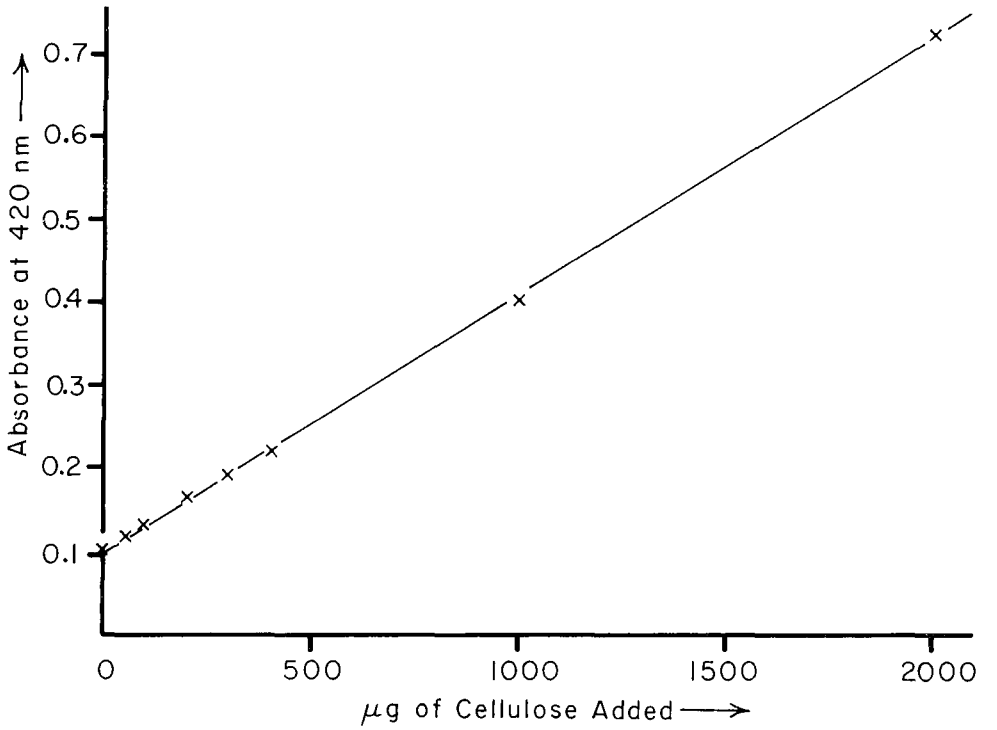

Figure 37. Normal working range for samples reported here (expansion of low absorbance portion of Figure 36).

close to that predicted from complete reaction with cellulase. We have no independent way to estimate the weight loss of cellulose in sediments resulting from pretreatment with acid and base, which obviously introduces some degree of uncertainty. Because of this uncertainty, we chose to report the weight of original sediment cellulose as equal to that of the glucose, omitting any correction factors based on molecular weights or the loss of cellulose by pretreatment which could vary in proportion between the Avicel standard and the cellulose in environmental samples. The maximum sediment weight that could be effectively analyzed with our procedures was found to be 800 mg. The amount of cellulose detected was found to be proportional to the weight of sediment analyzed, up to a sample weight of 800 mg. Larger weights of sediment were difficult to transfer quantitatively, and after centrifuging yielded supernatants with some discoloration and turbidity.

The analysis for cellulose proved extremely sensitive and reproducible in low ranges. In any given batch of samples the reaction blanks gave a glucostat absorbance of $\pm$ 0.002. Assuming a minimum sensitivity of 0.003 absorbance units, the minimum detectable amount of cellulose in an 800 mg sample was 0.001%.

RESULTS AND DISCUSSION

We have analyzed 14 samples of sediment from the Hudson River estuary and New York Bight and one sample of sewage sludge from Ward's Island sewage treatment plant in New York City for cellulose (Table 16). The locations of these samples range from near the upstream limit of saline water intrusion in the Hudson Estuary to beyond the edge of the continental shelf at depths of $\sim$ 2000 meters in the Hudson Submarine Canyon (Figure 38). Except for the sewage sludge sample with a cellulose content of $\sim$ 7%, all of the sediment samples had less than 0.06% cellulose by weight.

The variations in grain size of the Hudson estuary samples was relatively small, but in the New York Bight the samples ranged from predominantly clay and silt (< 63 μ) to predominantly sand (> 63 μ). We normalized the cellulose data by two procedures, one on the basis of the fraction of fine particles, and the other on the basis of the weight loss of the sediment when heated between 100°C and 500°C. This weight loss has been found to be approximately twice the organic carbon content of Hudson sediments (Gross, 1972), and thus provides an indicator of the fraction of organic matter which is cellulose. Assuming the organic carbon fraction is approximately half of the weight loss on ignition, all of the samples of sediment organic matter consist of less than 1% cellulose by weight, while sewage sludge organic carbon approaches 20% cellulose.

We analyzed several samples which are not recent sediments from cores in the Hudson estuary. One sample (mile point 19, 550 cm) is probably greater than 1000 years old, based on radiocarbon dating of shell layers higher up in the core. This sediment sample contained no measurable cellulose (< .001% by weight), although the total organic content was still appreciable ($\sim$ 2%). Another old sample from a core in New York harbor (mile point 0, 65-70 cm) had a very low cellulose value ($\sim$ 0.001%). This sample has a trace metal composition indicative of pre-industrial levels (unpublished data), but we do not have good age control on this sample other than that it is probably at least 50-100 years old.

Table 16

Cellulose Content of Hudson River Estuary and New York Bight Sediments

Location[a] (Mile Point)	Depth in Sediment (cm)	Weight % < 63μ	Weight[b] % lost on ignition (LIG)	Weight %[c] cellulose	Weight %[d] Crude Fiber by phenol	Weight %[e] total Carbohydrates by phenol	Cellulose / % < 63μ × 10^5	Cellulose / LIG × 10^4
54	20-25	98	6.4	.008			8	13
54	50-55	97	6.2	.008			8	13
43	0-10	95	9.5	.035	.08	1.5	37	37
19	550	90	4.1	.000		-	0	0
0	0-10	90	8.0	.028			31	35
0	5-10	95	9.2	.018			19	20
0	65-70	95	5.3	.001	-		1	2
Sewage Sludge		100[f]	70	7.3	9	20	7300	1050
-26	0-10	100[g]	12.7	.056			56	44
-38	0-10	33	5.0	.006	.05	.86	18	12
-67	0-10	17	2.8	.001	.02	.27	∿ 0[h]	∿ 0[h]
-117	0-10	5	1.8	.001	.007	.09	∿ 0[h]	∿ 0[h]
-136	0-10	87	9.7	.000	.04	.83	0	0
-147	0-10	98	10.6	.004	.04	.72	4	4
-157	0-10	93	10.9	.000	.03	.52	0	0

[a]Locations are given relative to the Hudson River mileage reference system, with the origin located at the southern tip of Manhattan. Positive numbers are upstream, and negative numbers downstream of the origin.

[b]Weight loss on ignition (LIG) represents the weight loss of samples heated from 110°C to 500°C. In Hudson sediments, this weight loss is usually about two times the organic carbon content.

[c]Data given in terms of the weight of glucose produced by enzymatic hydrolosis.

[d]Chemical analysis by method of Gerchakov and Hatcher (1972) after leaching with strong acid and base.

[e]Chemical analysis by method of Gerchakov and Hatcher (1972).

[f]No size fraction analysis was made because of the fibrous nature of dried sewage sludge. The weight < 63μ was assumed to be 100% for the purpose of the calculation in the next to last column.

[g]The sediment from this site was more than 90% sand (> 63μ). To increase sensitivity for cellulose determination, we removed all of the sand fraction, which had a weight loss on ignition of ∿ 1%, and thus had a relatively insignificant proportion of organic matter.

[h]The cellulose content of these samples was very hear the sensivitity limit of our analytical technique, so we have not reported ratios involving those concentrations.

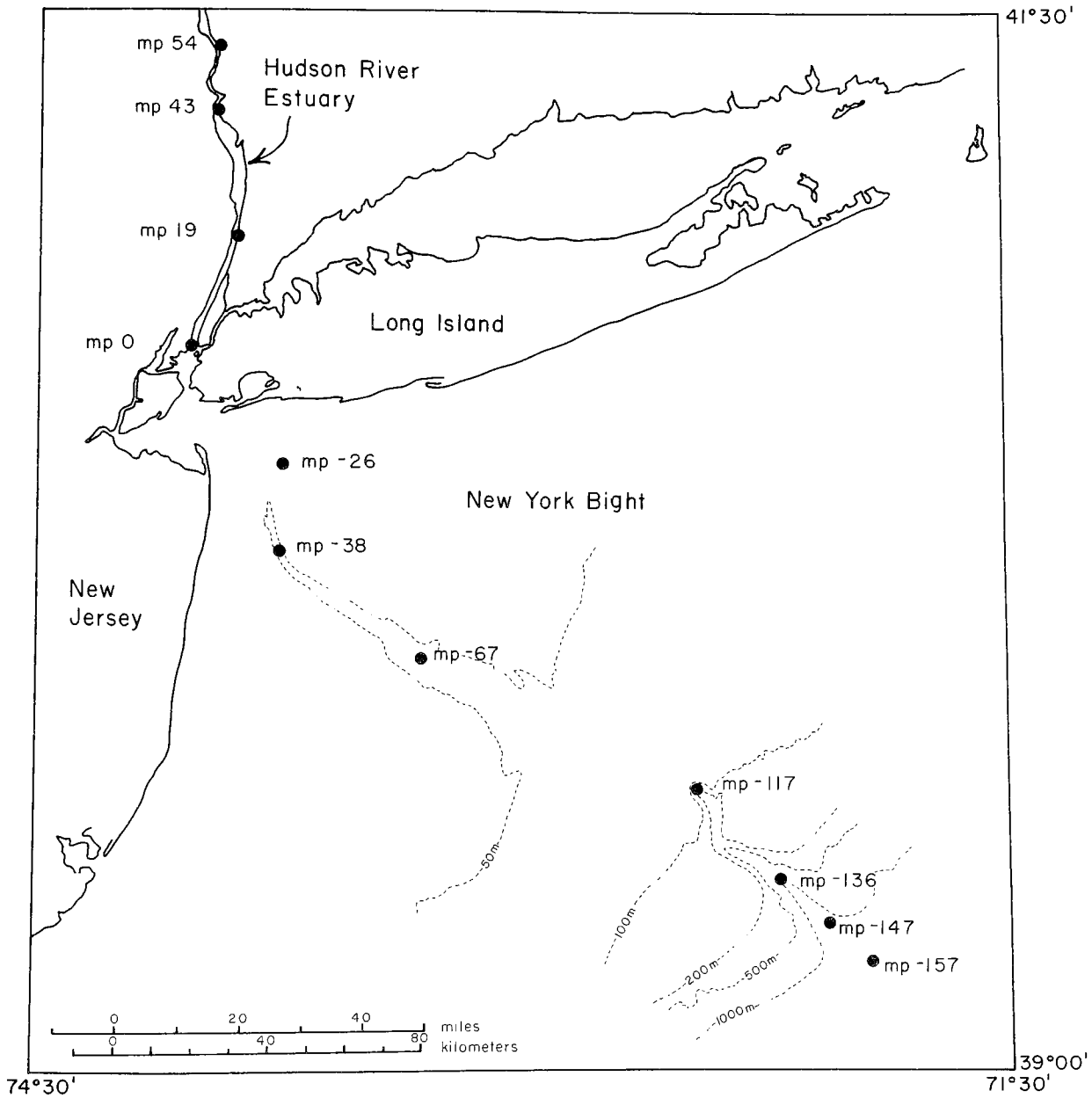

Figure 38. Locations of samples reported in Table 16. Samples range from near the upstream limit of saline intrusion (mp 54) to beyond the edge of the continental shelf (mp -157).

Recent sediments in the Hudson, both in the harbor (mile point 0, 0-10 cm, 5-10 cm) and upstream (mile point 43, 0-10 cm), have relatively high cellulose values, as does the fine fraction of sediment from near the sewage sludge dumping area in the New York Bight (mile point -26, 0-10 cm). Thus, recent sediments in the harbor and in the dumping area, both of which obviously contain appreciable sewage contamination, have high cellulose values (.02 - .06%). However, recent Hudson sediments (mile point 43) well upstream of the major sewage loading also are relatively rich in cellulose ($\sim$ .04%). We have analyzed organic matter from both the harbor and upstream for radiocarbon and found the harbor sediments to contain bomb carbon-14 in the organic matter (from sewage) while upstream the organic matter in surface sediments has a much lower carbon-14 content and thus appears to have a substantially lower component of recent sewage organics. We, therefore, conclude that high cellulose levels in Hudson sediments are not unequivocal indicators of sewage contamination. Presumably the same is true for the New York Bight, as is discussed in more detail below.

The magnitude of the cellulose values we observed indicates that total carbohydrate measurements [ranging from 10% to 60% of the organic carbon in New York Bight sediments (Hatcher and Keister, 1976)] provide very little information about the distribution of cellulose in sediments, and should not be interpreted as indicative of sewage cellulose.

It is also evident that there is little correspondence between cellulose and total carbohydrates or crude fiber. Cellulose concentrations are more than an order of magnitude smaller than crude fiber values in Bight sediments, while they are comparable to crude fiber and total carbohydrate numbers in sewage sludge and to crude fiber in one sample of Hudson sediment.

The lack of cellulose in old Hudson sediments, compared with the high values of recent sediments, indicates that cellulose is probably not stable in sediments on the time scale of hundreds to thousands of years, in contrast to condensed organic matter, such as humic acids which apparently can remain in soils and sediments for very long periods. The gradual breakdown of cellulose in sediments over long periods is reasonable considering that some soil fungi and certain wood eating organisms contain cellulases.

The time scale of breakdown of cellulose in coastal sediments would be very useful to know. We cannot place adequate constraints on the rate at which this process occurs from the data reported here, but a rough calculation indicates the half time may be at least 5 years.

If sewage sludge (SS) and dredge spoils (DS) were assumed to be present in the same weight proportion as that originally dumped (weight ratio of solids SS/DS $\sim$ 0.06; Gross, 1972) and contained the original cellulose values reported here (SS = 7% and DS = 0.02%), then composite dumped material should have $\sim$ 0.44% cellulose. Assuming a mean age of $\sim$ 15 years for dredge spoils and sewage sludge discharged to the dump site (dumping of these materials in the New York Bight has occurred over a number of decades) and also assuming that our one measured value (0.056%) is typical of composite waste discharges, the half time for destruction of cellulose would be $\sim$ 5 years. Our sample was from the fringe of the dumping area and was mostly coarse sand (> 90% by weight). We removed the sand fraction prior to analysis for cellulose, and

considered only the composition of the fine particles as relevant to this discussion.

Actually it is likely that substantially more of the sewage sludge particles than the dredge spoils would be carried well away from the discharge zone. Assuming cellulose to be stable, and that virtually all of the cellulose in our sample came from sewage sludge (ratio of cellulose in SS to DS = 350) the value of $\sim$ 0.06% in our sample is a little more than 10% of that expected from the composite of sewage sludge and dredge spoils dumped ($\sim$ 0.44% cellulose). Thus the two calculations indicate that if the sample we report is representative, (1) cellulose has a half time for breakdown of $\sim$ 5 years, or (2) assuming cellulose is stable, only 10% of the sewage sludge discharged is in the sediments. The most likely situation is between these extremes, i.e., cellulose has a half time for destruction of $\geq$ 5 years and only some fraction of sewage sludge ($\geq$ 10%) is found in the dumping area sediments.

The range of cellulose values we observed in the Hudson and New York Bight indicates that detailed studies of this component of the organic matter in sediments could provide valuable insights into the accumulation and diagenetic history of organic matter in recent sediments. Another possible application of enzymatic cellulose measurements is in the study of blooms of coastal planktonic organisms, such as Ceratium tripos, which may possibly play an important role in episodes such as the recent anoxic condition in the nearshore waters of the New York Bight (T. Malone, personal communication). These organisms have cell walls containing cellulose and appear to be capable of producing intense blooms under certain conditions. The cellulose from blooms would probably be relatively stable compared with most non-cellulose organic matter produced by coastal planktonic organisms, and could thus be traced for significant time periods in both the water column and the sediments.

SECTION 9

RADON-222 AS AN INDICATOR OF TRANSPORT RATES FROM THE SEDIMENTS TO THE WATER COLUMN IN THE HUDSON

INTRODUCTION

Striking differences in chemistry often exist across the sediment-water interface. Lake, river, and ocean waters are usually oxygenated and relatively depleted in nutrients. Interstitial waters of estuarine and nearshore sediments are usually anoxic very near the sediment surface and are often enriched in nutrients and in some transition metals. Thus, sediments consume oxygen from the water column and return nutrients and perhaps some transition metals. The movement of dissolved substances across the sediment-water interface can play an important role in establishing the composition of a water body and in regulating the rates of reactions which occur in sediments.

Three approaches have been employed to estimate the rate of exchange of dissolved substances across the sediment-water interface.

1. Direct measurement of flux into overlying water in either cores returned to the laboratory or in a confining device placed over the sediment in situ. Chemical flux is determined by a time series of analyses (Fanning and Pilson, 1974; Pamatmat and Banse, 1969).

2. Measurement of gradients in interstial waters and calculation of diffusive transport (Berner, 1971 and others).

3. Construction of a mass balance for a substance in the water column which includes transport into or out of sediments.

The first approach can be criticized as it alters the turbulent regime in the vicinity of the interface. The second approach is complicated for biologically active substances because the effects of reaction and variable diffusion on concentration vs. depth profiles are difficult to separate and because many of the critical processes may occur within a few millimeters of the sediment surface. Turbation by organisms and bottom currents can further complicate this approach. The third of these approaches avoids these difficulties, but averages flux temporally, spatially and is not always possible to employ.

Radon (Rn-222) is a noble gas with a four day half-life. Its parent, radium-226 (1600 year half-life) may be dissolved in the water column, but is primarily bound to or within solid phases. Thus high concentrations of

radon are found in sediment pore waters or in groundwaters, and much lower concentrations are found in the water column. In the Hudson, pore water has $\sim$ 600 dpm/l and overlying water $\sim$ 1.4 dpm/l. If Hudson water were in equilibrium with the atmosphere, the concentration would be $\sim$ 0.03 dpm/l at 25°C.

Since radon was originally proposed as a tracer for processes in aquatic systems by Broecker (1965), it has been used to study mixing rates and gas exchange rates in lakes and in the ocean. Figure 39 is a schematic radon profile in the open ocean. Throughout most of the water column, radon is in secular equilibrium with its parent. In the surface ocean, a deficiency of radon exists due to a net evasion to the atmosphere. In the deep ocean, an excess is found due to input from the sediments. The shapes of these deficiencies and excesses depends on the characteristics of the mixing processes in the ocean.

In the Hudson estuary the surface and bottom zones overlap. Figure 40 is a radon profile collected in 1971 at mp 25. Radon activity is clearly in excess of Ra-226 activity indicating that the rate of input from sediments is greater than the rate of evasion to the atmosphere.

Although first proposed more than ten years ago for studies of exchange across the sediment-water interface (Broecker, 1965), little has been done since then to exploit radon as a tracer for such processes. As a noble gas, radon is free of biological complications so its distribution will be controlled by a balance among production from its parent, radioactive decay and physical transport processes. Some fraction of the radon which is produced by decay of radium in sedimentary phases emanates into interstitial waters. It may decay there, or migrate into overlying waters before decaying. Migration can be effected by molecular diffusion or by turbation of sediments by currents and organisms. We will present results of radon measurements made in the Hudson estuary (Figure 40A) between 1971 and 1975 in an effort to quantify the importance of processes other than molecular diffusion as mechanisms for transport across the sediment-water interface in this estuary. Preliminary results of this research have been discussed by Hammond *et al.*, (1975).

ANALYTICAL METHODS

The technique for extraction and counting of Rn-222 from water samples has previously been described (Broecker, 1965). After radon analysis some samples were stored to permit ingrowth of radon and a second extraction for radium-226 analysis. Water samples (usually about 20 liters) were generally collected at least 200 m from shore to ensure that samples were representative of the major portion of the estuary. A few samples collected near shore in very shallow portions (< 1 m) of the estuary showed concentrations which sometimes approached twice those in the center of the channel.

Sediment samples were collected by gravity cores in plastic liners of either 3.5 or 6 cm diameter. To process each sample, the sediment was extruded, sections were cut and quickly dropped into a glass kettle which contained 100-200 cm^3 of distilled water. The kettle cover was sealed to

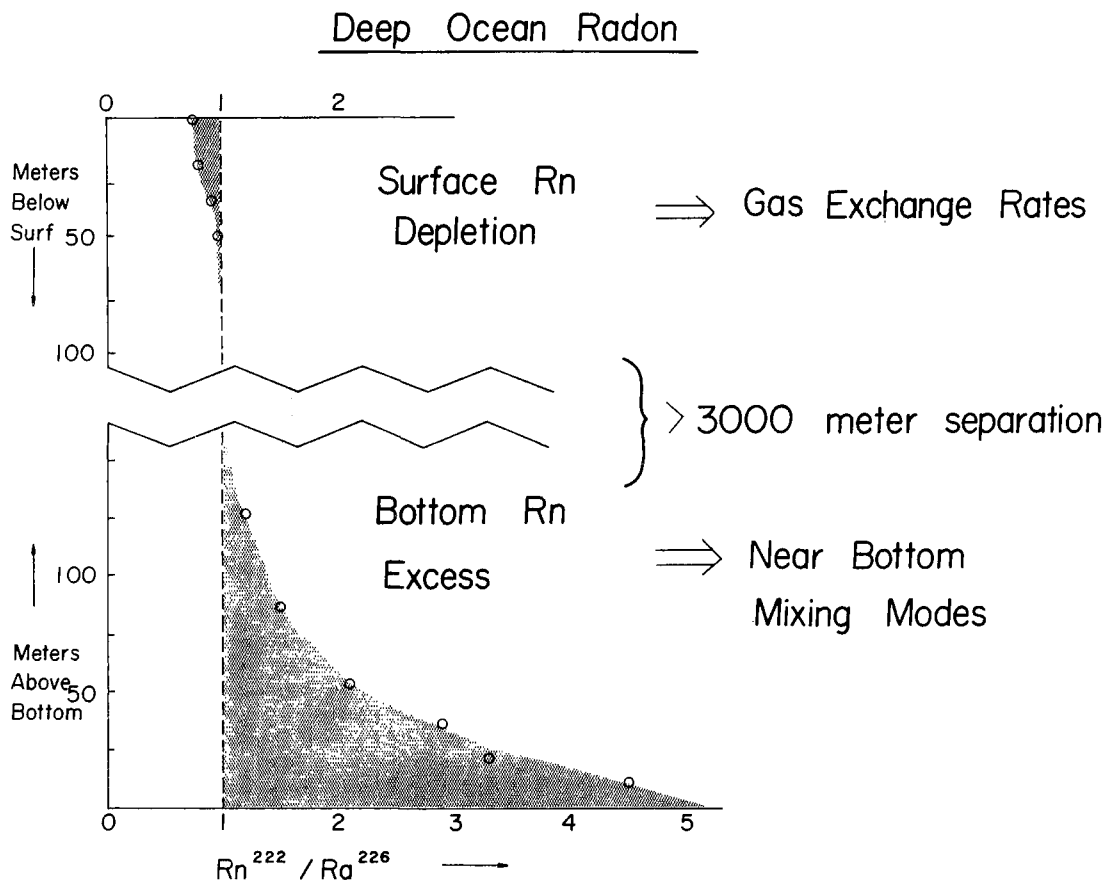

Figure 39. Deep ocean schematic radon profile: Through most of the water column radon-222 is in equilibrium with its dissolved parent radium-226. Near the surface a deficiency exists due to evasion to the atmosphere and near the bottom an excess exists due to diffusion from the sediment pore waters.

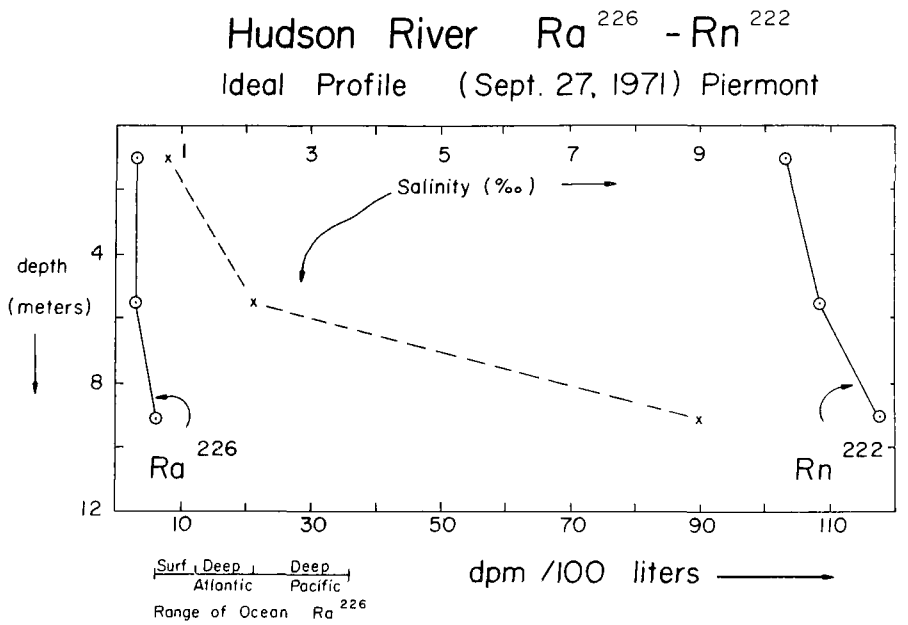

Figure 40. Hudson Estuary radon profile: Activity of radon-222 always greatly exceeds that of dissolved radium-226.

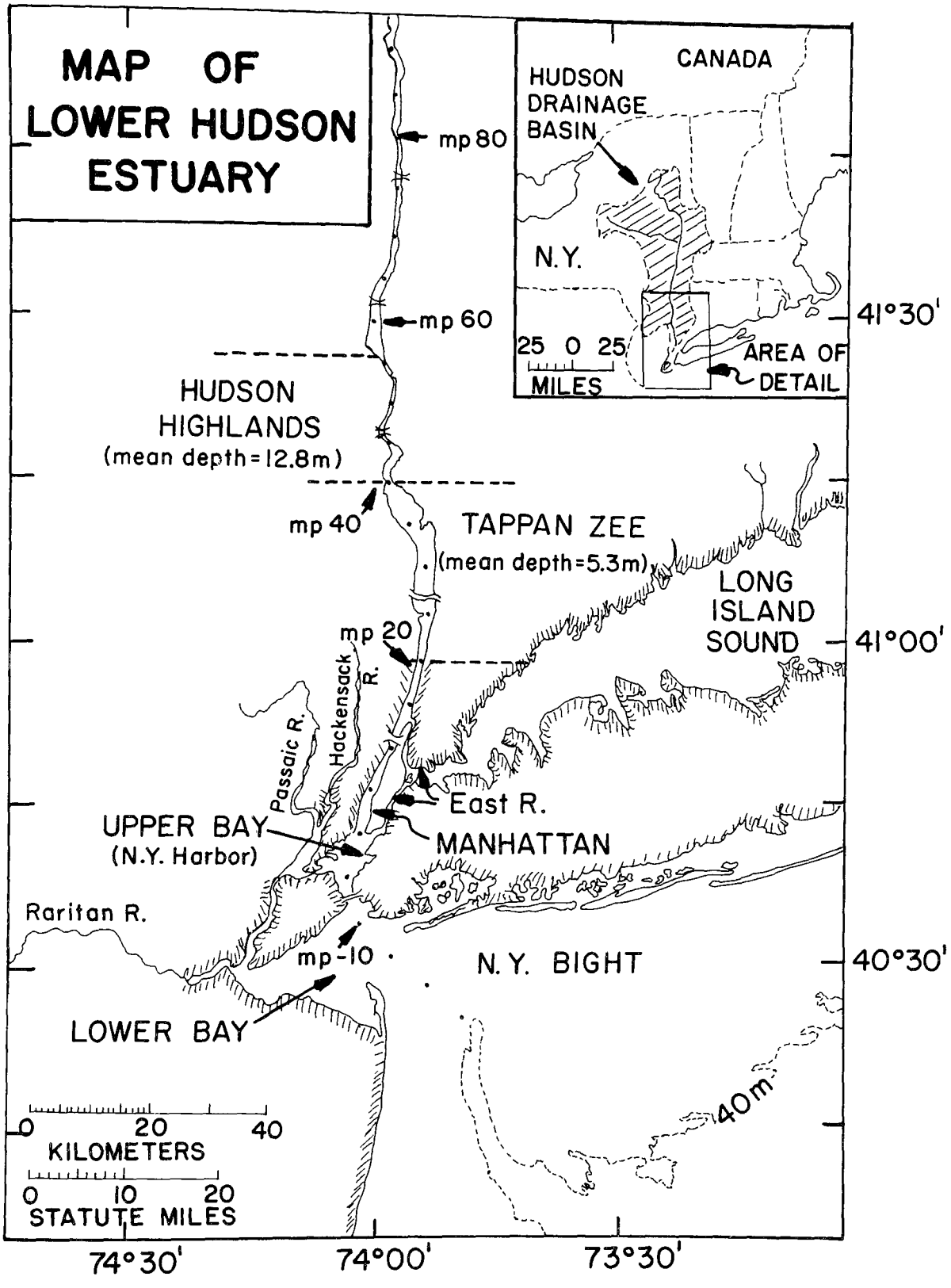

Figure 40a. A diagram of the lower Hudson Estuary indicating mean depths of the Tappan Zee and Highlands regions.

the base by an O-ring and contained 2 teflon stopcocks with O-ring seats. One of these stopcocks was connected to a bubbling tube. The kettle was shaken to create a slurry which could then be extracted and counted in the same manner as a water sample.

Radon extraction from sediments was accomplished within 2 days of collection and the kettle was resealed to allow regrowth of radon and measurement of the effective parent activity (C_{eq}). Results of sediment analyses are listed in Table 17. The rapid transfer of the kettles was apparently fairly efficient in preventing gas loss as the activity ratio of Rn-222 to Ra-226 was generally close to 1, with the exception of a sample from mp 53 which was apparently saturated *in situ* with CH_4 and formed large gas pockets while still in the core liner. One puzzling observation is that all sediments collected in the large diameter liner showed ∿ 20% radon deficiency while those from the small diameter liner showed none. Since gas escape should occur primarily from exposed sediment surfaces, one would have expected a larger diameter core to have less radon loss during sampling and transfer operations, not more. After the Ra-226 measurement was completed, the volume of the slurry was measured to compute the original volume of sediment sampled. The slurry was then dried and weighed.

RESULTS

The Hudson estuary is classified as a partially-mixed estuary whose circulation has been discussed by a number of authors, most recently by Abood (1974) and Simpson and Hammond (1977). The estuary is tidal as far upstream as a dam (at Green Island) located 154 miles from the southern tip of Manhattan (mp 154) with stage changes of 1-2 m and maximum current velocities of 50-100 cm/sec^{-1}. The estuary morphology is controlled significantly by the regional geology, recently summarized by Sanders (1974). The channel is narrow and quite deep where it passes through the Precambrian crystalline rocks of the Hudson Highlands, and then broad and shallow immediately south of the Highlands in the Tappan Zee region, an area formerly occupied by a large glacial lake. South of the Tappan Zee region, the Hudson is bounded on the west by the Palisades diabase, a thick sill formed in the Triassic (∿ 195 million years ago).

Initially, we expected to see a significant gradient in radon across the sharp depth discontinuity separating the deep waters of the Highlands from the shallow waters of the Tappan Zee. This was based on the assumption that a uniform radon flux from sediments into water of different mean depths would result in smaller concentrations in the deeper water. However, no discontinuity was ever observed, due to a number of processes discussed below.

Several surveys of radon concentration in the water column were made along the axis of the estuary. The first of these, made in late July 1972 (Figure 41), showed no consistent gradients, either with depth or with location along the channel of the estuary. Note that maxima may occur at the surface, the bottom, or at intermediate depth. To test the time variability, several profiles were taken at two locations throughout the summer of 1972 (Figure 42). Another series (primarily surface samples) was collected at more locations and shorter time intervals during August 1974 (Figure 43), and compared with

TABLE 17

Activity of Mobile Radon in Sediment

mp	Water Depth (m)	Coll. Date	Interval (cm)	$\frac{Rn^{222}}{Ra^{226}}$	Ra^{226} (dpm/gm dry)	C_{eq} (dpm/cm^3 sediment)
76	16	Aug 06 1974	2-10	1.02	.61	.45
			10-18	1.01	.58	.54
53	45	Mar 02 1974	2-10	.68	.88	.64
			10-18	.68	.69	.48
49	28	Aug 06 1974	2-6	.75	.59	.33
41	24	Apr 06 1974	2-10	1.01	.43	.25
			10-18	1.21	.39	.36
41	15	May 18 1974	2-6	--	.55	.39
37W	9	Aug 08 1974	2-6	.79	.52	.27
34	10	Apr 06 1974	2-10	1.05	.45	.32
			10-18	1.24	.40	.30
27		Nov 14 1973	0-4	.80	.05*	.06
			9-19	.69	.41	.29
			19-29	.71	.35	.29
			39-49	.71	.34	.29
			49-59	.78	.41	.26
25	5	Mar 02 1974	2-12	1.04	.37	.39
			12-22	--	.43	.39
25W	5	May 18 1974	2-6	--	.63	.56
18		Nov 05 1973	0-10	.81	.55	.29
			10-20	1.01	.34	.26
			20-30	1.17	.40	.40
			30-40	.78	.49	.43
			40-46	.68	.50	.52
18	13	May 19 1974	2-6	.38	.35*	.10
18W	1	Aug 27 1974	1-6	.50		.22
			13-15	.58	.48	.31
			22-24	.46	.48	.47
13W	8	Jan 18 1974	2-7	1.11	.34	.21
			7-12	1.03	.41	.25
			12-17	.94	.39	.27
9	15	Jan 18 1974	2-12	.98	.24	.16
			12-24	1.17	.19	.11
7	15	May 18 1974	2-6	--	.23**	.23**
1	15	Mar 02 1974	6-18	.93	.24	.28
-5	14	Mar 02 1974	2-10	.45	.06*	.08

*Sandy sediment with shell debris

**Assuming $Ra^{226} = Rn^{222}$

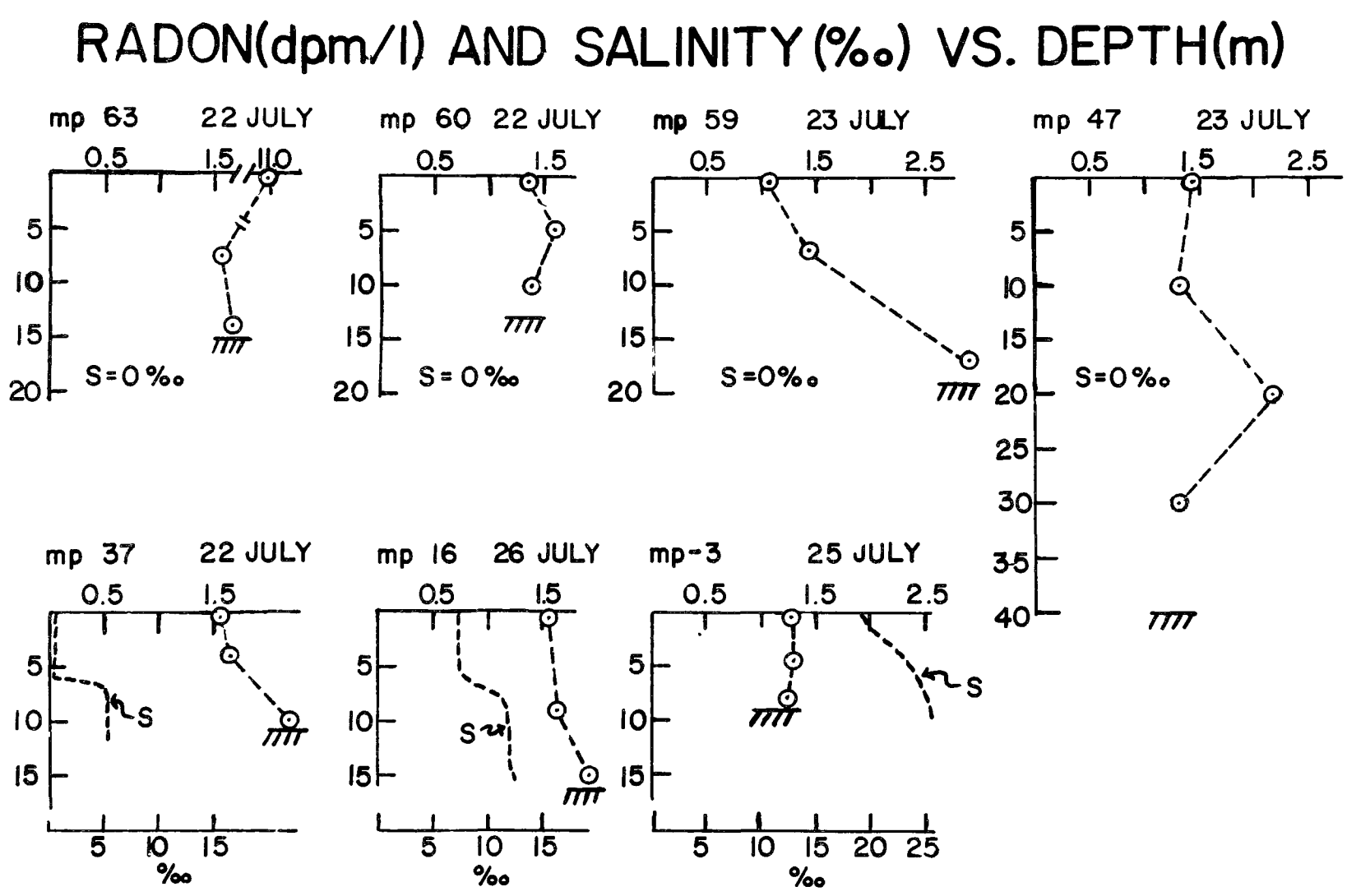

Figure 41. Radon sampling transect along the axis of flow - July 1972.

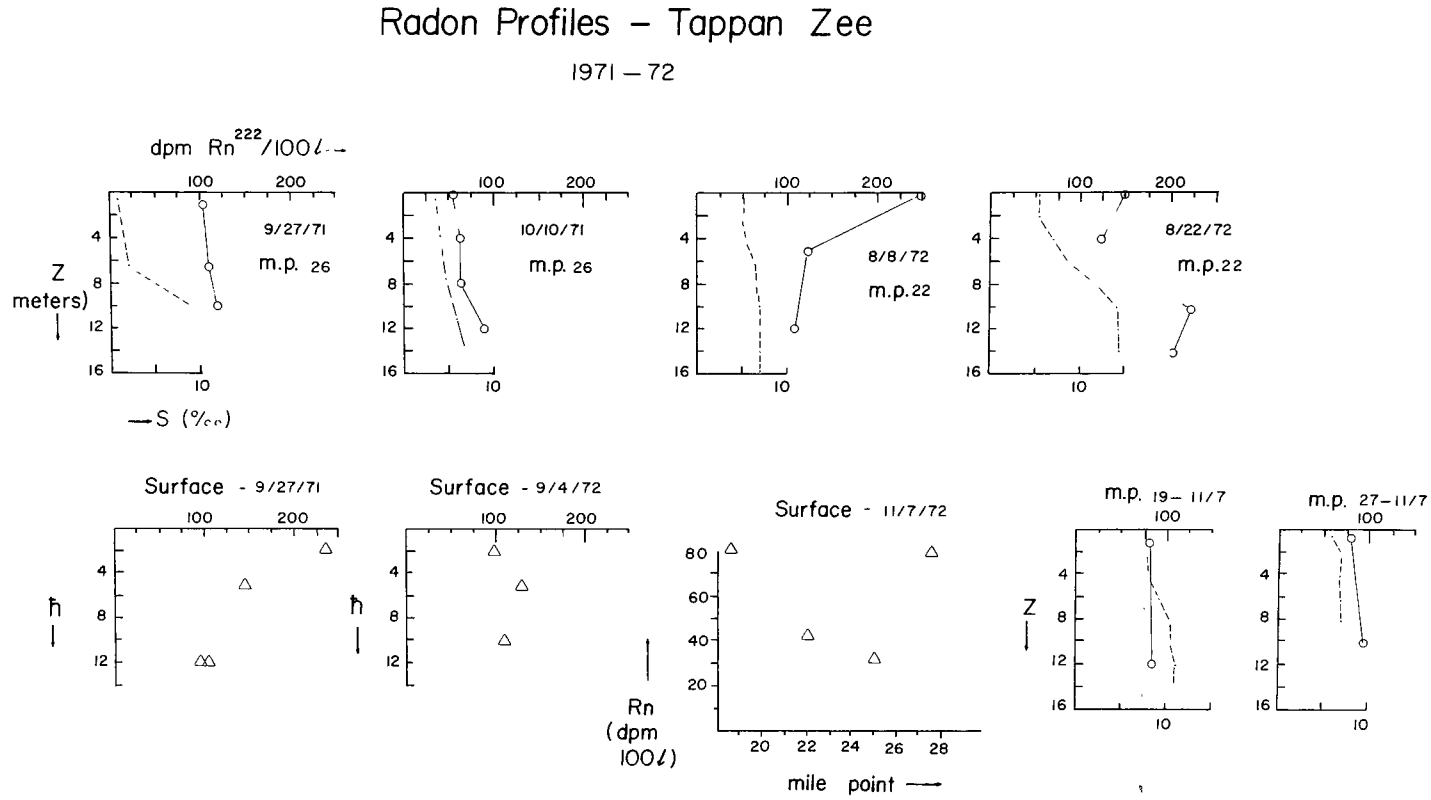

Figure 42. Time series of radon within a limited reach of the Hudson over a period of four months.

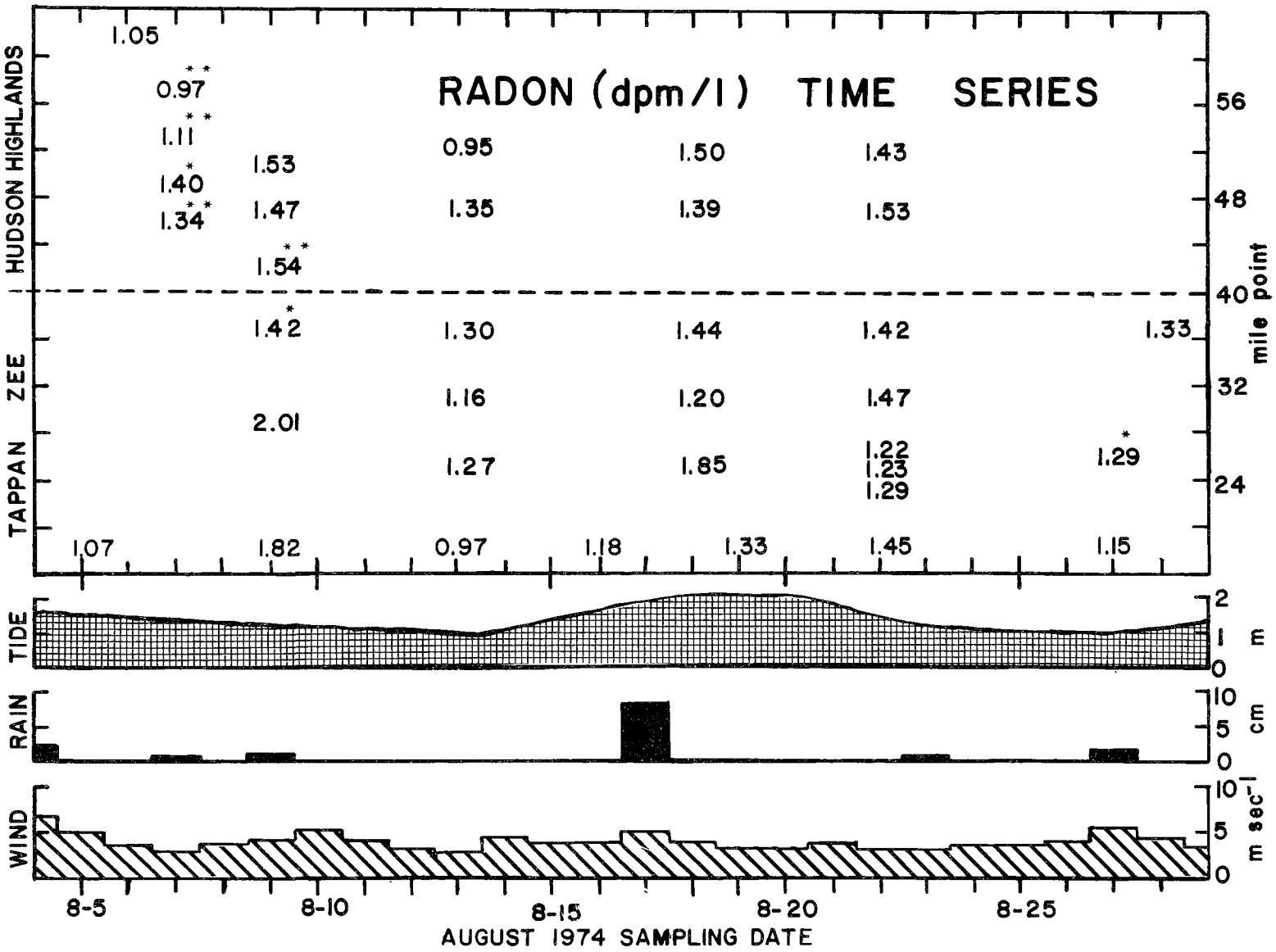

Figure 43. Time series of radon in the Hudson over one month: The number indicates activity (dpm/l) in a surface sample in mid-channel, * indicates a surface and deep sample were averaged, ** indicates a surface and two deeper samples were averaged. No correlation with rainfall, wind or tidal amplitude was apparent.

several potentially significant environmental variables. No consistent variation in radon levels could be correlated with tide heights (which varied by a factor of two) although the bottom currents and hence the rate of stirring of surface sediments by flow of water near the bottom (current turbation) might be expected to vary with tidal amplitude, with rainstorms, or with wind velocity. The median radon concentration for all of the summer (June-September) and winter (December-March) samples was determined for various segments of the estuary (Table 18). Since no consistent axial or vertical trends were observed, all samples from north of mp 16 were lumped to form the histogram in Figure 44, establishing a median for the estuary and displaying the extent of variability. The median is 1.43 $\pm$ 0.25 dpm/1 in summer and 1.30 $\pm$ 0.35 dpm/1 in winter.

A few measurements of Ra-226 were made on both filtered and unfiltered water samples. About half the Ra-226 is dissolved (passes .45 μ filter) and half is on suspended material. The total is 0.085 $\pm$ .04 dpm/1 (median of 36 analyses). The analytical precision was about 7% for both Ra-226 and Rn-222 analyses.

Several small streams entering the estuary have radon concentrations 5-10 times that of the estuary (Table 19), due to their shallowness and the contribution of groundwater flow. All of these cascade over dams or waterfalls shortly before entering the estuary. The turbulence introduced by this process is very effective in degassing radon from streams as shown by the measurements in Sparkill Creek on August 6, 1974.

McCrone (1967) has observed that the grain size, cation exchange capacity and percent organic carbon of Hudson estuary sediments are rather uniform with depth and location along the estuary between mp 20-76. This observation is supported by the rather constant value of radon released per gram of dry sediment (Ra-226 in Table 17), although samples north of mp 40 average $\sim$ 30% greater than those to the south. As one approaches the harbor, the release rate drops sharply and the variability increases, probably due to an increasing sand fraction and dredging activities. An average value in the top 20 cm was computed for each location and each location was weighted equally to estimate mobile radon in each of two large areas (listed in Table 21 as C_{eq} per wet sediment volume) with the uncertainty expressed equal to one standard deviation. Sandy samples from the navigation channel were not included in the average since they cover less than 5% of the total area.

DISCUSSION

The transport of radon across the sediment-water interface can be calculated by constructing a mass balance for radon in the water column (Table 20). The potential inputs are migration from sediments, production in the water column, stream inflow, and groundwater. The sinks are decay and evasion to the atmosphere. Gas bubbles which escape from sediment and rise through the water column are of negligible importance in transporting radon (Hammond *et al.*, 1975). When both sinks are considered, the mean residence time of a radon atom in the estuary is $T_2 \simeq 3$ days. With an effective horizontal eddy diffusivity of $K \simeq 700\ m^2/sec^{-1}$ computed on the basis of a one-dimensional advection-diffusion model (Simpson and Hammond, 1977), a radon atom will move

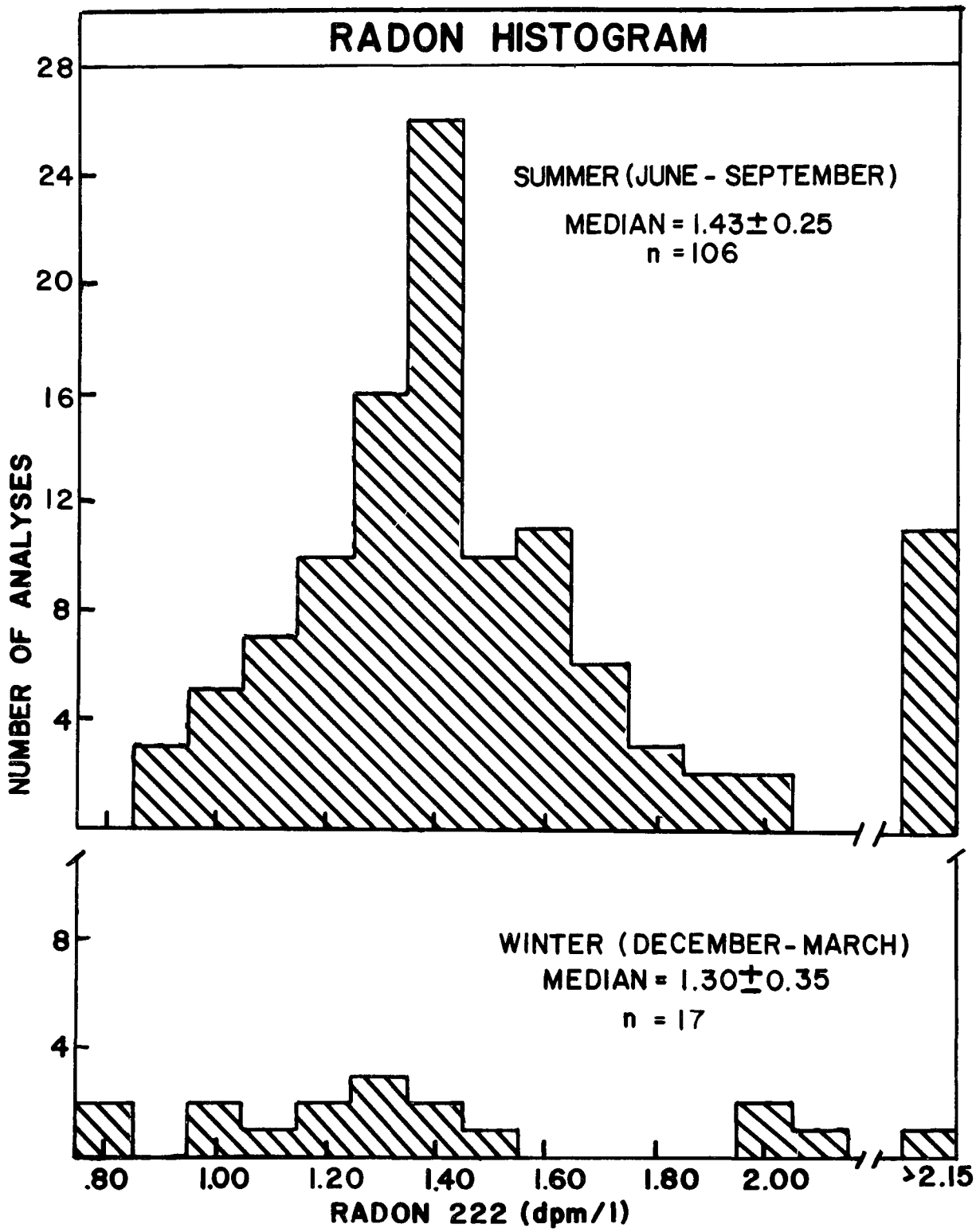

Figure 44. Histogram of radon data for the Hudson: All samples were collected at least 200 m from shore between mp 16 and mp 76.

TABLE 18

Estuary Geometry and Median Radon Concentrations

mp	16-20	20-40	40-57	> 57
Mean depth (m)	10	5.3	12.8	
Area (km^2)	9	116	29	
Median summer radon (dpm/l)	1.45±.31	1.43±.26	1.40±.27	1.50±.35
Number of samples	28	35	33	10
Median winter radon (dpm/l)	1.22±.15	1.42±.57	1.10±.30	
Number of samples	4	7	6	

TABLE 19

Radon (dpm/l) in Streams (mp 0-91) with Drainage Area > 100 km^2

mp			Date (1974)	Rn dpm/l	D.F.**	13 km Anomaly
18	Saw Mill River				.002	.02*
25	Sparkill Creek	(above dam, no ice)	Jan 29	39.6	.0006	
		(above dam, under ice)	Feb 13	62.5		
		(above dam, no ice)	Feb 20	37.6		
		(above dam)	Aug 6	23.8		
		(below dam)	Aug 6	9.8		.001
34	Croton River	(summer flow)			.002	.02*
45	Annsville Creek				.010	.10*
47	Popolopen Creek				.004	.04*
58	Moodna Creek	(below rapids)	Aug 7	9.3	.010	.09
59	Quassaick Creek				.006	.06*
60	Fishkill Creek	(in rapids)	Aug 7	0.9	.013	.01
67	Wappinger Creek	(below falls)	Aug 7	11.3	.011	.12
91	Wallkill River Rondout Creek	(below dam)	Aug 7	2.1	.087	.18

* Assuming Rn = 10 dpm/l

** D.F. = .01 yrs x 0.5 m x Drainage ARea/(River Cross-Section) x 13 km

TABLE 20

Radon Budget for Hudson Water Column
(atoms m^{-2} sec^{-1})

Region	Tappan Zee		Hudson Highlands	
Season	Summer	Winter	Summer	Winter
LOSSES				
Decay	126±23	125±50	298±58	234±64
Evasion	163±82	126±63	160±80	96±48
INPUTS				
Radium-226	8±4	8±4	18±8	18±8
Streams	3±5	3±5	36±10	36±10
Groundwater	0	0	80±40	0±40
From Sediments	278±85	240±81	324±107	276±80
TOTAL LOSS = TOTAL INPUT	289±85	251±80	458±99	330±80

TABLE 21

Comparison of Diffusive, Observed and Turbated Fluxes

	Tappan Zee		Hudson Highlands	
C_{eq} (dpm cm^{-3})	0.33 ± 0.10		0.42 ± 0.11	
Number of locations	8		5	
Season	Summer	Winter	Summer	Winter
D ($m^2 sec^{-1}$ x 10^9)	1.4	0.7	1.4	0.7
θ	1.2±.1	1.2±.1	1.2±.1	1.2±.1
Calculated diffusive flux (atoms $m^{-2} sec^{-1}$)	118±48	83±34	151±55	107±39
Observed flux (atoms $m^{-2} sec$)	278±85	240±81	324±107	276±90
Incremental flux (atoms $m^{-2} sec^{-1}$)	160±98	157±88	173±120	169±98
C_{eq} (dps cm^{-3}) x 10^{-4}	55±17	55±17	70±18	70±18
Minimum depth (cm)	3±2	3±2	2.5±2	2.5±2

an average of $(KT)^{1/2}$ = 15 km from its source. Thus, radon should be well mixed across the estuary, although large regional source variations could result in gradients along the flow axis. We have divided the estuary into segments and have constructed a mass balance for radon in two of these, the Tappan Zee region (mp 20-40) and the Hudson Highlands (mp 40-57). Since no consistent axial or vertical gradients exist, we treat each segment as a well-mixed box. In the absence of axial gradients, we can ignore horizontal advection and diffusion into and out of each box. The principles used to construct the mass balances are outlined below, and the construction is done for a unit surface area in each box.

Production in the Water Column

Radon is produced at a measurable rate by the radioactive decay of Ra-226 dissolved or suspended in the water. This rate can be calculated by integrating Ra-226 activity over the mean depth. No consistent seasonal or regional variation in this activity was observed, and the average concentration from all of the data of 0.085 $\pm$ 0.04 dpm/l was used. The variation is probably largely due to variations in the amount of suspended material in each sample. Suspended plus dissolved Ra-226 accounts for less than 5% of the total radon input.

Stream Inflow

The contribution of stream runoff was calculated by taking the average stream flow over the year, assuming an average concentration of 10 dpm/l, and dividing by the estuary area in the segment of interest. In the Tappan Zee, runoff is 0.13 $km^3 yr^{-1}$ and the input is 3 $\pm$ 5 atoms $m^{-2} sec^{-1}$. In the Hudson Highlands, runoff is 0.42 $km^3 yr^{-1}$ and the input is 36 $\pm$ 10 atoms $m^{-2} sec^{-1}$. This input is about 1% of the total in the Tappan Zee, and about 10% of the total in the Highlands.

The anomaly which a stream might produce in the estuary is listed in Table 19 and was calculated as follows. The tidal excursion of the estuary is about 13 km. Thus, a stream input will be mixed throughout at least this range. For each large stream a dilution factor (D.F.) was calculated, assuming rainfall of 100 cm/yr, runoff of 50%, estimating the stream drainage area, and assuming that in a mean radon life (0.01 years) this volume of water is added to 13 km. The anomalies (dpm/l) which could be expected from each stream is listed in Table 19, and are generally less than 10% of the median concentrations. An observed anomaly might be several times larger, since rainfall is episodic.

Groundwater

Supply of radon to the estuary by groundwater is the most difficult input parameter to characterize. Groundwater typically contains $\sim 10^3$ dpm/l and thus a small input could add significant amounts of radon. To introduce 50% of the total radon inputs would require groundwater flow amounting to 2.5% of the precipitation falling in the drainage basin surrounding the Hudson Highlands region and 22% in the drainage basin surrounding the Tappan Zee. Thus, the Tappan Zee should be free of major groundwater inputs derived locally. The bedrock geology does not indicate any outcrops of potential

aquifers and the highly impermeable glacial clays which underlie the Tappan Zee make groundwater flow even more unlikely.

We have observed a type of groundwater flow in the Hudson Highlands, however, along coarse fill used in embankments for railroad tracks. Pumping of water by the rise and fall of the tides occurs through these fill areas. As the tide rises, the banks accumulate water. As it falls, the water percolates back into the river. Water from one of these percolating outfalls was found to have a radon activity of $\sim$ 100 dpm/l. Assuming this is typical, that the banks occupy 2% of the estuary surface area, and that 0.25% $\pm$ .12 m of water exchanges each tidal cycle, the summer groundwater input to the water column in the Highlands is equivalent to 80 $\pm$ 40 atoms m^{-2} sec^{-1}. In winter, the embankments often should be frozen and tidal pumping greatly reduced. Railway embankments are not nearly as common along the Tappan Zee, and the great width of this region should make a tidal pumping input much less important than for the Highlands. Thus, we assume that groundwater is not a significant input to the Tappan Zee.

Radon Decay

The primary sink for radon in the water column is decay. The rate can be calculated by integrating the average concentration over the mean depth. Mean depths were computed from the Hudson River Navigation Charts and include marsh areas.

Although mixing in the estuary is rapid it is not instantaneous. If the combined effects of decay, evasion, and input from sediments (Table 20) were allowed to act on a column of water 1 m deep which was isolated from the rest of the estuary, this water would accumulate radon at a rate of about 90 atoms m^{-2} sec^{-1}. In half a tidal cycle (2×10^4 secs), this would amount to 0.2 dpm/l in concentration. Thus, incomplete mixing of marsh waters with the remainder of the estuary may create some variation in radon concentrations.

Evasion to the Atmosphere

During October 1974, two weeks of daily measurements were made to determine the concentration of radon in equilibrium with the atmosphere, by flushing air through 19 liters of distilled water for $\sim$ 2 hours at $\sim$ 3 l/min. Results ranged from 0.02-0.05 dpm/l at 15-20°C. Thus, estuary radon is considerably in excess of atmospheric equilibrium, and a net evasive flux occurs. The rate of evasion has been calculated by use of the Lewis and Whitman (1924) stagnant film model which envisions gas transport across the air-water interface to be limited by molecular diffusion through a thin film of water. The surface of this film is assumed to be in equilibrium with the atmosphere and the base of the film has a concentration equal to the measured surface water concentration. Film thickness has been related to wind speed (Broecker and Peng, 1974; Emerson, 1975) and we have estimated a thickness of 95 μ for the Hudson in summer (average wind speed - 4.4 m sec^{-1}) and 60 μ in winter (average wind speed - 5.9 m sec^{-1}). As discussed by Hammond and Simpson (1977), this estimate is based on more representative wind speed data than the film thickness used by Hammond *et al.* (1975). Using surface water concentrations listed in Table 18 and assuming atmospheric equilibrium to be 0.03 dpm/l in summer and 0.06 dpm/l in winter, the values in Table 20 were

calculated. Evasion and decay are of comparable importance.

Variations in evasion could cause changes in radon concentration. If the exchange rate was doubled in the Tappan Zee, radon would be lost at about 160 m^{-2} sec^{-1}, and in one day this would amount to a decrease of 0.35 dpm/1. If the exchange rate was halved, the anomaly would be +0.18 dpm/1. Variations in wind speed can produce changes in the water column concentrations similar to the observed variations.

Diffusional Input from Sediments

We have now established estimates of the loss terms for radon from two segments of the Hudson and all of the important input terms except one, the supply from sediments. This input must balance the radon budget, and its magnitude can be compared with the amount that molecular diffusion in the upper layers of the sediment should supply.

The problem of molecular diffusion in sediments has been discussed by Berner (1971) and equations for radon diffusion has been derived by Broecker (1965). Writing a balance for radon production, decay, and diffusion in one dimension

$$\frac{dC}{dt} = \lambda C_{eq} - \lambda C + \frac{d}{dx}\left(D_s \frac{dC}{dx}\right) \qquad (1)$$

where C = concentration of radon per wet sediment volume at x
C_{eq} = concentration of radon supported by emanation at x
λ = decay constant for radon
D_s = effective diffusivity of radon in sediments
x = depth in sediment

Porosity is assumed to be constant with depth and does not appear in the equation because of the definition of C. Assuming C_{eq} and D_s to be independent of depth, eq. 1 can be solved for the flux across the sediment-water interface per unit area,

$$J_o = (D_s\lambda)^{1/2} (C_{eq} - C_o) \qquad (2)$$

where C_o = concentration at the sediment-water interface, taken to be equal to that in the overlying water column.

Under molecular diffusion $D_s = \frac{Dm}{\theta^2}$ where D_m = molecular diffusivity and θ = the effect of tortuosity on diffusive path length ($\theta > 1$). D_m at 18°C has been measured by Rona (1971) and the effect of temperature has been calculated by Peng (1973). Li and Gregory (1974) have pointed out that diffusivity should increase by no more than 8% when salinity increases from zero to 35°/$_{oo}$. The effect of tortuosity is less well constrained. Li and Gregory (1974) found θ = 1.35 for Pacific red clay with a porosity of 50%. Hudson sediments typically have a porosity of 60-80%, so an estimate of θ = 1.2 should be accurate within 10%. The calculated diffusive flux is listed in Table 21. The uncertainty is primarily due to variability of measurements of C_{eq}. The calculated flux accounts for only 40% of the total input required by the budget (from Table 20). To supply the required flux, D_s must be increased by a factor of 6. It is unlikely that the measurement of D_m is this much in

error. Instead, we suggest that stirring of the surface layer of sediment (turbation) is significant in transporting radon across the sediment-water interface. Since the turbation effect appears to be similar in both summer and winter, and the benthic macrofauna are expected to be much less active at low temperatures, currents are probably the primary cause. An additional factor which appears to limit benthic organism activity in the area of the Hudson of interest is that of extremely variable salinity. Both the Hudson Highlands and Tappan Zee contain completely fresh water for appreciable periods of the year, although average salinities range from a few parts per thousand up to about 10 parts per thousand.

It is conceivable that roughness of the sediment surface might increase the total area of sediment sufficiently to enhance the radon flux above that computed using a planar surface. We can evaluate the significance of surface roughness with some simple calculations. Radon gradients should have a half-distance of about 2 cm, so topography with a wavelength greater than this will increase the surface area contributing to the diffusional flux beyond the surface area of a plane. Assuming a sinusoidal morphology with amplitude A and wavelength 2R, the path length dl covered by horizontal movement dx is:

$$dl = \left[1 + \left(\frac{A\pi}{R} \cos \frac{\pi x}{R}\right)^2\right]^{1/2} dx \qquad (3)$$

Large scale features of the channel examined with a PGR indicate that $A/R < 0.06$ for features with amplitudes of a few feet or more. The absence of microtopography is more difficult to demonstrate but an upper limit might be $A/R = 1/\pi$. This morphology would increase the diffusional area by 22%. However, it is unlikely that such topography exists in the muddy sediments of the Hudson and we take the surface area of the sediment-water interface to be equal to that of the map area.

Turbation Input from Sediments

To quantify transport due to turbation is a difficult problem. The actions of organisms have been modeled as a diffusive mechanism (Goldhaber et al., 1975; Hammond et al., 1975; Guinasso and Schink, 1975 and others). Transport in this type of model is characterized by an eddy diffusivity which exceeds molecular diffusivity within a turbated zone. Assuming that turbation is uniform spatially and temporally, we can calculate the minimum thickness of the turbated zone required to supply to observed flux (Table 21).

Alternatively, by assuming a depth to which turbation is effective, the eddy diffusivity required in the turbated zone to produce the observed flux across the sediment-water interface can be calculated, treating the sediments as a two-layer system. In the upper turbated layer (thickness = d), a uniform eddy diffusivity D_1 prevails. Below this, transport is by molecular diffusion and $D_2 = D_s$. A solution to the two-layer problem for radon in the surface ocean has been presented by Peng et al. (1974). Following this approach, the general solution to eq. 1 is:

$$(C_{eq} - C) = Me^{-ax} + Ne^{+ax} \qquad (4)$$

where a, M and N are constants. In the upper layer $a_1 = (\lambda/D_1)^{1/2}$ and in the lower layer $a_2 = (\lambda/D_2)^{1/2}$. The unknown quantities are M_1, N_1, M_2, N_2 and a_1.

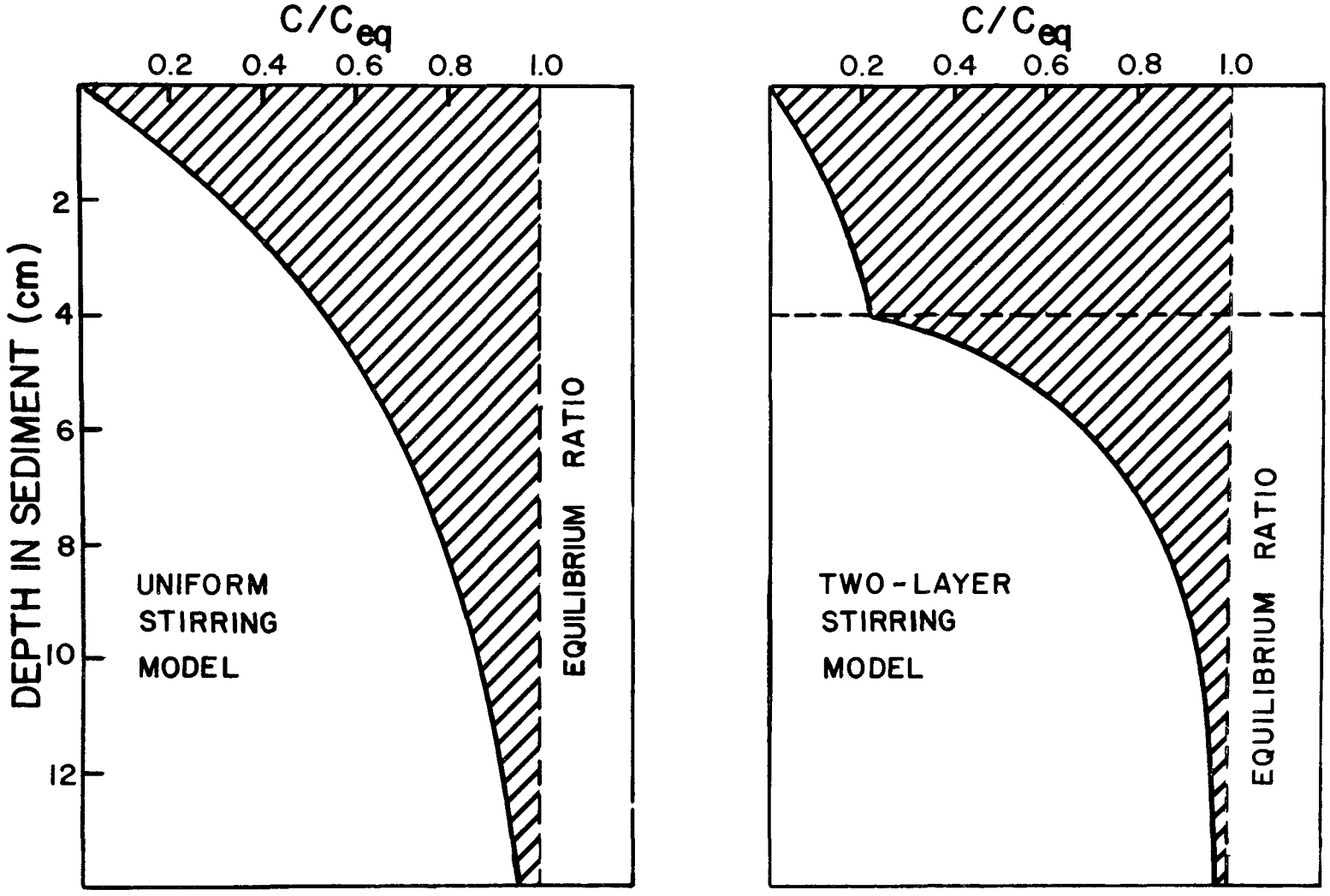

Figure 45. Calculated radon profiles in sediment which could produce the observed water column standing crop of radon. One model assumes a uniform eddy diffusivity, while the other assumes two layers, with the deep one characterized by molecular diffusion rates of radon.

Defining the lower layer to begin at y = 0 (so y = x-d), the boundary conditions are that radon concentration at the sediment-water interface must equal the concentration in the overlying water column

$$C_{x=o} = 1.43 \text{ dpm/l}$$

the flux across the interface must equal the observed flux

$$J_o = D_s \left.\frac{dC}{dx}\right|_{x=o} = 260 \text{ atoms } m^{-2} sec^{-1}$$

the concentration at the base of the upper layer must equal that at the top of the lower layer

$$M_1 e^{-a_1 x} + N_1 e^{a_1 x} = M_2 e^{-a_2 y} + N_2 e^{a_2 y} \quad \text{at } x = d,\ y = 0$$

the flux leaving the lower layer must equal the flux entering the upper layer

$$D_1 \left.\frac{dC}{dx}\right|_{x=d} = D_2 \left.\frac{dC}{dy}\right|_{y=0}$$

and deep in the sediment the concentration must equal the equilibrium value

$$C = C_{eq} \text{ at } y = \infty$$

With five boundary conditions and five unknowns, the concentration vs. depth profile can be calculated. If the thickness of the turbated zone is large, the calculated profile of radon deficiency (Figure 45) is a simple exponential and $D_1 = 8 \times 10^{-5}$ cm^2 sec^{-1}. If the thickness is chosen to be 4 cm in the Tappan Zee, the calculated summer profile (Figure 45) clearly reflects the two-layer character and $D_1 = 1.2 \times 10^{-4}$ cm^2 sec^{-1}. The predictive power of this model is limited, however, unless either D_1 or d can be evaluated independently since D_1 is quite sensitive to d. Surficial sediments in this estuary have high porosity and low viscosity (Olsen et al., 1976). The thickness of this soupy layer observed in cores averages about 2 cm in many areas. Below this depth, the viscosity increase is sufficient for sediment to retain its shape when extruded from core liners. On the basis of textural criteria, we chose d = 2 cm. This value is smaller than the minimum thickness required to produce the average observed flux, (Table 21), although it is within the estimated uncertainty.

It seems likely, however, that uniform stirring to 2 cm is not the only mechanism which can augment the diffusive flux in transporting substances across the interface. Ten of the 106 summer measurements had radon concentrations more than 3 σ from the median. This is more than twice the variability expected statistically. Three of these samples were collected on September 15, 1972 at mp 18 and are plotted vs. depth in Figure 45A. Their relationship to salinity indicates that the high values observed are not analytical contamination, but represent a localized and transient injection of radon into the water column. Assuming a mean water depth of 10 m and an average concentration of 6 dpm/l, to generate such an anomaly would require injection of 5×10^8 atoms m^{-2}, or all of the atoms stored in 5 cm of sediment at equilibrium. This estimate is a minimum since it neglects evasion, horizontal transport, and decay after injection. Portions of the estuary are dredged periodically, but not such activities were noted when samples were collected. Estuaries are regions of active erosion and redeposition, and it seems reasonable that

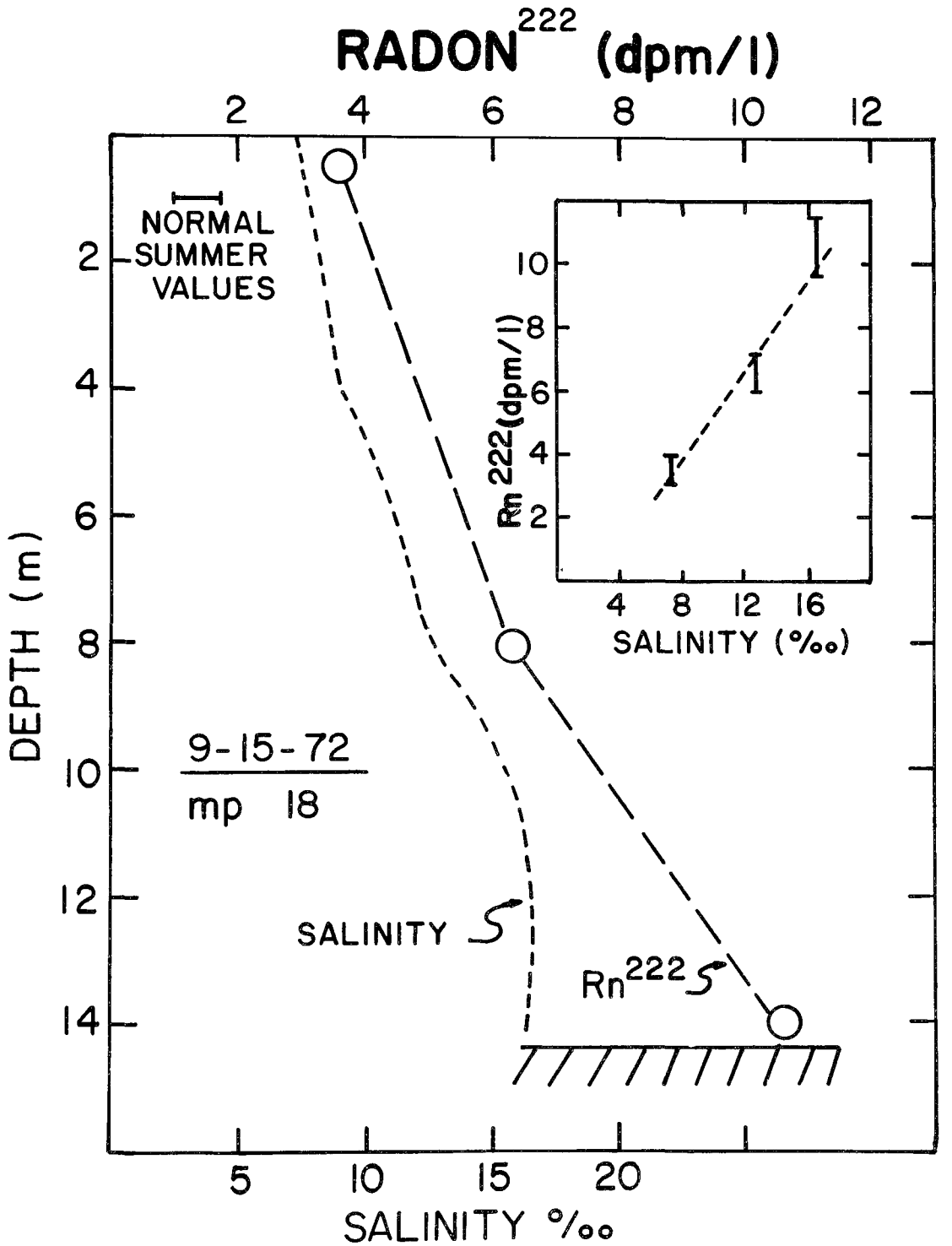

Figure 45a. Radon-222 concentration (dpm/l) vs. water depth (m) in the Hudson 15 September 1972. Salinity values are also shown.

transient anomalies can be produced by stochastic events such as slumps. The magnitude of the anomaly which a slump might produce depends on the thickness of sediment involved and the time which elapses between slumping and sampling.

Assuming that current turbation occurs uniformly and rapidly enough to remove all radon from the upper 2 cm of sediment, that transport occurs by molecular diffusion alone below 2 cm, and that values in Table 21 are accurate, stochastic reworking must supply a flux of about 50 atoms m^{-2} sec^{-1}. If this flux is supplied from sediments containing equilibrium concentrations of radon reworking can be characterized by a mass transport parameter, k, where

$$k = \frac{\text{reworking flux}}{C_{eq}} = \text{(depth of reworking) (frequency of reworking)}$$

On the basis of our data, an average radon flux due to stochastic reworking yields k = 0.6 m yr^{-1}, but the frequency and depth of reworking cannot be independently constrained. We can estimate the maximum frequency on the basis of time required for ingrowth of radon in sediment ($\sim 10^6$ secs), requiring a reworking depth of 2 cm (below the turbated layer). A maximum depth of 2 m might be estimated, requiring a reworking frequency of once every 3 years. If the relaxation time from a reworking event is one day (before radon concentrations in the water column return to "normal") and we observe an anomaly on one of twenty sampling trips, the frequency is about 5×10^{-7} sec^{-1} and the average reworking depth should be 4 cm.

CONCLUSIONS

Radon-222 is distributed rather uniformly throughout the water column of the Hudson estuary (Table 22). Vertical and axial variations are generally less than 20%. Slightly lower concentrations are observed in winter than in summer. By estimating the rate of gas exchange in the Hudson a mass balance for radon can be constructed. The sinks for radon are decay (40-65% of total) and evation (60-35% of total) with relative rates depending on mean depth. Inputs from radium-226 decay in the water column, stream runoff, and ground water are small in comparison to inputs from sediment.

The flux of radon supplied by molecular diffusion from sediments accounts for only 40% of the total input from sediments. This indicates at least one other transport mechanism involving the sediments must also be significant in the supply of radon. If we assume that the upper two centimeters of sediment, which has very low viscosity compared to underlying material, is stirred rapidly and continuously by tidal currents (relative to diffusion), a supply of radon comparable to that of molecular diffusion can be accounted for. A second mechanism, attributed to stochastic reworking of sediment by erosion and slumping, contributed a radon flux of approximately half of that supplied by molecular diffusion.

Quantitative application of these models to the transport of other dissolved species is not yet possible, because we cannot distinguish between the depth to which such processes operate and their rate of occurrence. Because nutrients, transition metals, and oxygen will have concentration vs. depth profiles which differ from that of radon, a one-to-one correlation between their transport and that of radon cannot be made. Detailed profiles

TABLE 22

Summary of Rn Measurements

Coll. Date	M.P.	Depth (m)	Sal. (°/₀₀)	Temp. (°C)	Excess Rn^{226} dpm/1	Rn^{226} dpm/1	Notes
1971							
9/23	25	0	1.0		1.89		from boat mooring
9/27	25	1	0.6	20.4	0.96	0.052	station no. 1
		6	1.9	20.6	0.99	0.052	
		10	8.1	21.7	1.12	0.085	
	26	1	0.5		1.23	0.032	station no. 2
		0	1.2		2.33	0.079	from west shallows, station no. 3
		0	0.9		1.31	0.038	at pier, station no. 4
11/10	25	0	3.7		0.42		
		4	4.0		0.49		
		8	4.7		0.45		
		12	7.3	∿13	0.73		
1972							
6/26	18	0	0.0	19.3	1.22	0.099	
		4			1.20	< 0	
		8	0.0		1.21	0.107	
7/10	18	0	0.2	21.6	1.25		
		3	0.4	21.4	∿1.2		(could not find
		15	2.0	20.9	∿1.0		analyses recorded)
7/18	18	0	0.0	24.4	1.62		
		5	2.0	23.7	1.55		
		15	12.3	21.6	1.44		
7/22	63	0	0.0		10.96		
		7.5	0.0		1.38		
		14	0.0		1.51		
7/22	60	0	0.0		1.23		
		5	0.0		1.46		
		10	0.0		1.28		
7/23	54	0	0.0		0.90		
		7	0.0		1.28		
		17	0.0	24.6	2.75		
7/23	47	0	0.0	24.5	1.30		
		10	0.0		1.16		
		20	0.0		2.02		
		30	0.0		1.14		
7/22	37	0	0.0	29.2	1.46		
		4	0.0	24.7	1.52		
		10	5.4	23.0	2.04		
7/25	-3	0	19.1	22.9	1.13		
		4.5	22.8	21.2	1.15		
		8	25.2	20.2	1.08		

(continued)

TABLE 22 (continued)

Coll. Date	M.P.	Depth (m)	Sal. (°/₀₀)	Temp. (°C)	Excess Rn^{226} dpm/1	Rn^{226} dpm/1	Notes
7/26	16	0	7.3	25.1	1.38		
		9	11.7	23.7	1.49		
		15	12.3	23.6	1.78		
8/1	18	0	5.1	25.0	1.25		
		5	6.9	23.9	1.25		
		7.4	7.4	23.8	1.19		
		14	10.3	23.4	1.47		
8/8	21	0	5.2		2.37		
		5	5.9		1.24		
		12	7.1		1.04		
8/14	18	0	4.2		0.95		
8/22	21	0	5.3		1.27		
		4	6.9		1.11		
		10	14.1		2.09		
		14	14.4		2.01		
9/4	25	0			1.16		station no. 1 east 8 1
		0			1.32		station no. 3, 8 1
		0			1.03		station no. 4, 8 1
9/15	18	0			5.20		bucket sample, 8 1
		0			3.58		8 1
		8			6.30		8 1
		12			10.62		8 1
9/23	18	5			1.44		8 1
		10			1.57		8 1
		14			1.27		8 1
10/18		0			0.56		8 1
		5			0.79		8 1
		9			0.86		8 1
		12.5			0.69		8 1
11/7		0			0.57		station no. 1 ∿16.5 1
		0			0.80		station no. 1, 8 1
		12			1.20		station no. 1, 8 1
		0			0.61	0.089	station no. 2, 19 1
		0			0.33	0.102	station no. 3, 19 1
		0			0.73		station no. 4, 8 1
		0			0.78		station no. 4, 19 1
		10			1.22		station no. 4, 8 1
1973							
8/23	31	0			1.27	0.13	
		6			1.45	0.15	
		>10			2.10	0.30	hit bottom, mud on Niskin

(continued)

TABLE 22 (continued)

Coll. Date	M.P.	Depth (m)	Sal. (°/₀₀)	Temp. (°C)	Excess Rn^{226} dpm/1	Rn^{226} dpm/1	Notes
1974							
8/5	25	0			1.73		
	18	0			0.92		
8/6	91	0	0.0		0.36		
	76	0	0.0		1.31		
	62	0	0.0		0.90		
8/7	57	0	0.1	25.8	0.77	0.049	
		10	0.1	25.7	0.78		
		20	0.1	25.7	0.90	0.083	
	53	0	0.5	25.5	1.03	0.089	
		20	0.5	25.6	1.04		
		40	0.4	25.6	0.82		
	49	0	0.7	25.7	1.30		
		24	1.3	25.5	1.20		
	46	0	1.4	25.8	1.14		
		12	1.6	25.8	1.29		
		24	1.7	25.7	1.13		
8/9	51	0	0.2	ND	1.38	0.154	
	47	0	0.5	ND	1.32		
	42	0	1.3	26.8	1.27		
		7	1.4	25.8	1.30	0.104	
		14	1.5	25.9	1.59		
	37	0	2.3	27.0	1.25		
		8	2.9	26.3	1.28		
	29	0	5.0		1.86		
	18	0	8.4		1.67		
8/13	52	0			0.80		
	47	0			1.20		
	37	0			1.15		
	31	0			1.01		
	25	0			1.12		
	18	0			0.82		
8/16	18	0			1.03		
8/18	52	0			1.35		
	47	0			1.24		
	37	0			1.29		
	31	0			1.05		
	25	0			1.70		
8/19	18	0			1.18		
8/22	52	0			1.28		
	47	0			1.38		
	37	0			1.27		
8/23	31	0			1.32		
	26	0			1.07		
	25	0			1.08		
	24	0			1.14		
	18	0			1.30		

(continued)

TABLE 22 (continued)

Coll. Date	M.P.	Depth (m)	Sal. (°/₀₀)	Temp. (°C)	Excess Rn^{226} dpm/l	Rn^{226} dpm/l	Notes
8/27	26	0			0.97	0.22	
		6			1.31		
	18	0			1.00		
8/28	37	5	3.6	27.1	1.18	0.22	
	1	0	18.8	25.2	1.01		
	-12	12	29.0	22.0	0.76		
9/10	76	0	0.0	ND	1.70	0.078	from dock
	47	0	ND	ND	1.56		from dock
12/13	25	1			1.18		from pier
	18	1			1.11		from dock
1975							
1/4	57	1			0.68	0.075	
	53	1			0.66	0.079	
		20			1.33	0.085	
	47	1			1.89	0.140	
	41	1			0.86	0.062	
		15			1.04	0.068	
	35	1			1.93	0.208	
		9			1.13	0.122	
	25	1			2.63	0.095	
		9			1.05	0.102	
	18	1			0.92	0.109	
2/10	25	1			1.27	0.054	from pier
	18	1			0.88	0.076	from dock
3/7	25	1			1.84	0.057	from pier
	18	1			1.27	0.073	from dock

of radon distribution in sediments could help provide answers to these questions. It is clear that uniform current turbation of surficial sediments will accelerate consumption of oxygen, decay of organic matter, and recycling of nutrients to the overlying water column. Stochastic reworking of sediments from depth may be effective at introducing trace metals to the overlying water column as this allows materials to bypass the zone of oxidized sediment near the sediment-water interface by mixing anoxic interstitial waters directly with the overlying water column.

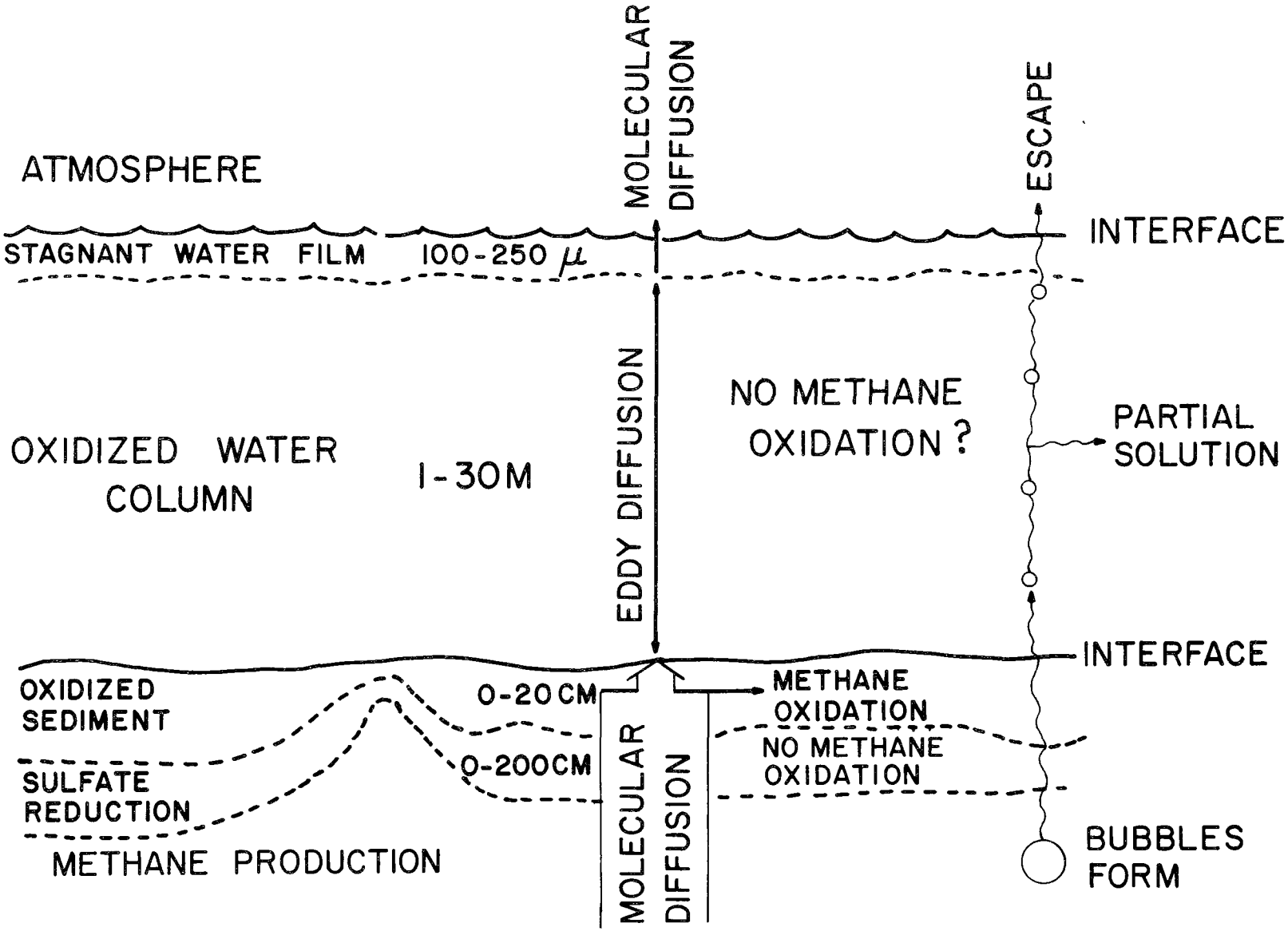

Figure 46. Biogeochemistry of methane in estuaries.

SECTION 10

METHANE AS AN INDICATOR OF TRANSPORT PROCESSES BETWEEN THE SEDIMENTS AND WATER COLUMN IN THE HUDSON

INTRODUCTION

Methane concentrations in natural waters are controlled by a balance among production, oxidation and mass transport. Methane production and oxidation have been studied in a wide variety of aqueous environments by both microbiologists and geochemists, although neither discipline has yet produced a fundamental understanding of the role of micro-organisms in either of these processes. Some of the controlling factors have recently been reviewed by Reeburgh and Heggie (in preparation). Methane production occurs by at least two mechanisms (Doelle, 1969; Mechalas, 1974), including reduction of CO_2 (Claypool and Kaplan, 1974) and acetate fermentation (Koyama, 1963). The microorganisms responsible for these processes are strict anaerobes but may be inhibited by the presence of sulfide (Cappenberg, 1975). This usually results in a lack of methane production in the presence of sulfate reduction (Atkinson and Richards, 1967; Tsou et al., 1973; Martens and Berner, 1974).

Methane oxidation can be carried out by a large number of aerobic microorganisms commonly found in lakes (Cappenberg, 1972; Rudd et al., 1974), rivers, river mud, soils (Whittenbury et al., 1970) and marine mud (Hutton and Zobell, 1949). Isotopic evidence and mass balance considerations suggest that methane oxidation can also be accomplished by sulfate reducers (Feely and Kulp, 1957; Nissenbaum et al., 1972; Reeburgh, 1976).

Methane transport through sediments may occur by diffusion, turbation and bubble migration (Figure 46). Diffusive processes have been discussed by a number of authors and a concise treatment can be found in Berner (1971). The importance of turbation by organisms and currents in transporting dissolved substances has recently begun to be quantitatively assessed (Goldhaber et al., 1975; Hammond et al., 1975). The importance of bubble transport across the sediment-water interface (hereafter called sediment flatulence) has been recognized by a number of authors (Koyama, 1963; Reeburgh, 1969; Emery, 1969; Martens, 1976 and others). To date, quantitative estimates of bubble transport have been difficult to make. Three approaches have been used: (1) examination of the decrease in organic carbon with increasing depth in the sediment, (2) counting the rate at which bubbles burst at the air-water interface, and (3) leaving a bubble trap above the sediment-water interface for a period of time. Each of these approaches presents complications. The first approach will be difficult to use in the presence of turbating organisms. Their activities may homogenize sediments and made the decreases in organic carbon with depth difficult to observe. The second approach is only useful for systems with

rapid flatulence and quiescent surfaces. Systems with slow flatulence would require observation of large areas for long periods of time to determine fluxes and while the number of bubbles can be counted, their mean size must be estimated to calculate fluxes. Estuaries rarely have surfaces sufficiently calm to permit use of this technique. The third method creates some logistical problems and is only useful for monitoring a rather small area. We present an application of an alternative approach for estimating flatulent releases, based on constructing a mass balance for methane in the water column.

MEASUREMENT TECHNIQUES

Water samples were collected in Niskin samplers and transferred through a tube to glass bottles ($\sim$ 115 cc) which were overflowed by one volume to minimize gas loss. To prevent oxidation during storage, 0.5 cc of $HgCl_2$ (saturated) solution was added and the bottle was capped with a serum cap pierced by a hypodermic needle, preventing bubble entrapment. In practice, a small bubble always forms. To minimize diffusive loss from this bubble through the cap, bottles were kept cool and stored upside down. An aliquot of this sample was injected into a stripping system patterned after those of Swinnerton et al. (1962) and Weiss and Craig (1973). Its dissolved gases were extracted by continuously purging with helium carrier. Methane was separated from O_2 and N_2 on a molecular sieve column (#5A) and measured on a flame ionization detector. Peak resolution is essential for samples containing less than 1 μM CH_4 since at hight sensitivity the detector we used gives a negative response to O_2 and a positive response to N_2. Since high sensitivity also increases baseline noise, peak height can be determined with greater reliability than peak area, although the latter must be known to compare the signal from samples to those from a gas standard which was injected periodically from a gas sampling loop for calibration. The relationship between peak height and area is a function of the condition of the column and, to a lesser extent, of both stripping temperature and sample salinity. The area/height ratio for water samples was determined periodically by use of a freshwater liquid standard with CH_4 $\sim$ 5 μM and is typically 1.1 to 1.3 times that of the gas standard. The sensitivity with the above procedures is 0.01 μM and the absolute accuracy is $\sim$ 6%, with the major uncertainty introduced by the peak area/peak height ratio. Precision for poisoned samples run on different days is about $\pm$ 3%.

A number of storage tests were performed at various temperatures, on waters of varying salinities, as a check on the procedure and to determine if CH_4 is oxidized by bacteria. The storage procedure for poisoned samples appears to be good for at least two weeks and is independent of temperature or light conditions. Storage temperature for unpoisoned samples was chosen to be within a few degrees of in situ temperature. These tests showed that the rate constant for methane oxidation is equivalent to a mean lifetime for methane of more than 20 days in Hudson waters with a salinity of less than a few parts per thousand and a lifetime much longer than this in higher salinity water.

Measurements of CH_4 in sediment were made by extruding sediment from a gravity core within a few minutes of collection, slicing a section of sediment and quickly sealing it in a glass kettle (volume $\sim$ 0.3 liters) along with

100 cm^3 distilled water. The resulting slurry was equilibrated with the gas phase and the concentration of CH_4 in the gas was determined by gas chromatography on a column of molecular sieve #5A with a flame ionization detector. Knowing the P_{CH_4} within the kettle, the air volume, the sediment volume sampled and the temperature, $[CH_4]$ per sediment volume can be calculated to $\pm$ 10%. This is the parameter required for calculating the diffusive flux of CH_4. Crude porosity measurements were made and these permit calculation of $[CH_4]$ to $\pm$ 20% in interstitial waters, the parameter necessary to determine the degree of *in situ* saturation. The kettle technique seems quite reliable for preventing gas loss as shown by measurement of Rn-222/Ra-226 activities on the same samples (Hammond, 1975). One core ($P_{in\ situ} \sim 5$ atm) was apparently saturated with CH_4 *in situ* and formed gas pockets when retrieved, causing $\sim$ 30% loss of Rn-222. The CH_4 measurement here was corrected for this. Oxidation of methane during kettle storage (usually < 24 hours) was apparently not a problem since a number of *in situ* values were observed.

RESULTS

A total of approximately 2.0×10^{10} m^3 of fresh water reaches the New York Bight each year by passing through lower New York Bay. About 85% of this enters the system via the Hudson River (mean annual flow $\sim$ 550 m^3/sec) and $\sim$ 15% is the combined inputs of the Raritan, Passaic and Hackensack Rivers. The average monthly freshwater flow varies by an order of magnitude between spring (high flow) and late summer (low flow), causing the distance of salt penetration (> 0.1°/$_{oo}$) to range between $\sim$ mp 25 and $\sim$ mp 65. Large volumes ($\sim$ 85 m^3/sec) of treated and untreated sewage from New York City and northern New Jersey (DeFalco, 1965) are introduced to the harbor complex. These discharges contribute more than 20% of the fresh water input during low flow conditions. The large sewage loading reduces summertime dissolved O_2 levels to 25-50% of saturation in the Upper Bay and has delivered large amounts of reduced carbon to the sediments. It is important to note that the Hudson Highlands and Tappan Zee reaches of the estuary have quite distinct morphologies. The mean depths are 12.8 m and 5.3 m respectively.

A number of synoptic sets of CH_4 samples were collected along the axis of the Hudson Estuary at different times of the year. Two typical transects (with surface and deep values averaged) are plotted in Figure 47. Their essential features are: CH_4 is greater in winter than summer; CH_4 is greater in reaches of the estuary with deeper water than those with shallow water; and CH_4 rises dramatically in the zone of major sewage loading.

Figure 48 illustrates the variation of CH_4 with depth at individual sampling stations. Fresher water in the upper half of the water column, low in CH_4, enters the northern end of the harbor complex, while more saline water, high in CH_4, flows upstream in the lower half of the water column. At the southern end of the harbor, lower salinity surface water leaving the estuary is high in CH_4, while saline water low in CH_4 is entering near the bottom. In a more pristine region of the estuary, the Hudson Highlands, variations with depth are less consistent. Methane sometimes increases with depth (mp 57, mp 49) but may also have mid-depth minima (mp 53) or maxima (mp 46). Samples collected in winter months show much less vertical variation, but the best

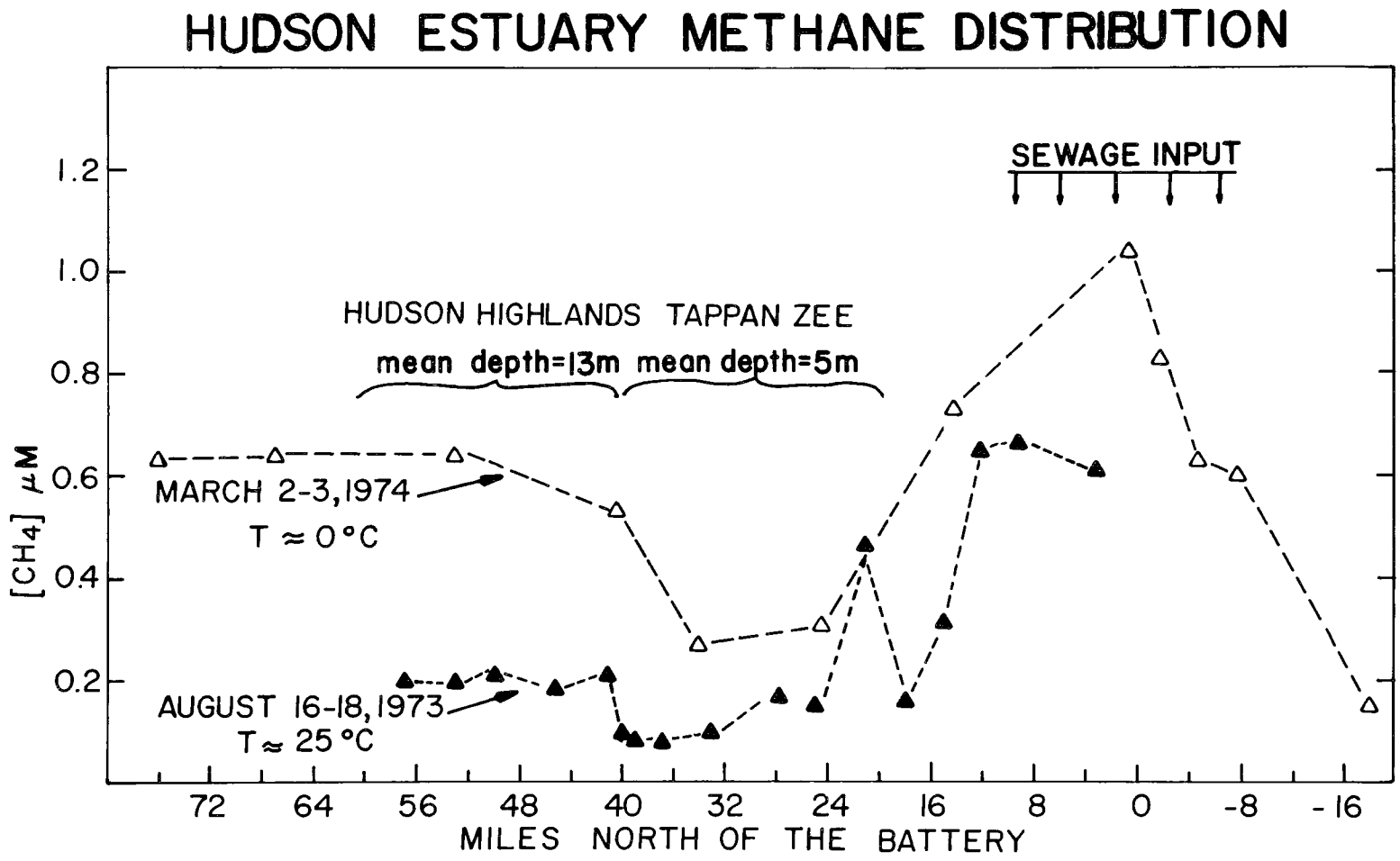

Figure 47. Methane and salinity versus depth in the Hudson.

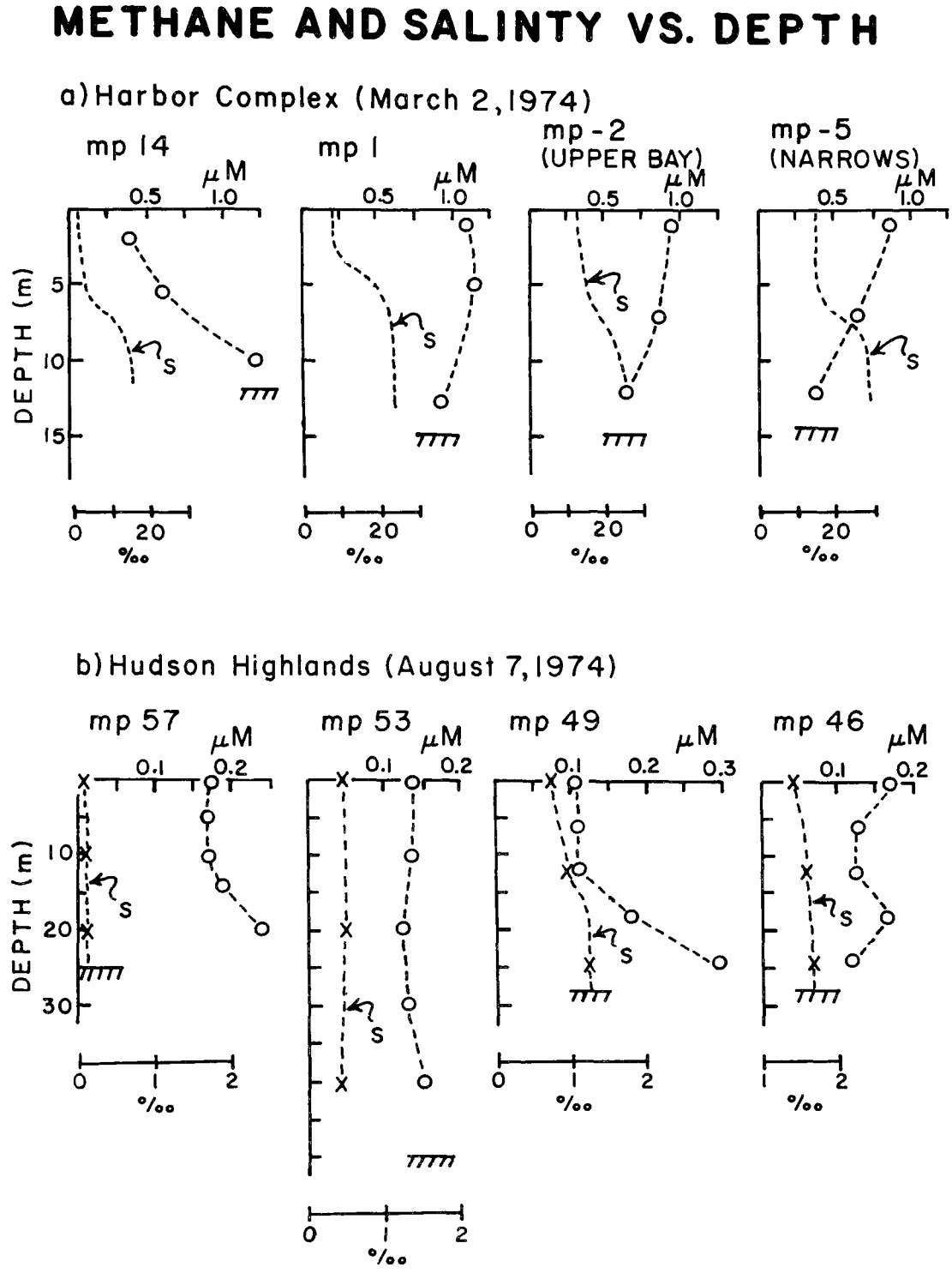

Figure 48. Methane versus mile point in the Hudson: Surface and deep samples were averaged.

generalization that can be made is that CH_4 is uniform in the Highlands within ± 30% (one standard deviation).

Hudson estuary sediments have been discussed by McCrone (1967), Gross et al. (1971) and Olsen et al. (1978). The predominant sediment type is a silty clay with ∿ 3-8% organic matter. Sandy sediments filled with shell fragments cover portions of the navigation channel, some sections of which are periodically dredged, and the sand fraction generally increases from the Tappan Zee to the very sandy sediments of the Lower Bay and New York Bight, with substantial areas of fine-grained sediments, accumulating rapidly in certain zones of the Upper Bay and between Manhattan and New Jersey.

Methane concentrations within surficial sediments show large variations, as abundances observed range over 4 orders of magnitude (Table 23). The upper limit seems to be controlled by saturation of CH_4 in interstitial waters. The ratio of observed concentration to in situ saturation (based on solubility data from Atkinson and Richards, 1967) is listed as S.F. in Table 23.

Clearly, the distribution of methane-saturated sediments is more heterogeneous than general sediment lithology variations. Surface (< 10 cm) sediments may be saturated with CH_4, but more commonly they are not. Cores from mp 49 and mp 37 evolved gas bubbles from ∿ 30 cm, although their surface sediments contained less than 10% of saturation. There is a trend toward greater incidence of surface saturation in the more northerly cores, but insufficient data is available to say this with much confidence. It is reasonable that this may be true, however, because less sea salt reaches these regions and thus sulfide inhibition of methane-producing bacteria in surficial sediments is less likely. The saturated sediments at mp 9 are located within ∿ 1 km of a major input of raw sewage and also in a zone of very rapid sediment accumulation. Methane distributions in Hudson sediments can be summarized by saying that interstitial waters of upper sediments at some locations are saturated in situ, but these are probably isolated pockets. All locations are probably underlain with CH_4-saturated material at some depth. The depth of this saturation is probably a complicated function of the amount and type of organic material present and the average annual salinity.

Three additional observations indicate the widespread nature of CH_4-saturated sediments in the Hudson estuary. Low seismic velocities reported by Worzel and Drake (1959) at mp 25 were attributed to gas-saturated sediments. Gas pockets have been observed to form at depth in several cores other than those described here (C. Olsen, personal communication). The authors have noted bubbles bursting at the river surface at various locations in the Tappan Zee and Hudson Highlands.

DISCUSSION

The distribution of methane in Hudson Estuary waters must be controlled by a balance between inputs and outputs. By treating parts of the lower estuary as well-mixed reservoirs, the importance of methane as a component of carbon cycling in Hudson sediments can be assessed. To develop these concepts, a budget for methane in the water column of the Hudson Estuary has been derived, which includes contributions of advective transport of methane along

TABLE 23

Methane Distribution in Hudson Estuary Sediments

mp	Depth (m)	Coll. Date	Interval (cm)	$[CH_4]$ µmol/l (in sed.)	$[CH_4]$ µmol/l (in IW)	(SF)[a]
76	16	4/6/74	2-10	3480	5520	.99
			10-18	3500	6360	1.14
53	45	3/2/74	2-10[b]	7830	12400	.92
			10-18[b]	6550	11900	.88
49	28	8/6/74	2-6	178	274	.05
41	24	5/18/74	2-6	20.8	32	<.01
			7-9			
41	15	4/6/74	2-10	1350	2140	.40
			10-18	2260	4520	.85
37	9	8/8/74	2-6	123	190	.07
34	10	4/6/74	2-10	19.6	31	<.01
			10-18	28.6	52	.01
25W	5	5/18/74	2-6	0.4	0.6	<.01
25	5	3/2/74	2-12	4.7	7.4	<.01
			12-22	6.0	11	<.01
18W	1	8/27/74	1-6	21	32	.02
			13-15	504	840	.55
			22-24	543	987	.64
18	13	5/18/74	2-6[c]	3.3	5.1	<.01
			14-16			
13W	8	1/8/74	2-7	3.1	4.8	<.01
			7-12	6.0	9.9	<.01
9	15	1/18/74	2-12	2390	3800	.93
			12-24	1500	2720	.67
7	15	5/18/74	2-6	6.1	9.4	<.01
			7-7.5			
1	15	3/2/74	6-18	74	123	.02
-2	19	5/18/74	2-6	12.7	19.6	<.01
-5	14	3/2/74	2-10[c]	1.8	2.9	<.01

[a] (Interstitial water $[CH_4]$)/(in situ saturation)

[b] Corrected value. Rn^{222} measurement on this sample indicated 32% gas loss

[c] Sandy sediment with shell debris

the estuary axis, evasion to the atmosphere, diffusion from the sediments, and the partial dissolution of bubbles created by sediment flatulence. Oxidation of methane in the water column is neglected since the storage tests indicated this process is much slower than evasion to the atmosphere. The reservoirs discussed are the Hudson Highlands (mp 56 to mp 40), the Tappan Zee (mp 40 to mp 20) and the Harbor complex (mp 20 to mp -5).

Advective Transport

It has been shown (Hammond, 1975) that for an estuary such as the Hudson, whose circulation can be approximated in terms of a two-layer advective model, the flux of a property C past any location is equal to the freshwater flux (Q_F) past that location, multiplied by the zero salinity intercept of a tangent on a plot of C vs. salinity at the location of interest. This approach is also valid for estuaries in which one-dimensional advection-diffusion models may be used (Boyle et al., 1974). If this is done at two different locations, the change in intercept, ΔC, can be used to calculate the net addition or loss of C between the two locations, equal to $Q_F \times \Delta C$. A plot of methane vs. salinity for March 1974 is shown in Figure 48A. Plots like this were used to calculate advective fluxes.

Evasion to the Atmosphere

Use of the stagnant-film model (Lewis and Whitman, 1924) for estimating the rate of exchange of gases across the air-water interface has met with considerable success in natural water systems (Broecker and Peng, 1974). This model envisions the rate of mass transport to be limited by molecular diffusion through a thin layer of water at the interface. The thickness of this film can be considered as a convenient parameter for characterizing the rate of gas exchange of an open water surface as a function of environmental variables. In marine systems, the most important forcing function on the rate of gas exchange is apparently wind velocity. Emerson (1975) has proposed an empirical calibration curve for wind speed and film thickness based primarily on exchange rates of Rn-222 in the ocean and in fresh water lakes. He notes that to use such a curve, observations of wind speed must be made at a fixed height above the air-water interface. Field data on which his curve is based are reproduced in Figure 48B with wind velocities taken to be those 10 m above the interface. The mean wind speeds (monthly average of observations at LaGuardia, Kennedy and Newark Airports) during 1973 and 1974 ranged from 4.1 to 6.3 ms^{-1}. This is equivalent to a film thickness of 110-50 μ. A previous estimate of 180 ± 60 μ based on wind speed at the Central Park Observatory (Hammond et al., 1975) must be too low. This film thickness would not permit evasion of methane from the Tappan Zee to keep pace with advective influx (primarily from the Highlands) during winter months, and consequently it must be an over-estimate. Wind measurements at the Central Park Observatory are typically 2 ms^{-1} lower than the regional average from other sites, possibly due to a sheltering effect from surrounding buildings, or to the general decrease in surface wind velocities usually observed in large cities.

The mean residence time of a methane molecule in a well-mixed column of water (depth h) before evasion will be $\frac{hz}{D}$ where z is film thickness and D is

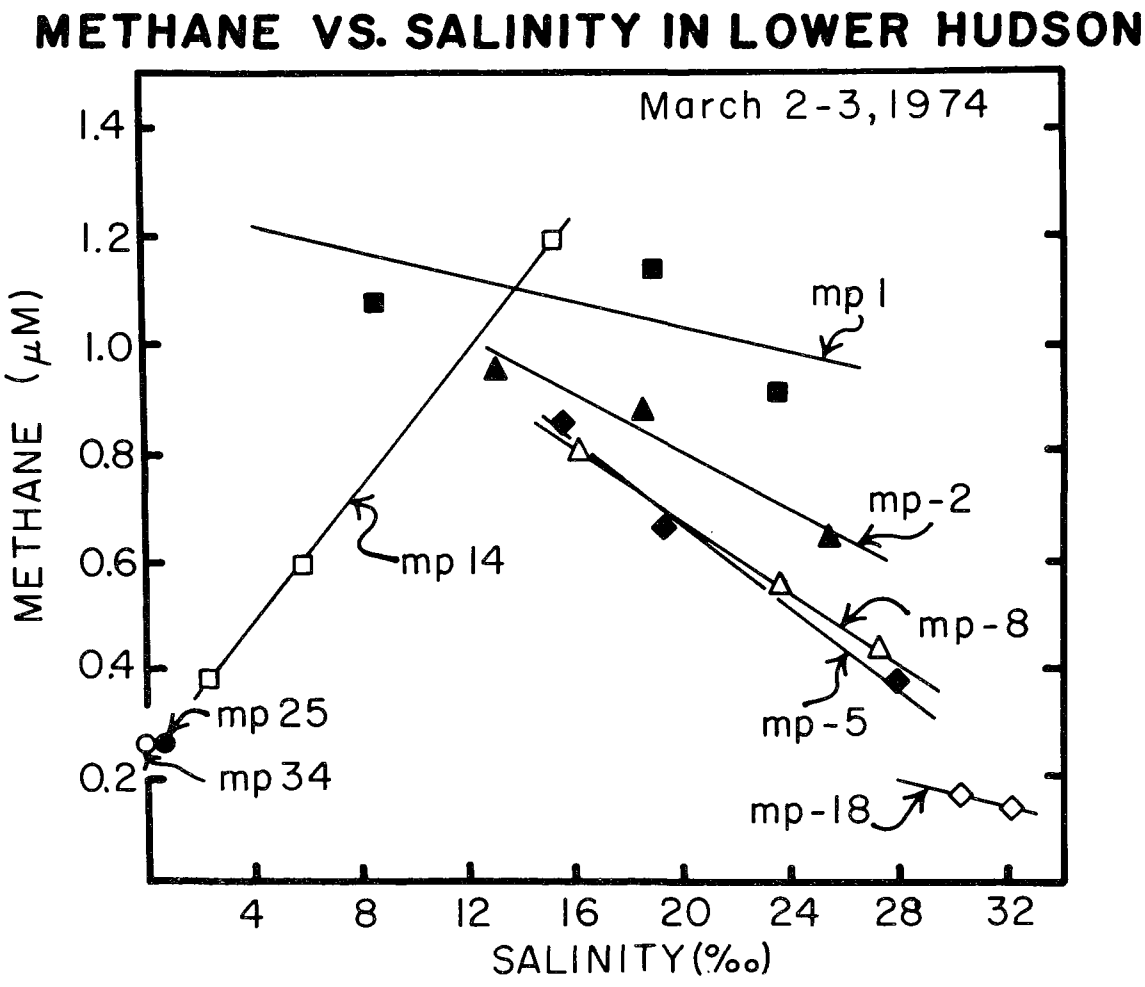

Figure 48a. Methane concentrations in μM/l vs. salinity in Lower Hudson Estuary, March 2-3, 1974, line indicate depth distribution at each sample station.

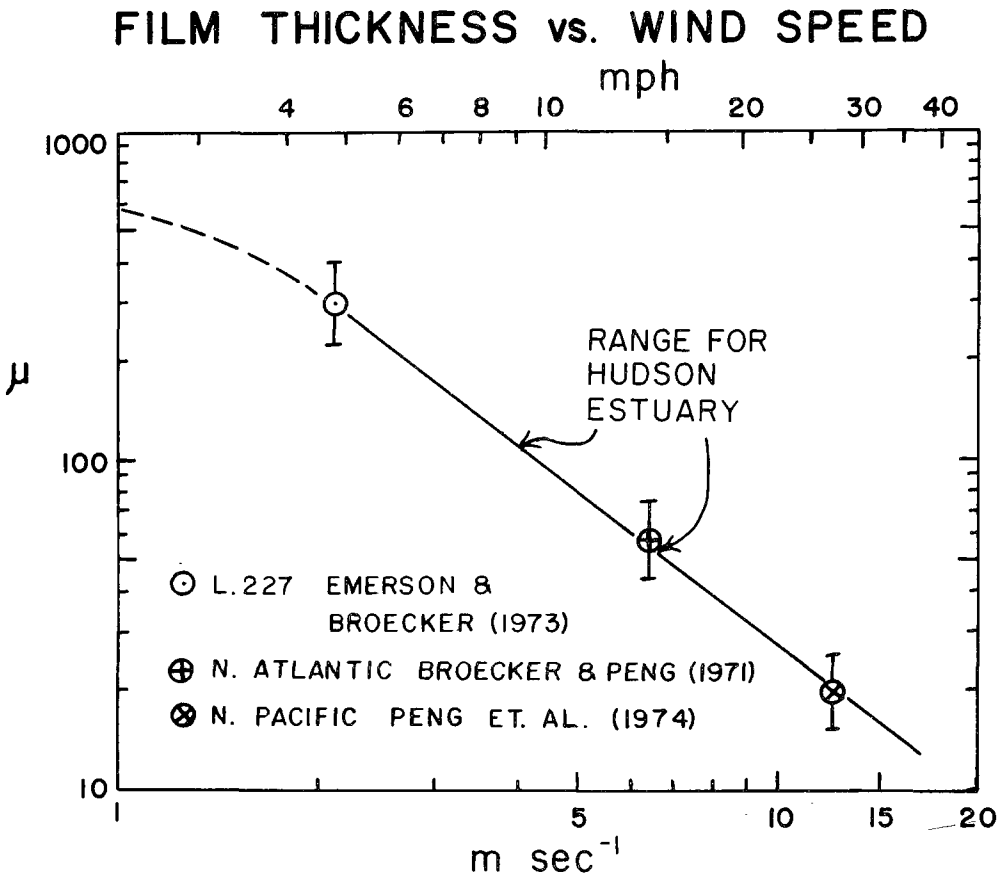

Figure 48b. Surface film thickness vs. wind speed as determined by gas exchange experiments on oceans and lakes

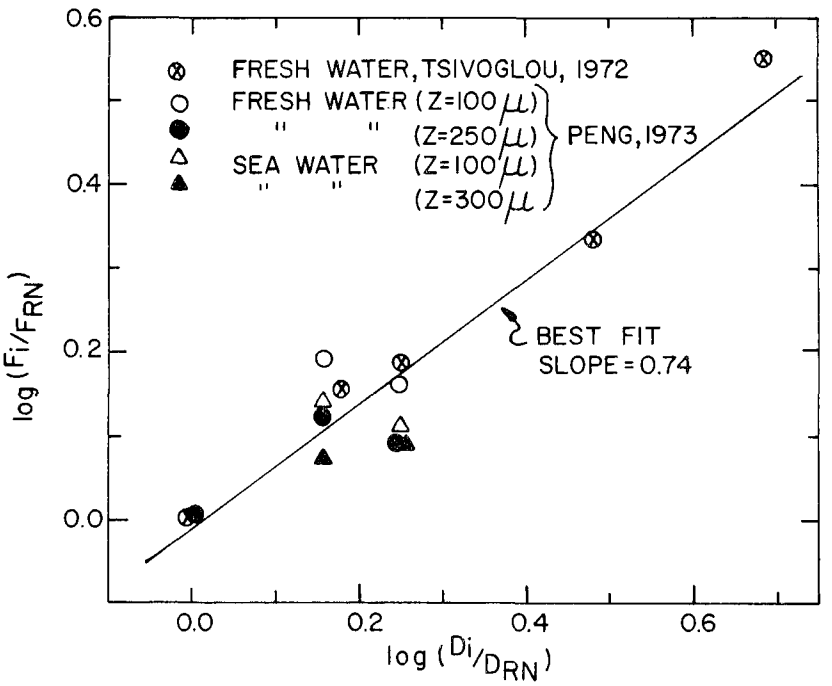

Figure 48c. The mass transfer (flux, i/flux, radon) vs. diffusion (diffusion, i/diffusion, radon) coefficients for various gases in several systems

molecular diffusivity of the molecule. In Tappan Zee waters this time is about three days during both summer and winter, since the temperature dependence of D is nearly compensated by higher winds in the winter. A film thickness for each sampling period was derived by averaging wind speed for a period beginning three days prior to sampling. The evasive flux of gas is then a function of the difference in concentrations between the bulk solution (C_W) and film surface (C_{eq}, assumed to be in equilibrium with the atmosphere):

$$\text{Flux} = D \frac{C_W - C_{eq}}{z} \qquad (1)$$

The average flux, assuming C_W = 0.2 μM, D = 2 x 10^{-5} $cm^2 s^{-1}$, and z = 100 μ, is 4 x 10^{-9} μ mol $m^{-2} s^{-1}$.

An alternative conceptual model for gas exchange in rivers and estuaries has been exploited by O'Connor and Dobbins (1958) based on the film replacement model of Higbie (1935). In this formulation, the exchange rate is limited by the replacement time (r) of a surface film through which molecular diffusion occurs and

$$\text{Flux} = (D/r)^{1/2} (C_W - C_{eq}) \qquad (2)$$

Each model is characterized by a mass-transfer coefficient, D/z or $(D/r)^{1/2}$, and a laboratory comparison of the fluxes of gases with differing diffusivity should test the relative superiority of the two models. Figure 48C is a plot of log ($Flux_i/Flux_{Rn}$) vs. D for experiments performed by Peng (1973) and Tsivoglou (1972) during which a tank of water was agitated and fluxes of different gases were monitored. The stagnant-film model predicts a slope of 1.0 and the surface renewal model predicts a slope of 0.5. The best fit line to the two sets of data has an intermediate slope of 0.74. The O'Connor-Dobbins model has previously been applied to the Hudson by O'Connor (1970) and Quirk et al. (1970), assuming that all turbulence is flow-induced. If the mass transfer coefficients calculated by these authors are equated to the stagnant-film model, a film thickness of z = 320 μ or 230 μ respectively, is predicted. This yields an exchange rate which is clearly too low, as pointed out earlier. This suggests that the empirical relationship between film thickness and wind speed is more accurate here.

Diffusion from Sediments

A first-order material balance calculation provides some important information about the effectiveness of diffusion in supplying methane to the overlying water column. Assuming that methane is unreactive in the upper 10 cm of sediment, a linear gradient should exist there, and if the data in Table 23 are representative of the estuary sediments as a whole, the diffusive flux is calculated to be 1 x 10^{-8} mol $m^{-2} s^{-1}$. This represents a minimum flux (if CH_4 is unreactive) because the diffusional gradient in methane-saturated sediments is probably greater than we assumed, and stirring of surficial sediments by currents and organisms has been neglected. This flux is about three times larger than the flux leaving the estuary by evasion alone, between mp 20 and mp 60, and consequently must be an over estimate. With so few sample locations it is possible that a representative suite of samples has not been collected, but in light of what is known about methane biogeochemistry, it seems much more likely that the major fraction of methane which diffuses into the upper layer of sediments (∿ 0 to 10 cm thick) is oxidized there by microorganisms before

it can diffuse into overlying waters. It is postulated that this layer forms an effective barrier to methane diffusion into overlying waters, certainly in saturated sediments and perhaps in all Hudson sediments. Since the seasonal and regional distribution patterns of methane can be accounted for in the absence of diffusion, we assume diffusion inputs to be small.

Bubble Transport

Diffusion is probably not the major mechanism supplying CH_4 to the estuary waters. The seasonal and depth characteristics of concentration in the water column can be most simply explained by another process. Bubbles can form in sediments if the total pressure of dissolved gases reaches *in situ* pressure. If a sufficient volume of gas accumulates, confinement is no longer possible and bubbles will migrate vertically through the sediment and escape. Martens (1976) has suggested that bubbles may follow tubes created by burrowing organisms. The escape of gas will result in a salvo of bubbles and the process may be termed sediment flatulence. The impact of this process in estuarine sediments has been described by Reeburgh (1969) and Martens and Berner (1974), but a quantitative estimate of its importance is not, to the author's knowledge, available. As the bubble of gas rises through the water column a portion of it will dissolve, resulting in a transfer of methane from the site of its production to the overlying waters.

The problem of diffusion into a water column from an ascending bubble has been dealt with by a number of authors. The treatment presented here, summarized in Table 24, is a modification of discussions presented by Levich (1962), LeBlond (1969) and Guinasso and Schink (1973). The mass flux entering the water from a gas bubble is given in equation 4 (Table 24). Bubbles of radius $r > 0.3$ cm are significantly non-spherical (Levich, 1962), but for simplicity, spherical geometry can be assumed. Neglecting surface tension (for $r > 0.01$ cm) the pressure within the bubble is given in equation 5. The rise velocity ($v = \frac{dz}{dt} < 0$) depends on water viscosity, bubble size and shape. Levich (1962) states that if $r < 0.01$ cm, v will be given by Stokes Law and if $r > 1.5$ cm, bubbles tend to become unstable, breaking into smaller bubbles. By analogy to Cape Lookout (Martens, 1976), bubbles are primarily methane and are likely to be within $0.05 \text{ cm} < r < 1.5 \text{ cm}$. According to data from Turner (1963) cited by Guinasso and Schink (1973), this size class of bubble has $v = -27$ cm/sec $\pm$ 30% at 20°C.

The input from one bubble rising through a water column of depth h is given by equation 6. If the gas is pure, from spherical geometry and the ideal gas law, equation 7 follows directly. Assuming that only a small fraction of the bubble dissolves (m = constant) and that $C_{eq} >> C_W$ (recalling that $C_{eq} = \alpha P$), equation 8 is obtained. Integrating equation 8 yields the input of methane from one bubble (equation 9, Table 24.

Equation 9 has two interesting functional characteristics: k/v depends only slightly on temperature since the viscosity effects on D and v should nearly cancel. Thus the temperature dependence of I should be close to that of solubility. If flatulence is uniform seasonally (at N bubbles sec^{-1}), and the concentration is controlled by a balance between bubbles and evasion (as is nearly true north of mp 20)

TABLE 24

Equations for Dissolution of a Rising Bubble

$$\frac{dm}{dt} = kA\ (C_{eq} - C_w)$$

k = mass transfer coefficient $(\frac{D}{z})$

= bubble boundary layer thickness

A = bubble surface area

$$P = P_o + aZ \tag{5}$$

P_o = pressure at top of water column (P_o = 1 atm. when Z = 0)

Z = vertical distance, positive down

$$a = \frac{dP}{dZ} = 10^{-3}\ \text{atm cm}^{-1}$$

$$I = \int_0^t (\frac{dm}{dt})\,dt = \int_h^0 \frac{1}{v}\,(\frac{dm}{dt})\,dZ \tag{6}$$

$$m = \frac{4\ Pr^3}{3RT}$$

R = ideal gas constant

T = absolute temperature

r_z = initial bubble radius

$$I = \frac{k\alpha}{v} \int_h^0 4\ (\frac{3mRT}{4P})^{2/3} PdZ = K\alpha \int_h^0 P^{1/3} dZ \tag{8}$$

where $K = \frac{4\ k}{v}\ (\frac{3mRT}{4})^{2/3} = \frac{4\ k}{v}\ r_z^2 P_z^{2/3}$

v = rise velocity (< 0)

$$I = (\frac{3\ r_z^2}{a})\ (\frac{k\alpha}{v})\ P_z^{2/3}\ (P_o + aZ)^{4/3} \int_h^0 \tag{9}$$

TABLE 25

Environmental Conditions and Methane Averages

Sample Date	Temp. (°C)	Wind Speed (ms^{-1})	Q_F (m^3s^{-1})	CH_4 (μM) Hudson Highlands (mp 40-60)	Tappan Zee (mp 20-40)	Harbor (mp -2 - 3)	TZ/HH
Aug. 16-18, 1973	24-27	3.6	280	0.20 (12)	0.11 (12)	0.61 (2)	.55
Aug. 24, 1973	24-27	4.4	280		0.13 (7)		
March 2-3, 1974	0-3	4.9	950	0.59 (6)	0.27 (4)	0.93 (6)	.46
April 6-7, 1974	4-7	6.0	1100	0.28 (6)	0.17 (6)	1.28 (6)	.61
Aug. 7, 1974	24-27	4.4	280	0.15 (22)			
Aug. 9, 1974	24-27	3.6	280	0.32 (7)	0.22 (4)		.69
Aug. 27-28, 1974	24-27	4.0	200		0.21 (8)	1.07 (6)	
Oct. 2-4, 1974	14-17	5.3	520	0.10 (5)	0.13 (4)	0.73 (3)	1.3

Predicted Ratio (h_{HH} = 12.8 m, h_{TZ} = 5.3 m)

*( ) is the number of samples collected

$$\frac{D}{z} C_W = IN$$

and since $\frac{D}{z}$ is also nearly constant,

$$C_W = \frac{INz}{D}$$

variations in concentration with temperature should be similar to those in solubility. This is approximately true (Table 25). Although Emery (1969) and Martens (1976) have observed seasonal variations in flatulent emissions (low at low temperature), we see no strong evidence for this. The reason may be that our bubbles originate at considerable depth in the sediment and do not "see" large temperature variations.

If flatulence is uniform areally, the model predicts high concentrations in reaches with deep water. If the mass flux is uniform and r_z is constant, N will be proportional to P_z^{-1}. Thus the ratio of methane concentration in the Tappan Zee to that in the Highlands should be

$$\frac{C_{TZ}}{C_{HH}} = \frac{(IN)_{TZ}}{(IN)_{HH}} = \frac{(P_Z^{-1/3} P_O - P_Z)_{TZ}}{(P_Z^{-1/3} P_O - P_Z)_{HH}} = 0.36$$

This is slightly lower than the observed ratio, but we have ignored the advective contribution from the Highlands to the Tappan Zee, which amounts to about 30% of the total budget there during high flow.

It is clear that the bubble model comes close to accurately predicing the observed seasonal and regional variations. It should be noted that alternative models could be constructed. The seasonal variations could be explained by assuming there is a reservoir of methane in the sediments which continuously supplies an upward flux of methane and that the oxidizing bacteria in the sediments are much less active at low temperatures. The observant reader will have noted that all saturated surficial sediments were collected in cool months rather than warm months. Thus, flatulence could be the controlling mechanism in warm months and diffusion in cold months. Regional variations could be explained by arguing that the Highlands contain a greater proportion of marsh areas than does the Tappan Zee, that marshes are areas of high sedimentation rates, and are consequently major sources of methane. We have measured dissolved methane in one marsh, and while it indicates the marsh area to be a somewhat more effective methane source than the adjacent river, marshes cannot supply the major fraction of methane inputs. We feel that although alternatives could be proposed, the assumptions required would be less general and the quantitative description of methane flux would require introduction of several adjustable parameters.

Budgets

The procedures described above were used to calculate methane input to the water column. These calculations include advective, evasive and flatulent components. Oxidation in the water column is assumed to be negligible and diffusive transport across the interface is also assumed to be negligible. Turbation is also neglected because of the apparent effectiveness of bacteria

in oxidizing methane as it diffuses upward into surficial sediments. Methane dissolved in sewage effluent accounts for 10% of the total input to the harbor and this correction was included in the calculations. By assuming values for δ and r_z, the flux of methane escaping from sediments can be calculated. These results are listed in table 26A. Several experimental schemes have been employed to find δ, but the problem is complicated because δ seems to depend on the "age" of the bubble, at least for the first few seconds (Deindoerfer and Humphrey, 1961). Since the rise time through an 8 m water column should be about 25 sec, the cleverly-devised experiments of Wyman et al. (1952) should yield the best value. They showed δ to be $\sim$ 20 μ and independent of bubble radius or temperature.

The escape of flatulence probably requires a certain buoyancy. Thus, it is likely that the spectrum of bubbles leaving sediments is fairly uniform in size. From visual observations we estimate r_z = 0.5 cm. This will certainly be correct within a factor of 3. Martens (1976) has estimated $0.3 < r_z < 1.0$, depending on mean depth and temperature. Between 4 and 16% of a bubble with r_z = 0.5 cm will dissolve as it rises, justifying the earlier assumption about a negligible loss of mass. Systematic errors introduced in Table 26 will be proportional to the systematic error in assuming an effective r_z. Note that the mass flux error which would be introduced by counting bubbles bursting at the surface is three times the percentage error in r. Clearly, we need a method to accurately determine bubble size spectrums.

The rate of flatulence can be compared to the rate of preservation of organic carbon (Table 26B). The latter was estimated on the basis of regional subsidence rates north of mp 20 and on the basis of dredging rates in the harbor complex. Flatulence and sedimentation rates are probably best constrained in the harbor complex, indicating that approximately 10% of the organic carbon which is buried escapes as flatulence. The fraction calculated for regions to the north is somewhat greater ($\sim$ 30%), but is reasonably consistent when the various uncertainties are considered. The diffusive flux calculated earlier is equivalent to 0.3 mol m^{-2} yr, suggesting that the major fraction of methane which is produced escapes as flatulence.

If the rate of CO_2 production is as great as the rate of CH_4 production, we expect to find a decrease of about 20% in organic carbon with depth in the sediment. Evidence for decreases of 30% or more have been observed in a few locations, but are not consistent (C. Olsen, personal communication). Decreases may be masked by turbation or may occur at depths below core penetration. Major questions which remain to be determined are identifying the depth at which methane is produced and the depth at which bubbles originate.

The rate of flatulence required by this model is approximately 10^{-3} bubbles $m^{-2} s^{-1}$. Emery (1969) has observed a rate about 15 times greater in a small coastal pond. Our rate is equivalent to 1 bubble min^{-1} in a 20 m^2 area. Since bubbles probably come in salvos of 10 or more, a visual observation to determine the rate would require survey of a large area for a long time, making such an observation in the Hudson impractical.

TABLE 26

Comparison of Flatulant Production Rate and Burial Rate of Organic Carbon

A) Flatulent Production[a] (mol m^{-2} sec^{-1} x 10^{8})

	Highlands	Tappan Zee	Harbor
Aug. 16-18, 1973	3.6	3.7	
Aug. 24, 1973		6.5	
March 2-3, 1974	4.9	2.2	22
April 6-7, 1974	3.5	3.4	43
Aug. 7, 1974	3.6		
Aug. 9, 1974	5.3	7.3	
Aug. 27-28, 1974		9.0	41
Oct. 2-4, 1974	1.6	4.9	24
Ave. (mol $m^{-2}s^{-1}$ x 10^{8})	3.8±1.3	5.3±2.4	33±11
(mol $m^{-2}yr^{-1}$)	1.2±0.4	1.6±0.7	10±3

B) Burial Rate of Organic Carbon

Sed. rate (gm cm^{-2} yr)	0.2±0.1[b]	3.5±1.0[c]
Dry wt. loss on ignition (%)	6	8
Carbon compounds (g mol^{-1})	30	30
Preservation of organic carbon (mol $^{-2}$ yr^{-1})	4±2	90±30

[a] Calculated as outlined in text from (evasion rate - advective rate)/(area x f)

[b] Assuming long-term sedimentation rate is equal to the subsidence rate (Fairbridge and Newman, 1968)

[c] Based on the rate of dredging in the Harbor Complex (averaged over the area from mp -8 to mp 20). The lower figure is derived from Panuzio's (1963) statistics for 1926-1960 and the upper figure is Gross (1972) estimate for 1964-1968

CONCLUSIONS

The factors which primarily control the distribution of methane in the waters of the Hudson Estuary are input by flatulence, advection and evasion to the atmosphere. Oxidation by bacteria in surficial sediments probably prevents significant amounts of methane from diffusing or being turbated into overlying waters.

Using wind speed data, evasion rates are estimated to occur at a rate equivalent to a film thickness of 100 μ and a budget for methane in the water column can be calculated. The budget requires an input from the sediments. A model accounting for this input by partial dissolution of sediment flatulence indicates that a bubble leaving the bottom, with an initial radius of 0.5 cm, will lose 4-16% of its methane to the water column as it rises, depending on temperature and depth. This model is used to calculate the production of gas bubbles in sediments. The rate of methane escape is equivalent to about 10% of the burial rate of organic carbon. We believe that this calculation is accurate within a factor of three, indicating that methane bacteria ultimately recycle a significant fraction of the organic carbon buried in these sediments.

SECTION 11

NUTRIENTS AND TRANSPORT MODELS IN THE HUDSON

NUTRIENTS IN URBAN ESTUARIES

In recent years substantial increases have occurred in algal populations in lakes including large systems such as Lake Erie. These increases are believed to result primarily from the loading of additional plant nutrient elements, phosphorus, and nitrogen. When excess algal growth can be directly related to man's activities, the changes are often ascribed to a loosely defined process called "cultural eutrophication". In most cases, the most practical management tool for decreasing algal standing crops in lakes is to reduce the input of phosphate. As a result, the general policy direction for nutrient management in several European countries and North American is to decrease the phosphate levels in detergents, to construct tertiary treatment facilities for phosphate removal from sewage whenever possible, and/or to divert sewage discharge from lakes if an acceptable alternative is available.

Excess algal growth problems have also developed in some large estuarine systems including the Potomac downstream of Washington, D.C., and removal of both phosphorus and nitrogen from sewage effluent has been proposed in several cases. Because of the costs of tertiary sewage treatment facilities and problems of sludge disposal from such facilities, it is important to examine critically the benefits of nutrient removal for estuaries on a case-by-case basis.

Mathematical representation of algal populations, nutrients, and even higher trophic levels such as zooplankton and fish, can be constructed in a similar way to those generated to describe the balance of dissolved oxygen in estuaries. The predictive capability of such models is sometimes not clear, since the response of phytoplankton communities, as well as higher trophic levels, to environmental parameters is more complex than for bacteria in their role as oxygen consumers. In light of large uncertainties in critical biological parameters, management alternatives can sometimes be reasonably examined using extremely simplified conceptual models of water circulation and nutrient-algae interactions. The approach described here (see also Simpson et al., 1975) is to examine the distribution of phosphate in the Hudson estuary and the rate of loading from sewage outfalls, in terms of a very simplified description of water circulation and phosphate behavior in the harbor region adjacent to New York City. Phosphate is the nutrient most frequently considered for nutrient removal from sewage effluent and is somewhat simpler to treat in estuarine budgets than nitrogen.

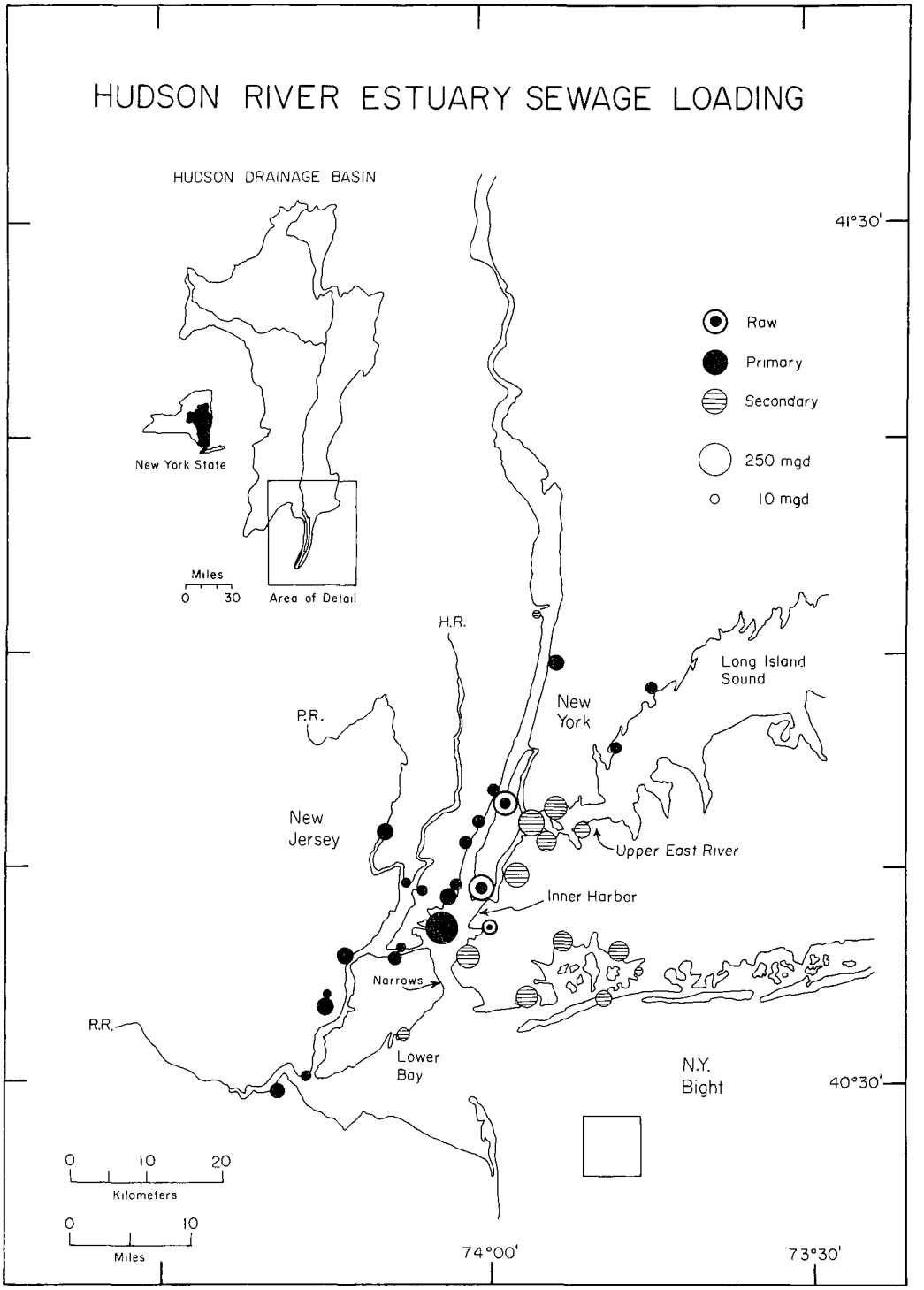

Figure 49. Location map for major sewage outfalls (> 10 million gallons per day) to the Hudson Estuary. Total discharges shown are ∿ 100 m^3/sec (∿ 2.3 billion gallons per day). Areas of the circles are proportional to the volume of sewage outfall at that discharge site. Square in the New York Bight indicates zone of sewage sludge and dredge spoil dumping.

SEWAGE AND PHOSPHATE IN THE HUDSON ESTUARY

The Hudson estuary, portions of which are entirely surrounded by the New York City metropolitan area, is an example of an estuarine system heavily loaded with sewage and other discharges which substantially alter the ambient water quality. Dissolved oxygen levels of less than 40% of saturation with atmospheric oxygen concentrations are not uncommon during summer months. Sewage is discharged to the Hudson Estuary near New York City from about a dozen major treatment plant outfalls and numerous smaller plants with a combined flow of approximately 80 m^3/sec ($\sim$ 1.8 billion gallons/day) plus a number of raw sewage outfalls, largely from Manhattan Island, which total about 20 m^3/sec ($\sim$ 0.5 billion gallons/day). Approximate locations of the largest outfalls are shown in Figure 49. Of the major treatment plant outfalls about 2/3 of the total volume is discharged from seconary treatment plants operated by New York City, while the remainder is supplied by primary treatment plants mostly from New Jersey.

The major secondary treatment plants in New York City, ranging in age from a few years to about 40 years, are reasonably efficient in reducing biological oxygen demand of sewage. Except for storm runoff periods when treatment plants are essentially by-passed, about two-thirds of the oxygen demand of the sewage is removed. Construction of major facilities is now underway to treat most of the remaining raw discharges which currently contribute on the order of 1/3 of the total dry weather biological oxygen demand to the lower Hudson estuary. Primary treatment outfalls, mostly from New Jersey, discharge about 1/3 of the total treated sewage flow and about 1/2 of the total oxygen demand. Thus in terms of the current oxygen budget, the largest impact of sewage discharge is from partially treated New Jersey outfalls. The oxygen demand from these sources will dominate to an even greater extent when the current construction projects in New York City provide secondary treatment for the raw discharge from Manhattan.

All of the major discharges of sewage to the lower Hudson estuary supply large amounts of primary plant nutrients, especially ammonia and phosphate, as well as organic materials which constitute the major load on the dissolved oxygen resources of the water. The supply rate of nutrients is more directly proportional to volume of sewage flow than is biological oxygen demand, since present treatment operations (raw, primary or secondary) do not have nearly as great an effect on nutrients as they do on dissolved and suspended organic carbon. It is important to establish to what extent and in what areas of the estuarine-coastal water system these sewage-derived nutrients are converted to organic matter by phytoplankton, and how this affects oxygen concentrations and other water quality factors.

The concentrations of dissolved phosphate as well as other primary nutrients in the harbor region of the Hudson estuary are approximately two orders of magnitude higher than those usually considered as limiting to phytoplankton growth. Phosphate concentrations do not vary greatly from one location to another in the harbor, despite the presence of a number of large discrete sources. The smoothness of observed phosphate concentrations indicates the effectiveness of mixing by tidal currents and density-induced non-tidal estuarine circulation. In general, the mean values of phosphate in the Inner Harbor range between 2 μm/l during spring high fresh water runoff

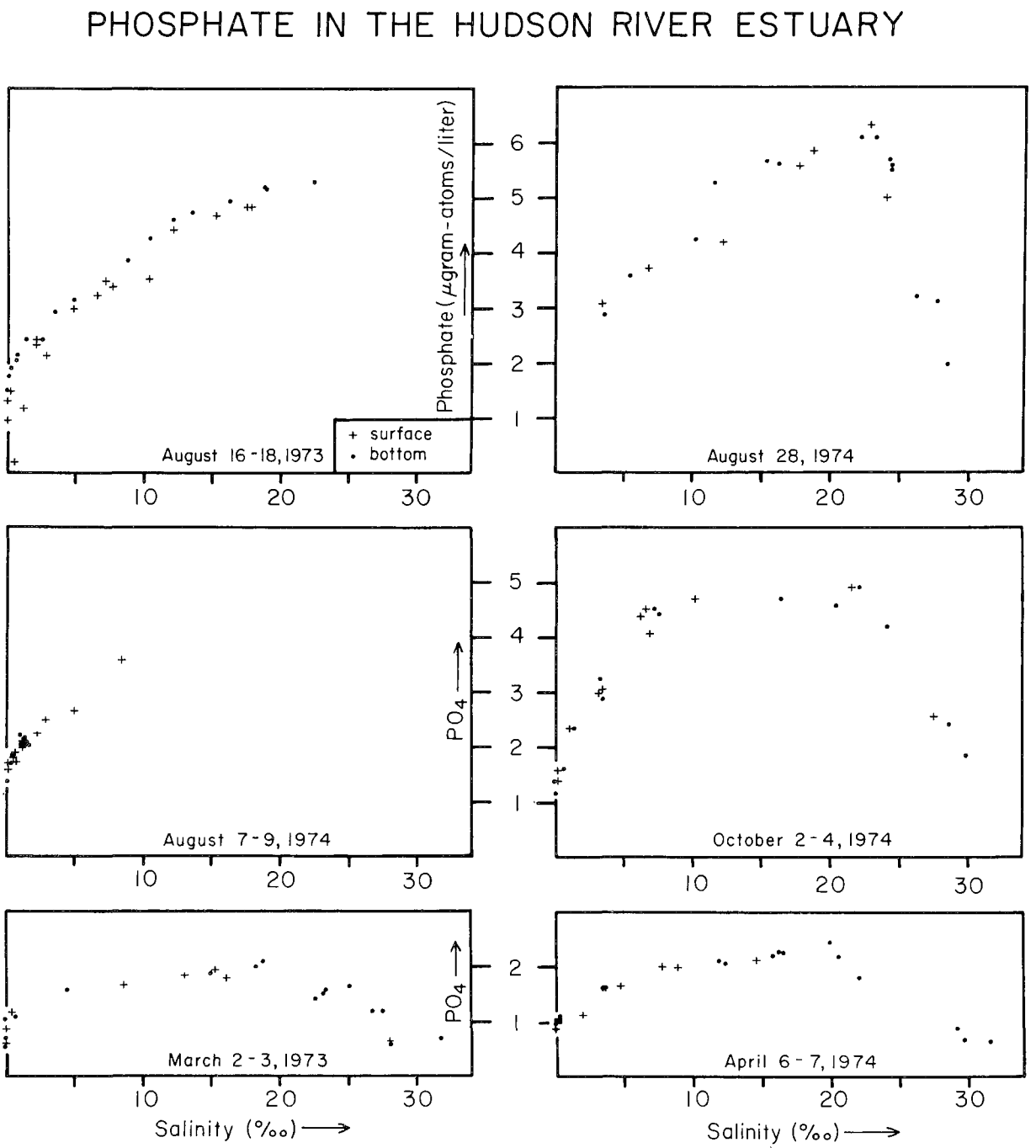

Figure 50. Phosphate (molybdate reactive) concentrations versus salinity: Fresh water flows were $\leq$ 300 m^3/sec for the August profiles, 450 m^3/sec for October, and $\sim$ 1250 m^3/sec for March and April.

and 6 μm/l during summer low fresh water discharge. To illustrate the general character of observed data several transects of phosphate and salinity for the Hudson are shown in Figure 50.

Total phosphorus measurements, as well as particulate organic phosphorus and dissolved organic phosphorus concentrations were made for most of the transects shown in Figure 50. In general, about 1/2 to 2/3 of the total phosphorus in the water was present as molybdate reactive phosphate, with most of the remainder as particulate organic phosphorus. During high fresh water flow (March and April) the fraction of particulate organic phosphorus was somewhat greater. The data shown are for samples collected along the axis of the Hudson, through the middle of the Inner Harbor, the Narrows, the Lower Bay, and the apex of the New York Bight (Figure 49). Samples collected in heavily loaded and more restricted zones of the Inner Harbor such as the East River plot above the trends shown, sometimes by as much as a factor of two in phosphate concentration, but the data shown are typical of most of the harbor volume.

Upstream of New York harbor, phosphate and salinity decrease at approximately the same rate until fresh water is reached, where the phosphate levels remain nearly constant at 0.5 to 1.0 μm/l, depending on the fresh water flow rate. Composite plots of the data for several survey periods indicate the general distribution of phosphate as a function of mile point (Figure 51) and salinity (Figure 52) during both low and high fresh water flows. The covariance of salinity and phosphate suggests that removal processes for phosphate such as algal uptake do not dominate phosphate concentrations in the salt intruded reach of the Hudson and that physical transport of the water by estuarine circulation is most critical in establishing the phosphate distribution.

The geometry of sewage loading is presented schematically in Figure 53. Most of the sewage is discharged directly to the Inner Harbor, with less than 5% of the total added upstream of the Inner Harbor (segments A, B, C and D of Figure 53). Saline water and sewage phosphate added to the Inner Harbor are spread well upstream of the discharge sites by estuarine circulation, as far upstream as segment D during low flow periods.

To illustrate the relative magnitudes of phosphate source terms to the Inner Harbor, and provide some sense of the time scale of removal by estuarine circulation, a one box model for phosphate in the Inner Harbor can be constructed (Figure 54). The mean concentration of phosphate in the Inner Harbor, multiplied by the volume of this portion of the estuary gives the total amount of phosphate in solution. Inputs of phosphate are (1) direct sewage discharge, (2) diffusion from the sediments, (3) downstream supply from the fresh water reach of the Hudson, and (4) particulate oxidation in the water column, with direct sewage discharge supply about 3/4 of the total. Dividing the total standing crop of phosphate in the Inner Harbor by the supply rate indicates a residence time for phosphate of 2 days during high flow and 7 days during low flow.

A similar calculation can be done using a first order estimate of the outflow rate of phosphate from the Inner Harbor. Removal of phosphate is predominantly through the Narrows, into the Lower Bay and then to the adjacent

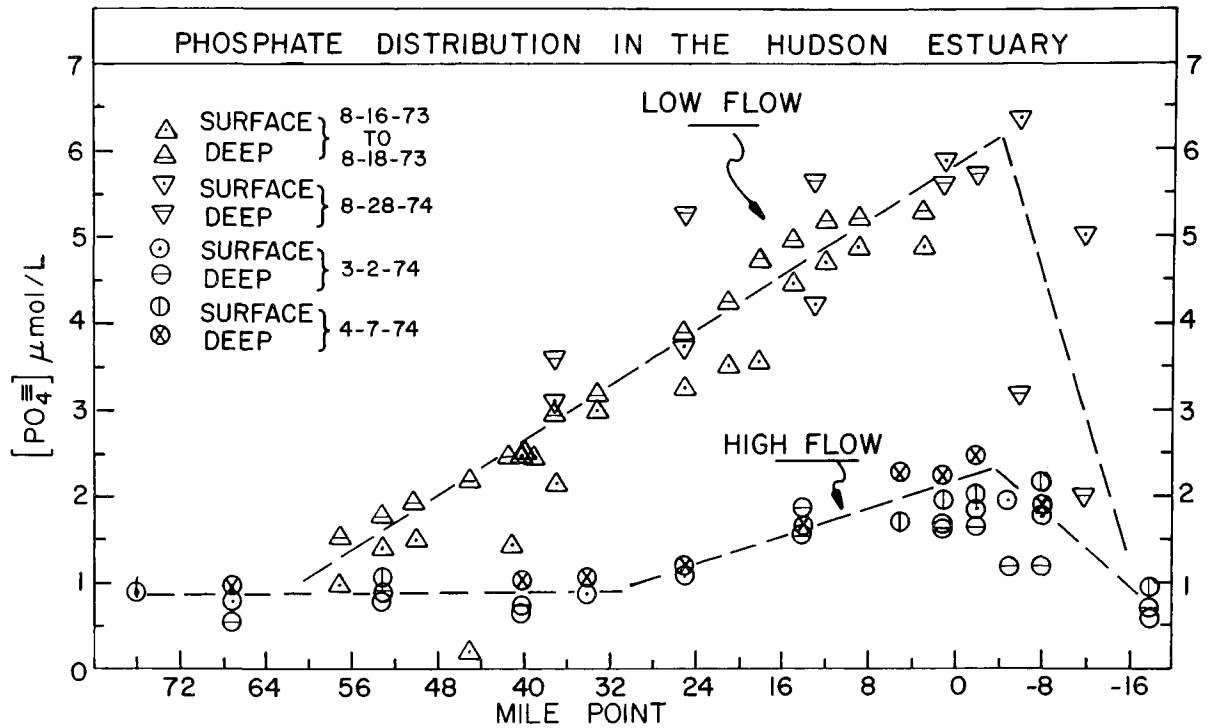

Figure 51. Phosphate (molybdate reactive) as a function of location for several surveys in the Hudson Estuary during high flow (March and April) and low flow (August).

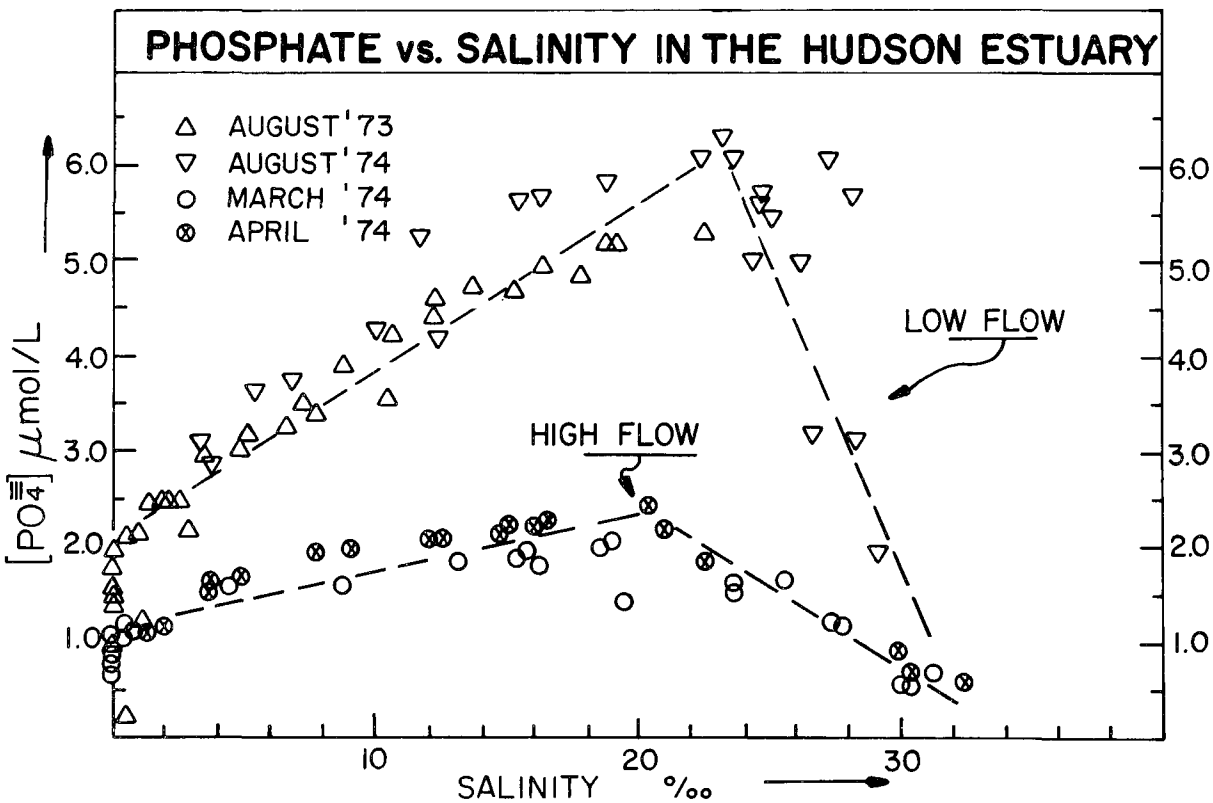

Figure 52. Phosphate (molybdate reactive) as a function of salinity for several surveys in the Hudson Estuary. Data are from Figure 51 plus samples from mid-depths.

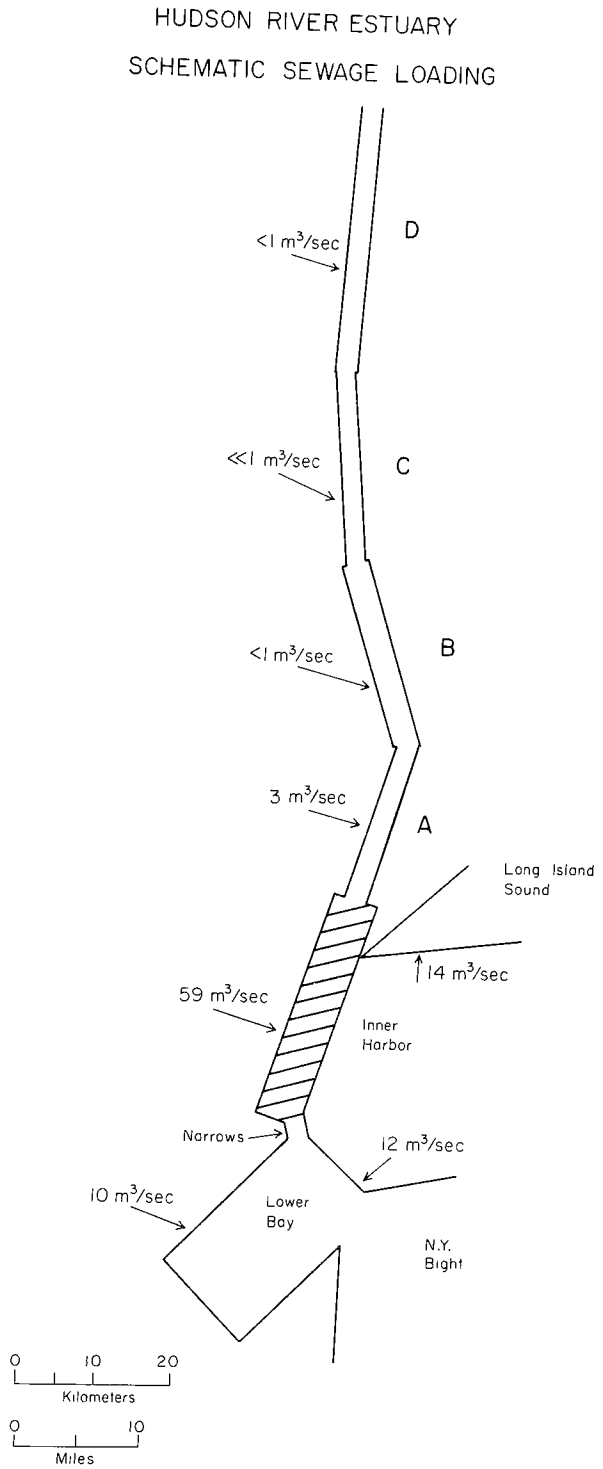

Figure 53. Schematic loading of sewage to segments of ∿ 30 km lengths of the Hudson.

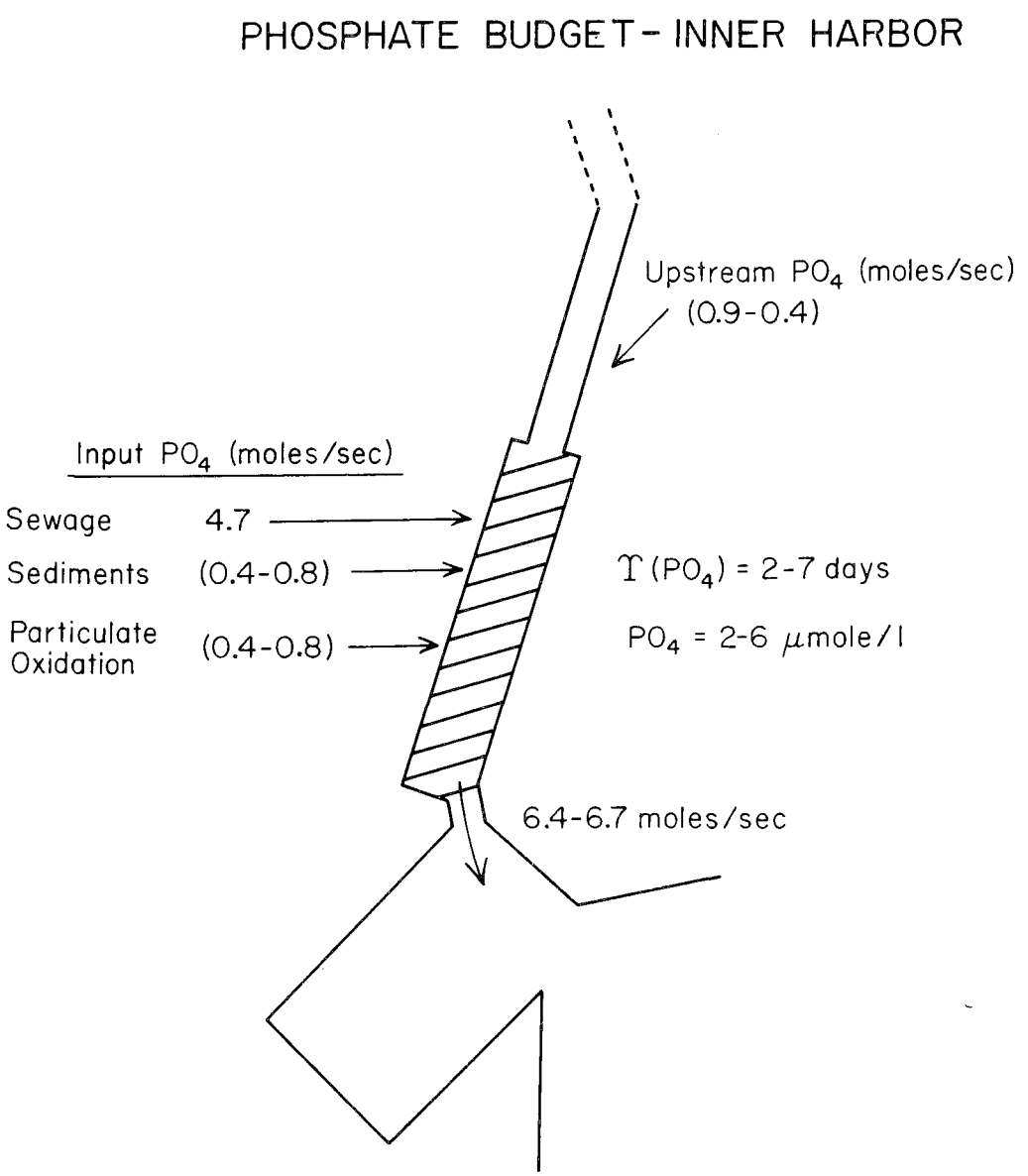

Figure 54. Approximate fluxes and concentrations of phosphate in New York harbor. The major cause of changes in residence time of phosphate in the harbor is change in the rate of fresh water discharge.

coastal waters of the New York Bight. Some phosphate discharge does occur through the Upper East River into western Long Island Sound. Based on estimates of the magnitude of this transport, we have decreased the loading rate of phosphate to the Inner Harbor used in Figure 54 by an equivalent amount, about 10-15% of the discharge rate through the Narrows. Water flowing out through the Narrows in the upper half of the water column has a mean phosphate concentration similar to that in the Inner Harbor, while that flowing upstream in the lower layer has a lower phosphate concentration and a higher salinity. Using a two-layer advective transport calculation (Figure 55 - two box model of phosphate transport in the harbor area) based on field salinity and phosphate concentrations during both high and low flow conditions, the removal rate of phosphate is comparable to that estimated in Figure 54 for the input rate. Thus to the first approximation, sewage phosphate is discharged to the lower Hudson into waters with salinities averaging about 2/3 of sea water salinity, mixed reasonably well through the Inner Harbor over a time period averaging between 4 and 14 tidal cycles, and discharged from the system by estuarine circulation.

These greatly simplified representations of nutrient transport rates in the Hudson can be expanded in the form of numerical models, and thus treated in terms which are more conventially applied in water quality transport calculations. The most common approach to one-dimensional descriptions of estuary transport is to use observed salinities to establish model parameters for the upstream transport of sea salt (and phosphate). Stommel (1953) suggested the use of one-dimensional advection-diffusion segmented models based on balancing downstream advection of fresh water with upstream diffusion of salt. Thus the complex upstream transport processes of density-driven circulation, tidal mixing and their interaction with channel morphology are lumped into a single "diffusion" constant for each segment boundary.

We can describe the tidal Hudson in terms of equal length segments, each of which are considered to be well mixed. The basis for the physical dimensions of volume elements used here for the Hudson between mp 0 and the head of the tide (about mp 154) is a report by Thatcher and Harleman (1972) on a one-dimensional physical transport model for the Hudson. We took channel dimensions reported in terms of a main "conveyance" channel and an adjacent "storage" channel at approximately two mile intervals, and converted all dimensions to metric units, combining the two-channel presentation into one channel.

The geometry of the Hudson estuary downstream of mp 0 is quite complex and not readily represented in one-dimensional terms, but we have chosen to do so as a simple extension of the linear geometry of the Hudson upstream of mp 0 (Figure 56). A summary is given in Table 27 of the segment dimensions used to approximate the Hudson as a chain of 6.4 km (4 mile) boxes extending from the seaward end of the Narrows (mp -8) to the head of the tide north of Albany ($\sim$ mp 154). The segments designiated A* and B* represent all of the harbor upstream of the Narrows, including Newark Bay, Kill van Kull, the Lower East River and Upper New York Bay, and thus are greatly simplified from the actual geometry. All dimensions of segments 1-38 were derived from approximating the main stem of the Hudson by rectangular cross-sections, based on dimensions reported for linear distances of slightly greater than 3.2 km (2 miles) (Thatcher and Harleman, 1972). We have rounded the segment lengths generated

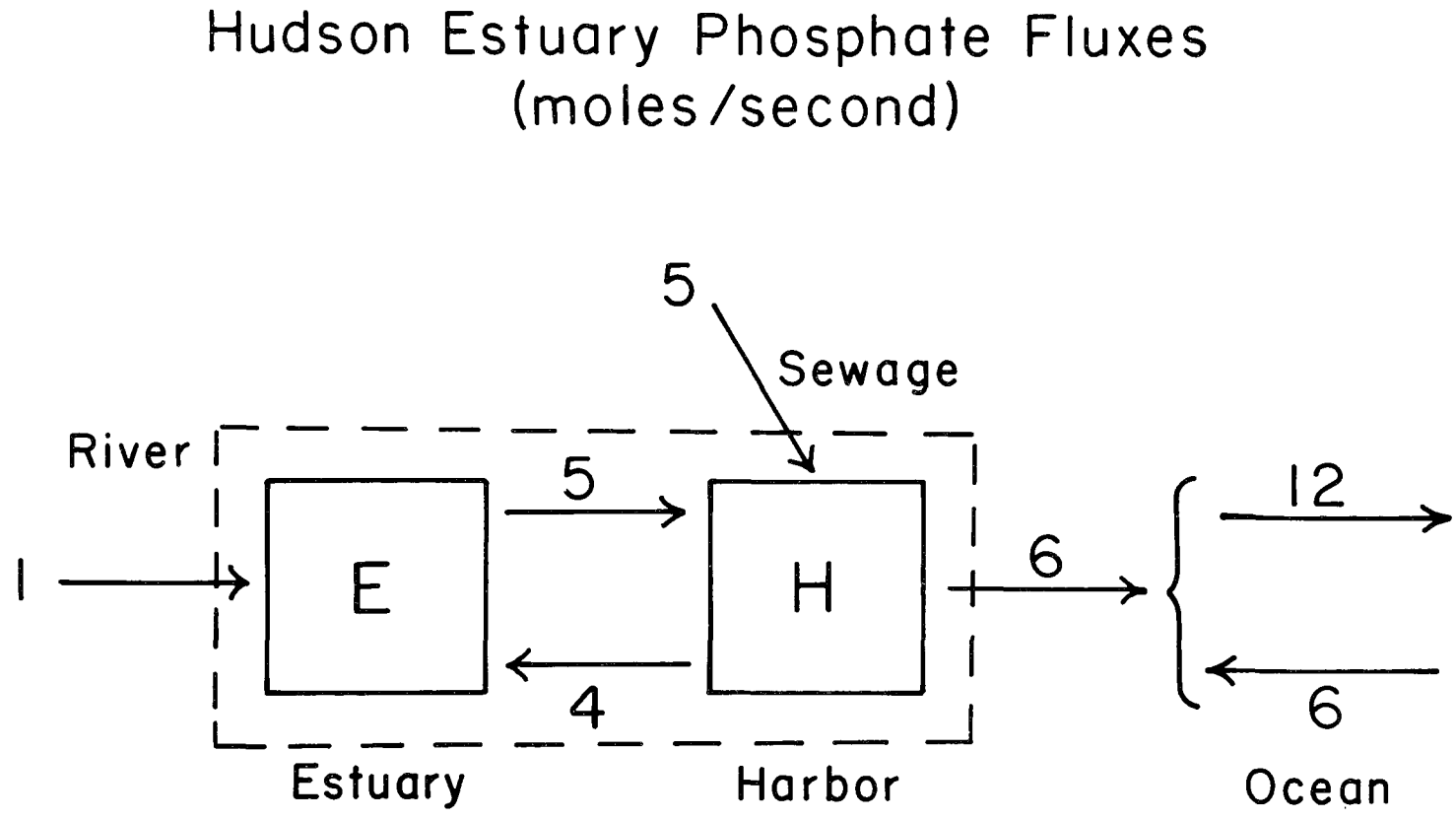

Figure 55. Simple two box model of phosphate fluxes in the Hudson, with discharge from the harbor expressed in terms of two layer advective fluxes.

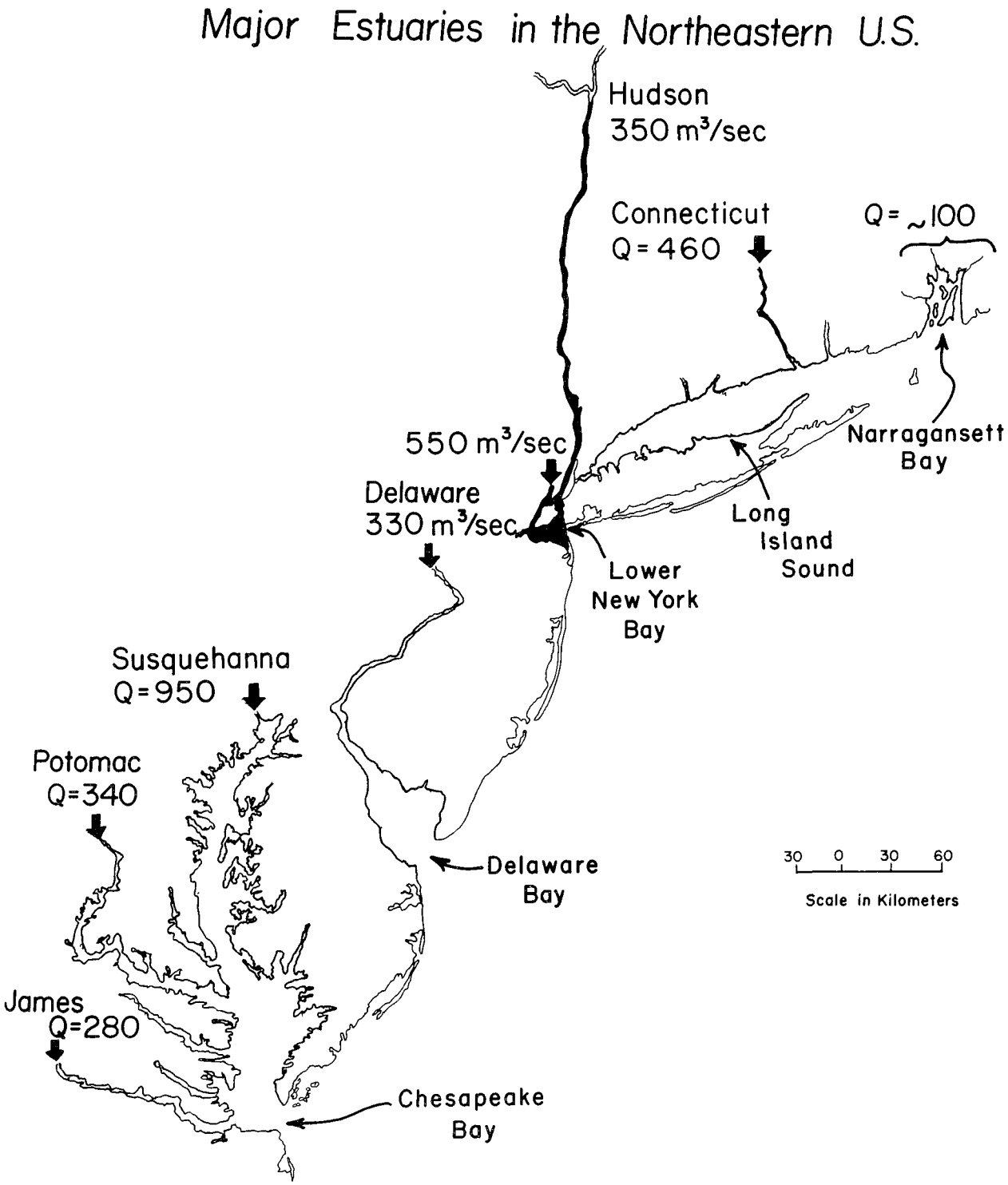

Figure 56. All of the major rivers flowing into the Atlantic between Rhode Island and Virginia enter estuarine systems (mean annual flows are shown for gauging stations above tidal influence).

TABLE 27

One-Dimensional Model Parameters for Tidal Hudson
Segment Lengths are 6.4 km (4 miles)

Segment No.	Mean Width (km)	Surface Area (km^2)	Mean Depth (m)	Segment Volume (10^6 m^3)
A*	2.00	12.8	16.8	216
B*	3.50	22.4	11.6	259
1	1.33	8.6	11.7	100
2	1.25	8.1	11.1	89
3	1.35	8.7	9.8	85
4	1.47	9.5	8.9	84
5	1.48	9.5	9.2	88
6	2.20	14.2	6.8	96
7	3.64	23.4	5.3	125
8	3.78	24.3	5.5	133
9	4.13	26.6	5.1	135
10	3.06	19.7	6.3	125
11	1.27	8.2	12.7	104
12	0.73	4.7	18.9	89
13	0.73	4.7	18.7	88
14	1.30	8.4	10.8	90
15	1.99	12.8	8.0	103
16	1.54	9.9	9.9	96
17	1.14	7.3	10.5	77
18	0.87	5.6	12.3	69
19	0.78	5.0	14.1	71
20	0.74	4.8	12.8	61
21	0.93	6.0	11.7	70
22	1.30	8.4	9.0	75
23	1.50	9.7	7.9	76
24	1.31	8.4	7.1	60

(continued)

TABLE 27 Continued

Segment No.	Mean Width (km)	Surface Area (km^2)	Mean Depth (m)	Segment Volume (10^6 m^3)
25	1.21	7.8	6.4	50
26	1.15	7.4	5.6	41
27	1.30	8.4	4.3	36
28	1.00	6.4	4.7	30
29	0.97	6.3	4.6	29
30	1.08	7.0	4.3	30
31	0.76	4.9	4.7	23
32	0.78	5.0	4.2	26
33	0.65	4.2	5.7	24
34	0.43	2.8	6.3	17
35	0.38	2.5	6.9	17
36	0.29	1.9	6.4	12
37	0.23	1.5	4.5	7
38	0.27	1.7	3.6	6

*Segments A and B are artificial in shape, and are designed to include the following:

	V (10^6 m^3)	A (km^2)	h (m)
Upper New York Bay	340	24	14
Lower East River	80	7	11
Newark Bay	34	11	3
Kill van Kull	21	3	7

The portion of the estuary seaward of the Narrows was excluded. Approximate dimensions of Lower New York Bay, Raritan Bay and Sandy Hook Bay are:

	V (10^9 m^3)	A (km^2)	h (m)
Estuary between Narrows and Sandy Hook-Rockaway Transect	$\sim$ 1.3	$\sim$ 250	$\sim$ 5

in our compilation to distances of 6.4 (4 miles) and hence show an upstream segment termination at mp 152, while the actual distance between the origin of the location system at mp 0 and the head of tide is located about mp 154. The mean depth of the entire estuary above the Narrows is slightly more than 8 meters.

The flushing characteristics of the lower estuary are difficult to describe because of the complexity of physical geometry and current patterns. We have chosen the Narrows as the logical seaward end of the estuary, primarily because the net transport past this location can be approximated reasonably well by a two-layer advective model (Hammond, 1975). We have used phosphate as an indicator of the rate of removal of pollutants from the harbor region through the Narrows, because the rate of addition can be described reasonably well (Hammond, 1975) and because its behavior to the first approximation appears to be conservative within the lower estuary (Simpson et al., 1975). Significant removal of sewage-derived nutrients from the harbor complex also occurs through the Lower and Upper East River, into western Long Island Sound, but this net transport appears to be substantially less than that through the Narrows. Our best estimate at this time is that approximately 85% of the total phosphate discharge upstream of the Narrows, including the discharge to the East River, leaves via the Narrows while the remaining 15% leaves the system via the Long Island Sound.

Table 28 summarizes the field data for salinity and phosphate which we have used to describe the flushing characteristics of the lower estuary. The seaward boundary values of salinity and phosphate represent the tidally-averaged characteristics of the upstream flowing water in the bottom half of the water column in the Narrows.

We have made a series of calculations of the equilibrium phosphate distribution in the Hudson with a one dimensional diffusion-advection numerical model. The predicted phosphate concentrations of several of these calculations are given in Figure 57. The calculations plotted are both low and high fresh water discharge conditions (Figure 58) using a constant input rate of phosphate from sewage of $\sim$ 5 moles per second. In one case all of the sewage phosphate is added to the second segment from the seaward end (B*) while in the other two cases the phosphate is added to each of the segments in amounts approximating those of the actual discharges (see Simpson et al., 1975 for a summary of sewage outfall geometry in the Hudson).

The primary difference in the calculations based on a distributed sewage phosphate source from those with a single aggregated source in segment B* is a more uniform distribution of phosphate within the harbor (segments A*, B*, 1, 2 and 3) but the differences were not large (Figure 57). Several of the calculations included additional inputs of phosphate from oxidation of sewage particulates within the harbor and diffusion from harbor sediments. The sum of these inputs was estimated to be 1/4 of the direct sewage discharge, which is comparable to the uncertainty of the sewage discharge estimate. We have not attempted to "tune" the calculations to provide a better fit to the observed data, which are also subject to substantial uncertainty since no really adequate time- and space-averaged data base exists. From the general similarity of the calculation outputs and "observed" phosphate data (Figure

TABLE 28

Segmented Model Observed Salinities
and Phosphate Concentrations

Segment No.	High Flow ($1130\ m^3/sec$) Salinity (°/₀₀)	High Flow ($1130\ m^3/sec$) Phosphate (µm/l)	Low Flow ($220\ m^3/sec$) Salinity (°₀₀)	Low Flow ($220\ m^3/sec$) Phosphate (µm/l)
Seaward Boundary	22	1.65	30	3.0
A*	19.7	2.0	26.7	5.5
B*	16.4	2.0	25.6	5.5
1	13.8	2.0	24.0	5.5
2	11.2	2.0	22.0	5.5
3	8.9	1.8	19.7	5.5
4	6.5	1.6	17.2	5.2
5	4.5	1.5	14.8	4.6
6	2.8	1.4	13.0	4.2
7	1.4	1.2	11.3	4.0
8	0.6	1.0	9.8	3.6
9	0	<1.0	8.3	3.4
10			6.6	3.2
11			4.9	2.9
12			3.4	2.6
13			2.5	2.2
14			1.9	2.1
15			1.5	2.0
16			1.2	1.9
17			0.7	1.7
18			∿0	<1.5

Fresh water flows for Segments A and B were slightly higher, due to the addition of sewage from the New York City area and the inflow of the Passaic and Hackensack Rivers. The totals during high and low flow for these segments were 1290 m^3/sec and 260 m^3/sec.

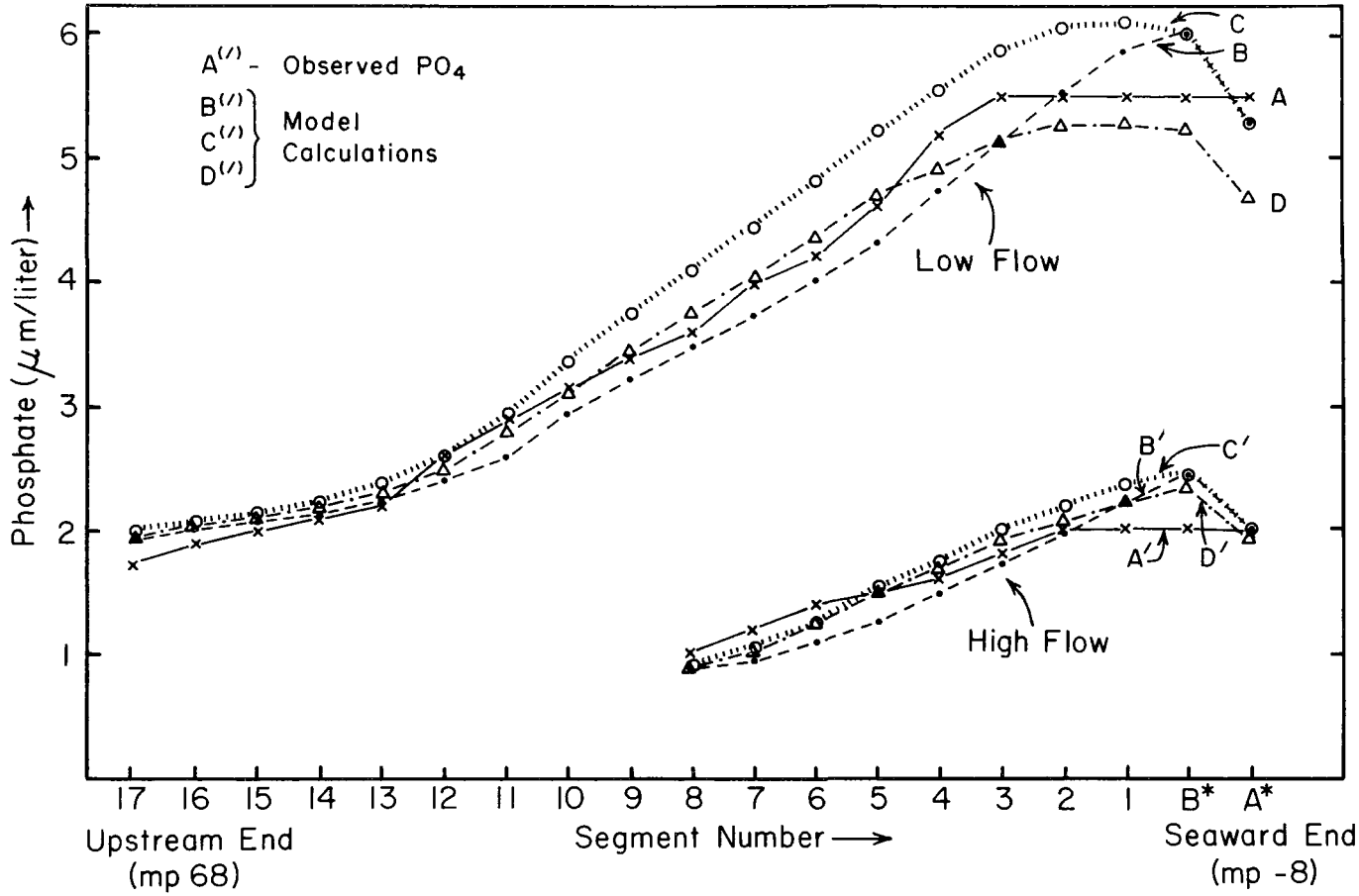

Figure 57. Observed (A and A') and computed (one dimensional diffusion-advection model calculations using ∿ 6 km, 4 mile, segments assumed to be well-mixed) phosphate concentrations in the Hudson Estuary. Curves B and B' assume all sewage added as point source, C, C', D and D' assume a distributed source approximately the actual pattern of discharge while C and C' include additional phosphate input by diffusion from sediments and particle oxidation in the water column. Primed letters indicate high flow, unprimed indicate low fresh water flow.

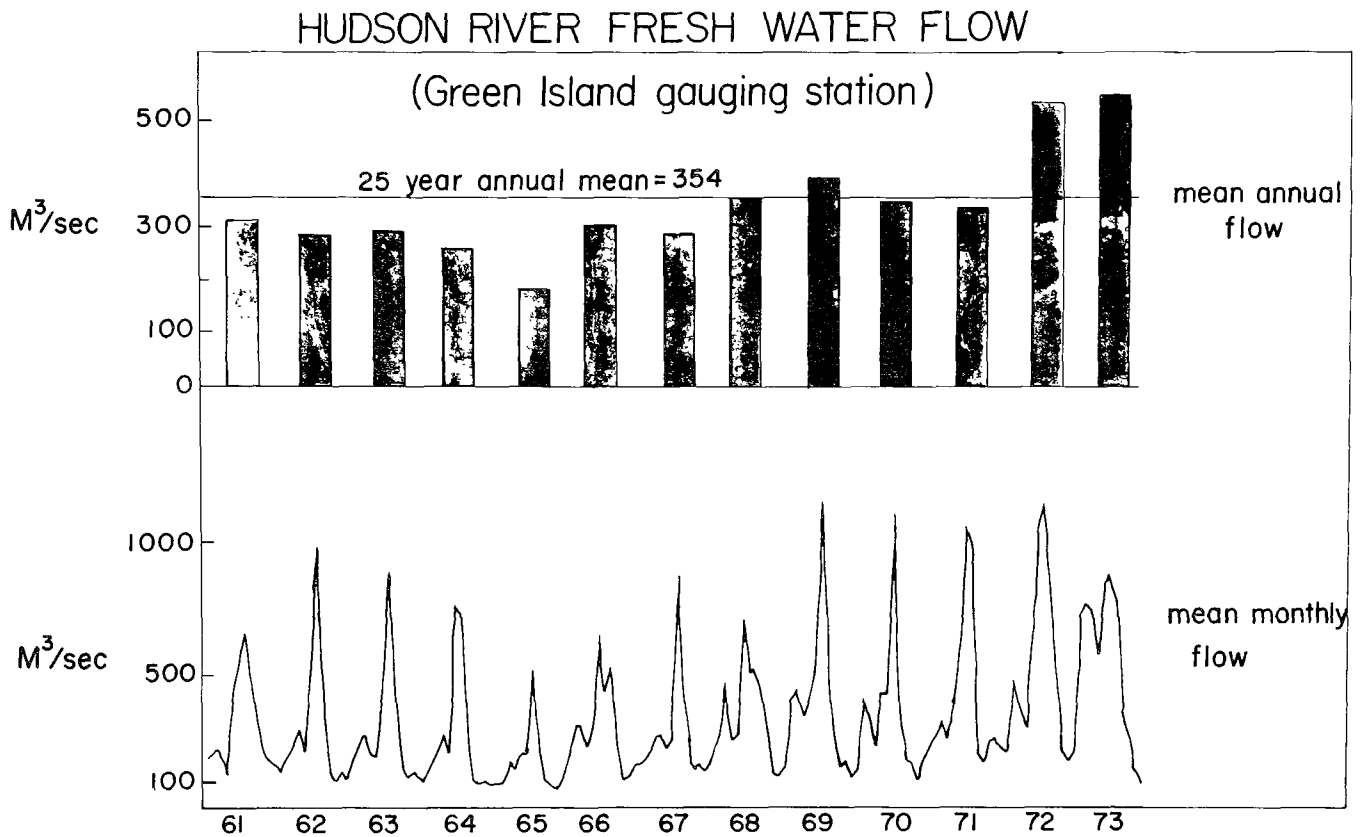

Figure 58. Gauged flows at the head of tide in the Hudson (Green Island mp +154) are approximately 2/3 of the fresh water flow at mp 0. Mean monthly flows usually range over about a factor of ten.

TABLE 29

Comparison of Phosphate Behavior in the Lower Hudson Estuary and Lake Erie

	Hudson	Lake Erie
Volume	0.6 km^3 (1)	500 km^3
Area	60 km^2	25,000 km^2
Mean Depth	10 m	20 m
Residence Time	2 days	1000 days
Basin Population	10^7 (2)	10^7
Σ P Loading Rate	-	26 mole/sec (3)
PO_4^{3-} Loading Rate	6 mole/sec	13 mole/sec (4)
Predicted PO_4^{3-} (5)	2 µmole/ℓ	2.5 µmole/ℓ
Measured PO_4^{3-}	2 µmole/ℓ (1)	.03-.06 µmole/ℓ (6)
Measured Σ P	2.7 µg- atom/ℓ	0.6-1.2 µg-atom/ℓ (7)
$\frac{\text{Measured } PO_4^{3-} \times 100\%}{\text{Predicted } PO_4^{3-} \times 100\%}$	100%	1-25% (6)

(1) High flow conditions (see Figure 52)
(2) Only populations discharging above the Narrows and not to the Upper East River is included (∿ 65% of total in basin).
(3) See Vollenweider et al., 1974.
(4) Assuming PO_4^{3-} = 50% of Σ P loading rate.
(5) Assuming conservative behavior for PO_4^{3-}.
(6) Summer epilimnion near the lower value, winter epilimnion near the upper value. See Dobson et al., 1974.
(7) See Dobson et al., 1974.

57) it is clear that very simple numerical models using observed salinities and estimated phosphate inputs from sewage can approximate reasonably well the gross features of the dissolved phosphate distribution within the salt intruded reach of the Hudson (Table 30).

If the general features of nutrient behavior in the Hudson are approximately correct as outlined here, then there are substantial implications for phosphate management policies in the New York City area. The primary purpose of decreasing phosphate discharge to receiving waters is to reduce adverse effects resulting from excess algal growth in the receiving water. The Hudson estuary upstream of the Narrows in the Inner Harbor has a large surplus of nutrients for algal growth. The algal population within this reach of the Hudson is surprisingly low. The maximum warm season standing crops of algae are on the order of only 10% of those of Lake Erie, a system that is generally accepted as having substantial areas that are clearly eutrophic. During winter months, algal standing crops in the Hudson are lower than summer months by more than an order of magnitude. Thus the Hudson Estuary is not now characterized by nuisance growth of algae. In addition, algal activity is not currently limited by available nutrients. Large excesses of ammonia and nitrate as well as phosphate are present. Thus reduction of the current discharge rate of phosphate by tertiary treatment of sewage for phosphate removal probably would have little effect on the activity of algae in this reach of the Hudson.

A first order budget for sewage-derived nitrogen in the Hudson has been presented (Garside et al., 1976), which also indicates that dissolved nitrogen and ammonia are removed from the Hudson estuary predominantly by estuarine circulation, and not by phytoplankton uptake. There seems little indication of nutrient limitation being significant for the Inner Harbor area of the Hudson estuary.

The factors which currently limit phytoplankton standing crops in the Hudson are not well defined, but growth rates have been clearly shown to be light and temperature regulated (Malone, 1976a). The most reasonable factors determining standing crops in the Hudson are light limitation due to the high suspended solids content of the water and rapid removal of algal cells from the estuary upstream of the Narrows by estuarine circulation. Neither of these factors could be readily affected by changes in sewage treatment processes since most of the suspended particulates are not supplied directly from sewage outfalls. If a substantial reduction in suspended solid levels during low flow summer months were to occur then algal growth rates would increase, perhaps reaching nuisance levels. This possibility should be carefully examined, but does not seem of primary concern for the next decade.

After leaving the Inner Harbor through the Narrows, the high nutrient estuarine waters support increasing phytoplankton standing crops, especially after reaching the adjacent coastal waters of the New York Bight. The magnitude of this increased phytoplankton activity can be clearly seen in higher chlorophyll contents in the New York Bight and even in the Lower Bay. Growth rates of phytoplankton in the nearshore waters are primarily light and temperature regulated and not nutrient limited (Malone, 1976b) and thus not very sensitive to control by nutrient discharge control upstream within the estuarine region.

TABLE 30

Nutrient Data

M.P.	Depth (m)	T (°C)	Sal. (°/₀₀)	CH_4 (µmol/l)	PO_4 (µmol/l)	Part P (µmol/l)	Excess [Rn] (dpm/l)
March 2-3, 1974							
103	1	1.5	0.1		0.59	1.31	
	5	1.5	0.1	0.24			
	11	1.5	0.1		0.52	1.65	
92	2	0.6	0.1		1.03	0.15	
	5	1.8	0.1	0.34			
	8	1.8	0.1		1.06	0.55	
76	2	0.6	0.1	0.62	0.85	0.96	
	11	0.7	0.1	0.64			
67	1	0.6	0.1	0.62	0.77	1.81	
	18	0.6	0.1	0.65	0.56	1.49	
53	1	0.5	0.1	0.63	0.77		
	21	0.5	0.1	0.66			
	43	0.5	0.1	0.64	0.85	1.26	
41	1	0.6	0.1	0.512	0.64	1.14	
	7	0.5	0.1	0.545			
	18	0.5	0.1	0.546	0.70	2.03	
34	1		0.1	0.260	0.85	2.51	
	3	1.2	0.1	0.276			
25	1	1.6	0.5	0.273	1.18	2.27	
	4	1.5	0.8	0.344	1.11	2.66	
14	2	1.5	2.2	0.386			
	6	2.8	4.5	0.60	1.57	0.42	
	10	3.0	15.0	1.19	1.88	2.24	
1	1	2.5	8.7	1.08	1.67	1.19	
	6	3.8	18.8	1.14	2.10	0.88	
	13	4.1	23.4	0.91	1.60	0.85	
-2	1	2.8	13.1	0.96	1.83	5.75	
	7	3.6	18.3	0.88	2.00	4.04	
	12	4.2	25.1	0.64	1.65	1.93	
-5	1	3.6	15.3	0.86	1.95	0.32	
	7	4.1	22.7	0.66	1.41	1.67	
	12	5.0	27.5	0.374	1.18	1.95	
-8	1	4.1	16.1	0.805	1.77	0.22	
	4	4.5	23.2	0.548	1.51	4.01	
	6	4.9	26.8	0.436	1.20	1.84	
-18	1	4.7	28.0	0.162	0.59	2.86	
	4	4.8	28.1	0.155	0.56	0.45	
	8	5.4	31.8	0.135	0.70	0.83	
East River							
	1	4.0	17.8	1.03	2.42	3.84	
	9	4.1	19.0	0.90	2.90	2.36	

(continued)

TABLE 30 (continued)

M.P.	Depth (m)	T (°C)	Sal. (°/₀₀)	CH_4 (µmol/l)	PO_4 (µmol/l)	Part P (µmol/l)	Excess [Rn] (dpm/l)
Kill Van Kull							
	1		14.6	1.16	1.81	6.67	
	11		16.7	1.45	1.77	3.94	
Lower Bay							
	1	4.0	20.3	0.545	0.96	1.14	
	4	4.1	20.4	0.572	0.90	2.53	
August 7, 1974							
57	1		0.1	0.174	1.48		0.77
	5			0.173			
	10		0.1	0.173	1.35		0.78
	14			0.188			
	20		0.1	0.239	1.57		0.90
53	1		0.5	0.141	0.75		1.03
	10			0.136			
	20		0.5	0.125	1.82		1.04
	30			0.131			
	40		0.4	0.155	1.73		0.82
49	1		0.7	0.180	1.89		1.30
	6			0.111			
	12		1.0	0.111	2.22		
	18			0.181			
	24		1.3	0.295	2.07		1.20
46	1		1.4	0.169	1.98		1.14
	6			0.127			
	12		1.6	0.122	2.02		1.29
	18			0.163			
	24		1.7	0.119	2.04		1.13
August 9, 1974							
57	1		0.2	0.324	1.62		1.38
47	1		0.5	0.241	1.80		1.32
42	1		1.3	0.310	2.18		1.27
	2.5			0.284			
	7		1.4	0.374	2.16		1.30
	10.5			0.501			
	14		1.5	0.507	2.11		1.59
37	1		2.3	0.217	2.23		1.25
	4			0.227			
	8		2.9	0.217	2.49		1.28
29	1		5.0	0.166	2.65		1.86
18	1		8.4	0.190	3.60		1.67
August 27, 1974							
26	1			0.158			0.97
	6			0.180			1.31
18	1			0.223			1.00
August 28, 1974							
37	1		3.4	0.379	3.09		
	5		3.6	0.378	2.90		
	10		5.4	0.84	3.62		

(continued)

TABLE 30 (continued)

M.P.	Depth (m)	T (°C)	Sal. (°/₀₀)	CH_4 (µmol/l)	PO_4 (µmol/l)	Part P (µmol/l)	Excess [Rn] (dpm/l)
25	1		6.8	0.301	3.72		
	6		10.1	0.191	4.24		
	11		11.5	0.190	5.26		
13	1		12.2	0.264	4.19		
	5		15.2	0.303	5.68		
	10		16.1	0.394	5.62		
9*	0		9.0	1.08	7.43		
1	1		18.6	0.94	5.84		
	5		22.1	1.00	6.09		
	10		24.2	1.01	5.57		
1**	1		16.7		5.59	1.01	
-2	1		18.8	1.13			
	6		23.2	1.28	6.10		
	12		24.2	1.23	5.70		
-6	1		22.8	1.21	6.34		
	10		24.3	1.44	5.51		
	20		27.7	0.79	3.14		
-12	1		24.0	0.93	5.00		
	6		26.2	0.655	3.20		
	12		28.5	0.307	1.98		

* By 125th St. sewage outfall
** 4 hours after previous sample

The total phytoplankton biomass of the coastal waters adjacent to the Hudson is, however, related to the quantity of nutrients reaching the area. Coastal waters adjacent to large rivers always support enhanced phytoplankton activity produced by injection of primary nutrients, and usually support greater fish populations as a result. Dissolved oxygen in bottom waters of small areas of the apex of the New York Bight approach values comparable to the Inner Harbor (< 40% of saturation). Bottom waters of the New York Bight well beyond the zone of influence of the Hudson estuary also show substantial oxygen depletion during the summer. The critical parameters for control of dissolved oxygen of bottom waters immediately offshore of the Hudson are still not well defined at this time. It is thus presently not clear if any major detrimental effects to the coastal waters are produced by enhanced nutrient discharge from the Hudson estuary.

In light of the current circumstances of sewage treatment, nutrient content, and water quality parameters in the Hudson estuary, the most reasonable policy for management of nutrient discharge during the next decade would not appear to be the initiation of tertiary treatment for phosphate removal (or for other primary nutrients). Considering the low summer dissolved oxygen levels within the Inner Harbor, the major efforts in sewage treatment should be to complete the secondary treatment facilities under construction in New York City, and to substantially upgrade the New Jersey discharges to include secondary treatment. Such an effort would require a minimum of a decade considering the current mix of political interests, but should significantly improve the dissolved oxygen content of the most heavily impacted region of the Hudson estuary. During that period, the question of nutrient removal and its potential effect on coastal water quality could be more extensively examined from the viewpoint of possible construction of tertiary sewage treatment facilities.

The conclusions presented here are based on extremely simple conceptual models of estuarine circulation which do not include any details of circulation or dynamics of the driving forces of the circulation. They involve some first-order approximations of net transport rates and time scales of flushing, as well as field data on the distribution of phosphate and chlorophyll as a function of salinity and location within the Hudson. More elaborate numerical models could certainly provide additional insights into the behavior of nutrients within the Hudson, but it is unlikely from a management viewpoint that major changes in the conclusions about phosphate behavior within the Inner Harbor of the Hudson estuary would result from more elaborate descriptions of the actual circulation.

SECTION 12

WATER COLUMN TRACE METALS IN THE HUDSON

INTRODUCTION

The data reported in this section were collected by Gary Klinkhammer of the University of Rhode Island as part of his masters thesis entitled, "The Distribution and Partitioning of Some Trace Metals in the Hudson River Estuary". All of the field sampling on the Hudson and laboratory work at URI were done by Gary Klinkhammer in cooperation with his thesis advisor, Mike Bender, a member of the faculty of the Graduate School of Oceanography at URI. Much of the discussion in this section was taken directly from this thesis (Klinkhammer, 1977).

Before the importance of dredge spoils and sewage sludge as sources of trace metals can be assessed, the distribution, sources and transport pathways of trace metals in the water column should be established. The data discussed in this section provide much of that information for the Hudson estuary during two periods of intensive sampling, April 1974 and October 1975. Both of these sampling periods were characterized by high fresh water discharge rates, early April 1974 being dominated by snow melt runoff, and October 1975 being dominated by abnormally rainy weather for several months preceding sampling.

SAMPLE COLLECTION AND ANALYTICAL METHODS

During April 1974, subsurface samples were collected using ordinary Niskin bottles on a hydrowire and surface samples were taken with a plastic bucket and polypropylene rope. In October 1975, subsurface samples were collected with a metal-free ten liter Niskin attached to a polypropylene rope. Samples were filtered through acid-washed 0.45 micron Millipore (T.M.) filters as soon as possible after collection, generally within 12 hours. Filtered samples were acidified to pH 2 with ultra-pure HCl and stored in acid-washed linear polyethylene bottles. Additional samples were stored cold in the dark, and analyzed for molybdate-reactive phosphate within three days after collection.

Soluble cadmium, zinc, copper, manganese and nickel were determined by atomic absorption spectrophotometry (AA) after ion-exchange preconcentration. Yields were determined by irradiating isotopically pure Cd-106, Zn-68, Cu-63, Mn-55 and Ni-64 to produce short lived radioactive tracers (Cd-107, Zn-69M, Cu-64, Mn-56 and Ni-65) which were added to the samples prior to passing through Chelex-100 and then analyzed on a Ge(Li) detector after elution with 10 ml of hot 3N HNO_3. Quantitative analyses of the stable metals were done

by flameless atomic absorption (graphite furnace) with a Perkin Elmer 503, except for zinc which was done by flame AA. A great deal of attention was devoted to blank determinations and intercalibration with other techniques including direct injection AA of raw samples for inorganic and isotope-dilution mass spectrometry for copper. Iron was done by direct injection into the graphite furnace, and by preconcentration with ammonium pyrillodine dithiocarbonate (APDC) followed by AA.

Particulate phase samples were oxidized on a low temperature asher, transferred to a polyethylene vial with 0.2 ml of pure HF, and allowed to digest for a week. Then 0.1 ml of pure HNO_3 was added and digestion proceeded for another week. Final volumes were made up to 1 ml with doubly-deionized H_2O. Aliquots of 0.1 ml were dispensed onto a small filter pad, dried, and analyzed for manganese and aluminum by neutron activation analysis utilizing 5 minute irradiations. Dilutions of the original 1 ml quenched digestion solutions were analyzed by flameless AA for cadmium, zinc, copper, manganese, nickel and iron.

RESULTS

Salinity, mile point locations, pH and the soluble concentration of trace metals are given in Table 31. Table 32 lists the concentrations in each water sample of these metals as particulates along with the suspended matter loads. Table 33 gives the dry weight metal abundances of the particulate matter itself. The total ranges of soluble concentrations tabulated in Table 31 for each of the metals are compared with metal data from Narragansett Bay, Rhode Island and the Saragasso Sea, which were also determined by similar analytical techniques in the laboratory at the University of Rhode Island (Table 34).

DISCUSSION

Figure 59 shows plots of soluble zinc, copper, manganese, nickel and reactive phosphate concentrations versus salinity for samples collected in April 1974, and October 1974. The importance of reactive-phosphate as a tracer for sewage input is clear from Figure 59. With the possible exception of copper these plots show maxima in metal concentrations which approximately coincide with those in the phosphate data. This suggests that three source mixing was the dominant process controlling the soluble concentrations of these metals throughout the estuary. Furthermore, in each case, these maxima occur at salinities corresponding to the New York harbor area.

The particulate phase also plays a major role in the transport of metals in the Hudson. Figure 60 is a plot of the concentration of particulate matter versus salinity. Bottom samples were consistently higher in suspended load, as might be expected, for both upstream and downstream tidal flow. Figure 60 also indicates that much of the suspended load of the river was being deposited in the area of New York harbor. This observation is consistent with the pattern of sedimentation rates based on the distribution of Cs-137 in sediments, which indicated a substantial zone of rapid deposition in the harbor.

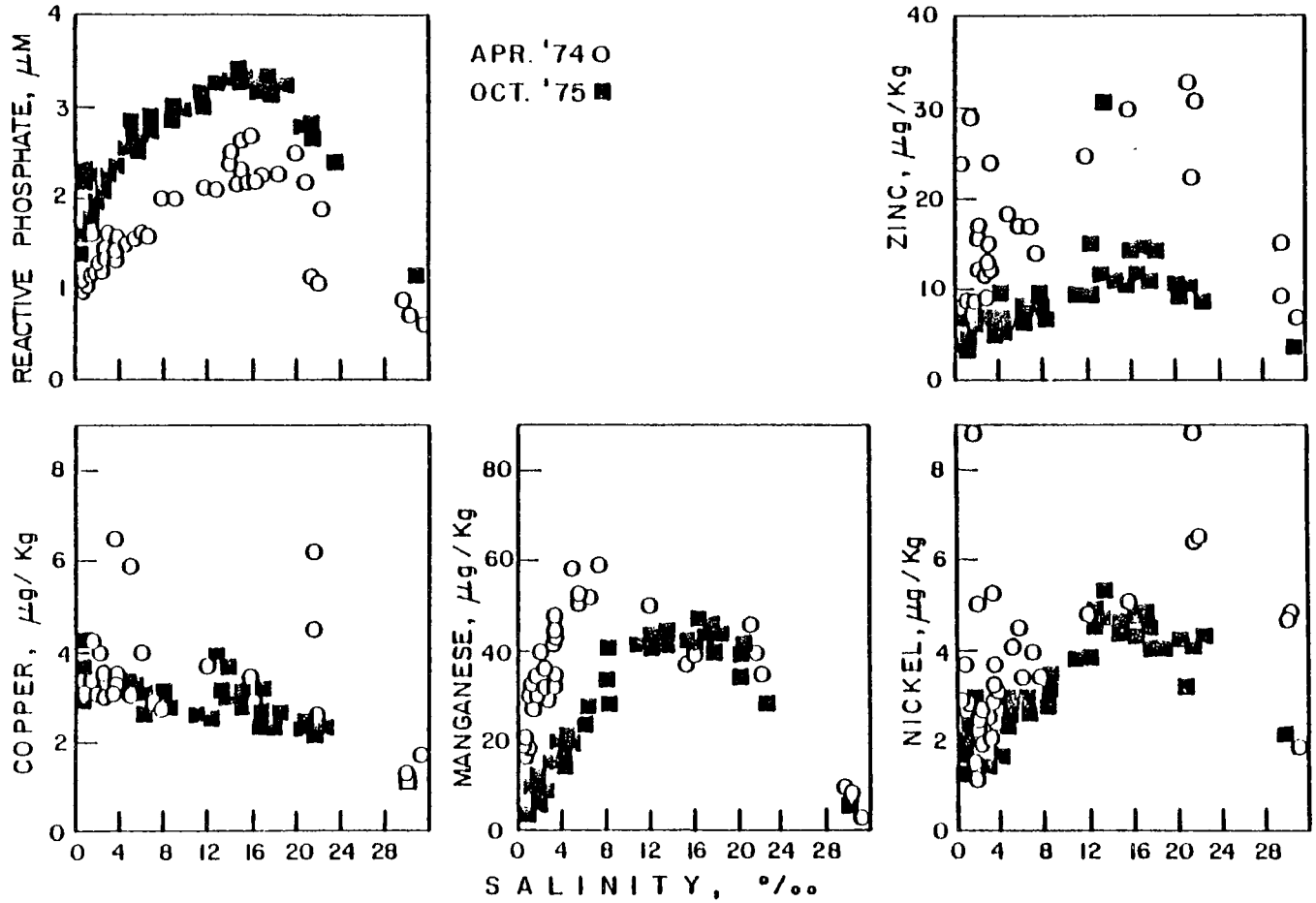

Figure 59. Soluble zinc, copper, manganese, nickel and molybdate-reactive phosphate concentrations versus salinity for samples collected in April 1974 and October 1975.

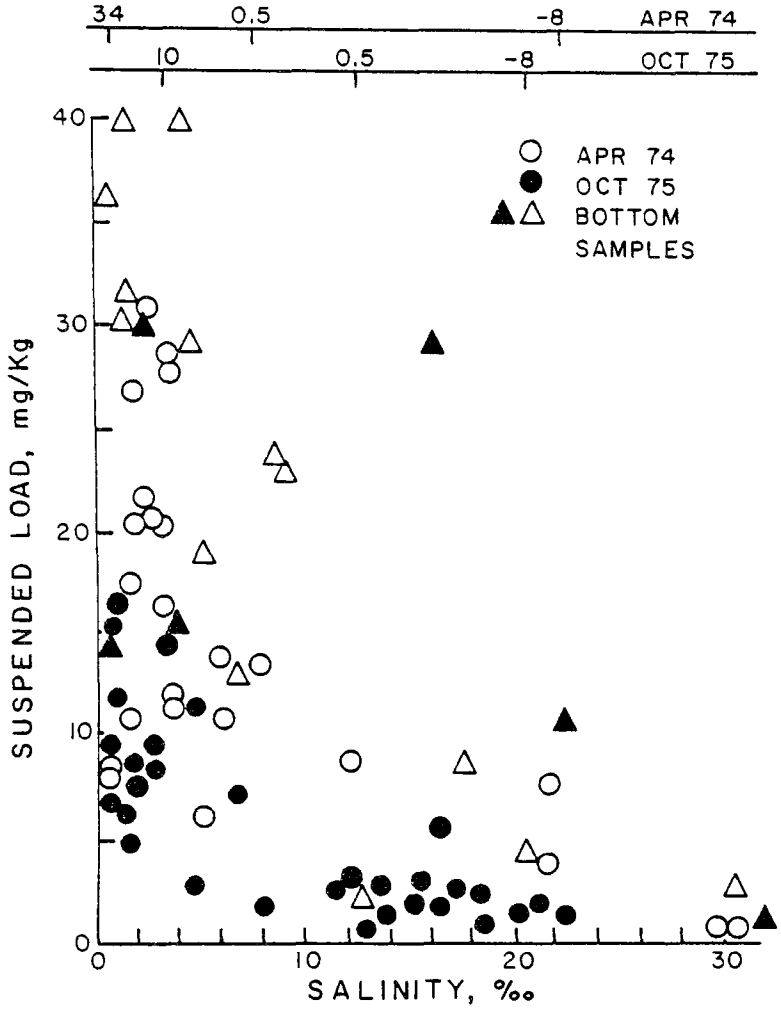

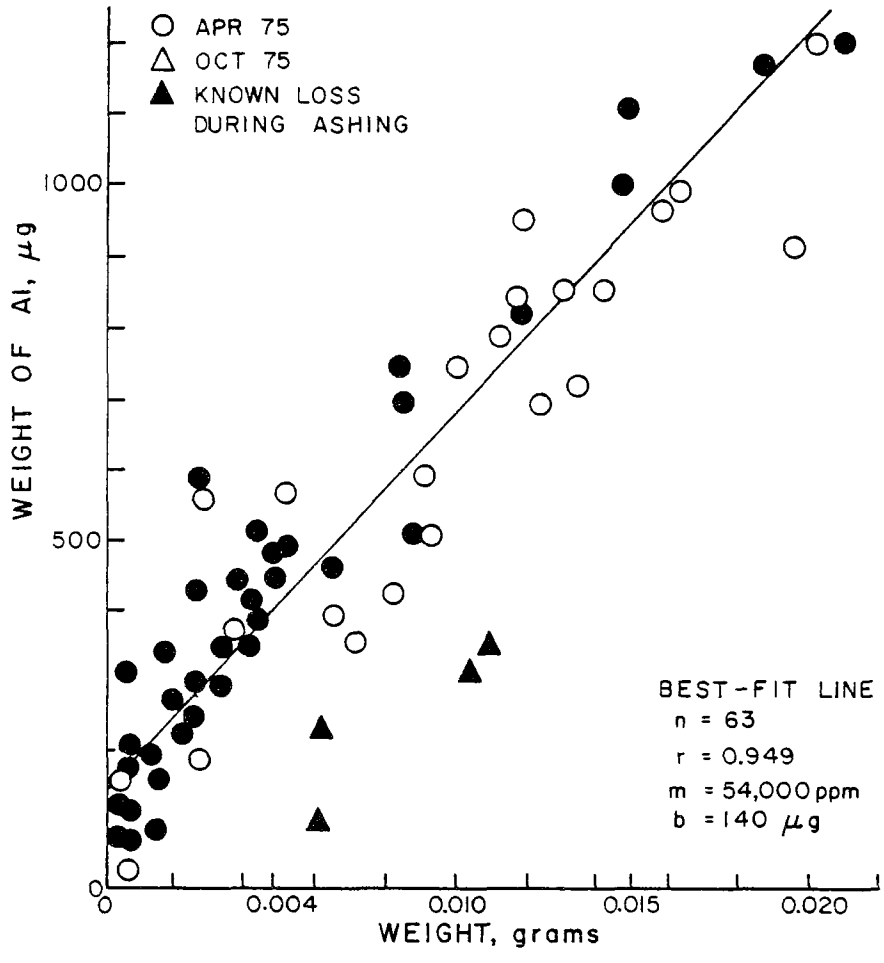

Figure 60. Concentration of the suspended material versus salinity and mile point (using surface salinities for April 1974 and October 1975).

Figure 61. Weight of aluminum collected on filters versus the total weight of suspended material - Hudson Estuary.

TABLE 31

Concentrations of Dissolved Trace Metals in the Hudson River Estuary (ppb)

April 1974

Mile Point	Depth*	Salinity (°/₀₀)	Cd	Ni	Zn	Cu	Mn
34	S	0.60	.317	3.70	23.7	3.22	20.7
	M	0.60	.309	2.89	7.46	3.23	21.0
	B	0.62	.286	2.53	8.00	3.34	16.7
24.5	S	1.99	.230	5.13	15.4	4.03	34.3
	B	2.00	.369	2.24	7.72	3.12	30.8
14	S	3.59	.194	2.35	8.00	3.02	43.5
	M	3.62	.272	3.78	14.5	3.17	44.9
	B	3.65	.395	5.29	23.4	6.49	-
Salinity	S	1.73	.271	9.30	28.4	4.09	26.6
Gradient	S	1.74	.230	1.51	7.62	4.21	31.4
	M	3.62	.284	3.20	11.0	3.35	42.4
	S	1.95	.152	1.12	15.6	3.29	34.0
	S	2.20	.259	1.93	15.0	3.46	29.2
	S	2.38	.279	2.73	16.6	3.51	35.8
	S	2.63	.319	2.38	11.0	3.48	39.4
	S	3.20	.284	2.51	8.55	3.30	32.5
	S	3.06	.187	1.95	11.2	3.26	31.8
	S	3.59	.237	3.11	11.3	2.85	47.5
	S	5.09	.498	4.12	17.7	5.94	58.6
	S	5.85	.231	3.37	11.0	3.14	50.7
	S	6.68	-	4.03	16.3	2.90	51.8
0.5	S	7.71	.302	3.38	13.6	2.68	59.7
	M	12.00	.325	4.80	24.5	3.72	49.6
	B	15.90	.343	-	29.4	2.91	38.7
-8	B	22.33	.339	6.60	30.8	2.25	34.6
-15	S	21.59	.503	10.8	32.9	6.28	45.5
	B	21.79	.361	6.40	21.8	4.50	40.1
-18.5	S	29.71	.301	4.71	14.9	2.84	9.75
	M	30.33	.091	4.79	9.02	1.29	8.36
	B	32.26	.187	1.82	6.11	5.53	2.11

(continued)

TABLE 31 (continued)

Mile Point	Depth*	Salinity (°/₀₀)	October 1975** Cd	Ni	Zn	Cu	Mn	Fe
33	S	.07	.162	1.49	3.48	2.86	1.9	91.7
31	S	.07	.142	1.80	7.25	2.94	1.5	20.8
29	S	.07	.134	1.60	4.38	3.19	1.2	16.2
27	S	.89	.139	1.26	2.59	3.15	1.2	37.5
26	S	1.03	.343	2.58	5.96	3.35	2.1	23.4
25	S	.31	.204	2.10	3.25	3.50	1.2	30.6
	B	1.49	.157	1.21	3.93	2.90	2.1	14.2
23	S	.48	.129	2.02	2.96	3.01	1.1	26.4
	B	1.25	.198	2.41	3.04	3.47	1.1	33.2
21	S	.83	.386	2.53	8.57	3.61	2.0	21.1
	B	1.25	.093	1.25	4.10	3.51	2.1	26.0
20	S	.89	.292	2.29	4.35	3.32	1.8	13.9
	B	4.90	.194	2.54	6.66	2.98	19.6	43.7
18	S	1.10	.245	2.00	4.78	3.07	2.2	10.0
	B	6.29	.216	2.85	3.58	2.99	23.1	57.5
16	S	1.68	.443	2.73	5.91	3.28	4.5	22.4
	B	4.31	.254	2.89	5.15	3.20	15.3	23.1
14	S	1.98	.196	2.55	5.92	3.22	6.7	32.9
	B	4.06	.177	2.97	4.66	3.32	17.1	26.0
12	S	2.66	.145	2.16	3.28	3.02	9.4	18.2
	B	8.22	.200	2.66	6.69	2.68	28.3	51.9
10	S	3.33	.175	2.62	6.87	3.20	14.8	16.9
	B	8.17	.391	3.15	7.63	2.76	40.5	30.9
8	S	4.19	.184	1.60	9.59	3.19	20.4	16.9
	B	12.40	.207	3.76	9.32	2.45	42.9	22.1
6	S	4.48	.200	2.37	6.79	3.04	21.0	24.4
	B	17.63	.257	4.54	14.5	2.28	45.5	13.2
4	S	6.83	.179	2.53	6.38	2.60	28.2	10.0
3	S	8.11	.343	3.43	9.62	3.14	33.7	15.9
1	S	11.47	.278	3.82	9.29	2.56	41.3	13.3
	M	18.46	-	4.00	14.3	2.64	43.6	51.2
0.5	S	12.40	.255	4.76	14.7	3.76	39.5	15.9
0	S	13.67	.627	4.69	11.8	3.00	42.4	12.3
-1	S	13.72	.362	4.67	14.3	3.15	40.7	14.9
	S	13.87	-	5.33	30.3	3.63	44.2	39.0
-2	S	15.43	.272	4.35	10.3	2.49	40.1	13.6

(continued)

TABLE 31 (continued)

Mile Point	Depth*	Salinity (°/₀₀)	Cd	Ni	Zn	Cu	Mn	Fe
-4	S	16.67	.157	4.82	11.6	3.13	42.9	13.3
	S	16.70	.608	4.83	14.4	3.08	46.9	12.3
	S	16.72	.261	4.29	11.8	2.59	44.8	14.6
	B	20.69	.136	4.19	10.3	2.32	38.8	10.6
-6	S	18.13	.170	3.99	10.8	2.33	39.9	10.6
-8	S	20.52	.167	3.22	9.84	2.37	34.4	8.3
-9	S	21.16	.221	4.08	10.2	2.35	40.5	4.7
-10	S	22.52	.234	4.29	8.75	2.32	28.2	7.0
	B	30.70	.100	2.10	3.60	1.08	5.8	20.3

* S = surface; M = mid-column; B = bottom
** All soluble concentrations in µg/kg

TABLE 32

Mile Point Locations, Depths, Salinities and the Particulate Concentrations of Six Metals for Samples Collected from the Hudson Estuary

Mile Point	Depth*	Salinity °/₀₀	Suspended load mg/kg	April 1974 ** Cd	Ni	Zn	Cu	Mn	Fe
34	S	0.60	8.4	.050	0.8	--	1.65	13.8	810
	M	0.60	7.0	.121	1.2	4.7	1.61	6.9	850
	B	0.62	14.3	.072	0.8	4.2	1.21	5.8	740
24.5	S	1.99	26.8	.112	6.4	6.7	2.8	11.5	1290
	B	2.00	30.0	.092	1.2	8.5	3.2	17.1	1360
14	S	3.59	27.7	.074	0.7	4.2	2.5	9.7	1080
	M	3.62	28.5	.201	8.0	7.7	4.8	14.9	1750
	B	3.65	15.6	.073	1.2	4.0	2.7	6.0	810
Salinity	S	1.73	17.5	.112	1.5	6.0	2.9	7.0	1180
Gradient	S	1.74	10.9	.057	0.7	3.3	1.19	5.6	650
	M	3.62	11.4	.048	1.1	3.7	2.1	6.1	730
	S	1.95	20.3	.077	1.2	5.8	3.3	10.5	1240
	S	2.20	21.6	.103	1.3	6.4	3.9	11.8	1302
	S	2.38	20.6	.106	1.1	5.7	3.7	12.0	1280
	S	2.63	30.9	.111	1.6	7.9	4.5	14.1	1570
	S	3.20	16.5	.030	0.2	2.0	3.6	3.5	430
	S	3.06	20.3	.060	0.7	5.2	2.3	8.2	941
	S	3.59	11.9	--	--	--	--	--	--
	S	5.09	0.6	.016	0.1	0.79	und	1.30	138
	S	5.96	13.9	.068	2.8	1.84	0.82	2.0	260
	S	5.85	11.0	.030	und	0.48	und	0.81	90
	S	6.68	11.8	.070	0.9	3.9	1.56	3.5	610
	S	7.71	13.5	.068	0.6	4.1	2.8	5.9	881
	M	12.00	8.8	.154	0.6	3.8	3.6	5.0	640
	B	15.90	28.9	--	--	--	--	--	--
	B	22.33	10.9	.049	0.4	1.77	1.89	3.4	350
	S	21.59	3.8	.044	0.4	4.1	3.2	3.1	300
	B	21.79	7.7	.027	und	3.00	1.98	2.7	260
	S	29.71	--	.013	und	0.20	und	0.91	40
	M	30.33	--	.006	und	0.04	und	0.22	7
	B	32.26	0.9	.010	und	0.29	2.5	0.40	30

* S = Surface; M = Mid-Column; B = Bottom
** All soluble concentrations are in µg/kg
und = undetectable

(continued)

TABLE 32 (continued)

Mile Point	Depth*	Salinity °/₀₀	Suspended load mg/kg	October 1975 ** Cd	Ni	Zn	Cu	Mn	Fe
33	S	.07	8.8	.055	0.75	4.2	1.52	11.7	690
31	S	.07	9.2	.072	0.72	4.6	1.83	12.0	690
29	S	.07	9.0	.062	1.03	7.1	1.34	19.9	1100
27	S	.89	8.2	.136	0.84	4.8	2.2	15.1	850
26	S	1.03	16.4	--	--	--	--	23	--
25	S	.31	7.0	.037	0.63	4.1	1.28	14.5	600
	B	1.49	30.3	.090	1.56	9.0	3.5	27	1420
23	S	.48	36.2	.079	1.42	7.6	3.4	26	1350
	B	1.25	31.2	.271	1.36	9.1	3.8	33	1400
21	S	.83	15.3	.051	0.91	5.3	2.4	22	970
	B	1.25	52.2	.132	2.23	13.9	5.7	40	2200
20	S	.89	6.6	.038	1.00	4.7	2.0	17.1	740
	B	4.90	19.0	.101	1.02	7.5	2.8	18.7	2200
18	S	1.10	11.8	.035	0.47	3.1	0.81	14.1	690
	B	6.29	13.2	.034	0.85	4.6	2.7	16.4	810
16	S	1.68	8.6	.029	0.68	4.5	1.63	11.6	530
	B	4.31	29.0	.058	1.27	9.3	4.3	18.7	1230
14	S	1.98	8.6	.024	0.40	2.7	1.08	10.6	430
	B	4.06	40.9	.066	0.26	8.1	5.0	15.7	1360
12	S	2.66	9.6	.025	0.68	4.6	1.50	16.9	530
	B	8.22	23.5	.066	1.09	7.4	4.7	12.8	1070
10	S	3.33	14.3	.039	0.82	4.9	2.6	13.1	770
	B	8.17	23.8	--	1.04	8.0	4.4	13.6	1070
8	S	4.19	11.5	.034	0.60	4.5	2.3	9.2	--
	B	12.40	12.5	.048	0.55	3.4	2.5	8.3	570
6	S	4.48	2.9	.030	0.45	3.9	2.6	6.1	390
	B	12.63	8.6	.035	0.50	3.1	2.6	4.4	500
4	S	6.83	7.0	.023	0.41	2.8	1.29	8.4	470
3	S	8.11	1.7	.022	0.33	2.9	0.98	3.0	290
1	S	11.47	2.6	.022	0.33	2.3	1.27	5.5	280
	M	18.46	0.8	.021	0.17	1.50	0.99	3.2	160
0.5	S	12.40	2.5	.012	0.17	1.31	0.48	2.2	160
0	S	13.67	2.8	.024	0.18	1.38	0.48	2.3	130
-1	S	13.72	0.7	.030	0.25	1.62	0.83	2.2	150
	S	13.87	0.7	.011	0.24	1.71	0.98	2.4	40
-2	S	15.43	2.6	.014	0.28	1.64	1.01	2.1	130
-4	S	16.67	5.5	.009	0.17	1.12	0.32	3.5	100
	S	16.70	2.1	.095	0.14	1.13	0.54	2.1	120
	S	16.72	2.2	.030	0.17	1.57	0.60	4.1	125
	B	20.69	4.4	.012	0.21	1.38	0.58	4.8	100
-6	S	18.13	2.5	.011	0.24	1.99	1.04	2.5	110
-8	S	20.52	1.4	.005	1.55	0.73	und	2.5	50
-9	S	21.16	1.8	.006	0.08	0.83	und	1.84	45
-10	S	22.52	1.4	.007	0.49	1.07	0.23	2.7	80
	B	30.70	2.9	.012	0.21	1.71	0.80	5.4	200

TABLE 33

Mile Point Locations, Depths, Salinities and the Metal Abundances of Six Metals in Particulate Matter Samples Collected from the Hudson Estuary

April 1974 **

Mile Point	Depth *	Salinity °/₀₀	Cd	Ni	Zn	Cu	Mn	Fe x 10^{-3}	Al x 10^{-3}
34	S	0.60	5.9	96	---	200	1300	96.5	111
	M	0.60	17	170	670	230	990	122.0	101
	B	0.62	5.0	56	300	90	400	51.5	54.4
24.5	S	1.99	4.2	240	250	110	430	48.1	61.5
	B	2.00	3.1	41	280	110	570	45.5	---
14	S	3.59	2.7	25	150	90	350	39.0	47.0
	M	3.62	7.1	280	270	170	520	61.4	60.0
	B	3.65	4.7	77	250	170	390	52.1	61.6
Salinity	S	1.73	6.4	86	340	160	400	67.4	75.5
Gradient	S	1.74	5.2	64	300	110	510	59.5	60.4
	M	3.62	4.2	97	330	190	530	64.3	72.7
	S	1.95	3.8	59	290	160	520	61.1	56.6
	S	2.20	4.8	60	290	180	550	61.1	81.0
	S	2.38	5.2	60	280	180	580	62.1	70.8
	S	2.63	3.6	52	260	150	460	50.8	67.1
	S	3.20	1.8	12	120	220	210	25.8	31.4
	S	3.06	3.0	34	260	120	400	46.4	53.7
	S	3.59	5.5	---	170	70	---	31.5	47.6
	S	5.09	---	80	---	und	---	---	302
	S	5.96	4.9	200	130	60	140	18.3	30.0
	S	5.85	2.7	und	40	und	70	8.2	16.1
	S	6.68	5.9	76	330	130	300	52.0	49.2
0.5	S	7.71	5.0	44	300	210	440	65.3	60.9
	M	12.00	18	68	440	400	570	73.7	65.2
	B	15.90	---	---	---	---	---	---	---
-8	B	22.33	4.5	38	160	95	320	32.0	51.9
-15	S	21.59	12	110	1090	830	820	79.0	66.6
	B	21.79	3.5	und	390	260	350	34.0	35.8
-18.5	S	29.71	---	und	---	und	---	---	---
	M	30.33	---	und	---	und	---	---	---
	B	32.26	11	und	340	und	460	33.6	29.7

* S = Surface; M = Mid-column; B = Bottom
** All abundances are in parts per million
und = Undetectable

(continued)

TABLE 33 (continued)

October 1975 **

Mile Point	Depth *	Salinity °/₀₀	Cd	Ni	Zn	Cu	Mn	F x 10^{-3}	Al x 10^{-3}
33	S	.07	6.3	85	480	170	1330	77.7	109
31	S	.07	7.8	78	530	200	1300	75.2	102
29	S	.07	6.9	110	790	150	2210	122.0	210
27	S	.89	17	100	590	270	1840	103.0	187
26	S	1.03	---	---	---	---	---	---	83.6
25	S	.31	5.3	90	580	180	2070	86.2	138
	B	1.49	3.0	52	300	120	880	47.1	90.0
23	S	.48	2.6	39	220	90	710	37.4	63.6
	B	1.25	8.7	44	290	120	1070	---	58.0
21	S	.83	3.3	60	350	160	1410	63.0	119
	B	1.25	2.5	43	270	110	760	42.3	75.7
20	S	.89	5.8	150	710	310	2590	113.0	181
	B	4.90	5.3	54	400	150	980	50.6	95.0
18	S	1.10	3.0	40	260	70	1200	43.5	85.5
	B	6.29	2.6	64	350	200	1240	61.6	118
16	S	1.68	3.3	79	520	190	1350	62.3	99.8
	B	4.31	2.0	44	320	150	650	42.6	75.9
14	S	1.98	2.8	47	310	130	1230	50.1	91.9
	B	4.06	1.6	60	200	120	380	33.3	57.9
12	S	2.66	2.6	71	480	160	1760	55.1	90.2
	B	8.22	2.8	46	320	200	550	45.8	69.0
10	S	3.33	2.7	57	340	180	920	54.1	87.6
	B	8.17	---	44	340	190	570	45.3	69.5
8	S	4.19	3.0	52	270	200	800	---	107
	B	12.40	3.8	44	270	200	660	262.0	---
6	S	4.48	10	160	1300	880	2100	138.0	252
	B	17.63	4.1	58	360	300	510	57.6	98.4
4	S	6.83	3.3	59	410	180	1200	68.0	---
3	S	8.11	13	210	1700	580	1700	166.0	267
1	S	11.47	8.5	130	880	490	2120	107.0	214
	M	18.46	26	210	1900	1200	4000	11.1	350
0.5	S	12.40	4.8	68	520	190	880	64.4	140
0	S	13.67	8.6	64	500	170	820	46.1	83.2
-1	S	13.72	43	360	2300	1200	3140	208.0	395
	S	13.87	16	340	2400	1400	3430	197.0	---
-2	S	15.43	5.4	110	630	390	810	50.7	128
-4	S	16.67	1.6	31	200	60	640	19.1	535
	S	16.70	45	67	540	260	1000	54.9	108
	S	16.72	14	77	710	270	1860	58.3	93.5
	B	20.69	2.7	48	310	130	1090	21.8	62.0
-6	S	18.13	4.4	96	800	420	1000	43.0	128
-8	S	20.52	3.6	1100	520	und	1790	31.4	96.5
-9	S	21.16	3.3	44	460	und	1000	25.1	98.4
-10	S	22.52	5.0	350	760	160	1930	60.8	128
	B	30.70	4.1	72	590	280	1860	68.8	109

TABLE 34

Comparison Between Ranges of "Soluble" Metal Concentrations Found in the Hudson Estuary, Narragansett Bay, Rhode Island, and the Sargasso Sea

Metal	Hudson Estuary (µg/kg)	[1]Narragansett Bay (µg/kg)	[2]Sargasso Sea (µg/kg)
Cd	.10 - .50	.05 - 1.0	.005 - .025
Zn	2.5 - 35	5.0 - 30	-----
Cu	2.0 - 7.0	1.0 - 7.0	.10 - .12
Mn	15 - 70	10 - 30	.01 - .15
Ni	1.0 - 10	3.0 - 10	.12 - .17

[1]Unpublished data of G. Klinkhammer.

[2]Cd, Cu and Ni values were taken from Bender and Gagner (1976). Mn data was taken from Bender et al (1976).

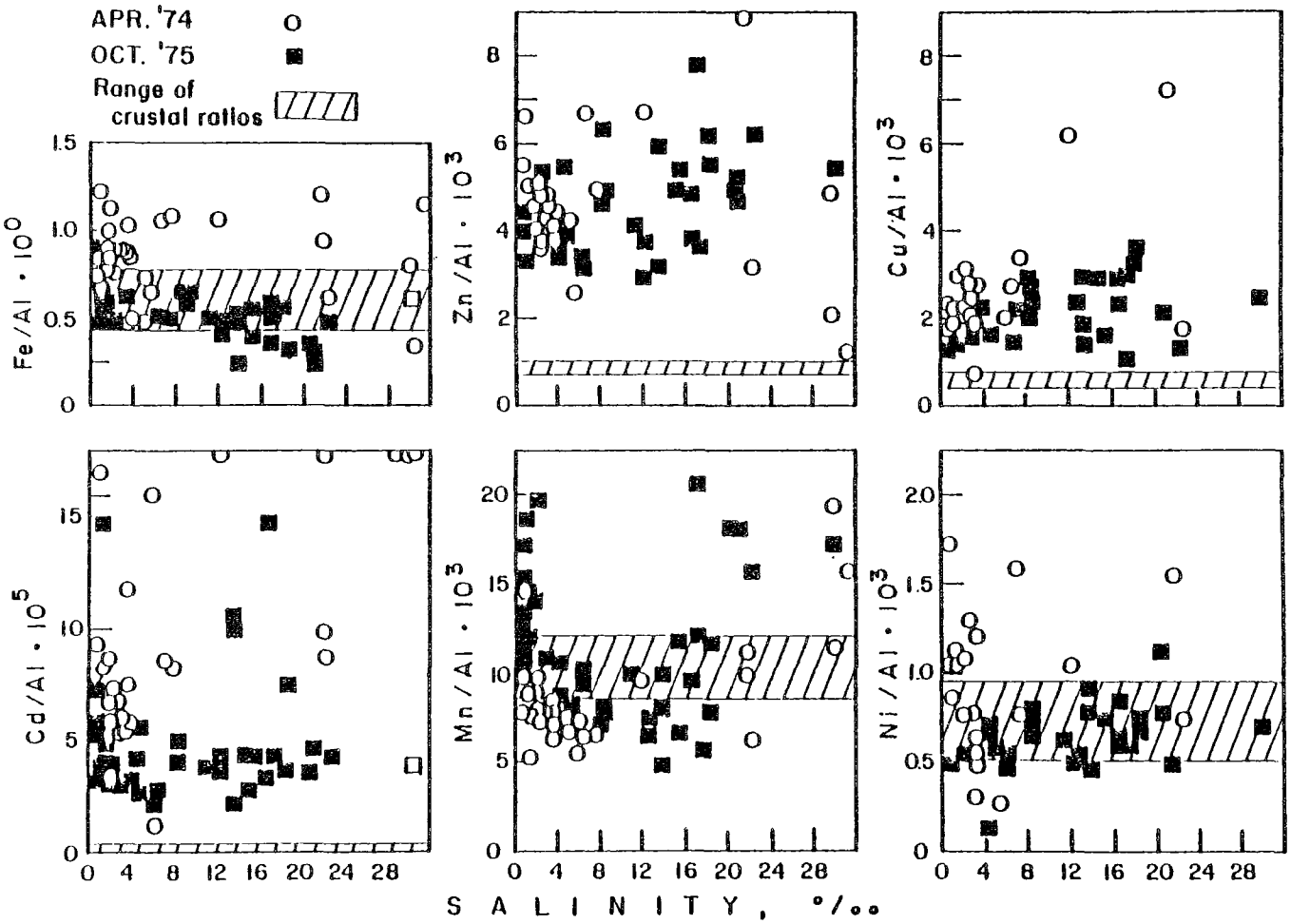

Figure 62. Metal to aluminum weight ratios of six metals in particulates filtered from the Hudson Estuary plotted versus salinity.

From the trends in soluble metals and suspended loads, it is clear that New York harbor is a zone of major perturbation, involving large addition of soluble metals from sewage and substantial decrease in suspended load due to changes in estuarine geometry and/or salting out effects (flocculation). Reactive-phosphate is apparently a useful tracer for sewage input of soluble metals, but an additional chemical tracer for the suspended load would be valuable for normalizing the metal abundances of the particulate matter. From Figure 61, it is apparent that particulate aluminum is a good indicator of the mass of suspended load. The metal abundances of the particulates have been normalized to aluminum and the weight ratios plotted versus salinity in Figure 62. Also shown are ranges in average crustal ratios of trace metals to aluminum as given by Turekian and Wedepohl (1961).

The concentrations of metals in sewage discharged from New York City are given in Table 35. One of the data sets (Klein et al., 1974) represents some approximation of total metals in New York City sewage from samples composited daily over a period of a month. Samples were taken unfiltered, and 15 ml of concentrated HCl and 5 ml of concentrated HNO_3 were added to each 100 ml aliquot (1.8 N in HCl and 0.8 N in HNO_3). The samples were then autoclaved and analyzed by flame atomic absorption spectrometry.

The plot of soluble manganese versus salinity in Figure 59 shows distinctive trends for the two collection periods. During April 1974, soluble manganese in the fresh water endmember was about 17 µg/kg. The concentration increased sharply toward Manhattan, reaching a maximum at a salinity of about 8°/$_{oo}$ (in the East River). Above this salinity the levels decreased gradually toward the Bight where the lowest concentration found was about 1 µg/kg at a salinity of 32°/$_{oo}$. The same trend is apparent for samples collected in October 1975, although the levels found were strikingly different. Here the average concentration of 14 fresh water samples was about 2 µg/kg. Again these levels increased sharply downstream reaching a maximum of about 45 µg/kg at a salinity of 14°/$_{oo}$ (also in the East River). Toward the Bight the levels again decreased to a minimum of about 6 µg/kg at 31°/$_{oo}$. The large maximum in the harbor is most likely due to sewage discharge, and based on a three source mixing model a sewage manganese concentration on the order of 1000 µg/kg is suggested for both sampling periods. The difference in the fresh water dissolved manganese during the two sampling periods is most likely due to a difference in the partitioning of Mn between the particulate and soluble phases, since the total Mn entering the estuary is similar during both surveys (Figure 63). We have not determined the cause of the difference in partitioning but several plausible explanations are the somewhat longer fresh water residence time (lower fresh water flow return) to allow time for oxidation to less soluble Mn(II) during the October period, and the higher water temperature during October.

There is evidence for desorption of manganese from suspended matter in the saline waters of the Hudson in the decrease in Mn to Al ratios downstream (Figure 62) and of loss of Mn from bottom sediments resulting in lower average Mn concentrations in deep water suspended matter, which contains a considerable amount of resuspended sediment (Figure 64). We have not measured directly the rate of remobilization of Mn from sediments deposited in the harbor, but a mass balance calculation for the flow conditions of the October survey indicates a rate of 1-2 µg/cm^2/cm^2/day (Klinkhammer, 1977), in good agreement

TABLE 35

Reported Metal Concentrations of Sewage
Being Discharged into the Lower Hudson Estuary

	* Cd	Zn	Cu	Mn	Ni	Fe	PO_4 μM
Interstate Sanitation Commission Report (1972)							
Number of Determinations	491	578	583	503	398	269	522
Average Concentration	<20	120	100	120	<100	600	60
Klein, et al. (1974)							
Number of Determinations	240	240	240	---	240	---	---
Average Concentration	10	260	150	---	100	---	---
Range in Concentrations Assumed in this Study	16± 8	180± 90	120± 60	825± 410	100± 50	600± 310	60

*All metal concentrations are in μg/kg.

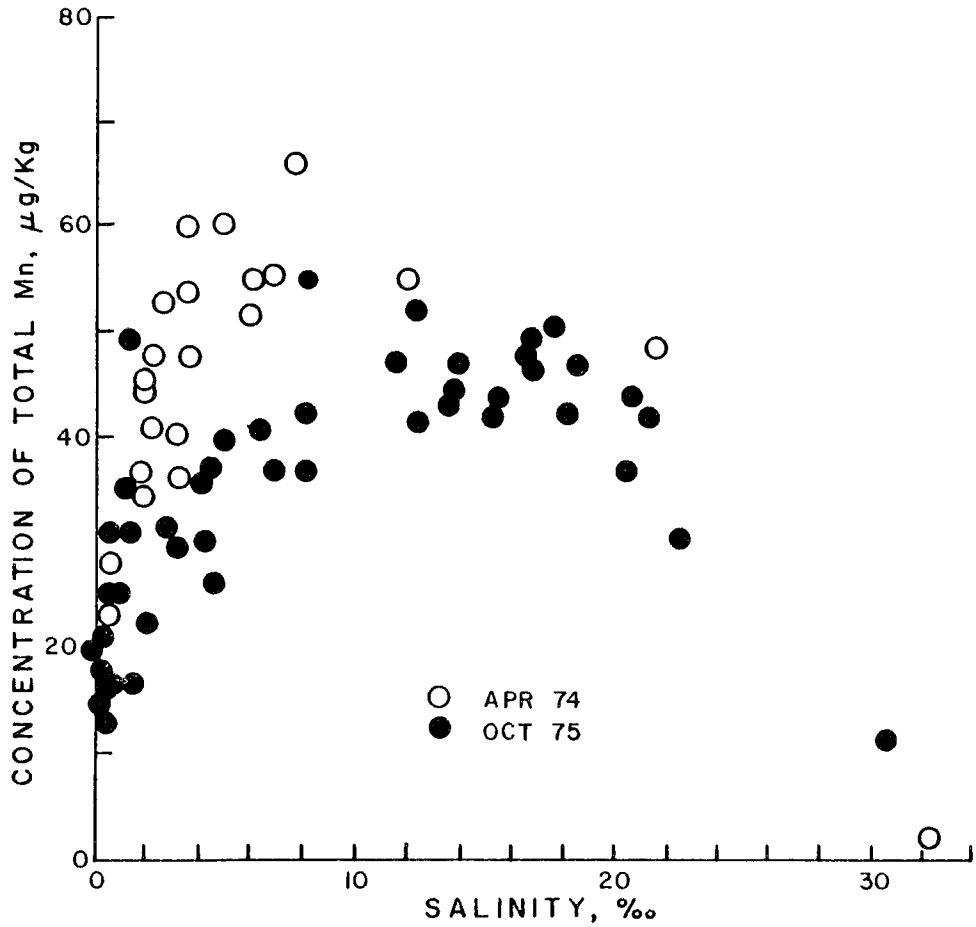

Figure 63. Plot of total manganese versus salinity for samples collected in the Hudson Estuary.

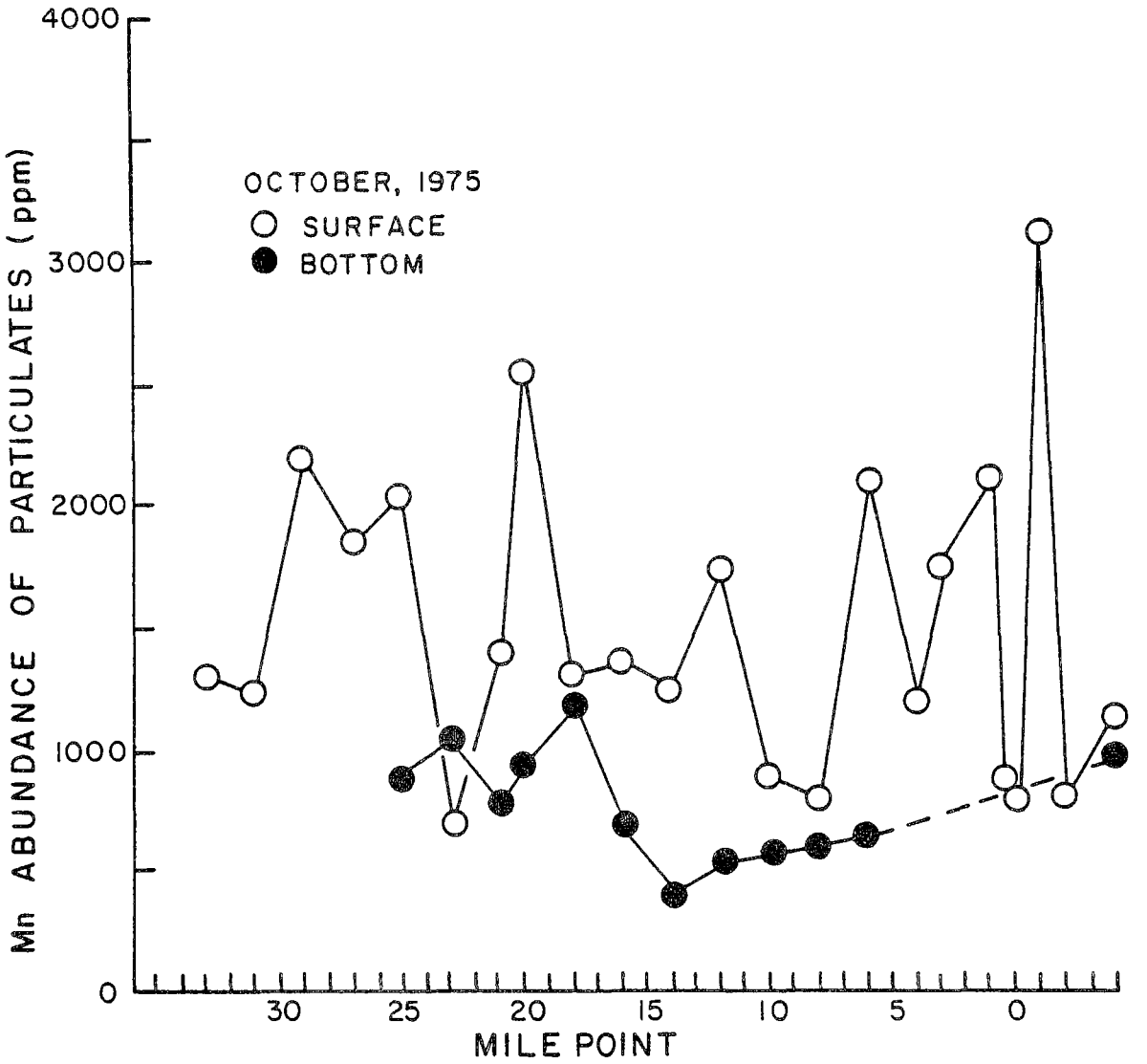

Figure 64. Manganese abundances of surface and subsurface particulates collected from the Hudson Estuary during October 1975 plotted versus mile point. The average manganese abundance of the surface particulates was 1500 ppm while it was 750 ppm for the subsurface samples.

with direct Mn flux measurements made in Narragansett Bay (Graham et al., 1976).

CONCLUSIONS

The partitioning of manganese between solid and soluble phases at the fresh water extremity of the estuary is apparently related to some temperature and/or time dependent process. An oxidation has been suggested here although other explanations cannot be eliminated by these data. In any case, the total manganese at low salinities was essentially constant during both collection periods at about 20 µg/kg. Downstream, manganese concentrations were dominated by a large anthropogenic input of soluble metal. This sewage Mn apparently remains soluble for the residence time of water in this section of the estuary (several days). The bulk of the particulate fraction was being deposited in New York harbor. These data further suggest that some desorption and/or reduction at the water-sediment interface may be occurring across the salinity gradient. However, the extent of any such process appears to be minor when compared to the direct supply of Mn from sewage.

The averaged partitioning of five metals between soluble and suspended load phases is shown for three regions of the Hudson in Figure 65. Except for iron, which was predominantly ($\sim$ 99%) on particles, most of the transport of metals in the Hudson was occurring in solution. The general trends were consistent for both sampling periods, except for manganese which was discussed earlier.

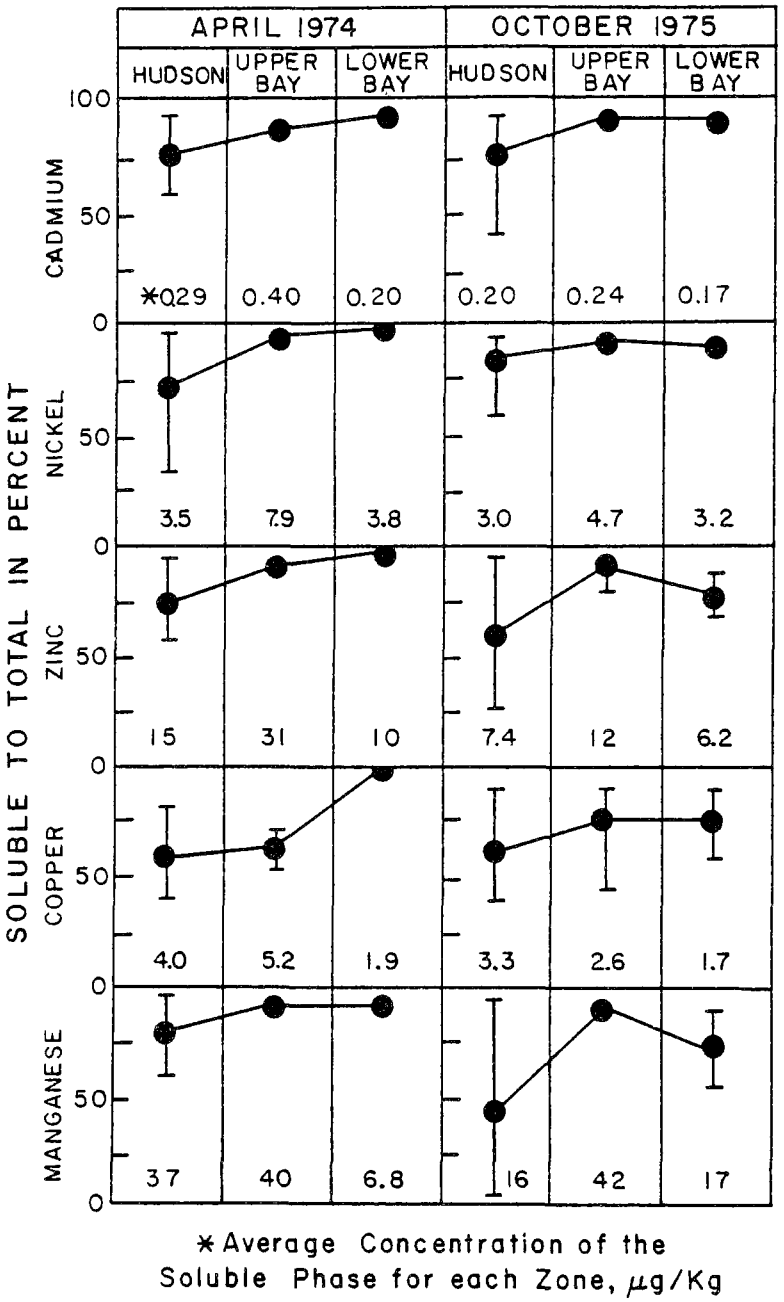

Figure 65. The partitioning of five trace metals in the Hudson Estuary. Iron data is not shown but about 99% of this metal was present in the particulate phase in all three boxes during October 1975.

SECTION 13

SUMMARY OF HUDSON FIELD RESEARCH RESULTS

In Section 4 we discussed the distribution and sources of several metals in Hudson estuary sediments in terms of the background trace metal composition of fine-grained sediments and the levels of pollutant metals added from diffuse sources throughout the Hudson estuary and from the concentrated sources in the New York City area. The observed concentrations of Zn, Cu and Pb were generally 3-6 times background levels with the highest values, especially for Cu, in New York harbor. We have not attempted to derive the total burden of pollutant metals in New York harbor sediments, although that would probably be feasible to do from the information we are developing about recent sediment deposition pattersn in the Hudson based on the distribution of Cs-137. Considerable attention has been directed to the elevated levels of trace metals in New York Bight sediments due to disposal of dredge spoils and sewage sludge. Although the levels of trace metals in the sediments of the dumping area are very high relative to those of more distant sandy shelf sediments and thus make very dramatic and useful mapping tools, the concentrations of metals in most of the surface sediments of the Hudson, and especially in New York harbor are comparable to those in the dumping areas. Thus if the pollutant metal concentrations in the sediments of the Bight apex are considered as a serious environmental problem, then similar concern should also be directed to the condition of much of the sediments of the Hudson estuary.

The area of most intense metal pollution that we have observed in the Hudson is in a small cove about 60 km north of New York City. Effluents of a battery factory released over several decades have contaminated sediments of a small portion of Foundry Cove to levels above a percent for both Cd and Ni. We have completed a survey of the Cd and Ni distribution in the least contaminated portion of this cove ($\leq$ 1000 ppm in Cd and Ni) adjacent to the main channel of the Hudson. Of the total burden of Cd (and Ni) in Foundry Cove of 25-50 tons, we estimate that at least 2 tons have been transported away from the area of most contamination, through a narrow connecting channel, and accumulated in the outer area of the cove. We believe most of this transport probably occurred by resuspension and deposition of fine particles in the sediments over a number of years, mobilized by tidal currents, and perhaps to some extent by a dredging operation in the most contaminated area of the inner cove. The covariation of Cd and Ni in outer cove sediments and the pattern of reactor radionuclide distribution in the sediments argue against transport of Cd and Ni in solution to the outer cove, and against a single episode of Cd and Ni deposition in the outer cove (i.e. dredging remobilization) which has been spread through the upper 20 cm of sediments by biological or physical mixing processes.

Our studies of interstitial water (pore water) Cd in Foundry Cove have been promising, but have not progressed sufficiently to reach many conclusions. The new pore water sampling technique developed in our laboratory appears to be quite a valuable addition to the study of sediment chemical processes, especially in relatively shallow waters accessible by divers. The concentrations of dissolved Cd in Foundry Cove sediments appear to be much higher than water column Cd concentrations, even in the most heavily impacted area of the Hudson. Thus these sediments definitely appear likely to be a source of soluble Cd, as opposed to the sediments of Narragansett Bay, which do not appear to be a source of soluble Cd. We cannot make a good estimate of the strength of the source of Cd from these sediments, based on our experiments to date, but can place some probable limits on flux estimate budget calculations by relating the pore water Cd data to that of Mn. In Foundry Cove the most contaminated sediment area which we studied had pore water Cd concentrations of approximately 30 ppb, about two orders of magnitude less than Mn in the same samples. The flux of Mn from Narragansett Bay sediments has been directly measured to be 1-2 $\mu g/cm^2/day$. If the same flux were to characterize Foundry Cove sediments the total flux of Mn per year over the area of the cove ($\sim$ 0.5 km^2) would be $\sim$ 3 tons. If the flux of Cd were in the same proportion to Mn as the ratio of pore water concentrations ($\sim$ 1/100) the annual flux of Cd would be $\sim$ 0.3 T or about 10^{-3} of the sediment burden of Cd in the Cove. There are several reasons why this might be expected to be an upper limit of the Cd flux from Foundry Cove sediments, but without more field experiments we cannot be more definite at this time. It does appear likely that Foundry Cove sediments during fresh water conditions that existed during the experiments described here are a net source of soluble Cd and not a net sink as indicated for the estuarine conditions of Narragansett Bay sediments.

We have found the distribution of a number of reactive pollutants, including Zn, Cu, Pb, Cd, Ni and polychlorinated biphenyls (PCB's) and Pu-239,240 to be strongly correlated with the distribution of Cs-137 in recent Hudson sediments. This covariation indicates that fine particles in estuaries are a transport vector for a large spectrum of pollutants and greatly simplifies the task of mapping the distribution of reactive pollutants in coastal zone sediments.

We have explored the use of C-14 as an indicator of the source of pollutant carbon in Hudson sediments, and found that the presence of recent sewage carbon in New York harbor overwhelms the presence of fossil fuel contaminated carbon which produce old apparent C-14 ages of organic matter in a number of environments contaminated with recent pollutants (Baltic Sea coastal sediments, Narragansett Bay, and Lake Washington).

In addition to exploiting C-14 measurements to learn about the source of pollutant carbon in contaminated sediments, we have developed a new type of analytical approach based on enzymes for quantitative determination of cellulose in coastal zone sediments. A preliminary survey indicates that this technique could provide substantial new insights into the diagenesis of large organic molecules in the coastal environment.

On the basis of a large number of water column and sediment measurements of Rn-222, a radioactive daughter of Ra-226, we were able to establish quantitatively the rate of transfer of a chemically-inert natural tracer from

the sediment to the water column in the Hudson estuary. One major conclusion was that the flux of Rn-222 from the sediments could be computed to within a factor of two based on a simple model of molecular diffusion within the sediments. The observed flux was approximately a factor of two greater than predicted from molecular diffusion and could be attributed to a combined effect of bioturbation, sediment stirring by currents, and other poorly defined processes which might enhance the flux of material from sediment interstitial waters.

We also explored the use of dissolved methane as an indicator of sediment-water exchange rates. The supply from the sediments appears to be dominated by partial solution of methane bubbles which are produced in the sediments and then pass up through the water column. Thus methane is not a useful analog for trace metal fluxes, but some new insights were gained. An extremely large range of dissolved methane concentrations within the sediments was observed ($\geq$ x 1000), indicating that the rate of anaerobic fermentation of organic matter and/or bacterial consumption of methane in sediments in the Hudson must be greatly variable. Since sulfate reduction (and sulfide production) is to some extent a competing process with that of methane production for destruction of organic matter in anaerobic sediments, and since trace metal solubilities in sediments may be strongly influenced by sulfide concentrations, the relationship between methane concentration in sediments and metal mobility should probably be explored.

We have invested substantial effort to establish the amounts of sewage components discharged to the Hudson near New York City and to develop simple model descriptions of the flushing characteristics of the Hudson estuary. This is essential for interpreting water column metal data in terms of transport processes and fluxes to the adjacent coastal waters. We have found dissolved phosphate to be a valuable indicator of both sewage loading rate and residence time of water in the Hudson near New York City. Thus phosphate is valuable as an indicator of the rate of sewage metal discharge and of the transport rates of dissolved metals out of the estuary. The rapid transport of phosphate from the Hudson by physical mixing compared with removal rates by phytoplankton activity indicates that nutrient removal in the New York City area probably would have little immediate benefit to water quality in the Hudson estuary, and thus tertiary treatment of sewage should not be introduced until clear evidence of beneficial results from such treatment can be developed.

Extensive surveys (by Gary Klinkhammer of the University of Rhode Island) of dissolved and suspended phase metals in the Hudson have been completed for two high fresh water flow periods. Most of the water column transport of metals out of the Hudson is accomplished by soluble metals, while deposition of large amounts of suspended particles causes accumulation of large amounts of particulate phase trace metals in New York harbor. Using the measured concentrations of soluble metals and phosphate in New York harbor, and our estimate of the discharge rate of phosphate through the Narrows from simple transport models ($\sim$ 6 moles/sec) we can calculate the discharge rate of soluble metals (Mn, Fe, Zn, Cu, Cd and Ni) from the Hudson estuary to the New York Bight apex (Table 36). From the estimated metal deposition rates by rain and dry fallout to the New York Bight (Duce et al., 1976), we derived maximum estimates of the delivery of total Fe, Zn and Cd from the atmosphere

TABLE 36

Soluble Metal Fluxes to the New York Bight Apex
(first order estimates - grams per second)

	Hudson Discharge April 1974[1]	Hudson Discharge October 1975[2]	Air Deposition to Apex (2×10^3 km^2)[3]	Benthic Flux (150 km^2)[4]
Mn	104	76	-	+ 15 ± 5
Fe	-	36	47	+ 1.5 ± 1
Zn	81	22	10	-
Cu	14	5	-	+ 0.1 ± 0.2
Cd	1	0.4	0.2	-0.01 ± 0.02
Ni	21	9	-	0 ± 0.1

[1]Derived from data in Sections 11 and 12

[2]Derived from data in Sections 11 and 12

[3]Derived from atmospheric deposition rate estimates by Duce et al., 1976.

[4]Derived from studies of Narragansett Bay at the University of Rhode Island by M. Bender.

(Table 36). Assuming all of the atmospheric metals are rapidly dissolved, it is possible that this flux could be significant for soluble Fe, Zn and Cd relative to the dominant estuarine discharge of soluble metals. These estimates of atmospheric deposition have a very large degree of uncertainty (Duce et al., 1976) and probably are less significant in the New York Bight apex relative to other fluxes than indicated in Table 36. We have also attempted to derive first order estimates of the flux of metals from waste area sediments (Gross, 1976), assuming an area of 150 km^2 of fine-grained, metal-contaminated sediments. The flux estimates per unit area we used were derived from studies in Narragansett Bay by the University of Rhode Island. Except for Mn, where the benthic flux approaches 15-25% of the estuarine discharge rate of soluble Mn, the waste area sediments do not appear to be significant sources of metals (Fe, Cu and Cd). Extrapolation of the Narragansett Bay results to the New York Bight waste area was done because these data are the best available data of which we are aware for organic rich, reducing sediments in a coastal environment.

Our conclusions about the lack of importance of soluble phase mobliization of metals from the waste area in the Bight, except for Mn, is consistent with the observations of Segar and Cantillo (1976), where the only consistent difference between dump site water column dissolved metals and a distant shelf central site was also for Mn.

There do appear to be considerable differences in published New York Bight metal concentrations far from zones of contamination (Segar and Cantillo, 1976) compared with those obtained by Windom (1977) for southeastern coastal waters, especially for Zn and Cu. Despite the uncertainty of the absolute concentrations of soluble metals in the New York Bight, the data do not seem inconsistent with the interpretation that the waste area sediments are a relatively insignificant source of soluble metals in the New York Bight apex, compared with the flux of soluble metals from the Hudson.

Our opinion is that, although more effort should be devoted to the understanding of trace metal transport pathways in coastal waters impacted by dredge spoil and sewage discharges, it is at least equally important to intensify studies of the environmental pathways and significance of pollutants such as PCB's and other toxic organic compounds, especially for the New York City area.

REFERENCES

1. Abood, K.A. Circulation in the Hudson Estuary. In: Hudson River Colloquium, Annals of the New York Academy of Sciences, 250:36-111, 1974.

2. Artem'yev, V.Y. Carbohydrates in the bottom sediments of the Central Pacific. Oceanology, 10:508-513, 1970.

3. Atkinson, L.P., and F.A. Richards. The occurrence and distribution of methane in the marine environment. Deep-Sea Research, 14:673-684, 1967.

4. Bender, M.L. Does upward diffusion supply the excess manganese in pelagic sediments? Journal of Geophysical Research, 76:4212-4215, 1971.

5. Berner, R.A. Principles of Chemical Sedimentology. McGraw-Hill, New York, 1971. 240 pp.

6. Biggs, R.B., and C.D. Wetzel. Concentration of particulate carbohydrate and the halocline in Chesapeake Bay. Limnology and Oceanography, 13: 169-171, 1968.

7. Bondeitti, E.A., F.H. Sweeton, T. Tamura, R.M. Perhac, L.D. Hulet, and T.J. Kneip. Characterization of cadmium and nickel contaminated sediments from Foundry Cove, New York. In: Proceedings of the National Science Foundation Trace Contaminants Conference, 1973.

8. Boyle, E.A., J.M. Edmond, and E.R. Sholkovitz. The mechanism of iron removal in estuaries. Geochimica et Cosmochimica Acta, 41:1313-1324, 1977.

9. Bowen, V.T., and W. Roether. Vertical distributions of strontium-90, cesium-137 and tritium near 45° North in the Atlantic. Journal of Geophysical Research, 78:6277-6285, 1973.

10. Bower, P.M. Cadmium and nickel in the sediments of Foundry Cove. Master's Thesis, Queens College of the City University of New York, Flushing, New York, 1976. 162 pp. with appendicies.

11. Broecker, W.S., and E.A. Olson. Lamont radiocarbon measurements, VI. Radiocarbon 1:111-132, 1959.

12. Broecker, W.S., and A. Walton. The geochemistry of C^{14} in fresh water systems. Geochemica et Cosmochimica Acta, 16:15-38, 1959.

13. Broecker, W.S., and E.A. Olson. Lamont radiocarbon measurements, VIII. Radiocarbon, 3:176-204, 1961.

14. Broecker, W.S. Radiocarbon dating: A case against the proposed link between river mollusks and soil humus. Science, 143:596-597, 1964.

15. Broecker, W.S. The application of natural radon to problems in ocean circulation. In: Symposium on Diffusion in Oceans and Fresh Waters, Lamont Geological Observatory, Palisades, New York, pp. 116-145, 1965.

16. Broecker, W.S., E.R. Bonebakker, and G.G. Rocco. The vertical distribution of cesium-137 and strontium-90 in the oceans, 2. Journal of Geophysical Research, 71:1999-2003, 1966.

17. Broecker, W.S., and T.H. Peng. Gas exchange rates between air and sea. Tellus, 26:21-35, 1974.

18. Bruland, K.W., K. Bertine, M. Koide, and E.D. Goldberg. History of metal pollution in Southern California coastal zone. Environmental Science and Technology, 8:425-432, 1974.

19. Buehler, K., and H.I. Hirshfield. Cadmium in an aquatic ecosystem: Effects on planktonic organisms. In: Trace Contaminants in the Environment, Proceedings of the Second Annual NSF-RANN Trace Contaminants Conference, Asilomar, Pacific Grove, California, 1974.

20. Cain, W.F., and H.E. Suess. Carbon-14 in tree rings. Journal of Geophysical Research, 81:3688-3694, 1976.

21. Cappenberg, T.E. Ecological observations on heterotrophic, methane oxidizing and sulfate reducing bacteria in a pond. Hydrobiologia, 40:471-485, 1972.

22. Cappenberg, T.E. A study of mixed continuous cultures of sulfate-reducing and methane-producing bacteria. Microbial Ecol., 2:60-72, 1975.

23. Carmody, D.J., J.B. Pearce, and W.E. Yasso. Trace metals in sediments of New York Bight. Marine Pollution Bulletin, 9:132-135, 1973.

24. Chow, T.J., K. Bruland, K. Bertine, A. Soutar, M. Koide, and E.D. Goldberg. Lead pollution: Records in Southern California coastal sediments. Science, 181:551-552, 1973.

25. Claypool, G.E., and I.R. Kaplan. The origin and distribution of methane in marine sediments. In: Natural Gases in Marine Sediments, I.R. Kaplan, ed., Plenum Press, New York, 1974. 324 pp.

26. Craig, H. Isotopic standards for carbon and oxygen and correction factors for mass spectrometric analysis of carbon dioxide. Geochimica et Cosmochimica Acta, 12:133-149, 1957.

27. Deevey, E.S., M.S. Gross, G.E. Hutchinson, and H.L. Kraybill. The natural C-14 content of materials from hard-water lakes. Proceedings National Academy of Science, 40:285-288, 1954.

28. deGroot, A.J., W. Salomons, and E. Allersma. Processes affecting heavy metals in estuarine sediments. In: Estuarine Chemistry, J.D. Burton and P.S. Liss, eds., Academic Press, London, pp. 131-157, 1976.

29. Deindoerfer, R.N., and D.E. Humphrey. Mass transfer from individual gas bubbles. Ind. Eng. Chem., 53:755-759, 1961.

30. Doelle, H.W. Bacterial Metabolism. Academic Press, New York, 1969.

31. Dreywood, R. Qualitative tests for carbohydrate materials. Ind. Eng. Chem., 18:499, 1946.

32. Dubois, M., K.A. Gilles, J.K. Hamilton, P.A. Rebers, and F. Smith. Colorimetric method for determination of sugars and related substances. Analytical Chemistry, 28:350-356, 1956.

33. Duce, R.A., G.T. Wallace, Jr., and B.J. Ray. Atmospheric trace metals over the New York Bight. NOAA Technical Report, ERL 361-MESA 4, 1976, 17 pp.

34. Edgington, D.N., J.J. Alberts, M.A. Wahlgren, J.O. Karttunen, and C.A. Reeve. Plutonium and americium in Lake Michigan sediments. In: Transuranium Nuclides in the Environment, IAEA-SM-199/47, IAEA, Vienna, pp. 493-516, 1976.

35. Elderfield, H. Manganese fluxes to the oceans. Marine Chemistry, 4:103-132, 1976.

36. Emerson, S.R. Gas exchange rates in small Canadian shield lakes. Limnology and Oceanography, 20:754-761, 1975.

37. Emerson, S.R. Early diagenesis in anaerobic lake sediments. Geochimica et Cosmochimica Acta, 40, 1976.

38. Emery, K.O. Estuaries and lagoons in relation to continental shelves. In: Estuaries, G.H. Lauff, ed., American Association for the Advancement of Science, Pub. 83:9-11, 1967.

39. Emery, K.O. A coastal pond, studied by oceanographic measurements. American Elsevier, New York, 1969.

40. Erlenkeuser, H., E. Suess, and H. Willkomm. Industrialization affects heavy metal and carbon isotope concentrations in recent Baltic Sea sediments. Geochimica et Cosmochimica Acta, 38:823-842, 1974.

41. Evans, D.W., and N.H. Cutshall. Effects of ocean water on the soluble-suspended distribution of Columbia River radionuclides. In: Radioactive Contamination of the Marine Environment, International Atomic Energy Agency, Vienna, pp. 125-138, 1973.

42. Evans, D.W., N.H. Cutshall, F.A. Cross, and D.A. Wolfe. Manganese cycling in the Newport River estuary, North Carolina. Estuarine and Coastal Marine Science, 5:71-80, 1977.

43. Fairbridge, R.F., and W.S. Newman. Postglacial crustal subsidence of the New York area. Zeitschrift für Geomorphologie, 12(3):296-317, 1968.

44. Fanning, K.A., and M.E.Q. Pilson. The diffusion of dissolved silica out of deep-sea sediments. Journal of Geophysical Research, 79:1293-1298, 1974.

45. Farmer, J.G., V.T. Bowen, and V.E. Noshkin. Long-lived artificial radionuclides in Lake Ontario, I. Supply from fallout, and concentrations in lake water of plutonium, americium, strontium-90 and cesium-137. Submitted to Limnology and Oceanography, 1977.

46. Feely, H.W., and J.L. Kulp. Origin of Gulf coast salt-dome sulfur deposits. Bulletin of American Association of Petrol. Geol., 41:1802-1853, 1957.

47. Folsom, T.R., N. Sreekimaran, Hansen, J.M. Moore, and R. Grismore. Some concentrations of Cs-137 at moderate depths in the Pacific 1965-1968. USAEC Report HASL-217, 1970, 109 pp.

48. Fritz, P., and S. Poplawski. ^{18}O and ^{13}C in the shells of freshwater molluscs and their environments. Earth and Planetary Science Letters, 24:91-98, 1974.

49. Garside, C., T.C. Malone, O.A. Roels, and B.C. Sharfstein. An evaluation of sewage-derived nutrients and their influence on the Hudson Estuary and New York Bight. Estuarine and Coastal Marine Science (in press).

50. Garrels, R.M., and C.L. Christ. Solutions, minerals and equilibria. Freeman, Cooper and Company, San Francisco, California, 1965.

51. Gerchakov, S.M., and P.G. Hatcher. Improved technique for analysis of carbohydrates in sediments. Limnology and Oceanography, 17:938-943, 1972.

52. Goldhaber, M., R.A. Berner, R.C. Allen, and J.K. Cochran. Sulfate reduction, diffusion and bioturbation in Long Island Sound. In: Symposium on Marine Chemistry in the Coastal Environment, American Chemical Society Middle Atlantic Region, 1975 (abstract).

53. Graham, W.F., M.L. Bender, and G.P. Klinkhammer. Manganese in Narragansett Bay. Limnology and Oceanography, 21:665-673, 1976.

54. Gross, M.G. Geologic aspects of waste solids and marine waste deposits, New York metropolitan region. Geological Society of America Bulletin, 83:3163-3176, 1972.

55. Gross, M.G. Waste disposal. MESA New York Bight Atlas Monograph, 26, 1976, 32 pp.

56. Gross, M.G., J.A. Black, R.J. Kalin, J.R. Schramel, and R.N. Smith. Survey of marine waste deposits, New York metropolitan region. Marine Science Research Center Technical Report No. 8, State University of New York at Stony Brook, 1971, 72 pp.

57. Guinasso, N.L., and D.R. Schink. A simple physiochemical acoustic model of methane bubbles rising in the sea. Unpublished report No. 73-15T, Texas A&M University, College Station, Texas, 1973, 24 pp.

58. Hammond, D.E., and H.J. Simpson. Methane distribution and sediment flatulence in the Hudson River Estuary. Limnology and Oceanography, revisions submitted, 1977.

59. Hammond, D.E., H.J. Simpson, and G. Mathieu. Methane and radon-222 as tracers for mechanisms of exchange across the sediment-water interface in the Hudson River Estuary. In: Marine Chemistry in the Coastal Environment, T. Church, ed., ACS Symposium Series 18: 119-132, 1975.

60. Hammond, D.E., H.J. Simpson, and G. Mathieu. ^{222}Rn distribution and transport across the sediment-water interface in the Hudson River Estuary. Journal of Geophysical Research, in press, 1977.

61. Handa, N. Examination of the applicability of the phenol sulfuric acid method to the determination of dissolved carbohydrates in sea water. Journal of Oceanogr. Soc. Japan, 22(3):1-8, 1966.

62. Hardy, E.P. Depth distributions of global fallout Sr-90, Cs-137 and Pu-239,240 in sandy loam soil. USAEC Report HASL-286, pp. 2-10, 1974.

63. Hardy, E.P., and L.T. Alexander. Rainfall and deposition of Sr-90 in Clallam County, Washington. Science, 136:881-882, 1962.

64. Harley, N., I. Fisenne, L.D.Y. Ong, and J. Harley. Fission yield and fission product decay. USAEC Report HASL-164, 1965.

65. Hatcher, P.G., and L.E. Keister. Carbohydrates and organic carbon in New York Bight sediments as possible indicators of sewage contamination. In: The Middle Atlantic Shelf and New York Bight, Limnology and Oceanography Special Symposium, 2, M.G. Gross, ed., in press.

66. Hesslein, R.H. An in situ sampler for close interval pore water studies. Limnology and Oceanography, 22:913-915, 1976.

67. Higbie, R. The rate of absorption of a pure gas into a still liquid during short periods of exposure. Trans. Am. Inst. Chem. Eng., 35:365-389, 1935.

68. Hunter, J.V., and H. Heukelekian. The composition of domestic sewage fractions. Journal of Water Pollution Control Fed., 37:1142-1163, 1965.

69. Hutton, W.E., and C.E. Zobell. The occurrence and characteristics of methane oxidizing bacteria in marine sediments. Journal of Bacteriology, 58:463-473, 1949.

70. Keith, M.L. and G.M. Anderson. Radiocarbon dating: fictitious results with mollusk shells. Science, 141:634-637, 1963.

71. Keith, M.L., G.M. Anderson, and R. Eichler. Carbon and oxygen isotopic composition of mollusk shells from marine and freshwater environments. Geochimica et Cosmochimica Acta, 28:1757-1786, 1964.

72. Klein, L.A., M. Lang, N. Nash, and S. Kirschner. Sources of metals in New York City waste waters. Department of Water Resources Report, City of New York, Journal of Water Pollution Control, 46(12):2653-2662, 1974.

73. Klinkhammer, G.P. The distribution and partitioning of some trace metals in the Hudson River Estuary. Master's Thesis, University of Rhode Island, Kingston, Rhode Island, 1977, 136 pp.

74. Kneip, T.J. Cadmium in an aquatic ecosystem: distribution and effects. First Annual Progress Report to the National Science Foundation, New York University Institute for Environmental Medicine, New York, New York, 1974.

75. Kneip, T.J. Cadmium in an aquatic ecosystem: distribution and effects. Second Annual Progress Report to the National Science Foundation, New York University Institute for Environmental Medicine, New York, New York, 1975.

76. Kneip, T.J., T. Hernandez, and G. Re. Cadmium in an aquatic ecosystem: transport and distribution. In: Trace contaminants in the Environment, Proceedings of the Second Annual NSF-RANN Trace Contaminants Conference, Asilomar, Pacific Grove, California, 1974.

77. Kolle, W., H. Ruff, and L. Stieglitz. Die belastung des Rheins mit organischen schadstoffen. Naturwissenschaften, 59:299-305, 1972.

78. Koyama, T. Gaseous metabolism in lake sediments and paddy soils and the production of atmospheric methane and hydrogen. Journal of Geophysical Research, 68:3971-3973, 1963.

79. LeBlond, P.H. Gas diffusion from ascending gas bubbles. Journal of Fluid Mechanics, 35:711-791, 1969.

80. Levich, V.G. Physiochemical Hydrodynamics, Prentis Hall, New York, 1962.

81. Lewis, G.J., and N.W. Rakestraw. Carbohydrates in sea water. Journal of Marine Research, 14:253-258, 1955.

82. Li, Y.H., J. Bishoff, and G. Mathieu. The migration of manganese in the Artic Basin sediment. Earth and Planetary Science Letters, 7: 265-270, 1969.

83. Lovegren, J.R. Paleodrainage history of the Hudson Estuary. Master's Thesis, Columbia University, New York, New York, 1974. 152 pp.

84. Lowman, F.G., D.K. Phelps, R. McClin, V.R. DeVega, I.O. DePodavani, and R.J. Garcia. Interactions of the environmental and biological factors on the distribution of trace elements in the marine environment. In: Disposal of Radioactive Wastes into Seas, Oceans and Surface Waters, International Atomic Energy Agency, Vienna, pp. 249-265, 1966.

85. Lynn, D.C., and Bonatti, E. Mobility of manganese in diagenesis of deep sea sediments. Marine Geology, 3:457-474, 1965.

86. Malone, T.C. Environmental regulation of phytoplankton productivity in the lower Hudson Estuary. Estuarine and Coastal Marine Science, 5:157-171, 1977a.

87. Malone, T.C. Phytoplankton productivity in the Apex of the New York Bight: environmental regulation of productivity/chlorophyll a. In: The Middle Atlantic Continental Shelf and New York Bight, M.G. Gross, ed., Limnology and Oceanography Special Symposium, 2, 1977b, 260 pp.

88. Martens, C. Control of methane sediment-water bubble transport by macroinfaunal irrigation in Cape Lookout Bight, North Carolina. Science, 192:998-1000, 1976.

89. Martens, C.S., and R.A. Berner. Methane production in the interstitial waters of sulfate-depleted marine sediments. Science, 185:1167-1169, 1974.

90. McCrone, W.W. The Hudson River Estuary: sedimentary and geochemical properties between Kingston and Haverstraw, New York. Journal of Sedimentary Petrology, 37:475-486, 1967.

91. Meade, R.H. Landward transport of bottom sediments in estuaries of the Atlantic coastal plain. Journal of Sedimentary Petrology, 39: 222-234, 1969.

92. Mechalas, B.J. Pathways and environmental requirements for biogenic gas production in the ocean. In: Natural Gases in Marine Sediment, I.R. Kaplan, ed., Plenum Press, pp. 11-25, 1974.

93. Mook, W.G., and Vogel, J.C. Isotopic equilibrium between shells and their environment. Science, 159:874-875, 1968.

94. Morel, F.M.M., J.C. Westall, C.R. O'Melia, and J.J. Morgan. Fate of trace metals in Los Angeles County waste water discharge. Environmental Science and Technology, 9:756-761, 1975.

95. Morris, L.D. Quantitative determination of carbohydrates with Dreywood's anthrone reagent. Science, 107:254-255, 1948.

96. Newman, W.S., D.L. Thurber, H.S. Zeiss, A. Rokach, and L. Musich. Late Quaternary geology of the Hudson River Estuary: A preliminary report. Trans. New York Academy of Science, 31(2):548-570, 1969.

97. Nissenbaum, A., B.J. Presley, and I.R. Kaplan. Early diagenesis in reducing fjord, Saanich Inlet, British Columbia, I. Chemical and isotopic changes in major components of interstitial water. Geochimica et Cosmochimica Acta, 36:1007-1027, 1972.

98. Noshkin, V.E., and V.T. Bowen. Concentrations and distributions of long-lived fallout radionuclides in open ocean sediments. Radioactive Contamination of the Marine Environment, IAEA, Vienna, pp. 671-686, 1973.

99. O'Connor, D.J. Water quality analysis for the New York Harbor complex. In: Water Pollution in the Greater New York Area, A.A. Johnson, ed., Gordon and Breach, New York, 1970. 121 pp.

100. O'Connor, D.J. and W.E. Dobbins. Mechanism of reaeration in natural streams. Trans. Am. Soc. of Civil Eng., 123:641-666, 1958.

101. Oliver, B.J. Heavy metal levels at Ottawa River sediments. Environmental Science and Technology, 7:135-137, 1973.

102. Olsen, C.R., H.J. Simpson, R.F. Bopp, S.C. Williams, T.H. Peng, and B.L. Deck. A geochemical analysis of the sediments and sedimentation in the Hudson Estuary, Journal of Sedimentary Petrology, 1978 (in press).

103. Owens, J.P., K. Stefansson, and L.A. Sirkin. Chemical, mineralogic and palynologic charater of the Upper Wisconsin-Lower Holocene fill in parts of Hudson, Delaware and Chesapeake estuaries. Journal of Sedimentary Petrology, 44:390-408, 1974.

104. Pamatmat, M.M., and K. Banse. Oxygen consumption by the seabed. II. In situ measurements to a depth of 180 m. Limnology and Oceanography, 14:250-259, 1969.

105. Panuzio, F.L. Lower Hudson River siltation. In: Proceedings of the Federal Inter Agency Sedimentation Conference, Agricultural Research Service, Miscellaneous Publication No. 970, pp. 512-520, 1963.

106. Peng, T.H. Determination of gas exchange rates across sea-air interface by the radon method. Ph.D. Thesis, Columbia University, New York, New York, 1973. 324 pp.

107. Quirk, Lawler and Matusky, Engineers. Hudson River water quality and waste assimilative capacity study, a final report submitted to the State of New York, Department of Environmental Conservation, 1970, 198 pp.

108. Rafter, T.A. and B.J. O'Brien. Radiocarbon in the atmosphere and in the South Pacific ocean. In: Proceedings of the 8th International Conference on Radiocarbon Dating, The Royal Society of New Zealand, Wellington, pp. 241-266, 1972.

109. Rapaire, J.L., and G. Hugues. Monaco radiocarbon measurements, V. Radiocarbon, 19:44-61, 1977.

110. Reeburgh, W.S. Observations of gases in Chesapeake Bay sediments. Limnology and Oceanography, 14:368-375, 1969.

111. Reeburgh, W.S. Methane consumption in Cariaco Trench waters and sediments. Earth and Planetary Science Letters, 28:334-337, 1976.

112. Reeburgh, W.S., and D.T. Heggie. Microbial methane consumption reactions and their effect on methane distributions in freshwater and marine environments. Limnology and Oceanography, 22:1-9, 1977.

113. Reese, E.T., and M. Mandels. In: Methods in Carbohydrate Chemistry, Vol. III, Academic Press, New York, 1963.

114. Riel, G.K. The distribution of fallout cesium-137 in the Chesapeake Bay. In: Proceedings of the Second International Symposium on the Natural Radiation Environment, J.A.S. Adams, W.M. Lowder, and T.F. Gesell, eds., pp. 883-896, 1972.

115. Ritchie, J.C., P.H. Hawks, and J.R. McHenry. Deposition rates in valleys determined using fallout cesium-137. Geol. Soc. Amer. Bull., 86:1128-1130, 1975.

116. Rogers, M.A. Carbohydrates in aquatic plants and associated sediments from two Minnesota lakes. Geochimica et Cosmochimica Acta, 29:183-200, 1965.

117. Rosen, A.A., and M. Rubin. Natural carbon-14 activity of organic substances in streams. Science, 143:1163-1164, 1964.

118. Rubin, M., and D.W. Taylor. Radiocarbon activity of shells from living clams and snails. Science, 141:632, 1963.

119. Rudd, J.W.M., R.D. Hamilton, and N.E.R. Campbell. Measurement of microbial oxidation of methane in lake water. Limnology and Oceanography, 19:519-524, 1974.

120. Sackett, W.M., and W.S. Moore. Isotopic variations of dissolved inorganic carbon. Chemical Geology, 1:323-328, 1966.

121. Sanders, J.E. Geomorphology of the Hudson Estuary. In: Hudson River Colloquium, Ann. New York Academy of Science, 250:5-38, 1974.

122. Schink, D.R., N.L. Guinasso, and K.A. Fanning. Processes affecting the concentration of silica at the sediment-water interface of the Atlantic Ocean. Journal of Geophysical Research, 80:3013, 1975.

123. Segar, D.A., and A.Y. Cantillo. Trace metals in the New York Bight. Am. Soc. Limnology and Oceanography Spec. Symp., 2:171-198, 1976.

124. Simmons, H.B., and F.A. Herrmann. Effects of man-made works on the hydraulic, salinity and shoaling regimes of estuaries. In: Environmental Framework of Coastal Plain Estuaries, B.W. Nelson, ed., Geological Society of America Memoir, 133:555-570, 1972.

125. Simpson, H.J., R. Bopp, and D.L. Thurber. Salt movement in the lower Hudson, Ch. 9. In: Third Symposium on Hudson River Ecology, Hudson River Environmental Society, New York, 1974.

126. Simpson, H.J., and D.E. Hammond. Application of one-dimensional transport models to circulation in the Hudson Estuary. Submitted to the Journal of Estuarine and Coastal Research, 1977.

127. Simpson, H.J., D.E. Hammond, B.L. Deck, and S.C. Williams. Nutrient budgets in the Hudson River Estuary. In: Marine Chemistry in the Coastal Environment, Amer. Chem. Soc. Sym. Series, T.M. Church, ed., 18:616-635, 1975.

128. Simpson, H.J., C.R. Olsen, T.H. Peng, and S.C. Williams. Radiocarbon dating of Hudson Estuary cores. In preparation.

129. Simpson, H.J., C.R. Olsen, R.M. Trier, and S.C. Williams. Man-made radionuclides and sedimentation in the Hudson River Estuary. Science, 194:179-183, 1976.

130. Simpson, H.J., S.C. Williams, C.R. Olsen, and D.E. Hammond. Nutrient and particulate matter budgets in urban estuaries. Estuaries, Geophysics and the Environment, National Academy of Sciences, Washington, D.C., pp. 94-103, 1977.

131. Solozono, L. Determination of ammonia in natural waters by the phenolhypochlorite method. Limnology and Oceanography, 14:799, 1969.

132. Spiker, E.C. Carbon isotope variations in San Francisco Bay. Trans. American Geophysical Union, 4:255, 1976.

133. Spiker, E.C., and M. Rubin. Petroleum pollutants in surface and groundwater as indicated by the carbon-14 activity of dissolved organic carbon, 61-64, 1975.

134. Standard Methods, 13th edition. American Public Health Association, New York, 1971.

135. Stommel, H. Computation of pollution in a vertically mixed estuary. Sewage and Industrial Wastes, 25:1065-1071, 1953.

136. Stookey, L.L. Ferrozine - A new spectrophotometric reagent for iron. Analytical Chemistry, 42(7):779-781, 1970.

137. Strickland, J.D.H., and T.R. Parsons. A practical handbook of sea water analysis. Bull. Fisheries Research Board of Canada, 167, 1968, 311 pp.

138. Swinnerton, J.W., V.J. Linnenbom, and C.H. Cheek. Determination of dissolved gases in aqueous solutions by gas chromatography. Analytical Chemistry, 34:483-485, 1962.

139. Taylor, S.R. Abundance of chemical elements in the continental crust: A new table. Geochimica et Cosmochimica Acta, 28:2173-2185, 1964.

140. Thatcher, M.L., and D.R.F. Harleman. A mathematical model for the prediction of unsteady salinity intrusion in estuaries. Technical report No. 144, Ralph M. Parsons Laboratory for Water Resources and Hydrodynamics, Department of Civil Engineering, Massachusetts Institute of Technology, 1972.

141. Thomas, R.L. The distribution of mercury in the sediments of Lake Ontario. Canadian Journal of Earth Sciences, 9:636-651, 1972.

142. Thomas, R.L. The distribution of mercury in the surficial sediments of Lake Huron. Canadian Journal of Earth Sciences, 10:194-204, 1973.

143. Tsivoglou, E.C. Relative gas transfer characteristics of krypton and oxygen. In: Symposium on Direct Tracer Measurement of the Reaeration Capacity of Streams and Estuaries, U.S. Environmental Protection Agency, Water Pollution Control Research Series, 16950:19-30, 1972.

144. Tsou, J.L., D. Hammond, and R. Horowitz. Interstitial water studies, Leg 15 - Study of CO_2 released from stored deep sea sediments. In: Initial Reports of the Deep Sea Drilling Project,, B.C. Heezen, I.D. MacGregor, eds., Washington, D.C., 20:851-863, 1973.

145. Turekian, K.K., and K.H. Wedephol. Distribution of elements in the earth's crust. Geological Society of America Bulletin, 72:174-192, 1961.

146. Turner, W.R. Physics of microbubbles. Report Tech. Note 01654-01-2. Vitro Laboratories, Silver Springs, Maryland, 1963.

147. Volchok, H.L. The global strontium-90 budget. Journal of Geophysical Research, 71:1515-1518, 1966.

148. Volchok, H.L., and M.T. Kleinman. Global Sr-90 fallout and precipitation: Summary of the data by 10 degree bands of latitude, USAEC Rep. HASL-245, 2-83, 1971.

149. Wakeham, S.G., and R. Carpenter. Aliphatic hydrocarbons in sediments of Lake Washington. Limnology and Oceanography, 21:711-723, 1976.

150. Wahlgren, M.A., and J.S. Marshall. The behavior of plutonium and other long-lived radionuclides in Lake Michigan: I. Biological transport, seasonal cycling and residence times in the water column. In: International Symposium on Transuranium Nuclides in the Environment, IAEA-SM-198/39, IAEA, Vienna, 1975, 227 pp.

151. Weiss, D. Late Pleistocene stratigraphy and paleoecology of the lower Hudson River Estuary. Bull. Geological Society of America, 85:1561-1570, 1974.

152. Weiss, R.F., and H. Craig. Precise shipboard determination of dissolved nitrogen, oxygen, argon, and total inorganic carbon by gas chromatography. Deep Sea Research, 20:291-303, 1973.

153. Whittenbury, R., K.C. Phillips, and J.F. Wilkinson. Enrichment, isolation and some properties of methane-utilizing bacteria. Journal of General Microbiology, 61:205-218, 1970.

154. Windom, H.L., K.C. Beck, and R. Smith. Transport of trace metals to the Atlantic Ocean by three southeastern rivers. Southeast Geology, 12:169-181, 1971.

155. Windom, H.L. Preprint. 1977.

156. Wong, K.M. Radiochemical determination of plutonium in sea-water, sediments and organisms. Anal. Chim. Acta, 56:355-364, 1971.

157. Worzel, J.L., and C.L. Drake. Structure section across the Hudson River at Nyack, New York, from seismic observations. Annals New York Academy of Science, 80:1092-1105, 1959.

158. Wrenn, M.E., J.W. Lentsch, M. Eisenbud, G.J. Laver, and G.P. Howells. Radiocesium distribution in water, sediment and biota in the Hudson River estuary from 1964 through 1970. In: Proceedings of the Third National Symposium on Radioecology, Oak Ridge, Tennessee, 1971.

159. Wyman, J., P.F. Scholander, G.A. Edwards, and L. Irving. On the stability of gas bubbles in seawater. Journal of Marine Research, 11:47-62, 1952.

160. Zafiriou, O.C. Petroleum hydrocarbons in Narragansett Bay, 2. Chemical and Isotopic Analysis. Estuarine Coastal Marine Science, 1:81-87, 1973.

161. Zein-Eldin, A.P. and B.Z. May. Improved N-ethylcarbazole determination of carbohydrates with emphasis on sea water samples. Analytical Chemistry, 30:1934-1941, 1958.

TECHNICAL REPORT DATA
(Please read Instructions on the reverse before completing)

1. REPORT NO.	2.	3. RECIPIENT'S ACCESSION NO.
EPA-600/3-79-029		

4. TITLE AND SUBTITLE	5. REPORT DATE
DREDGE SPOILS AND SEWAGE SLUDGE IN THE TRACE METAL BUDGET OF ESTUARINE AND COASTAL WATERS	March 1979 issuing date
	6. PERFORMING ORGANIZATION CODE

7. AUTHOR(S)	8. PERFORMING ORGANIZATION REPORT NO.
H. James Simpson	

9. PERFORMING ORGANIZATION NAME AND ADDRESS	10. PROGRAM ELEMENT NO.
Lamont-Doherty Geological Observatory of Columbia University Palisades, New York 10964	1BA819
	11. CONTRACT/GRANT NO. 803113

12. SPONSORING AGENCY NAME AND ADDRESS	13. TYPE OF REPORT AND PERIOD COVERED
Environmental Research Lab. - Narragansett, RI Office of Research and Development U.S. Environmental Protection Agency Narragansett, Rhode Island 02882	Final
	14. SPONSORING AGENCY CODE EPA/600/05

15. SUPPLEMENTARY NOTES

--

16. ABSTRACT

Many reactive pollutants, such as Zn, Cu, Pb, Cs-137, Pu-239, 240 and PCB's appear to be transported and accumulated together in association with fine-grained particles in the Hudson River estuary. Anthropogenic increases of 3-6 times natural levels of Zn, Cu, and Pb were found for Hudson sediments. Mobilization of Cd and Ni in the sediments of a small embayment of the Hudson with very high contamination levels appears to be primarily by resuspension of fine particles, although elevated concentrations of Cd in pore waters were also observed. Radiocarbon measurements indicate the predominant source of organic carbon in New York harbor sediments is recent sewage and not petroleum hydrocarbon contamination. A new enzymatic technique was developed to trace the distribution of cellulose, a significant component of sewage sludge, in coastal sediments. Radon-222, a natural radioactive gas dissolved in the Hudson, is supplied primarily from the sediments at approximately twice the rate predicted by molecular diffusion. Methane measurements provided additional information on the flux of materials from sediments. The behavior of phosphate and trace metals derived from sewage was examined on the basis of field data and the use of simple models to examine management alternatives. The most reasonable course appears to be completion of secondary sewage treatment plants in New York City and major upgrading of primary treatment in New Jersey.

17. KEY WORDS AND DOCUMENT ANALYSIS

a. DESCRIPTORS	b. IDENTIFIERS/OPEN ENDED TERMS	c. COSATI Field/Group
Geochemistry Sediments Radioactive isotopes	Dredge spoil Coastal waters	08/A 08/D 08/H

18. DISTRIBUTION STATEMENT	19. SECURITY CLASS *(This Report)*	21. NO. OF PAGES
RELEASE TO PUBLIC	UNCLASSIFIED	223
	20. SECURITY CLASS *(This page)*	22. PRICE
	UNCLASSIFIED	

☆ U. S. GOVERNMENT PRINTING OFFICE: 1979 — 657-060/1634

U.S. ENVIRONMENTAL PROTECTION AGENCY
Office of Research and Development
Environmental Research Information Center
Cincinnati, Ohio 45268

POSTAGE AND FEES PAID
U.S. ENVIRONMENTAL PROTECTION AGENCY
EPA-335

Special Fourth-Class Rate
Book

If your address is incorrect, please change on the above label tear off; and return to the above address.
If you do not desire to continue receiving these technical reports, CHECK HERE ☐; tear off label, and return it to the above address,

EPA-600/3-79-029